

The Structure and Function of V_{1b} Vasopressin Receptors

Yukie Goto

A thesis submitted to the University of Birmingham
for the degree of Doctor of Philosophy

School of Biosciences
University of Birmingham
Edgbaston, Birmingham
B15 2TT, United Kingdom
September 2009

UNIVERSITY OF
BIRMINGHAM

University of Birmingham Research Archive

e-theses repository

This unpublished thesis/dissertation is copyright of the author and/or third parties. The intellectual property rights of the author or third parties in respect of this work are as defined by The Copyright Designs and Patents Act 1988 or as modified by any successor legislation.

Any use made of information contained in this thesis/dissertation must be in accordance with that legislation and must be properly acknowledged. Further distribution or reproduction in any format is prohibited without the permission of the copyright holder.

Acknowledgement

Firstly I would like to thank my supervisor Professor Mark Wheatley for giving me this opportunity to participate in his research, and for his support and guidance throughout my study. I would also like to thank those who have worked in his research group: in particular John for providing us with molecular models of vasopressin receptors; Alex, Mattew, Denise, Cymone and Amelia, for equipping me with the laboratory techniques required for carrying out this study; and Rachel and Richard for their companies and supports in the research group for last few years. I am truly grateful to Dr. David Poyner and Prof. Ian Martin for their inspiring teachings on this subject area in my undergraduate years. My gratitude goes to Rosemary for her conscientious hard work in looking after laboratories, equipments, and students; and to Eva, David, Karthik, Prof. Wharton, Bob, Pei, Tim, Umbrene, Yiu Pin, Raul, Martin and Mohammed for their companies in the laboratories and in the office; and also to Eric for his support in general outside the university. I am also thankful to Dr. Dove and Dr. Ladds for reading manuscripts and giving me advices on corrections.

I would like to acknowledge Dr. Jeremy Presland, Dr. Grant Wishart, Dr. Mark Craighead and their co-workers in Organon Laboratory, a part of Schering-Plough Research Institute (Newhouse, Scotland) for collaboration, intellectual input, and all the supports provided.

Finally, I am truly grateful to BBSRC and Schering-Plough for financial and material supports given to this project.

Abstract

The V_{1b} vasopressin receptor ($V_{1b}R$) is a receptor for a neurohypophysial nonapeptide [arginine⁸] vasopressin (AVP). $V_{1b}R$ is a G-protein coupled receptor (GPCR) belonging to the Family A GPCR superfamily. The structures of seven α -helical transmembrane domains of this family members can be predicted based on the crystal structure of bovine rhodopsin (bRho) and human β_2 adrenergic receptor (β_2AR) obtained by the X-ray diffraction techniques. This study aimed to identify amino acid residues which participate in ligand binding of the $V_{1b}R$ by site-directed mutagenesis with the aid of molecular models of vasopressin receptors based on the crystal structure of bRho.

The $V_{1b}R$ is a potential drug target in treating stress-related conditions such as depression, anxiety and post-traumatic stress disorders. Since it is the latest subtype identified among the mammalian neurohypophysial hormone receptors, it remains as the least studied subtype. A closely related subtype V_{1a} receptor ($V_{1a}R$) has been studied in far more detail for its potential of being a drug target in treating cardiac conditions and epilepsy. Hence, effective means of studying the $V_{1b}R$ can be accomplished by exploring the information already available on the $V_{1a}R$ and thereby defining the differences and similarities existing between the two. Detailed subtype comparisons are also fundamental for designing subtype selective drugs for effective therapy with fewer side-effects. This project was designed also to elucidate amino acid residues which determine selectivity of ligands for the $V_{1b}R$ over the $V_{1a}R$.

This study demonstrated that the charged residues Glu^{1.35} and Arg^{3.26}, polar residues Gln^{2.61} and Tyr^{5.38}, and cyclic residue Pro^{2.60} are crucial in AVP binding to the $V_{1b}R$. These residues are all

located at the extracellular facing surface of transmembrane domains (TMs). Also at the vicinity, charged residues Arg^{1.27} and Asp^{2.65}, and aromatic Trp^{2.64} are shown to be important components of the AVP binding cavity. The study demonstrated that two residues Trp^{6.48} and Phe^{6.51} located at the TM6 are required for high affinity binding of non-peptide antagonists to the V_{1b}R.

The reciprocal mutagenesis between V_{1b}R and V_{1a}R residues revealed that Phe^{7.35} located at the exofacial surface of TM7 is a key residue required for a high affinity binding of a non-peptide antagonist with selectivity for the V_{1b}R over V_{1a}R. Also on the TM7, Met^{7.39} was shown to be involved in a high affinity binding of an antagonist with selectivity for the V_{1b}R over V_{1a}R. Two residues on the top of TM5, Leu^{5.39} and Thr^{5.42} were also shown to participate in V_{1b}R-selective binding of non-peptide antagonists.

From the perspectives of drug development, the variants of V_{1b}R were studied in two streams: firstly to characterise pharmacological properties of single nucleotide polymorphism (SNP) variants of human V_{1b}R; and secondly to determine differences in TM architectures between rat and human V_{1b}Rs. The study showed that a SNP variant of the V_{1b}R with a residue substitution of Gly to Arg at position 191 is more readily expressed on the cell-surface in comparison to the wild-type. The variant was also found to generate InsP-InsP₃ accumulation effectively in response to AVP stimulation. The mutagenesis involving introduction of specific rat V_{1b}R residues into human V_{1b}R revealed that there is a slight difference in the local environment of TM4 between the V_{1b}Rs found in the two species.

Abbreviations

In the production of this thesis, the abbreviations recommended by the Journal of Biological Chemistry (<http://www.jbc.org/misc/ifora.shtml>) have been applied. In addition, the following abbreviations were used:

A ₁ AR	A ₁ Adenosine receptor
A ₂ AR	A ₂ Adenosine receptor
αAR	α adrenergic receptor
AC	Adenylyl cyclase
ACTH	Adrenocorticotropin
AIMAH	ACTH-independent macronodular adrenal hyperplasia
AKA	A-kinase anchoring protein
ARF6	ADP-ribosylation factor 6
ARNO	ADP-ribosylation factor nucleotide site opener
AT _{1A} R	Angiotensin receptor type 1A
AVP	[Arginine ⁸]vasopressin
AVT	[Arginine ⁸]vasotocin
β ₁ AR	β ₁ adrenergic receptor
β ₂ AR	β ₂ adrenergic receptor
bRho	Bovine rhodopsin
BSA	Bovine serum albumin
BNST	Bed nucleus of the stria terminalis
BRET	Bioluminescence energy transfer
CA	Cyclic antagonist: [d(CH ₂) ₅ Tyr(Me)Arg ⁸]vasopressin
CA2	<i>Cornu Ammonis 2</i>
CaM	Calmodulin
CAM	Constitutively active mutant
cAMP	Cyclic AMP
CCK _B R	Cholecystokinin B receptor

CCR ₅	C-C chemokine receptor type 5
CD8	Cluster of differentiation 8
CHO	Chinese hamster ovary cell-line
CNS	Central nervous system
CP	Carboxy-terminal of glycopeptide
CRF	Corticotrophin releasing factor
CRFR1 α	Corticotrophin releasing factor receptor 1 α
CRLR	Calcitonin receptor-like receptor
DAG	1, 2-diacylglycerol
dAVP	[deamino-Cys ¹ , Arg ⁸]vasopressin
d[Cha ⁴]AVP	[deamino-Cys ¹ , Cyclohexylalanine ⁴ , Arg ⁸]vasopressin
dDAVP	[deamino-Cys ¹ , <i>D</i> -Arg ⁸]vasopressin
DI	Diabetes insipidus
dVDAVP	[deamino-Cys ¹ , Val ⁴ , <i>D</i> -Arg ⁸]vasopressin
DMEM	Dulbecco's modified Eagle's medium
DMSO	Di-methyl-sulfoxide
EGFR	Epidermal growth factor receptor
ECL	Extracellular loop
ELISA	Enzyme-linked immunosorbent assay
ERK	Extracellular signal regulated kinase
FBS	Foetal bovine serums
FRET	Fluorescence energy transfer
FSH	Follicle-stimulating hormone
G-protein	Guanine-nucleotide-binding protein
GABA	Gamma-aminobutyric acid
GIT	G protein-coupled receptor kinase-interactor
GPCR	G-protein-coupled receptor
GDP	Guanosine diphosphate
GEF	Guanine nucleotide exchange factor
GRK	G-protein-coupled receptor kinase

GSK	Glycogen synthase kinase
GTP	Guanosine triphosphate
H ₂ R	H ₂ Histamine receptor
H8	Helix 8
HA	Haemagglutinin
HEK	Human embryonic kidney
HPA	Hypothalamic-pituitary adrenal
5-HT	5-hydroxytryptamine
InsP	Inositol monophosphate
InsP ₃	Inositol 1,4,5-trisphosphate
ICL	Intracellular loop
LA	Linear antagonist: [PhACD-Tyr(Me) ² Arg ⁸ Tyr-(NH ₂)]-vasopressin
LH	Luteinising hormone
MA	Medial amygdaloid nucleus
mAChR	Muscarinic acetylcholine receptor
MAPK	Mitogen activated protein kinase
MCS	Multiple cloning sequence
MD	Molecular dynamic
mGluR	Metabotropic glutamate receptor
MLCK	Myosin light chain kinase
MLCP	Myosin light chain phosphatase
μOR	μ opioid receptor
NDI	Nephrogenic diabetes insipidus
NF-AT	Nuclear factor of activated T-cells
NMR	Nuclear magnetic resonance spectroscopy
NP	Neurophysin
OT	Oxytocin
OTR	Oxytocin receptor
PDL	Poly-D lysine
PDZ	PSD-95-discs-large-ZO-1

PEI	Poly-ethylenimine
PKC	Protein kinase C
PLC	Phospholipase C
PTSD	Post-traumatic stress disorders
PVN	Paraventricular nucleus
RAMP	Receptor activity modifying protein
RGS	Regulator of G-protein signalling
RMSD	Root mean square deviations
RTK	Receptor tyrosin kinase
SCN	Suprachiasmatic nucleus
SEM	Standard errors of means
SH3	Src homology 3
SON	Supraoptic nucleus
SNP	Single nucleotide polymorphism
TM	Transmembrane domain
TSH	Thyrotropin stimulating hormone
V _{1a} R	V _{1a} vasopressin receptor
V _{1b} R	V _{1b} vasopressin receptor
V ₂ R	V ₂ vasopressin receptor
VTR	[Arginine ⁸]vasotocin receptor
Wt	Wild-type

Contents

Acknowledgements	i
Abstract	ii
Abbreviations	iv
Contents	viii
Chapter 1. Introduction	1
1.1. Mammalian neurohypophysial hormones	1
1.1.1. Structure	3
1.1.2. Receptor subtypes and distributions	6
1.1.3. Physiological distribution of vasopressin receptors	6
1.1.4. Physiological actions	7
1.1.5. Pathophysiology	8
1.2. G-protein coupled receptors	10
1.2.1. Classification	10
1.2.2. Post-translational modifications	13
1.2.3. G-proteins and their regulators	14
1.2.4. Oligomerisation of GPCRs	19
1.2.5. Cellular regulations of GPCRs	21
1.2.6. Receptor theory and pharmacological models for GPCR function	24
1.2.7. Allosteric modulators on GPCR pharmacology	29
1.2.8. Cellular influences on GPCR pharmacology	30
1.3. Family A GPCRs	33
1.3.1. Structure of Family A GPCRs	33
1.3.2. Functional motifs and molecular mechanisms of activation	40
1.4. Vasopressin receptors	45
1.4.1. G-protein coupling	45
1.4.2. Oligomerisation	45
1.4.3. Synthetic peptide ligands	47
1.4.4. Non-peptide antagonists	49

1.4.5.	Mutagenesis, molecular modelling and docking studies	51
1.5.	Aims of this study	53
Chapter 2.	Material and Methods	54
2.1.	Materials	
2.1.1.	Radiolabbed compounds	54
2.1.2.	Ligands	54
2.1.3.	Molecular biology reagents	54
2.1.4.	Cell culture reagents	55
2.1.5.	Plasmid cDNA expression vector	55
2.1.6.	Oligonucleotide primers	56
2.2.	Methods	
2.2.1.	Expression constructs and site-directed mutagenesis	57
2.2.2.	Agarose gel electrophoresis	57
2.2.3.	Gel-purification of the PCR products	58
2.2.4.	Restriction digestion	58
2.2.5.	Ligation of cDNA	59
2.2.6.	Transformation of <i>E.coli</i>	59
2.2.7.	Plasmid cDNA extractions	59
2.2.8.	Automated dideoxy sequencing	60
2.2.9.	Sequence Alignment	60
2.2.10.	Cell culture and transfection	60
2.2.11.	Preparation of membrane extract	61
2.2.12.	Protein assay	61
2.2.13.	Competition radioligand binding assay	62
2.2.14.	Thermal denaturation assay	63
2.2.15.	Determination of Cell-Surface Expression of Receptors by Enzyme-linked Immunosorbent Assay (ELISA)	63
2.2.16.	Determination of Agonist-induced Internalisation of Receptors	64
2.2.17.	Determination of the Effect of a Non-peptide Antagonist on the Cell-Surface Expression and Internalisation by ELISA	64
2.2.18.	Inositol phosphate assay	65
2.2.19.	Data analysis	65
Chapter 3.	Investigating the role of conserved residues among vasopressin receptors in V_{1b}R ligand binding	67
3.1.	Introduction	67

3.2.	Results	71
3.2.1.	Identification of conserved residues among vasopressin receptors by primary structure comparisons	71
3.2.2.	The role of conserved residues in the N-terminal, juxtamembrane regions and the upper region of TM2	77
3.2.3.	The participation of TM2 residues in the ligand binding to the V _{1b} R	87
3.2.4.	The roles of the highly conserved residues of TM3 in the juxtamembrane region and the putative ligand binding site	99
3.2.5.	The role of conserved aromatic, or polar residues of TM4 and TM5 in the ligand binding and receptor stability of V _{1b} R	104
3.2.6.	The role of conserved residues in TM6	120
3.3.	Discussions	129
3.3.1.	The residues required for the AVP binding to the V _{1b} R	129
3.3.2.	The roles of TM Gln residues in the ligand binding of V _{1b} R	137
3.3.3.	The involvement of Tyr in the ligand binding of V _{1b} R	140
3.3.4.	The participation of Ile ^{6.40} and Trp ^{6.48} in the V _{1b} R ligand binding	143
3.3.5.	The roles of conserved Phe residues in TM domains of the V _{1b} R	144
3.3.6.	Pharmaco-chaperone activity of the selective antagonist 5234B	146
3.4.	Future works	148

Chapter 4. Exploring the molecular basis for ligand selectivity between V_{1b}R and V_{1a}R
..... 150

4.1.	Introduction	150
4.2.	Results.....	152
4.2.1.	The characteristics of the V _{1b} R constructs containing the corresponding V _{1a} R residue	157
4.2.2.	The characteristics of the V _{1a} R constructs containing the corresponding V _{1b} R residue	165
4.2.3.	Alanine mutagenesis	173
4.3.	Discussions	183
4.3.1.	Phe ^{7.35} and Leu ^{5.39} are involved in 5234B binding to V _{1b} R	183
4.3.2.	The residues possibly contributing indirectly in constructing the binding cavity of 5234B in V _{1b} R	186
4.3.3.	The residues interacting SSR149415 and SR49059	187
4.3.4.	The role of Thr ^{5.42} in the ligand binding of V _{1b} R	190
4.3.5.	The mode of LA binding to V _{1b} R and V _{1a} R	190

4.4.	Future Studies	191
Chapter 5.	The investigation on the variants of V_{1b}R	192
5.1.	Introduction	192
5.2.	Results.....	194
5.2.1.	SNP variants of human V _{1b} R	194
5.2.2.	Characterisation of the SNP variant V _{1b} R constructs	197
5.2.3.	Characterisation of the human V _{1b} R constructs containing the equivalent residue of rat V _{1b} R	203
5.3.	Discussions	212
5.3.1.	Characteristics of SNP variants distinct from the Wt V _{1b} R	212
5.3.2.	Comparisons of TM domains between human and rat V _{1b} Rs	215
5.4.	Future studies	216
Chapter 6.	Summary and concluding remarks	216
References	223
Appendix	pEC ₅₀ values determined for InsP-InsP ₃ assay	249

Chapter 1 Introduction

1.1. Mammalian neurohypophysial hormones

In the majority of mammalian hypothalamo-neurohypophysial systems, the magnocellular neurones within the paraventricular nucleus (PVN) and the supraoptic nucleus (SON) synthesise oxytocin (OT) and [arginine⁸]vasopressin (AVP). In some species, [lysine⁸]vasopressin replaces AVP. These are synthesised as prohormones in the cell bodies of the magnocellular neurones along with neurophysins (NP) which act as carriers. After the synthesis, AVP and OT are carried by specific NP, NP-I for AVP and NP-II for OT, whilst being transported along the axons into the posterior lobe of the pituitary gland. The peptides are then released into the systemic circulation as required. These peptides are known as neurohypophysial hormones. The functions of the hormones were initially found to induce uterine contraction [1], milk ejection and to increase blood pressure [2].

In addition to their original recognition as hormones, the neuromodulatory roles of these peptides have been identified [3, 4]. The parvocellular neurones in the PVN also synthesise both peptides, extending the axons to the other parts of the central nervous system (CNS) including the hypothalamus, brain stem and spinal cord [5, 6]. AVP was also shown to be present in the suprachiasmatic nucleus (SCN) [7-10]. AVP-producing neurones were also found in the bed nucleus of the stria terminalis (BNST), the subparaventricular zone, lateral septum and the medial amygdaloid nucleus (MA), [11-14].



Figure 1.1 A schematic representation of the AVP-neurophysin I prohormone:

AVP and its carrier NP are synthesised altogether as a prohormone comprising: SP (signal peptide), AVP ([arginine⁸]vasopressin), NP-I (neurophysin-I), CP (carboxy-terminal of glycopeptide).

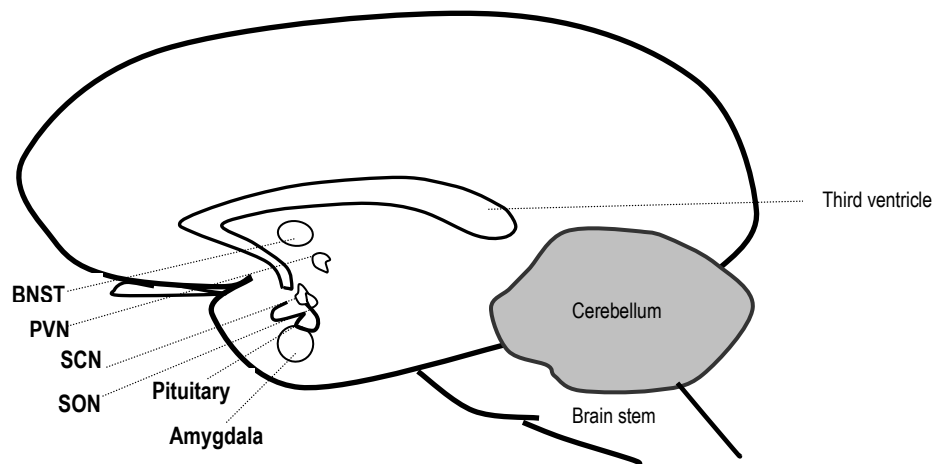


Figure 1.2 A simplified schematic diagram of the mammalian brain:

The figure shows relevant brain regions mentioned in the previous page. The sites where AVP was found are shown in **bold**. Abbreviations: BNST (the bed nucleus of the stria terminalis), PVN (the paraventricular nucleus), SCN (suprachiasmatic nucleus), SON (the supraoptic nucleus). Viewed from the left-hand side.

1.1.1. Structure

AVP and OT are structurally very similar nonapeptides, each of which comprising a hexapeptide ring and a tripeptide tail that terminates with glycineamide. The ring is formed by a covalent disulfide bond between Cys residues at positions one and six. Figure 1.3 displays the molecular structure of AVP. AVP and OT are distinguished by two amino acid differences at positions 3 and 8. AVP has Phe at position 3 whereas OT has aliphatic amino acids Ile at position 3, and Leu at position 8 in place of Arg of AVP.

Peptides which are structurally and functionally similar to vasopressin or oxytocin have been found in other animal species. The neurohypophysial hormones which have been identified to date are summarised in table 1.1. The existence of such analogous peptides in numerous species implicates the evolution of the neurohypophysial system in the animal kingdom. An exceptionally interesting case is found in molluscs of the genus *Conus* which may contain such analogous peptides in their venom, utilising the structural similarity of the peptide to the endogenous peptides found in predators. Conopressin-T found in the venom of *C. tulipa* has been shown to be an antagonist at the V_{1a} vasopressin receptor [15]. In conopressin-T, the conserved Pro⁷ and Gly⁹ are replaced with Leu and Val, making the conformation less flexible and more hydrophobic at the tripeptide tail.

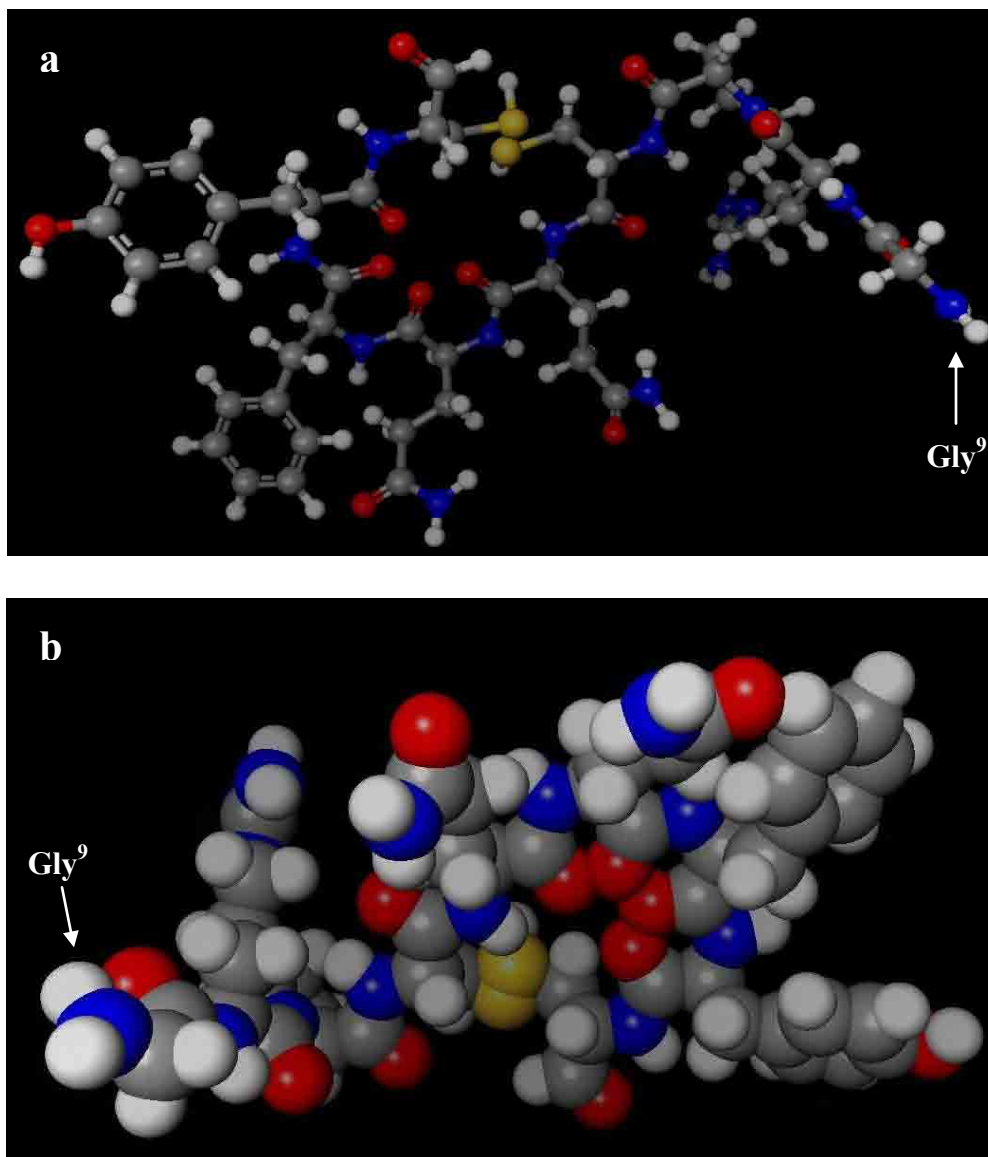


Figure 1.3 Molecular model of AVP: standard chemical colour codes applied.

a. The balls and sticks model;

b. The space-filled model (rotated 180° from the above figure a, and tilted slightly).

Figures made using Sirius (San Diego, Supercomputer Centre, USA).

Name	Amino acid sequence	Source identified
Arginine vasopressin	<u>C</u> YFQ <u>N</u> <u>C</u> PRG (NH ₂)	Mammals
Lysine vasopressin	<u>C</u> YFQ <u>N</u> <u>C</u> PKG (NH ₂)	Suiforms (Pigs, Hippopotamus)
Phenypressin	<u>C</u> FFQ <u>N</u> <u>C</u> PRG (NH ₂)	Macropods (Kangaroos, Wallabies)
Vasotocin	<u>C</u> YIQ <u>N</u> <u>C</u> PRG (NH ₂)	Non-mammalian vertebrates
Inotocin	<u>C</u> LI <u>TN</u> <u>C</u> PRG (NH ₂)	<i>L. migratoria</i> , <i>T. Castaneum</i> <i>N. vitripennis</i> (Insects)
Crustacean OT/AVP-like peptide	<u>C</u> FI <u>TN</u> <u>C</u> PPG (NH ₂)	<i>D. pulex</i> (Plankton)
Conopressin-T	<u>C</u> YIQ <u>N</u> <u>C</u> LRV (NH ₂)	<i>C. tulip</i>
Conopressin-Vil	<u>C</u> LIQ <u>D</u> <u>C</u> PγG (NH ₂)	<i>C. villepini</i>
Conopressin-S	<u>C</u> IIR <u>N</u> <u>C</u> PRG (NH ₂)	<i>C. stratus</i>
Conopressin-G	<u>C</u> FI <u>RN</u> <u>C</u> PKG (NH ₂)	<i>C. geographus</i>
Annetocin	<u>C</u> FVR <u>N</u> <u>C</u> PTG (NH ₂)	<i>E. foetida</i> Annelid (ringed worm)
Octopressin	<u>C</u> FWT <u>S</u> <u>C</u> PIG (NH ₂)	<i>O. vulgaris</i> Cephalopod (Octopus)
Cephalotocin	<u>C</u> YFR <u>N</u> <u>C</u> PIG (NH ₂)	
Phasvatocin	<u>C</u> YF <u>NN</u> <u>C</u> PVG (NH ₂)	Chondrichthyes (Cartilaginous fishes)
Aspargtocin	<u>C</u> YI <u>NN</u> <u>C</u> PLG (NH ₂)	
Valitocin	<u>C</u> YIQ <u>N</u> <u>C</u> PVG (NH ₂)	
Glumitocin	<u>C</u> YIS <u>N</u> <u>C</u> PQG (NH ₂)	
Isotocin	<u>C</u> YIS <u>N</u> <u>C</u> PIG (NH ₂)	Osteichthyes (Bony fishes)
Mesotocin	<u>C</u> YIQ <u>N</u> <u>C</u> PIG (NH ₂)	Dipnoi (Lungfishes), Marshupials
Oxytocin	<u>C</u> YIQ <u>N</u> <u>C</u> PLG (NH ₂)	Mammals

Table 1.1 Vasopressin/Oxytocin-like peptides: Disulfide-bonding cysteine residues are in **underlined bold**. Highly conserved, with an exception of conopressin-T, proline and glysinamide are also shown in **bold**. γ stands for γ-carboxyglutamate. Modified from Dutertre *et al.* 2008 [15].

1.1.2. Receptor subtypes

Three subtypes of receptors have been identified for AVP: V_{1a} vasopressin receptor (V_{1a}R), V_{1b} vasopressin receptor (V_{1b}R) and V₂ vasopressin receptor (V₂R). There is only one type of oxytocin receptor (OTR) identified. AVP is a high affinity partial agonist of OTR, but OT is not a high affinity agonist for any of the three subtypes of vasopressin receptors.

1.1.3. Physiological distribution of the vasopressin receptors

Each subtype has distinct patterns of distribution throughout the body. Being expressed on the vasculature [16-19] and platelets [20] make V_{1a}R probably the most widely expressed subtype amongst the three. The V_{1a}R is also present in the spleen, the liver [21, 22], the adrenal cortex [23] and the CNS [24, 25]. In the brain, V_{1a}R is found mainly in the lateral septum, the fundus striatum, the hypothalamic stigmoid nucleus and the area postrema-nucleus of the solitary tract complex [26, 27]. OTR is expressed on reproductive tracts [28-31], mammary glands [32, 33], T-cells in thymus [34], vascular endothelial cells [35] and the CNS [36-38]. V₂R is found on the kidney tubules where it mediates the anti-diuretic effect [39, 40]. The expression of V₂R mRNA was also found in the brain of newborn rats; however, the level of expression showed age-dependent decline and no V₂R transcript was found in the brains of rats older than two-weeks [41]. V_{1b}R is expressed in the pituitary corticotrophs [42], the adrenal medulla [43, 44], the pancreas [45], white adipose tissue, cluster of differentiation 8 (CD8) cells in the thymus [34] and the CNS [45]. In the brain, the mRNA of V_{1b}R have been identified in the olfactory bulb, CA2 pyramidal neurones in the hippocampus, supraoptic, surachiasmatic dorsomedial hypothalamic nuclei, piriform and entorhinal cortices, substantial nigra, and dorsal motor nucleus of the vagus [46-48].

1.1.4 Physiological actions

As a hormone, AVP is released into the hypophysial portal system and the circulation to act on several target tissues including: i) the vasculature at which AVP induces vasoconstriction [49, 50]; ii) the heart and hypothalamus where AVP increases secretion of atrial natriuretic factors [51, 52]; iii) the kidney tubule where AVP alters permeability of renal collecting duct to water [53]; iv) the pancreas where the secretion of pancreatic hormones, insulin and glucagon, are regulated [54-57]; v) the pituitary corticotrophs where AVP up-regulates adrenocorticotropin (ACTH) secretion predominantly by potentiating the effect of corticotrophin releasing factor (CRF) [58-60]; vi) the adrenal gland at which AVP increases glucocorticoids secretion [61] and aldosterone secretion [23]; vi) the liver in which AVP regulates protein catabolism, lipid metabolism [62] and glucose homeostasis [63, 64]; and viii) platelets where AVP induces aggregation [65, 66]. AVP has also been shown to have mitotic effects by activating the epidermal growth factor receptor (EGFR) in certain cell types [67].

The central effects of AVP have been shown by studies, predominantly on rodents. AVP is involved in regulating: i) the brain water and electrolyte composition [68, 69]; ii) circadian rhythms [8, 70, 71]; iii) social and reproductive behaviour [72-76]; iv) spatial memory via $V_{1a}R$ [77, 78]; v) inter-male aggression [79-82] and behaviours related to dominant/subordinate social status [14, 83, 84]. The expression of AVP can be influenced by gonadal steroids androgens and oestrogen in BNST and MA regions [85-88] and therefore certain actions of AVP can be sexually dimorphic. In monogamous prairie voles, affiliative pair-bonding formation is induced by AVP in males but by OT in females [89-92]. Male $V_{1a}R$ knockout mice were found to have a profound social recognition deficit [93].

Neuromodulatory roles of AVP have been identified in recent years. AVP excites motor neurones via V_{1a}R [94, 95]. AVP can enhance glycinergic and gamma aminobutyric acid (GABA)-ergic inhibitory transmission also via V_{1a}R [96, 97]. AVP has been found to increase glutamate release in hippocampus and cortical regions [98], and dopamine release in the medial prefrontal cortex [99]. Recently knock-out studies of V_{1a}R and V_{1b}R revealed the involvement of AVP in nociceptive responses and morphine-induced hyper-locomotion and hypothermia likely via ACTH and dopaminergic neurones in the mesolimbic system [100]. AVP has also been shown *in vitro* to act as a neurotrophic factor in cultured embryonic neurones from *Xenopus laevis* [101], rat hippocampus [102, 103] and rat ventral spinal cord [104].

OT appears to participate predominantly in physiological roles involving reproduction and parental care both centrally and hormonally [105-108]. OT modulates myometrial contractility, facilitates induction of labour, and stimulates milk secretion by mammary glands.

1.1.5 Pathophysiology

The combination of vasoconstriction, water retention, and mitotic effects of AVP is thought to be involved in the pathogenesis of atherosclerosis, heart failure and hypertension. AVP has also been suggested to be involved in cerebral vasospasm following subarachnoid haemorrhage [109]. Such life-threatening conditions can potentially be treated by administration of V_{1a}R antagonists [69, 110-112].

The loss of function of AVP at the renal ducts results in nephrogenic diabetes insipidus (NDI), which is characterised by polyuria due to severe abnormality in water homeostasis. The majority of NDI cases are congenital caused by X-linked mutations in the V₂R gene, AVPR2. The mutations can be missense, frameshift, inframe deletion, insertion, nonsense, or combined;

but missense is the commonest among all, in particular involving Arg or Tyr residues [113]. An example of such missense mutations is Trp substitution of Arg¹¹³ which results in dysfunctional misfolded V₂R. Modified AVP, [deamino-Cys¹, D-Arg⁸]vasopressin (dDAVP) also known as desmopressin, is a relatively selective V₂R/V_{1b}R agonist with weaker potency at V_{1a}R. It has been clinically proven for its use in preventing bed-wetting or milder cases of acquired DI, as it increases water retention in the kidney as well as increasing water retention via ACTH secretion upregulated by V_{1b}R. As for NDI, desmopressin is ineffective due to the loss of functional V₂R. On the other hand, excessive V₂R activity may result in hyponatremia with excessive fluid uptake. V₂R-selective antagonist could provide effective treatment for such conditions [114].

Inadequate central functions of OT have been suggested to result in subnormal parent-child bonding, lack of social recognition, or possibly autism [115-118]. On the other hand, excess central OT activity in late pregnancy can induce anxiety behaviour in the mother, which can be reversed by OTR antagonist [119].

The dysregulation of hypothalamic-pituitary adrenal (HPA) axis caused by synergistic increase of AVP and CRF has been related to pathophysiology of depression and post-traumatic stress disorders (PTSD) [120]. AVP is released rapidly from the median eminence into the pituitary portal circulation in response to stress [121], and prolonged stress causes AVP to up-regulate V_{1b}R [122]. It has also been suggested that the V_{1b}R-specific antagonists could possibly be applied in treating aggressive behaviours associated with dementias and traumatic brain injuries [123, 124]. Reduction of aggressive behaviour following administration of a V_{1b}R antagonist has been demonstrated in hamsters [125]. When the functional suppression of either V_{1b}R or CRFR1 was performed in mice, it reversed stress-induced suppression of neurogenesis [126]. Several other studies have also demonstrated that the V_{1b}R antagonists are potential

therapeutic agents to treat depression and stress-related disorders [127-132]. $V_{1b}R$ antagonists can also be used to alleviate the symptoms of ACTH-secreting tumours, since $V_{1b}R$ has been found to be over-expressed in certain ACTH-secreting adenoma associated with Cushing's syndrome [133]. Moreover, ectopic expressions of $V_{1b}R$ and V_2R were found in the adrenal gland of patients affected by a rare case of Cushing's syndrome caused by ACTH-independent macronodular adrenal hyperplasia (AIMAH) [134, 135]. Since AIMAH can potentially be treated by $V_{1a}R$ antagonists to some extent [136], more effective treatments for the individuals exhibiting the phenotype may possibly be achieved by administration of dual antagonists of $V_{1a}R/V_{1b}R$ or $V_{1a}R/V_2R$ depending on the nature of ectopic expression identified in each patient.

1.2. G-protein coupled receptors

The GPCR superfamily is the largest class of the transmembrane receptor proteins in the human genome [137]. It is generally estimated that approximately 40 % of all drug targets are GPCRs. GPCRs commonly have seven α -helical transmembrane domains with an extracellular N-terminus and an intracellular C-terminus. In this section, the key characteristics of GPCRs are addressed regarding the receptor pharmacology.

1.2.1. Classification

Mammalian GPCRs can be divided into three families based on types of native ligands, and on similarities in the primary and the secondary structures. Family A is the largest, containing

about 90% of all GPCRs. The members of Family A include visual pigment rhodopsin, biogenic amine receptors, purine receptors, and neurohypophysial hormone receptors as well as some other neuropeptide receptors. Rhodopsin and β_2 adrenergic receptor (β_2 AR) are the two most explored among those. The structures of Family A GPCRs are described in detail in the next sub-chapter 1.3. The second largest is Family B, of which members have relatively larger ligands, and the extracellular domains contribute largely in the binding of their endogenous ligands. Glucagon and secretin receptors often represent Family B members. Family C is a group of GPCRs with small ligands such as amino acids. GABA_B receptors and metabotropic glutamate receptors (mGluRs) are well-studied members of this family. The members characteristically have a large N-terminal domain and a very short intracellular C-terminal tail. The figure 1.4 illustrates the characteristic architectures of GPCRs which belong to the three major mammalian families.

Fungal GPCRs which have been identified are categorised into the following three small families. Yeast pheromone receptors are divided into Family D and Family E. Family F contains cAMP receptors found in the slime mould *Dictyostelium discoideum*.

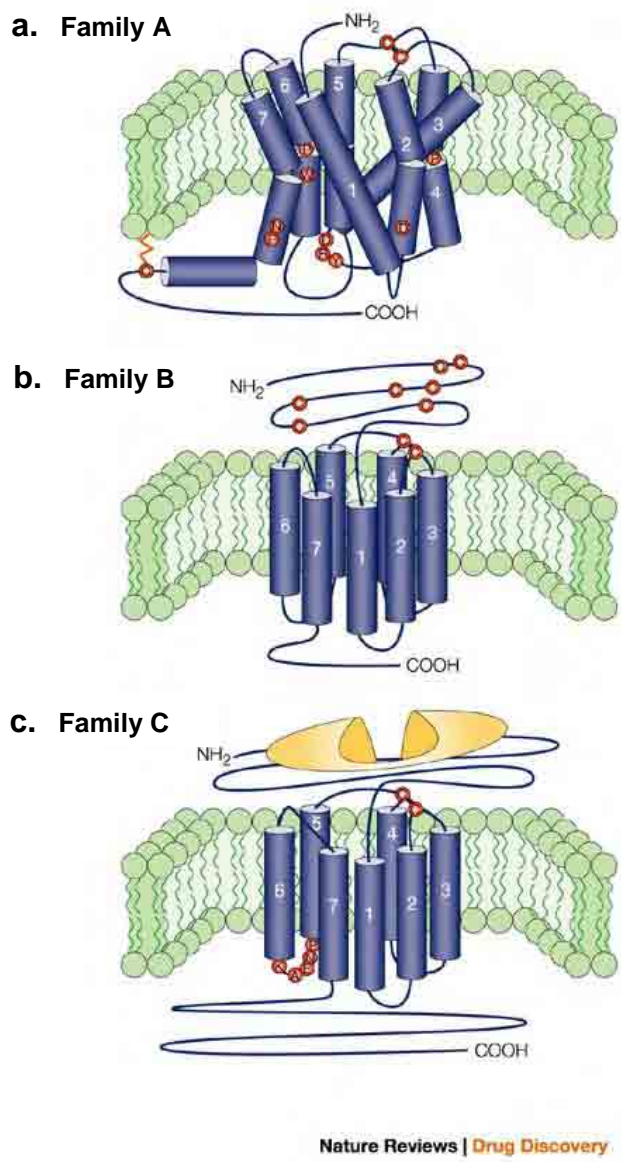


Figure 1.4. a-c. The characteristic features of three major mammalian GPCR families:

The figure illustrates key features of three mammalian GPCR families: **a)** Family A members are characterised by several highly conserved residues (indicated by red circles) and a disulfide bond that connects ECL1 and ECL2. Most of these receptors have palmitoylated cysteine residues (orange zigzag) which serve as an anchor to the membrane by the C-terminal domain. **b)** Family B GPCRs are characterised by a large N-terminal domain containing several cysteine residues that form a network of disulfide bridges. The palmitoylation site, the conserved residues and motifs typically present in Family A GPCRs are not found in Family B. **c)** Family C members have a large characteristic N-terminal domain with the ligand-binding domain (shown in yellow), which is often described as a venus fly trap that can open and close with the agonist bound. Family C members have short and highly conserved (red circles) ECL3. Except for two cysteines in ECL1 and ECL2 that form a putative disulfide bridge, the Family C members have none of the features that characterise Family A and B members. Taken and modified from George *et al.*, 2002 [138].

1.2.2. Post translational modifications

Most GPCRs have putative sites (NxS/T) for N-linked glycosylation in the N-terminus, while some may also contain the site within the extracellular loop (ECL) regions. Family A GPCRs do not have signalling peptides for cellular trafficking of secretory or membrane proteins. For such GPCRs, the glycosylation appears to have significance in cell-surface expression of the receptors [139]. Neither ligand binding nor signalling properties appear to be affected by the glycosylation [140, 141].

Many Family A GPCRs have at least one Cys residue which can be thio-acylated with palmitate by the juxtamembrane region of the C-terminal domain. The palmitoylation provides an anchor by embedding the acyl groups into the hydrophobic region of the cell membrane. Palmitoylation may also favour the receptor interaction with lipid rafts, which are regions rich in glycosphingolipids, cholesterol and also signalling molecules such as kinases. The palmitoylation of V_{1a}R at two residues, Cys³⁷¹ and Cys³⁷² has been confirmed. The study showed that the receptor appeared to be less phosphorylated and more sequestered in the absence of palmitoylation while ligand binding properties appeared to be unaffected [142].

Cytoplasmic Lys residues of GPCRs have been shown to be ubiquitinated, initially in Family E yeast GPCRs Ste2p and Ste3p, upon agonist stimulation [143, 144]. Ubiquitination is a covalent attachment of a 76 amino acid protein ubiquitin via an isopeptide bond between Lys residues. Family A GPCRs such as β_2 AR [145], and V₂R [146] have also been shown to be ubiquitinated following agonist binding to facilitate the receptor degradation by proteosomes.

1.2.3. G-proteins and their regulators

G-proteins are enzymes comprising three subunits: α , β , and γ . The α -subunit (G_α) has a GTPase domain, an α -helical domain with modulatory function, and the N-terminal domain which is disordered as a monomer but ordered by β -subunit (G_β) binding [147-150]. The G_α is inactive as guanine di-phosphate (GDP) bound state. The activation of GPCR initiates exchange of guanine nucleotide, favouring binding of guanine tri-phosphate (GTP) to the G_α . The G_α at GTP-bound state dissociates from the other subunits. The effectors of G_α include phospholipase C_β (PLC_β), adenylyl cyclase (AC), guanine nucleotide exchange factor (GEF), src tyrosine kinase, and components of the mitogen-activated protein kinase (MAPK) pathway. Both $V_{1a}R$ and $V_{1b}R$ are coupled to $G_{\alpha q/11}$ which activates PLC_β . PLC_β hydrolyses phosphatidylinositol 4,5 bisphosphate ($PtdIns(4,5)P_2$) to produce inositol 1,4,5-trisphosphate ($InsP_3$) and 1,2-diacylglycerol (DAG). $InsP_3$ binds to its receptor at the endoplasmic reticulum (ER) to release calcium ions (Ca^{2+}), whilst DAG activates family of protein kinase C (PKC) to initiate cellular responses (figure 1.5). The β - and γ - subunits ($G_{\beta\gamma}$) dimer also has many effectors including PLC_β [151], AC [152], Ca^{2+} pump [153], and K^+ channel [154]. G_β has a β -propeller structure, containing seven motifs of Asp-Trp repeats known as WD-40 repeats [148] which stabilises the N-terminal domain of G_α . G_γ binds G_β by the N-terminal coiled coil domain that spreads over the base of G_β [148]. The binding of $G_{\beta\gamma}$ to G_α inactivates it while enhancing its association with the GPCR [155, 156].

The contact site between G-protein and GPCR involves the C-terminal domain [157], cytoplasmic portions of TM5, TM6 [158, 159], and intracellular loops (ICLs) [160, 161]. Figure 1.6 shows sites of receptor contact in G_α . GPCRs have preferences in coupling to a particular type of G-protein; however, certain GPCRs are known to couple to more than one

type of G-protein [162]; thereby having the potential to activate numerous signalling pathways [163] under different circumstances and environments.

At least 17 G_α , 5 G_β , and 14 G_γ have been cloned so far [164]. In theory, such variations allow a diversity of G-protein population to emerge in different combinations. To simplify, G-proteins can be classified into four groups: G_s , $G_{i/o}$, $G_{q/11}$, and $G_{12/13}$, based on the similarities in the primary structures of the G_α and the intracellular signalling events associated with each.

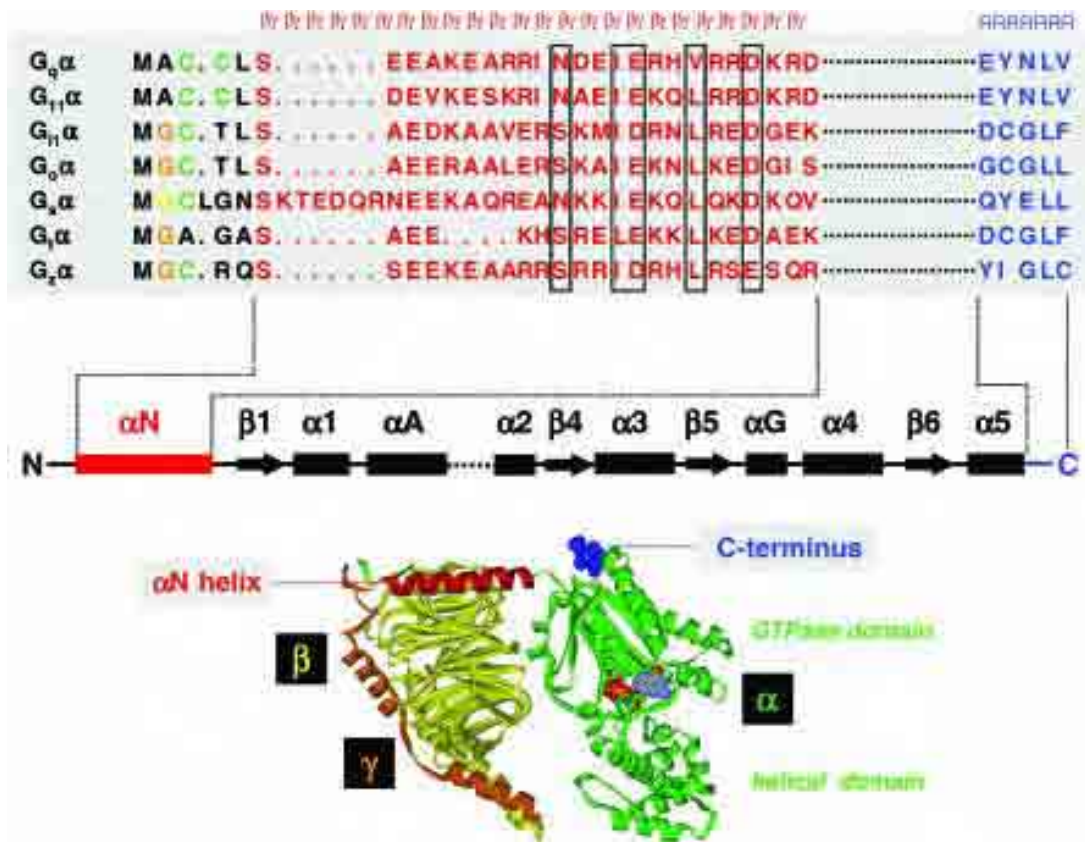


Figure 1.6 $G_{\beta/\gamma}$ and receptor contact sites on G_{α} .

Top: Sequence alignment of the N- and C- terminal regions of selected G_{α} -subunits. Residues that are subject to N-linked myristoylation, thio-palmitoylation or N-linked palmitoylation are highlighted in orange, green and yellow, respectively. Residues comprising the N-terminal αN helix are highlighted in red and residues at the extreme C-terminus of G_{α} are shown in blue. The αN helix is required for binding $G_{\beta/\gamma}$ -subunits, and $G_{\beta/\gamma}$ contacts are boxed in black, the extreme C-terminus plays a key role in specific receptor recognition. In the secondary structure diagram below the aligned sequences, $G_{\beta/\gamma}$ and receptor interaction sites are highlighted in red and blue, respectively. Only selected domains of G_{α} are shown, and for simplicity the domains between αA and the $\alpha 2$ helix have been omitted as indicated by the dotted line. Bottom: Illustration of the N-terminal αN helix (red) and the C-terminal receptor contact region (blue) in the context of the tertiary and quaternary structure of the resting state, inactive $G_{i1}\alpha\beta_1\gamma_2$ heterotrimer. The GDP molecule is buried between the GTPase and helical domain of G_{α} (green), the β -subunit (yellow) and the γ -subunit is shown in orange.

Taken from Milligan and Costenis, 2006 [165]

There are several regulators of G-proteins that have been identified. Phosducin, originally isolated from bovine brain, is a protein kinase A which inhibits the GTPase activity of G_{α} [166, 167]. GEF is a positive regulator that promotes G_{α} binding to GTP, and is activated by $G_{\alpha 12/13}$. There is a family of regulators of G-protein signalling (RGSs). RGSs accelerate the hydrolysis of GTP by G_{α} ; thereby acting as positive regulators by increasing the turn-over of G-protein activation in a short time-period. RGSs can also act as negative regulators by the same means of accelerating the hydrolysis of GTP when competing GTP- G_{α} binding with the effectors. The property whereby RGSs can act as both positive and negative regulators in a concentration-dependent manner has been demonstrated experimentally *in vivo* and *in silico* by Smith *et al.* [168]. Certain RGSs have been shown to interact with the C-terminal regions of the receptors. RGS2 and RGS5 were also shown to bind to the C-terminal tail of OTR [169].

A domain homologous to RGS is found in the N-terminal region of G protein-receptor kinases (GRKs) [170], which phosphorylate the agonist-bound GPCRs and recruit arrestins to initiate receptor internalisation [171]. The activity of GRK2 and GRK3 was shown to be positively regulated by free $G_{\beta\gamma}$ subunits [172, 173]. GRK2 was shown also to be able to bind to GTP- $G_{\alpha q}$, and inhibit activation of PLC_{β} via the RGS domain [174]. Moreover, GRKs and RGSs may compete for binding to the active receptors: RGS14 was shown to prevent GRKs from phosphorylating the morphine-bound μ OR [175]. Cells are thought to utilise different RGSs and GRKs as either positive or negative regulators to adjust the signalling to appropriate level.

1.2.4. Oligomerisation of GPCRs

GPCRs in living cells have been demonstrated by fluorescence resonance energy transfer method (FRET) to pre-couple to specific G-proteins [176]. Leucotrien B4 receptor has been shown to exist within the cell-membrane as pentamer, comprising GPCR homodimer and a trimeric G-protein at resting state [177]. Homodimerisation appears to occur in many Family A members [178-181] and Family C members [182]. Formation of heterodimers by related receptor subtypes were also demonstrated in Family A members [183, 184] and Family C members [185]. Heterodimerisation is not limited within closely related subtypes and some distantly related receptors are also capable of forming heterodimers [186-188]. Heterodimers of GPCRs belonging to different families have also been reported [189, 190].

The dimerisation of GPCRs occurs in the endoplasmic reticulum (ER) and also in the Golgi apparatus during protein synthesis and maturation [191, 192], and the process might be necessary for efficient protein folding preventing aggregation. Dimerisation of GPCRs may involve several domains, with slight variations among different receptors. The extracellular domains, TMs [193, 194] and the C-terminal domain were all shown to participate in formation of GPCR dimers by several studies [178-180, 195-198]. Family C member mGluRs form disulfide-linked homodimers [182]. Dimerisation is a necessity for the mGluRs to be functional [195, 196].

Dimerisation appears to have effects on the functionality also of certain Family A GPCRs. The studies of cross-linking at the TM4 of D₂ dopamine receptor revealed that agonist binding accelerates homodimerisation, in contrast to inverse agonist decelerating it [199]. Diminished signalling by D₃ dopamine receptor was observed by heterodimerising with

adenosine 2A receptor ($A_{2A}R$) [200]. Enhancement of signalling by avian CRFR1 by heterodimerisation with arginine vasotocin receptor has also been documented [190].

Many Family B members also form oligomers with a group of single α -helical transmembrane proteins known as receptor activity modifying proteins (RAMPs). RAMPs are known to alter pharmacological properties of calcitonin receptor-like receptor (CRLR) by direct association [201, 202].

The abundance of evidence proving GPCRs exist as dimers or oligomers might make one wonder whether monomeric GPCRs actually exist. Bioluminescence resonance energy transfer (BRET) study with a realistic optimisation has shown that some Family A GPCRs, including the members previously shown to form dimers in over-expressed systems, can exist as monomers at a moderate level of expression while Family C GABA_BR heterodimers were detected readily [203].

Some GPCRs, including β_2AR , V_2R , parathyroid hormone receptor and angiotensin receptor, have been shown to activate intracellular signalling cascades independent of G-proteins [204-207]. GPCRs may form complexes with other signalling proteins either directly or via scaffolding proteins. These scaffolding proteins can include a-kinase anchoring protein (AKA)79/150, Homer [208], spinophilin, adaptor proteins containing PDZ domain or SH3 domain [209-212]. These interactions are to facilitate signalling cascade while allowing cross-talk between independent signalling events to occur.

1.2.5. Cellular regulations of GPCRs

Within the cells there are various components which regulate the functionality of GPCRs in response to any stimulus. GPCRs can be regulated at the molecular level to adjust the signalling properties of the receptor, and also by adjusting the population of the receptor.

Shortly after agonist induced activation, GPCRs attenuate strength of signals and become less responsive in the phenomena known as desensitisation. Upon activation, GPCRs become phosphorylated at the intracellular loop domains (ICLs) and at the C-terminal domain by kinases such as PKA, PKC and GRK. The phosphorylation reduces the receptor signalling by causing uncoupling of the G-protein from the receptor [213-215]. The phosphorylated GPCRs are internalised into the intracellular membrane compartment by interacting proteins such as β -arrestin [216], clathrins [217], or dynamin [218]. Figure 1.7 describes the receptor internalisation initiated by the β -arrestin association. The receptors internalised by endocytosis can be degraded within lysosomes, or by proteases following ubiquitination. Prolonged and excess signalling cascades may result in down-regulation of the receptors at the level of gene expression and protein synthesis, as well as by degrading existing receptors [219-222]. GPCRs can be internalised in the absence of agonist binding by interaction with β -arrestin. β -arrestin acts as an adaptor between GPCRs and clathrin-coated pits, thereby impairing the G-protein association with the receptor [223, 224]. Agonist-independent internalisation of AT_{1A}R and cholecystokinin receptor A has been documented [225-227].

Cells can maintain minimal levels of the receptors, and the de-sensitised cells can be re-sensitised within a short-period of minutes. In the endosomes containing phosphatases, the receptors are de-phosphorylated to be recycled back to the cell-surface.

GPCRs can also be up-regulated in response to inverse agonist, which prevents agonist-independent activity of the receptor. Many Family A GPCRs are known to have constitutive activity in the absence of agonist stimulation. Inverse agonists have been used as therapeutic agents in order to reduce the constitutive activity of the receptors. However, the uses have been associated with development of tolerance to chronic treatments. The phenomenon has been studied on histamine H₂ receptor (H₂R). Inverse agonists of H₂R, cimetidine and ranitidine both increased receptor density, while no significant increase was associated with the competitive antagonist burimamide [228]. The finding provided an explanation for the tolerance observed in treating ulcers using H₂R specific drugs [229, 230].

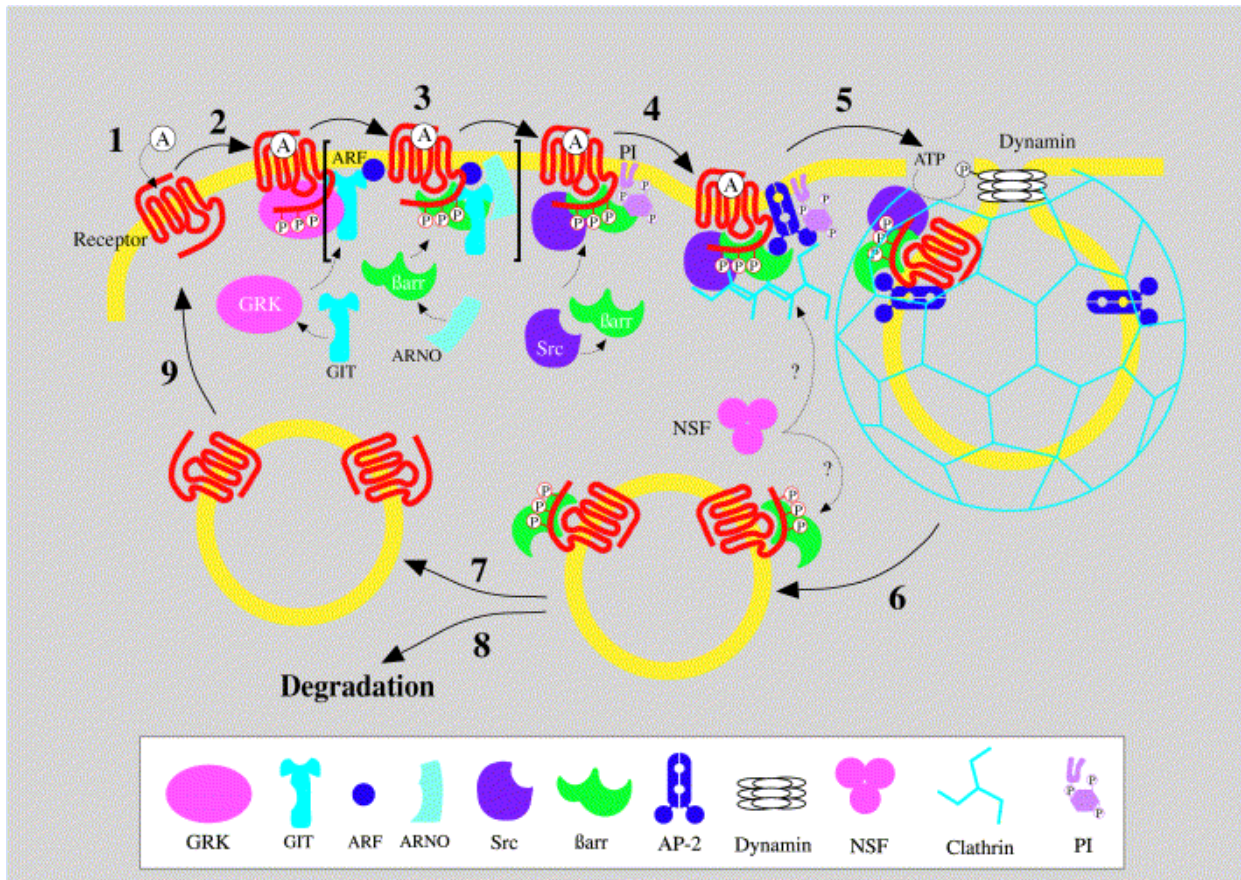


Figure 1.7 Model depicting the steps leading to endocytosis of G protein-coupled receptors: Agonist binds to receptors leading to the activation of G proteins and effectors (step 1). GRKs are recruited to the activated receptor to initiate the desensitization and internalization process. GRKs phosphorylate Ser and Thr residues on the intracellular domains of the receptors to create high affinity binding sites for β -arrestins (Barr) (step 2). Once β -arrestins are translocated from the cytosol to the activated receptors, this protein can act as an adaptor molecule and interact with many other proteins (step 3). β -arrestin interact with AP2 and clathrin to regulate formation of clathrin-coated pits and vesicle. β -arrestin and GRKs both interact with membrane lipids, as GRKs are found in complex with GRK-interactor (GIT), β -arrestin, GTP-binding protein ARF, nucleotide binding site opener ARNO (step 3). The exact events regulated by these interactions remain to be elucidated. β -arrestin can also bind to Src, which regulate the phosphorylation of dynamin (step 4). The participation of ATPase NSF in the receptor endocytosis remains to be confirmed. Once the clathrin-coated vesicles are formed, dynamin and possibly other associated proteins regulate fission of the vesicles, which are then processed to intracellular compartments to allow dephosphorylation of the receptors (step 6), recycling (steps 7 and 9) or degradation (step 8).

Taken from Claing *et al*, 2002 [231]

1.2.6. Receptor theory and pharmacological models for GPCR function

The initial theory governing receptor-ligand interaction emerged as Hill and Langmuir discovered the equilibrium binding equation [232, 233]. Clark then published his theory of receptor and ligand association based on the law of mass action in 1930s [234]. Around the same time, Gaddum carefully quantified competition binding between two ligands at a receptor site, and derived an equation for obtaining receptor occupancy (ρA), shown below:

$$\rho A = \frac{[A]}{K_A} \left(\frac{[A]}{K_A} + (1 + \frac{[B]}{K_b}) \right)^{-1} \quad \text{Equation 1}$$

Where A is tracer ligand, B is competitive antagonist, and K_A and K_b are the dissociation constants of tracer ligand and competitive antagonist.

The concept of efficacy was raised by Stephenson as partial agonism was identified with recognition that response is not necessarily proportional to occupancy [235]. In order to describe the receptor activation, the two-state model in which the receptors were described to be either in an inactive state (R) or in an active state (R*), was initially proposed by Del Castillo and Katz based on the study of ion channels [236] (figure 1.9a). With the realisation that R* can exist in the absence of ligand, the reversible two-state model was later proposed to include a ligand-free conformational equilibrium between R and R* (K^*) (figure 1.9b). Ligands which selectively bind to R* are agonists. The more selective the agonist is for R*, the greater the efficacy associated with the agonist. Ligands which bind indiscriminately both R and R* do not shift K^* , and thus behave as competitive antagonists; -also known as neutral antagonists. Competitive or neutral antagonists have no effect on the signalling properties of the receptors. Subsequently, many GPCRs have been described that have basal activity in the absence of agonist. Such constitutive activity of GPCRs led to discovery of inverse agonists which have negative efficacy, influencing K^* to favour R. Figure 1.8 illustrates the effect of agonists,

partial agonists, inverse agonists and antagonists on GPCRs. The two-state model of ligands selectively binding to pre-existing conformations is favourable energetically compared to an alternative idea of the conformational induction, in which ligand creates the conformation through the binding process to a receptor of a single conformation [237, 238]. In reality, ligands are thought to select initially certain receptor conformations to be able to bind, and may induce a slight conformational change for a better fit momentarily while binding.

In order to adapt the two-state model for GPCRs, the model was further elaborated to include G-protein binding to the receptor, and consequentially allosteric transitions or isomerisation of the receptor conformation. The agonist binding and G-protein coupling appears to cooperate positively [239]. The derived model is known as ternary complex model. De Lean *et al.* first applied this model to describe ligand binding to β -adrenergic receptor (β AR) and its G-protein activation [240]. The extended ternary complex model was proposed to describe constitutive activities of GPCRs [241] (figure 1.9c). The model has an isomerisation constant (L) which gives the amount of R^* available for G-protein coupling. By increasing the relative stoichiometry of receptor to G-protein, the elevated R^* G-protein complex was obtained in the model. However, the model remained thermodynamically incomplete. The ternary complex model was further revised to include pre-coupling of G-protein to GPCR. The model was named cubic ternary complex receptor occupancy model by Weiss *et al.* [242] (figure 1.9d) and it was thermodynamically complete. The model includes four cooperativity factors designated with Greek alphabets: i) activation cooperativity of ligand (α); ii) activation cooperativity of G-protein (β); iii) binding cooperativity between ligand and G-protein (γ) and iv) activation cooperativity between ligand and G-protein (δ).

Ternary complex models described above are limited in that these do not fully describe functionality of certain GPCRs with tendencies of coupling with more than one particular type of G-protein. The three-state model was proposed by Leff *et al.* for such GPCRs which couple to two types of G-proteins [243]. The model contains two active states (R^* and R^{**}) each of which couples to specific G-protein. Both R^* and R^{**} competes with one another in parallel, and the preference of ligands by the receptor determines which active state to dominate. An alternative, 'the multi-state model' was suggested by Schwartz allowing a receptor to alternate between several active and inactive conformations [244]. The probabilistic model or 'stimulus trafficking' was another alternative proposed by Kenakin with a theoretical assumption that a receptor can exist in a limitless number of possible conformations inducible by different ligands which can either enhance or deplete depending on the efficacy associated with the ligand [245].

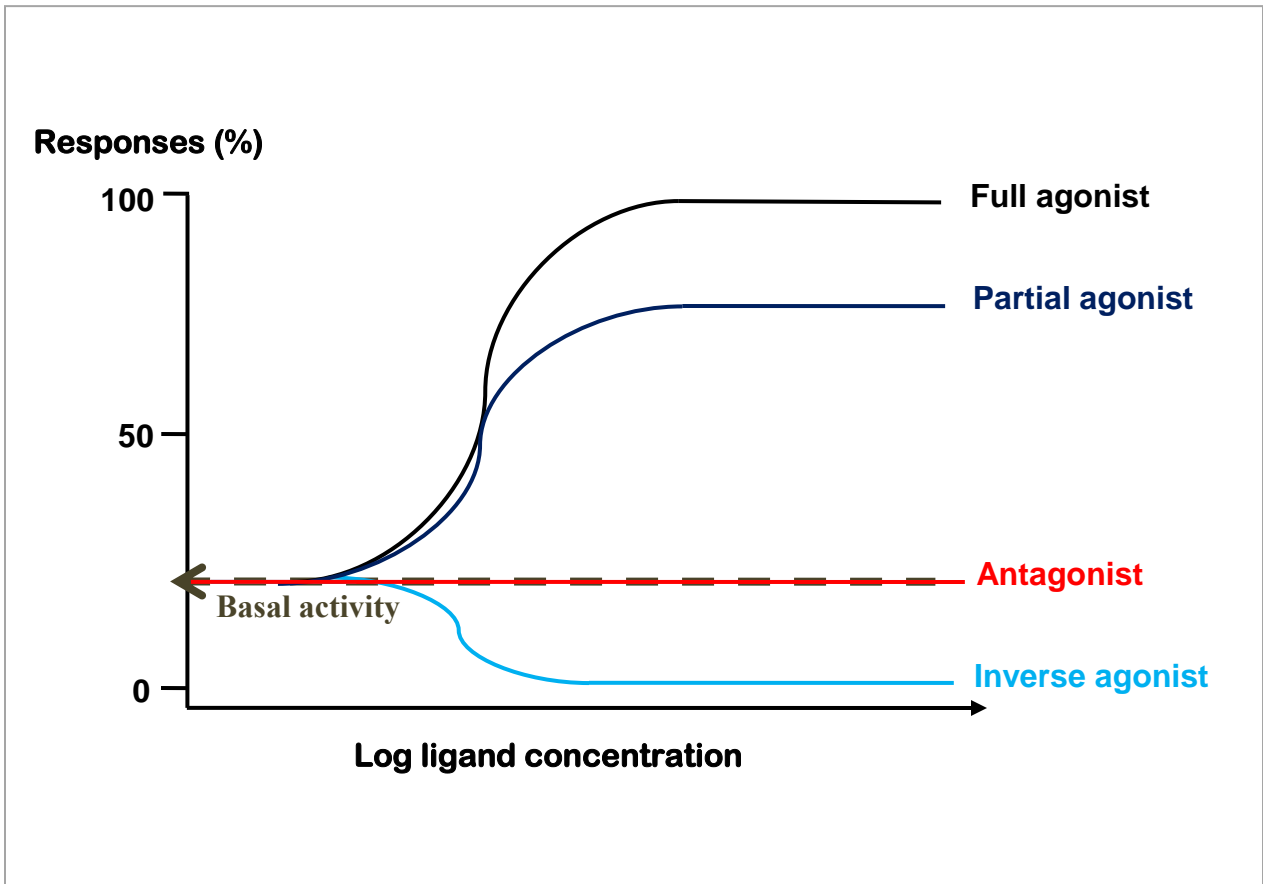


Figure 1.8. Classification of ligand efficacy for GPCRs:

Many GPCRs exhibit certain levels of basal activity in the absence of agonist. Inverse agonists inhibit this agonist-independent activity of the receptors (the line in turquoise), while antagonists do not affect the activity (in yellow). Full agonists produce maximal biological responses capable of the system (in black). Partial agonists do not elicit such large responses at high concentrations, as can another agonist in a given system under specified conditions. The designation of full versus partial agonist is system dependent, and a full agonist for one tissue may be a partial agonist in another [246].

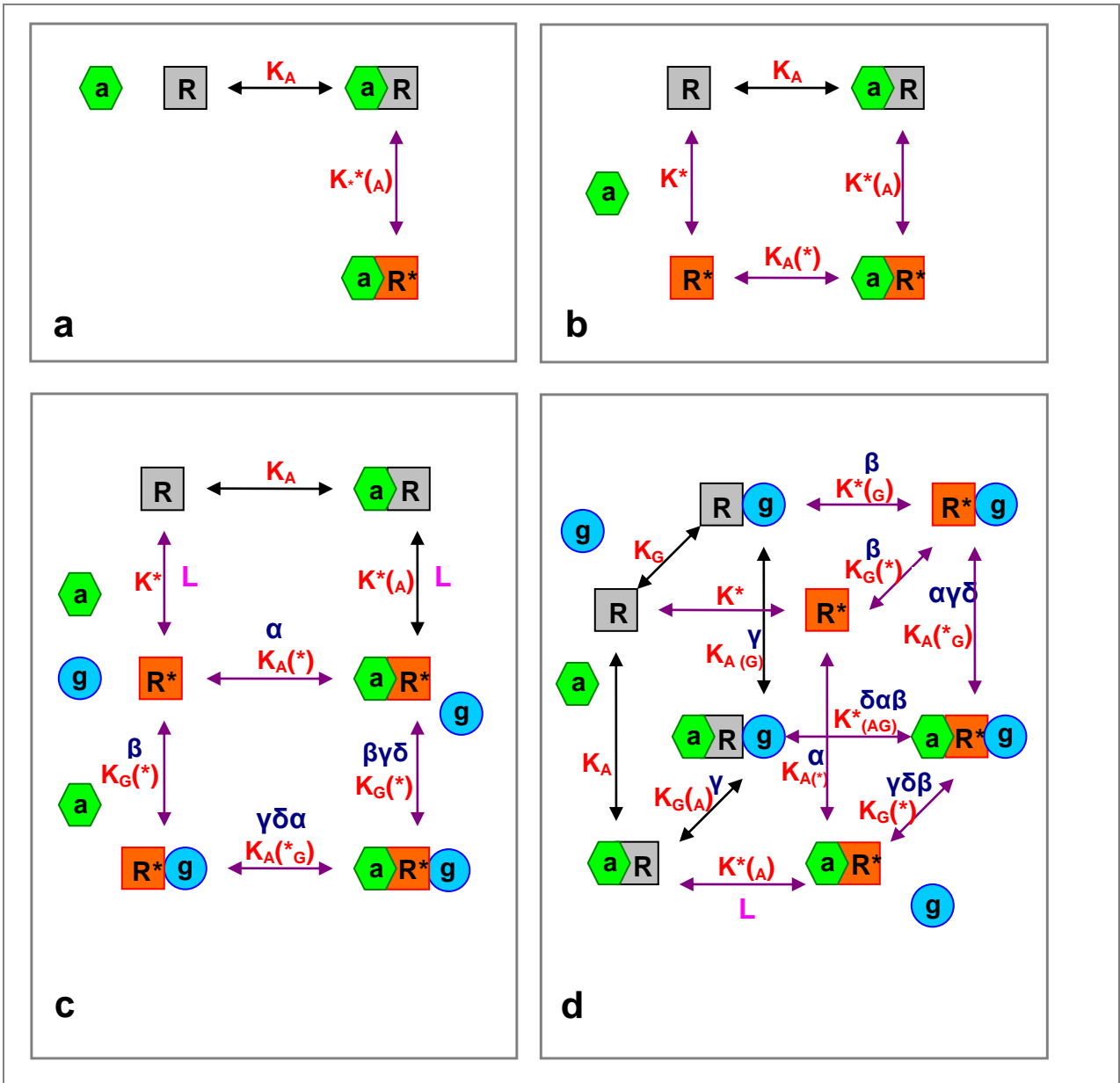


Figure 1.9 a-d Models of receptor activation:

(a) Basic two-state model, (b) Reversible two-state model, (c) Extended ternary complex model, and (d) Cubic ternary complex model. In the presence of agonist (a), receptors can go through several conformational states at inactive (R) and at active (R*) states governed by ligand-independent conformational equilibrium between R and R* (K^*), equilibrium dissociation constants of agonist (K_A) and of G-protein (K_G). Ternary complex models contain G-protein (g) to show transitional processes influenced by cooperativity factors $\alpha, \beta, \gamma, \delta$ and isomerisation constant (L) (see text).

1.2.7. Allosteric Modulators in GPCR pharmacology

Allosteric modulators of GPCRs are compounds that bind to alternative sites of the receptor opposed to the orthodox ligand binding site. In this context, the ligands which bind to the latter site are called orthosteric ligands. As these occupy different sites, allosteric and orthosteric ligands can co-occupy the same receptor, and allosteric ligands can either be negatively or positively cooperative to the orthosteric ligand. Allosteric modulators were discovered on observations that certain antagonists can show different affinities to the same receptor under different experimental conditions. Such studies on adrenergic receptors are relatively well documented [247-250]. CGP12177 is a competitive antagonist at orthosteric site of β_1 AR; however, it activates receptor at a high concentration in a non-counteractive way by other classical β_1 AR antagonists [251-253]. CGP12177, and also two other ligands, LY362884 and carvedilol, have all been identified to bind allosteric sites of the receptors as positive allosteric modulators [252-255].

Negative allosteric modulators and competitive antagonists both exhibit inhibitory action to receptor activation. However, both are clearly distinguishable by saturation assay. A Schild plot of competitive antagonism gives a straight linear line with slope 1, while that of negative allosteric modulators are curvilinear [248]. The Schild plot is a graph of \log_{10} (concentration-ratio (r) minus one) plotted against \log_{10} antagonist concentration; the graph yields a straight line of unit slope for competitive antagonism which obeys the Schild equation below:

$$r - 1 = [B] \cdot K_B^{-1} \qquad \text{Equation 2}$$

Where r is the ratio of the agonist concentration which produces 50% response in the presence of antagonist to the agonist concentration produces the same response in the absence of antagonist; B is the concentration of a reversible competitive antagonist; and K_B is the equilibrium dissociation constant for the B with the receptor [256].

The two antagonisms can be distinguished by competition assay, because maximal displacement of orthosteric ligands by allosteric modulators is limited regardless of concentrations used, as the binding process is restricted by cooperativity factor α . On the other hand, competitive antagonists can displace the bound ligands down to non-specific binding level when sufficient concentration is used.

1.2.8. Cellular influence on GPCR pharmacology

Some GPCRs such as adrenergic receptors and muscarinic acetylcholine receptors (mAChRs) were shown to have different pharmacological profiles depending on the cellular environment. The experimental evidence and observations on this subject are extensively reviewed by Nelson and Challiss [257], and Baker and Hills [258]. Several plausible mechanisms at different levels of the cellular events have been discussed.

Firstly, receptors can be processed differently depending on the cell-types at the level of post-transcriptional modifications. RNA editing at up to five distinct sites of the 5-hydroxytryptamine 2c receptor (5-HT_{2c}R) have been demonstrated to influence constitutive activity and efficacy [259]. Alternative splicing product of mu-opioid receptor (μ OR) showed less sensitivity to opioid peptide and more selectivity to opiate alkaloid [260]. On the other hand, four alternative splice variants of α ARs remained to show functional consistency among them [247]. Alternative splicing affecting functionality of GPCRs is rare, since over 90% of GPCRs do not contain introns within the open reading frames and therefore do not undergo alternative splicing [261].

Another possible factor is phosphorylation. As cell types may vary in expression of kinases, differential phosphorylation of GPCRs might also contribute to pharmacological

profiles dependent on cell-types. Phosphorylation of β_2 AR has been shown to alter its affinity for antagonists [262].

Heterodimerisation can also contribute unique pharmacology associated with some GPCRs. For instance, 6'-guanidinonaltrindole causes analgesia by selectively activating heterodimers of κ/δ opioid receptors but not homodimers of either subtype [263]. Alteration of agonist selectivity of CRLR by RAMPs has been well documented [264]. RAMP3 has also been shown to have an effect on the affinity of antagonists for CRLR [265]. The cell-specific expressions of GPCRs, which can potentially heterodimerise, and/or accessory proteins such as RAMPs are therefore thought to contribute to the cell-type dependent pharmacology profile.

Since cell-types may vary in G-protein content and certain GPCRs have been shown to couple to more than one G-protein subtype, differential G-protein coupling might also have effect on GPCR pharmacology. The influence of G-protein coupling on agonist efficacy has been reported. The study of 5-HT_{2C}R in Chinese hamster ovary (CHO) cell-line showed that agonists can activate multiple signalling pathways via two different G-proteins with a different rank order [266]. Affinities of antagonist for the adenosine A₁ receptor (A₁R), which couples to both G_{ai} and G_{as} in CHO cells [163, 267], were not affected by the level of the relevant gene expressions [268]. Chini and Manning have shown that the synthetic peptide ligand Atosiban is an agonist at OTR by promoting G_{ai} coupling, while it acts as a competitive antagonist of the G_{aq} coupling to the same receptor [269].

Signalling properties of a GPCR can also influence the pharmacology. Propranolol has been reported to be an inverse agonist at β_2 AR preventing cAMP accumulation in CHO or human embryonic kidney (HEK) cell-lines [270]. However, it can also be a partial agonist at the same receptor for initiating extracellular signal regulated kinase (ERK) 1/2 activation [271].

Since β_2 AR has also been reported to be capable of signalling independently of G-protein via interacting with β -arrestin [205], such actions of propranolol indicate the ligand discrimination between different GPCR signalling complexes.

A final point is on the composition of plasma membranes, which may vary in the proportion of lipid rafts and caveolae, depending on cell types. Caveolae are indentations of the plasma membrane with lipid composition similar to lipid rafts, but these are associated with caveolin which appears to have versatile roles including inhibition of signalling enzymes such as AC [272], kinases [273-276] and phosphatases [277, 278]. A role of caveolin as a molecular chaperone in GPCR trafficking to the cell surface has also been reported [279, 280]. Caveolae tend to be rich in signalling molecules, and the expression of the signalling molecules in caveolae can vary in a tissue-specific manner [281] and some proteins such as AC localise to these lipid-rich area in a cell-dependent manner [282]. The compartmentalisation of GPCR may also be cell-specific. β_2 AR was found to be enriched in the lipid rafts of cardiac myocytes, but not in the vascular smooth muscle cells [282]. GPCRs may differ in their pharmacology within or outside the lipid rafts or caveolae. Signalling properties may be affected in the protein-rich caveolae. Moreover, the ligand affinity of some GPCRs can be modified by cholesterol [283]. The localisation of OTR in lipid rafts was shown to correlate positively with an increased agonist affinity for the receptor [284].

1.3. Family A GPCRs

1.3.1. Structure of Family A GPCRs

GPCRs have seven alpha-helical transmembrane domains (TM1~ TM7) with connecting extracellular loops (ECL1-3) and intracellular loops (ICL1-3). In Family A GPCRs, the upper TM3 and ECL2 are covalently bonded by a disulfide bond formed between cysteine residues. In addition to the 7TMs, a short helix designated as helix 8 (H8) is present immediately after TM7, perpendicular to it and parallel to the membrane (figure 1.10). The receptor forms a barrel-like shape as seven transmembrane alpha-helices associate with one another within the lipid bilayer.

Family A members have highly conserved residues within TMs, each of which possesses at least one strictly conserved residue. Using the most conserved residues as guidance points, Ballesteros and Weinstein proposed a numbering scheme for TM residues in order to facilitate structural comparisons between different receptors studied [285]. In the numbering scheme, each residue is presented as $n^{\text{TM}}.50$, in which n^{TM} refers to the number of TM domain, and 50 represents the most conserved residue in the TM domain. This thesis employs this numbering scheme when discussing individual residues in or nearby TMs.

The three dimensional structure of bovine rhodopsin (bRho) to 2.8 angstrom (\AA) resolutions was obtained by X-ray crystallography in 2000 by Palczewski *et al.* [286]. The crystal structure and a schematic representation of Family A GPCR are shown in figure 1.10 and 1.11 below. Another crystal structure of bRho containing internal water molecules at 2.6 \AA resolution was obtained several years later [287]. The crystal structures of meta-rhodopsin I has also become available to provide a GPCR structure at an alternative functional state [288]. In addition, an engineered human $\beta_2\text{AR}$ structure with a bound inverse agonist has been obtained at 3.8 \AA

resolution stabilised with fab fragment of antibody [289, 290]. The structure of chimeric human β_2 AR fused to T4-lysozyme at 2.4 Å was also obtained with an associated inverse agonist [291]. A chimeric human adenosine A_{2A} receptor fused to T4 lysozyme was also crystallised with a bound inverse agonist at 2.6 Å with a high salt concentration [292]. The structure of avian β_1 AR, engineered to increase thermal stability, has also been determined in the presence of an antagonist [293].

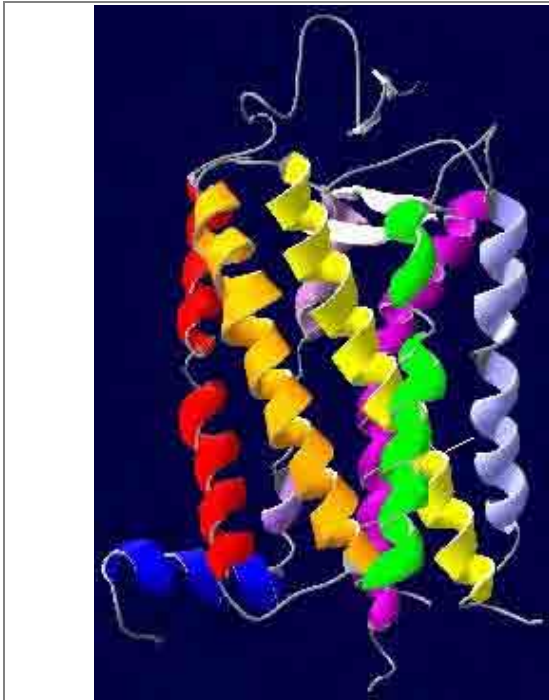


Figure 1.10
The tertiary structure of bovine rhodopsin obtained by X-ray crystallography at 2.8 Å resolutions:

Anticlockwise from: TM1 (red), TM2 (Orange), TM3 (yellow), TM4 (green), TM5 (pale blue), TM6 (purple), TM7 (lilac) and helix 8 (blue). ICL2, ICL3 and the C-terminal region are not shown.

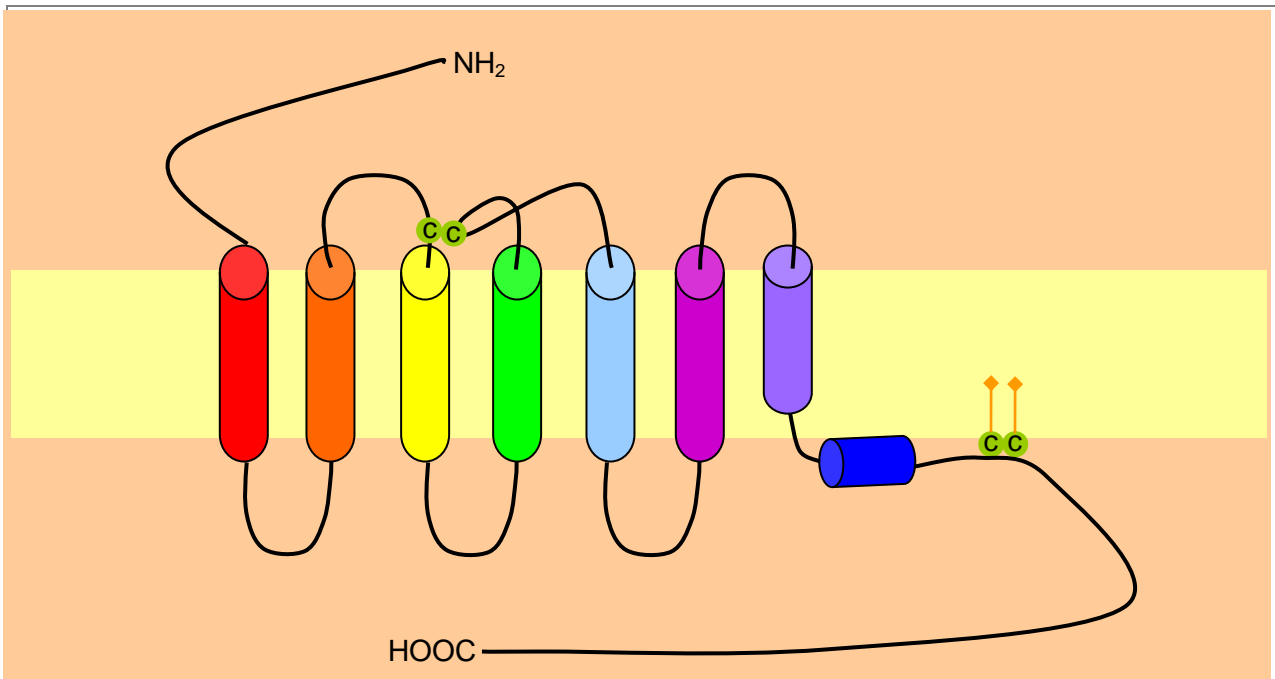


Figure 1.11 **The schematic representation of a rhodopsin-like, Family A GPCR:**
 GPCRs have the extracellular N-terminal domain and the intracellular C-terminal domain with seven transmembrane domains each of which are joint by intracellular or extracellular loops in a single polypeptide. Family A GPCRs have a disulfide bridge linking the upper TM3 and ECL2. Cys residues in the C-terminal preceding H8 (blue) are often palmitoylated.

Since most GPCRs naturally express at low levels, crystallisation of native GPCRs without extensive modifications has so far been successful only for rhodopsin, which expresses at high density and also contains a covalently bonded inverse agonist 11-*cis*-retinal stabilising the structure. Lately, the structure of opsin crystals, formed at a low pH, in which the active conformation resembling metarhodopsin II was stabilised was obtained as a ligand-free opsin [294], and also as a complex with transducin derived peptide [295].

Combined with other experimental studies of engineered GPCRs, the crystal structures revealed characteristic features which might be shared amongst the Family A members, as well as emphasising differences between the receptors studied. As seen in the secondary structure comparison, relative similarities were seen in TM domains. When the structures of bRho and human β_2 AR obtained were superimposed, the similarities in the TM regions were shown with relatively small root mean square deviation (RMSD) of 1.56Å [290].

Crystal structures revealed that some TM domains have bends and kinks. Such intrahelical kinks can be produced at the imino acid residue proline, and also glycine which can produce negative phi torsion angles at the peptide backbone. Dipole properties in serine, threonine and cysteine residues can also introduce significant bending or twisting as hydrogen bonds can be formed between the hydroxide or sulfhydryde moieties of these residues and the carbonyl of the peptide backbone [286, 296]. Each of TM5, 6 and 7 has a conserved proline residue, and this conservation of proline-inducible flexibility is consistent with the functional importance of the three TMs. Between TM7 and H8, there is a NPXXY motif that is highly conserved [297]. The proline residue in the motif allows the amphipathic H8 to bend almost perpendicular relative to TM7 by glycine residue joining TM7 and H8. In both GPCR Family A and B, proline residue in TM6 are essential [298], and the same applies to Family D yeast pheromone receptors [299]. A proline residue has been identified to be important also in loop

regions, and a conserved Pro-Leu motif in the middle of ICL2 is often seen in GPCRs. The mimetic peptide studies using a synthetic ICL2 of V_{1a}R showed that the motif allows the peptide to adapt to different conformations [300].

The association between helices in the lipid bilayer was shown to be important for folding of GPCRs. When the TM-TM interactions of human adenosine A_{2A} receptor were investigated in a synthetic environment using circular dichroism spectroscopy and Föster resonance energy transfer, some TM domains were shown to require neighbouring helices for proper folding to be achieved [301]. The studies by the same group showed that compact and weakly polar residues are important in helix packing [299]. Similar interactions to dipoles occur between cation and conjugated π electrons of aromatic rings. The interactions are, however, regarded as somewhat more complicated since the forces occurring can be either repulsive or attractive due to the nature of π electrons [302]. Notable forces appear to be the cation- π interaction occurring between amphipathic Lys and aromatic residues. Such forces are likely to contribute to the effective packing of TM domains as the interaction energy involved has been proposed to be twice that of the van der Waals interactions [303-305].

Four crystal structures of inverse agonist carazolol-bound β_2 AR, antagonist cyanopindolol-bound β_1 AR, antagonist ZM241835-bound A_{2A}R and rhodopsin were compared and studied by Rosenbaum *et al.* [306]. When the four structures were examined, particularly prominent structural differences are visible in the ECL regions (figure 1.12). In rhodopsin, a part of ECL2 adopts a short β -hairpin structure. This structure, together with the N-terminal domain covers the interior of the receptor to prevent hydrolysis of Schiff base in 11-*cis*-retinal [307, 308]. In both β_1 AR and β_2 AR, ECL2 contains a short α -helix which is stabilised by the disulfide bond

while the N-terminal domain is disordered [289, 291, 293]. Another recognised difference was in ICL2. A short α -helix was seen in ICL2 of β_1 AR and A_{2A} R, but neither in the β_2 AR nor in rhodopsin [306].

Superimposition of the ligand binding sites of the four structures showed that binding sites of rhodopsin, β_1 AR and β_2 AR are partly overlapping. Polar and hydrophobic residues from TM3, TM5, TM6 and TM7 are involved in the ligand binding in rhodopsin and adrenergic receptors. However, the ligands bound to adrenergic receptors appeared to be located slightly above 11-*cis*-retinal. The ionone ring of retinal was seen making direct contact with Trp^{6.48} which has been associated with functional significance. The role of Trp^{6.48} is described in the Section 1.3.2. In contrast, ZM241835 binds A_{2A} R in a manner almost perpendicular to the plane of the cell membrane, extending along TM6 and TM7 from the ECL to Trp^{6.48} [292].

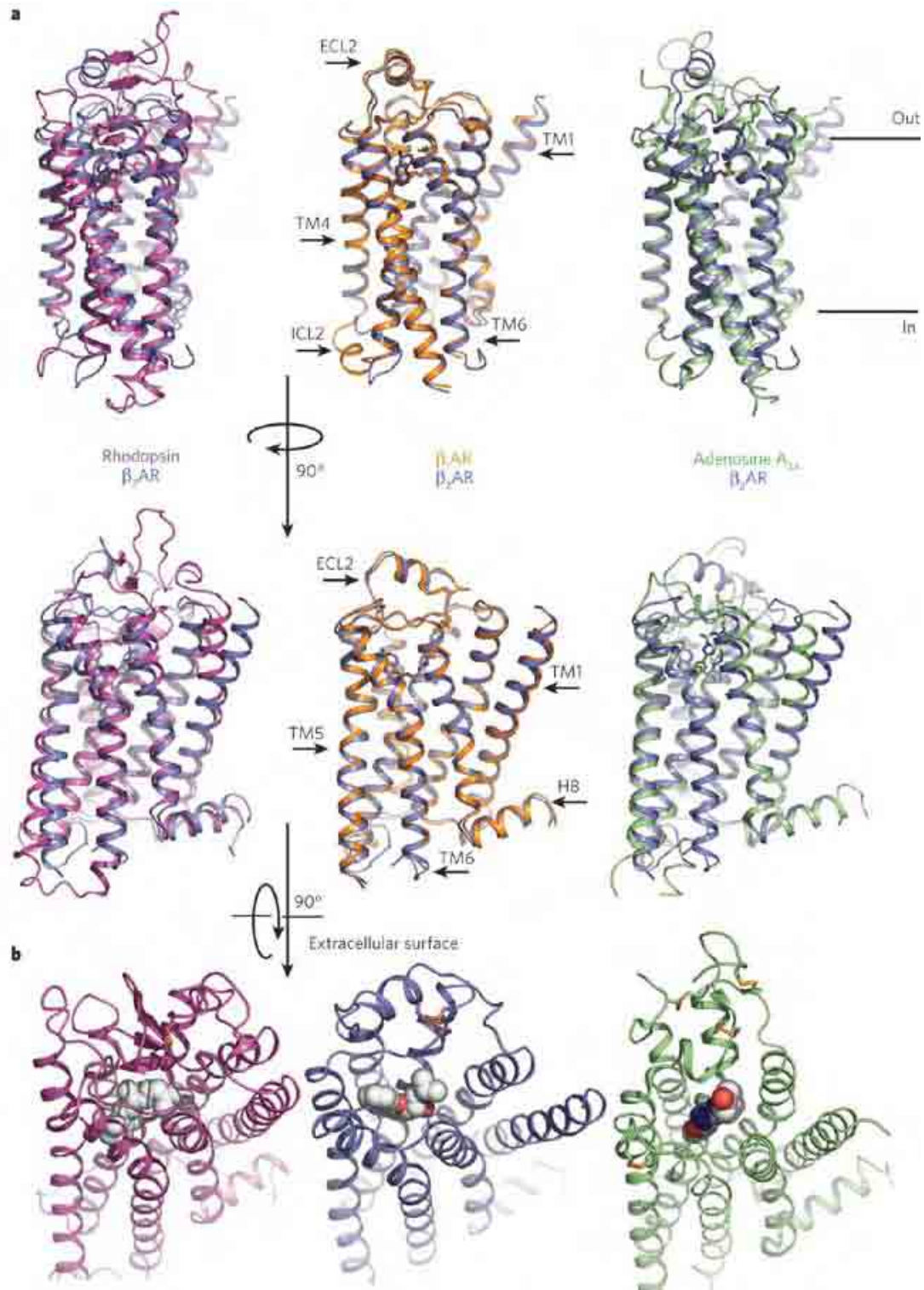


Figure 1.12 Crystal structures of GPCRs:

Bovine rhodopsin (purple), avian β_1 AR (orange) and human A_{2A} adenosine receptor (green) are each superimposed on the human β_2 AR structure (blue). **b**, Extracellular views of rhodopsin, the β_2 AR and the A_{2A} adenosine receptor. The ligands are shown as spheres.

Taken from Rosenbaum *et al.*, 2009 [306].

1.3.2. Functional motifs and molecular mechanisms of activation

There have been two motifs established to be crucial in the function of Family A GPCRs. Firstly, Arg^{3.50} and Asp/Glu^{3.49} of a conserved D(E)RY motif at the cytosolic end of TM3 have been shown to be important for G-protein activation [309, 310]. The two residues have been demonstrated to stabilise inactive conformation by a strong intra-helical salt bridge [311]. The D(E)RY motif stabilising inactive conformation is in a general term known as an ‘ionic lock’. The inactive state is enforced by additional interactions of Arg^{3.50} with Glu^{6.30} and Glu^{6.32} forming a hydrogen bonding network between TM3 and TM6 in catecholamine receptors, opsins and glycochormone receptors. The neutralising substitution of Asp^{3.49} or Glu^{6.30} in a catecholamine receptor results in constitutive activation and increased accessibility of water molecules to the TM domains [312]. Glu^{6.30} and Glu^{6.32} are however not strictly conserved in Family A GPCRs. In V_{1a}R, V_{1b}R and OTR, Lys^{6.30} and Arg^{6.32} are found. Since Lys^{6.30} can possibly interact with Tyr^{3.51} by cation- π interaction and Arg^{6.32} may interact with Asp^{3.49}, the mechanism in holding inactive state involving the regions of TM3 and TM6 may also be proposed in these receptors with slightly altered molecular interactions in details.

Another motif involved in activation of Family A GPCRs is present in TM6, a conserved CWXP motif, in which X can be any, but often relatively hydrophobic residues. Several studies have shown that Cys^{6.47} is pointing towards TM7 in the water accessible binding-site crevice [313-316]. Since Trp^{6.48} has been proposed to exist in two probable rotamer states depending on the freedom of rotational angles of the indole side chain of Trp^{6.48} (i.e. Chi-angle of -60° in inactive and 180° in active approximately) this residue has been suggested to act as a micro-switch to initiate the receptor activation upon ligand binding [244, 317]. Trp^{6.48} was predicted to be vertical at the interface between TM3 and TM6 in an inactive state by molecular model-

based studies, one of which also predicted Cys^{6.47} hydrogen bonding to a water molecule [318, 319]. The positioning of Trp^{6.48} relatively vertical to the TM was observed in crystal structures (figure 1.13). The conserved Pro^{6.50} causes TM6 to kink in the inactive state. The crystal structures of both inactive and ligand-free active receptors showed the vertical positioning of the indole of Trp^{6.48} (figure 1.13.a.ii). The alternative rotamer state may possibly be captured when a crystal structure of agonist-bound Family A GPCR is obtained. During the activation, TM6 and TM7 have been suggested to move vertically around Pro^{6.50}, inducing straightening of TM6. As a result, the cytoplasmic end of TM6 moves away from TM3 thereby unlocking ‘the ionic lock’ described above. This mechanism of GPCR activation is known as a global toggle switch model [244].

Comparisons between rhodopsin and opsin crystal structures revealed a few structural changes with insights in the activation mechanisms. Firstly, the ligand binding cavity becomes relatively wider in opsin. The opening appears to be induced by the displacement of the ionone ring of retinal by Trp^{6.48}. The movement of Trp^{6.48} causes the interaction between Lys^{7.43} and Glu^{3.28}, which is a counterion to the Schiff-base, to be broken, resulting in the slightly wider cavity [306]. At the cytosolic end, TM6 moved away from the helical bundle core, over 6Å relative to the inactive state, towards TM5. The space left after the TM6 migration was stabilised by newly adjusted conformation of Tyr^{7.53} of NPXXY motif. The active structure is also stabilised by new interactions formed between Glu^{6.30} and Lys^{5.66}, and between Arg^{3.50} and Tyr^{5.58} as Arg^{3.50} dissociates from Glu^{3.49}. Another interaction with Arg^{3.50} is also formed with the backbone of Gα peptide as a binding cavity for transducin forms between TM3, TM5 and TM6. A hydrogen bonding network is also formed between the transducin peptide and TM3, TM5 and H8 of opsin. The transducin derived C-terminal peptide adapted α-helical

conformation, as the amphipathic nature of hydrophobic interactions occurs in associating with the cytoplasmic ends of TM5 and TM6 in the co-crystallised structure [295].

In addition to the mechanisms described above, a mechanistic role of H8 has been suggested as a conformational switch for GPCRs between active and inactive forms. H8 region has been suggested to be destabilised during activation [320, 321] while the amphipathic helix enforces the receptor association with the membrane at resting state [322]. Located above H8 at the bottom of TM7, is a conserved NPXXY motif. The crystal structures of GPCRs showed the distortion of TM7 caused by Pro^{7.50} directing Tyr^{7.53} towards a water-containing cavity lined by TM2, TM3, TM6 and TM7. The network of water molecules facilitates distortion of TM7 as well as providing interacting partners to polar residues [291, 292, 307, 308]. This so-called ‘water pocket network’ appears to stabilise the inactive state. The interactions involving solvents provide a rapid toggle switch which can be altered easily as an agonist binds [307, 308, 323].

Biophysical studies on β_2 AR provided an insight into the allosteric modulation of GPCRs. A highly conserved, disulfide bonding Cys^{3.25} has been suggested to function as a molecular switch in an acid-base equilibrium, since the transition of the residue in the β_2 AR between the acid and base states alters TM-TM interactions. The differences in inter-helical interacting energy observed suggested that the interaction between TM3-TM6, TM3-TM4, TM6-TM7 and TM1-TM7 discriminate the agonist and antagonist binding [324].

The movement of TM domains in GPCRs have been studied by various groups. The movement of TM3 and TM6 in light-activated rhodopsin was recorded [325]. Two-dimensional dipolar-assisted rotational resonance NMR studies confirmed this TM interaction in rhodopsin and metarhodopsin II. The studies showed the motion of TM6 migrating away from TM3 during activation [326]. Solid-state magic angle spinning NMR studies by the same group

showed that strong hydrogen bond formed between Glu¹²² in TM3 and His²¹¹ in TM5 was disrupted in metarhodopsin II, implicating that alternative interactions become available for accessing TM3 upon activation [327]. The other TM-TM interaction which has been demonstrated to occur during activation is TM7 and TM1. Agonist induced rotational movement of the cytosolic side of TM7 towards TM1 was confirmed by disulfide cross-linking and modelling studies on M₃ acetylcholine receptor [328, 329].

The evidence for structurally important conformational changes involving TMs and ECL2 has been provided by a solid-phase NMR study. The network of hydrogen bonding occurs between ECL2 and the extracellular ends of TM4, TM5 and TM6 are disrupted in metarhodopsin II forming opsin [330]. The disruption results in formation of a wider cavity.

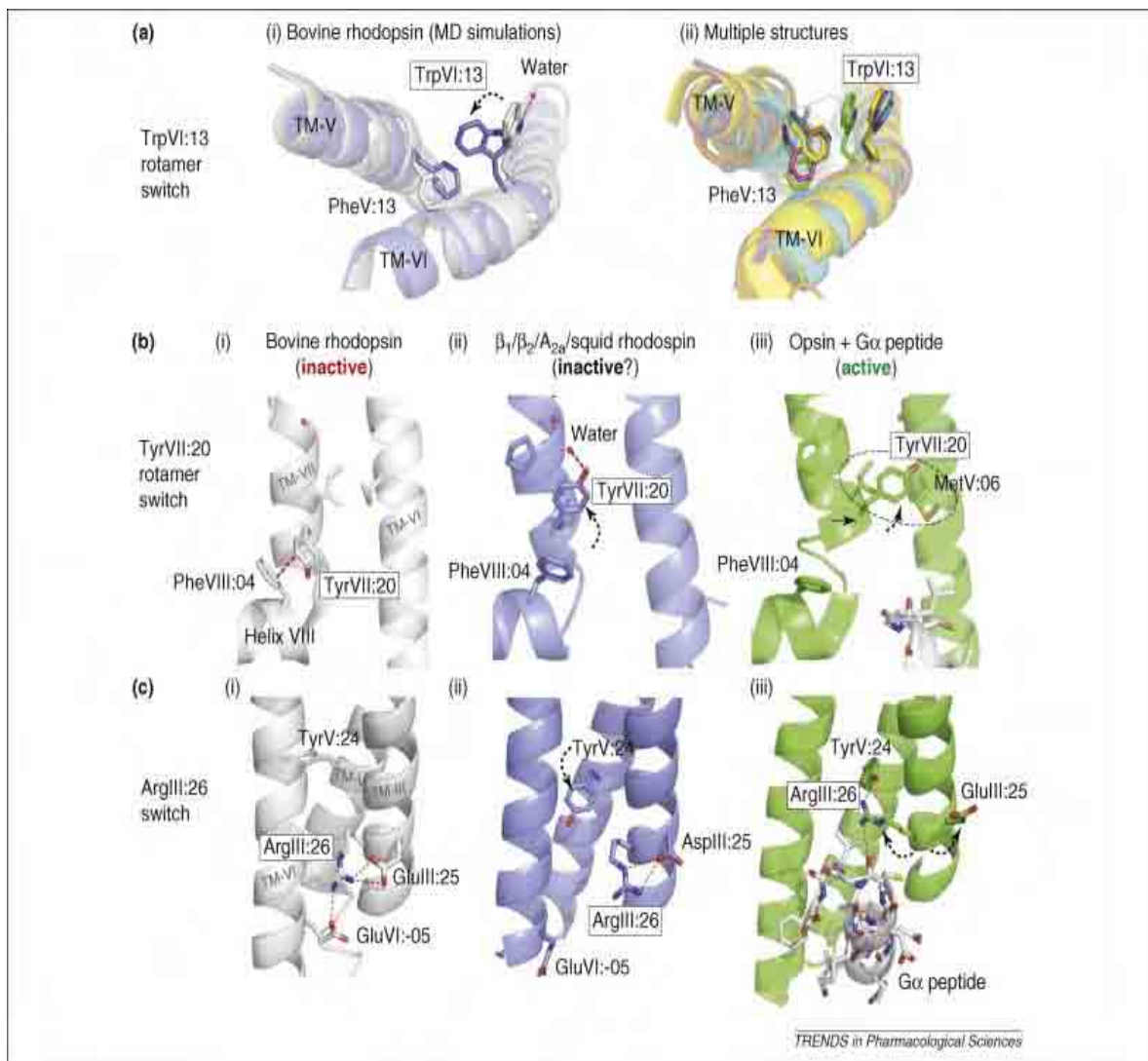


Figure 1.13 Proposed mechanical activation switches of Family A GPCRs:

The residues are indicated with Baldwin numbering scheme in which the central TM residues are counted as 13 following TM number in Roman numerals. **(a) (i)** Trp^{6.48} (TrpVI:13) shown after molecular dynamic simulations to interact with water molecules in the inactive state of bRho. Upon activation, the residue has been proposed to be attracted towards Phe^{5.47} (PheV:13) by van der Waal's forces. **(ii)** Overlay of 6 crystal structures showing Trp^{6.48}: bovine rhodopsin (purple), β_2 AR (dark blue), β_1 AR (Orange), A_{2A}R (light blue), squid opsin (yellow) and opsin (green). **(b)** Three states of Tyr^{7.53} (TyrVII:20) viewed from TM3 **(i)** interacting with PheVIII:04 in inactive bovine rhodopsin. **(ii)** Tyr^{7.53} rotated upward interaction with a water molecule in 'water pocket' in the intermediate state. **(iii)** Tyr^{7.53} rotated upwards engaging in hydrophobic interactions in a TM6 and TM7 interface (indicated as a dotted circle) in opsin. **(c)** The ionic lock in three states **(i)** Arg^{3.50} (ArgIII:26) interacts with Glu^{3.49} (GluIII:25) and Glu^{6.30} (GluVI:05) in the inactive state. **(ii)** Arg^{3.50} interacting only with Glu^{3.49} in the intermediate state. **(iii)** Arg^{3.50} interacts with Tyr^{5.58} (Tyr V:24) and also with the backbone of G α peptide in the active opsin.

Taken from Nygaard *et al.*, 2009 [331]

1.4. Vasopressin receptors

The three subtypes of vasopressin receptors are described in this section with a slight focus on $V_{1a}R$ and $V_{1b}R$. Closely related oxytocin receptor (OTR) is also briefly mentioned. The molecular cloning and expression of rat $V_{1a}R$ was first achieved in 1992 by Morel *et al.* [21]. Lolait *et al.* also cloned rat V_2R in the same year [332]. Subsequently, the cDNA of human $V_{1a}R$ was obtained by two groups in 1994 [22, 333]. In the same year, the cDNA of human $V_{1b}R$ was cloned and sequenced by Sugimoto *et al.* [42].

1.4.1. G-protein coupling

$V_{1a}R$ and $V_{1b}R$ both preferentially couple to G-protein with $G_{q/11}$ subunits, both of which activate phospholipase C_β (PLC_β) to produce $InsP_3$ and DAG as second messengers. $InsP_3$ releases Ca^{2+} from the ER to increase the intracellular Ca^{2+} concentration. DAG activates PKC to further initiate the cellular response (figure 1.5, section 1.2.3). OTR also prefers to couple to $G_{q/11}$. V_2R couples preferentially to G_s which activates AC to increase cyclic AMP production. $V_{1b}R$ is capable of activating multiple signalling pathways by also coupling to G_s , depending on the level of the receptor expression [334]. $V_{1a}R$ has been shown to couple to G_{i3} in fibroblast cell-line at G_0/G_1 phase of the cell cycle but not in the other phases [335].

1.4.2. Oligomerisation

Homo- and hetero-dimerisation of $V_{1a}R$, V_2R and OTR have been demonstrated experimentally by Terrillon *et al.* in 2003 using co-immunoprecipitation and BRET. All subtypes can form either homo- or hetero-dimers when co-expressed, in both fully glycosylated and immature

forms in the ER. Neither agonist- nor antagonist-treatment appeared to have affected dimerisation as measured by BRET measurement [191].

V_{1a}R and V₂R can both be internalised by associating with β -arrestin. Following the internalisation, V_{1a}R is rapidly recycled as it tends to dissociate from β -arrestin. V₂R, on the other hand, remains in the endosome longer by a stronger association with β -arrestin. Co-expression studies revealed that heterodimerisation of the two subtypes is strong enough to entrap the V_{1a}R with weaker association to β -arrestin. The recycling of V_{1a}R was inhibited by co-expression with V₂R [336].

The oligomerisation of neurohypophysial receptors were also confirmed by Albizu *et al.* using a series of radioligand binding assays: saturation, dissociation and competition binding experiments. The studies revealed that there is a cooperative nature associated with the receptors to various ligands including endogenous AVP or OT, and the type of cooperativity, either negative or positive, does not depend on the agonist or antagonist properties of the ligands. Since the study eliminated the possibility of G-protein coupling as a cause of cooperativity, the process of dimerisation was assumed to be the reasons for the phenomena observed [337]. The group also observed a negative cooperativity of V_{1b}R binding to vasopressin when expressed in COS-7 (simian kidney fibroblast cell-line) or CHO cell-lines.

Examples of neurohypophysial hormone receptors forming heterodimers were shown in the studies on human V_{1b}R and corticotrophin releasing factor receptor 1 (CRFR1) dimers, and avian CRFR1 and [Arg⁸]vasotocin receptor (VTR) [189, 190]. Specificity in heterodimerisation was shown by a study on OTR. The study showed that OTR can dimerise with V_{1a}R or V₂R, but not with the remotely related bradykinin receptor [338].

1.4.3. Synthetic peptide ligands

In order to study functionalities of each receptor subtypes, a series of cyclic and linear peptide antagonists each of which are selective to V_{1a}R or V₂R were derived from AVP by Manning in collaboration with Sawyer in the 1980s. A highly selective V_{1a}R antagonist, d(CH₂)₅Tyr(Me)²AVP (CA), has often been used as a reference in studies of V_{1a}R-specific compounds [339-341]. A linear antagonist [phenylacetyl-D-Tyr(Me)²Arg⁸Tyr⁹-(NH₂)]vasopressin (LA) was also produced [342]. LA is less selective as it also binds to both V_{1a}R and V_{1b}R with relatively high affinities but with a significant preference to V_{1a}R.

A group in SmithKline and French Laboratories was also actively developing peptide V₂R antagonists [343]. However, compounds which displayed potency as V₂R antagonists in several animal models turned out to be V₂R agonists in human because of existing species differences [344]. This case highlights the necessity of investigating the differences in the species relevant in the process of drug development.

There are a few peptide compounds which have exhibited specificity towards V_{1b}R but with existing species differences in subtype selectivity. [deamino-Cys¹, D-3'-(pyridyl)Ala²]AVP proved to be specific V_{1b}R agonist in rats [345]. However, it has been reported to behave as a V_{1a}R/V_{1b}R agonist in humans. [deamino-Cys¹, Arg⁸]vasopressin (dAVP) modified at position 4, [deamino-Cys¹, Cyclohexylalanine⁴, Arg⁸]vasopressin (d[Cha⁴]AVP), also displayed a high affinity agonism to V_{1b}R in human and bovine species, but the compounds showed less selectivity over V₂R in rats [346]. Recently, [deamino-Cys¹, Leu⁴, Lys⁸]vasopressin has been proven to be a selective rat V_{1b}R agonist with a nanomolar affinity [347]. Some of the subtype-selective peptide ligand developed are summarised in table 1.2 below.

Table 1.2 Subtype-selective peptide ligands of vasopressin receptors

Receptor	Ligand name	Properties	Ref.
V _{1a}	CA	Antagonist	[348, 349]
V _{1a}	HO-PhAc- <i>D</i> -Tyr(Me)-Phe-Gln-Asn-Arg-Pro-Arg-(NH ₂)	Antagonist	[350]
V _{1a}	LA	Antagonist	[339, 342]
V _{1b}	dP[Tyr(Me) ²]AVP	Antagonist	[351]
V _{1b}	d[<i>D</i> -3'-(pyridyl)Ala ²]AVP	Agonist	[345]
V _{1b}	dDAVP	Agonist	[352]
V _{1b}	d[Cha ⁴]AVP	Agonist	[353, 354]
V _{1b}	d[Leu ⁴ , Lys ⁸]vasopressin	Agonist	[355]
V ₂	desGly ⁹ -d(CH ₂) ₅ [<i>D</i> -Ile ² , Ile ⁴]AVP	Antagonist	[356]
V ₂	D(CH ₂) ₅ [<i>D</i> -Ile ² , Ile ⁴]AVP	Antagonist	[357]
V ₂	dDAVP	Agonist	[358]
V ₂	dVDAVP	Agonist	[359]

Abbreviations: CA = d(CH₂)₅[Tyr(Me)²]AVP; LA = [phenylacetyl-*D*-Tyr(Me)²Arg⁸Tyr⁹-(NH₂)]vasopressin; dDAVP = [deamino-Cys¹-*D*-Arg⁸]vasopressin; d[Cha⁴]AVP = [deamino-Cys¹, cyclohexylalanine⁴, Arg⁸]vasopressin; dVDAVP = [deamino-Cys¹-Val⁴, *D*-Arg⁸]vasopressin.

1.4.4. Non-peptide antagonists

In the past years, various orally-active, nonpeptide antagonists have been designed for vasopressin and oxytocin receptors. A few of them are selected here to be described briefly. Table 1.3 summarises non-peptide antagonists developed for vasopressin receptors. The first two nonpeptide $V_{1a}R$ antagonists, quinolinone derivative OPC-21268 [360] and N-sulfonyl-indoline SR49059, were synthesised in the early 1990s [361]. Based on OPC-21268, a selective OTR antagonist was developed by Merck & Co to treat preterm labour [362]. Rational modification of SR49059 yielded N-arylsulfonyl-oxindole SSR149415 as the first $V_{1b}R$ -selective nonpeptide antagonist [363]. However, SSR149415 has been reported to be a mixed antagonist to $V_{1b}R$ and OTR [364].

A few compounds have successfully entered clinical trials (table 1.3). Some of these are benzazepine derivatives. The benzazepine moiety appears to provide a good fit in some GPCRs. Benzazepine-derived compounds have been developed as selective ligands for other Family A GPCRs including: D_1 dopamine receptor (D_1R) agonists [365-367] or antagonists [368-370], 5-HT_{2c}R antagonist [371] or agonist [372], C-C chemokine receptor type 5 (CCR_5) antagonists [373-375], μ OR antagonist [376], and M_3R antagonist [377]. $V_{1b}R$ and V_2R selective compounds were derived from oxindole by Sanofi-Aventis. Other ligands derived from oxindole include cholecystokinin B receptor ($CCK_{B}R$) antagonist [378], β_3AR agonist [379], and growth hormone secretagogue receptor agonists [380-382].

Table 1.3 Non-peptide antagonist of vasopressin receptors

Subtype	Name	Company	Chemical Derivatives	Development	Ref.
V _{1a}	OPC-21268	Otsuka	Quinolinone	Stopped	[360, 383]
V _{1a}	SR49059	Sanofi-Aventis	N-sulfonyl-indoline	Stopped	[384]
V _{1a}	SRX251	Azevan	Azetidinone	Phase I	[385, 386]
V _{1a}	SRX246	Azevan	Azetidinone	Phase I	[386]
V _{1a}	LY307174	Eli Lilly	Azetidinone	Preclinical	[386]
V _{1a}	YM218	Yamanouchi /Astella	Benzazepine	Preclinical	[387]
V _{1a}	FR218944	Fujisawa/Astella	Benzazepine	Preclinical	[388]
V _{1a}	None	Yamanouchi /Astella	Triazole	Preclinical	[389]
V _{1a}	JNJ17308616	Johnson&Johnson	Spirobenzazepine	Preclinical	[390]
V _{1b}	SSR149415	Sanofi-Aventis	N-arylsulfonyl-oxindole	Phase II /Stopped	[363, 391]
V _{1b}	Org52186	Organon/Schering Plough	<i>Undisclosed</i>	Preclinical	[392, 393]
V ₂	OPC31260	Otsuka	Benzazepine	Phase II	[394]
V ₂	OPC41061	Otsuka	Benzazepine	Phase II / III	[395, 396]
V ₂	SR121463	Sanofi-Aventis	N-arylsulfonyl-oxindole	Phase II / III	[397-400]
V ₂	VPA985	Wyeth-Ayerst/ Cardiokine	Benzodiazepine	Phase II / III	[401-404]
V ₂	WAY140288	Wyeth-Ayerst	Benzodiazepine	Preclinical	[405]
V ₂	VP343	Wakamoto	Quinoxaline	Phase I	[406]
V ₂	VP365	Wakamoto	Benzodiazepine	Preclinical	[406]
V ₂	None	Johnson&Johnson	Indolazepine	Preclinical	[407]
V _{1a} / V ₂	YM087	Yamanouchi /Astella	Benzazepine	Phase IV	[408, 409]
V _{1a} / V ₂	YM471	Yamanouchi /Astella	Benzazepine	Preclinical	[410]
V _{1a} / V ₂	JVT605	Japan Tobacco	Thiazepine	Preclinical	[411]
V _{1a} / V ₂	CL385004	Wyeth-Ayerst	Benzodiazepine	Preclinical	[412, 413]
V _{1a} / V ₂	None	Wyeth-Ayerst	Tricyclic benzazepine	Preclinical	[414]
V _{1a} / V ₂	RWJ676070	Johnson&Johnson	Spirobenzazepine	Preclinical	[415, 416]

1.4.5. Mutagenesis, molecular modelling and docking studies

When molecular modelling is successfully achieved by a comparative method based on a known structure, the accuracy of the model can be tested by empirical experiments. The ligand binding cavities can initially be predicated by molecular docking of the compound to a model of the receptor, thereby providing some target residues for site-directed mutagenesis. The experimental data are then used to confirm, or make corrections to, the molecular model so as to generate a realistic representation.

In the process of docking, most algorithms generate a large number of possible structures. The likely structure needs to be identified among those candidates. The problem of generating and evaluating a plausible structure can be solved manually using interactive computer graphics, with six degrees of translational and rotational freedom of a molecule relative to the other. This process is said to be rather more complex than it sounds, since very similar compounds have been shown to adopt quite different binding modes in reality. In automated docking methods, scoring functions typically approximate the binding free energy of the ligand to the receptor. Relatively fast approximations can be made by adding each contributing factor in a single equation as:

$$\Delta G_{\text{bind}} = \Delta G_{\text{solvent}} + \Delta G_{\text{conf}} + \Delta G_{\text{int}} + \Delta G_{\text{rot}} + \Delta G_{\text{t/r}} + \Delta G_{\text{vib}} \quad \text{Equation 3}$$

Six contributing factors are included in the equation 3: i) the effects of solvent ($\Delta G_{\text{solvent}}$); ii) the free energy arising from conformational changes (ΔG_{conf}); iii) the free energy changes due to molecular interactions (ΔG_{int}); iv) the free energy loss for freezing internal rotations due to entropic contributions (ΔG_{rot}); v) the free energy loss in rotation and translation by association of two bodies into one ($\Delta G_{\text{t/r}}$); and vi) the free energy due to vibrations (ΔG_{vib}) [417]. Alternative equations which allow fast approximations can be written by finding a linear

relationship between parameters which reflects the overall free energy change. Such parameters can be hydrogen bonding, ionic interactions, hydrophobic interactions, and the loss of internal degrees of freedom by the ligand. The equation must include a penalty function that considers deviation of the bond distance from the ideal geometry [418].

Several docking studies have been published for vasopressin receptors and the oxytocin receptor. For instance, docking of a nonpeptide antagonist OPC-21268 and AVP into the human $V_{1a}R$ was performed by Thibonnier *et al.* one by one, using the docking program LIGIN. The program is based on a built-in complementary function as a sum of the surface area of atomic contacts, and it has the capability of optimising the length of hydrogen bonds [419]. Their structures showed that the orientation of the antagonist binding was distinct from the AVP binding. A partial overlap was recognised only by the extracellular surface, where the polar part of the antagonist was located. The hydrophobic portion of the antagonist was buried much deeper in the TM region. The binding pocket was composed of TMs 4,5,6,7 and ECL3. Their structure was shown to be plausible by rational analysis of findings from mutagenesis experiments [420]. Docking studies of subtype-selective antagonists and vasopressin receptors have been performed by Tahtaoui *et al.* with SR49059 and $V_{1a}R$, and by Derrick *et al.* with SSR149415 and $V_{1b}R$, using the automated docking program Gold 1.2 which employs bond lengths, interaction energies as parameters. The findings of the two studies are discussed in the chapter 4 of this thesis, which concerns the subtype differences in ligand binding between $V_{1a}R$ and $V_{1b}R$.

1.5. Aim of this study

The V_{1b}R has been shown to have a distinctive role involved in eliciting physiological responses to stress. The discovery of a high affinity V_{1b}R-selective and orally active non-peptide antagonist would allow further investigation of the V_{1b}R functions and the related physiology, as well as having a therapeutic potential. The aim of this study was to investigate the ligand binding sites of the human V_{1b}R, regarding peptide and non-peptide ligands. The residues at which ligands may contact in the putative binding cavities were identified by engineering specific mutations in the receptor, with the aid of molecular models of V_{1b}R and also V_{1a}R. In doing so, firstly the residues which are conserved among vasopressin receptors were studied. Secondly, the residues which may distinguish V_{1b}R and V_{1a}R in the binding of V_{1b}R-selective non-peptide antagonists were also studied. Thirdly, the species-specific interactions of the V_{1b}R-selective antagonists regarding rat and human V_{1b}Rs would be investigated. Single nucleotide polymorphic variants of V_{1b}R occurring in the human population and pharmacological ramification of these would be investigated.

Chapter 2 Materials and Methods

2.1. Materials

2.1.1. Radio-labelled compounds

[Phe³-3,4,5-³H]AVP (specific activity of 44 ~ 62 Ci·mmol⁻¹) and myo-[2-³H]inositol (specific activity of 22 Ci·mmol⁻¹) were purchased from PerkinElmer (Stevenage, UK).

2.1.2. Ligands

AVP, OT, the cyclic antagonist d(CH₂)₅[Tyr(Me)²]AVP (CA), the linear antagonist [PhAc-*D*-Tyr(Me)²Tyr⁹-(NH₂)]AVP (LA), dDAVP, AVP-free acid were purchased from Bachem (St. Helens, UK). [Glu⁸]AVP and [β-Ala⁹]AVP were custom synthesised by Alta-Biosciences (University of Birmingham, UK). d[Cha⁴]AVP was purchased from Tocris Biosciences (Tocris Biosciences, Bristol, UK). (2S)-1-[(2R,3S)-5-chloro-3-(2-chloro-phenyl)-1-(3,4-dimethoxybenzene-sulfonyl)-3-hydroxy-2,3-dihydro-1*H*-indole-2-carbonyl]-pyrrolidine-2-carboxamide (SR49059) was a gift from Dr. C. Serradiel-Le Gal (Sanofi Recherche, France). (2S, 4R)-1-[(5-chloro-1-[(2,4-dimethoxyphenyl)-sulfonyl]-3-(2-methoxy-phenyl)-2-oxo-2,3-dihydro-1*H*-indol-3-yl]-4-hydroxy-*N,N*-dimethyl-2-pyrrolidine-carboxamide (SSR149415) and the V_{1b}-selective non-peptide antagonist N0083 PICK 5234B (5234B) were gifts from Schering-Plough Research Institute (Newhouse, UK).

2.1.3. Molecular Biology Reagents

Pfu polymerase was purchased from Promega (Southampton, UK). *Dpn-I* was purchased from New England Biolabs (Hitchin, UK). dNTPs were purchased from Bio-line (London, UK).

Kits used for DNA purification and preparation were obtained from Qiagen (QiaQuick PCR purification kit, QiaQuick Gel Purification kit), Promega (WizardTM mini-prep kit) and Marligen Life Technologies (High Purity Plasmid Maxiprep System). Oligonucleotide primers, desalted, and cartridge purified for bases longer than 33 bases, were synthesized by Invitrogen (Paisley, UK). Di-methyl-sulfoxide (DMSO) molecular biology grade, bovine serum albumin (BSA), monoclonal mouse anti-HA antibodies clone HA-7, monoclonal anti-FLAG antibodies clone M2, monoclonal goat anti-mouse antibodies conjugated with horseradish peroxidase, horseradish peroxidase substrates and associated buffer were purchased from Sigma Aldrich (Poole, UK).

2.1.4. Cell Culture Reagents

Dulbecco's modified Eagles medium (DMEM), inositol-free DMEM, foetal bovine serum (FBS), phosphate buffered saline (PBS) were purchased from Gibco-BRL (Paisley, UK). DMSO cell culture grade and poly-*D*-lysine, poly-ethylenimine (PEI) and glucose were purchased from Sigma Aldrich. Cell culture flasks, plates and dishes were purchased from TPP® (Sunderland, UK), BD Biosciences (Oxford, UK), and Orange Scientific (Braine-l'Alleud, Belgium).

2.1.5. Plasmid Expression Vector

pcDNA3.1(+) (figure 2.1) was purchased from Invitrogen (Paisley, UK). The vector is 5.4 kb in length, containing an ampicillin resistance gene for selection in *E. coli*, a human cytomegalovirus (CMV) immediate-early promoter for high expression, and a SV40 element for episomal replication in HEK293T cell-line which expresses the SV40 large T antigen.

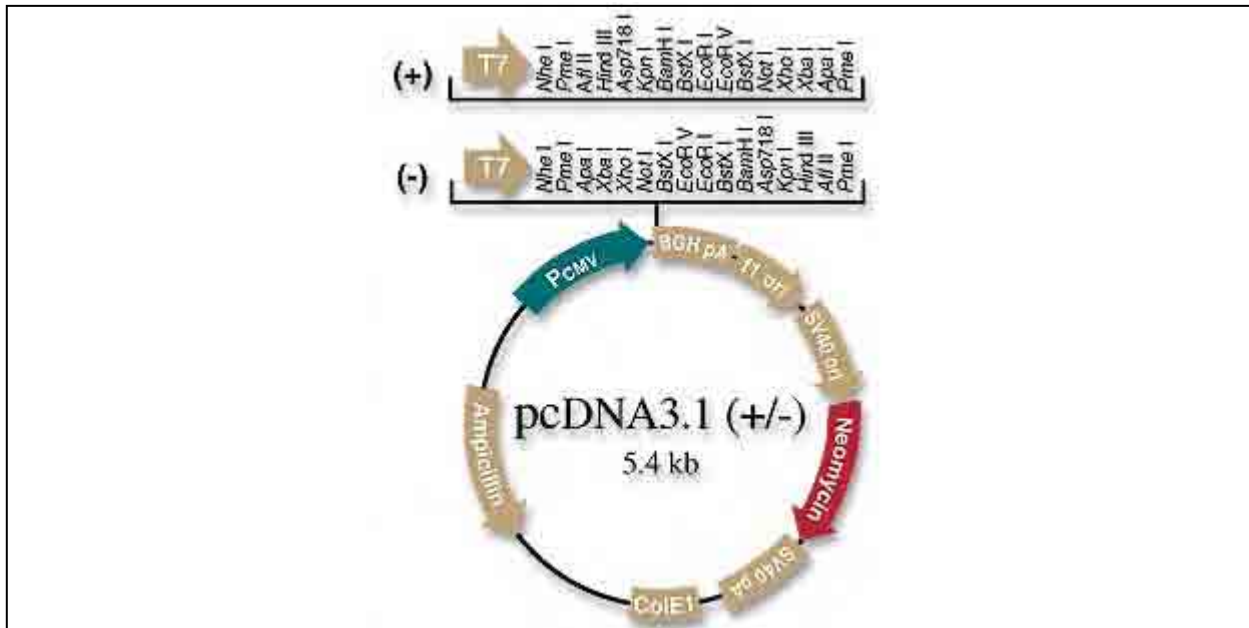


Figure 2.1 The expression vector pcDNA3.1: The figure shows the functional elements and restriction digestion sites of pcDNA3.1.

2.1.6. Oligonucleotide Primers

Primer pairs were designed to keep differences in melting temperature (T_m) between sense and antisense primers to be no more than 5 °C. T_m for each primer was estimated based on the proportion of GC and AT pairs. A web page, Stratagene QuickChange™ Primer T_m calculator (<http://www.stratagene.com/OPCR/tmCalc.aspx>) was used to assist designing the primers. The sequences of the primers used for the site-directed mutagenesis are shown in the result sections. The sense (S) and antisense (AS) primer sequences for the vector pcDNA3.1(+) used to confirm the entire construct sequences were: 5'-CGA-CTC-ACT-ATA-GGG-AGA-CCC-AAG-C-3' (S) and 5'-CCA-GGG-TCA-AGG-AAG-GCA-CGG-3' (AS).

2.2. Methods

2.2.1. Expression Constructs and the Site-Directed Mutagenesis

Human V_{1b}R and V_{1a}R, each fused to an N-terminal haemagglutinin (HA) epitope tag with protein sequence YPYDVPDYA, were subcloned into pcDNA3.1(+). The presence of the tag was previously shown not to have any significant effect on the receptor pharmacology (Hawtin, S.R. Doctoral thesis, 1999; Baker, A.J., Doctoral thesis 2008, University of Birmingham).

Site-directed mutagenesis was performed using the QuickChange™ method (Stratagene, Cambridge UK), following the manufacturer's instructions. Briefly, a reaction mixture of the final volume 50 µL was prepared to contain approximately 100 ng of plasmid cDNA as templates, sense and antisense mutagenic primers with the final concentration of 100 µg.mL⁻¹, dNTP mixture with the final concentration of 40 mM, and *Pfu* polymerase (0.5 ~ 2.0 units). Using a Biometra TRIO-thermoblock, a thermal cycling program was set to have an initial denaturing period of 1 min at 90°C, and 12 repeated cycles comprising 30 s denaturing period at 90°C, 1 min annealing period at 55 ~ 63 °C, and 14 min extension period at 68 °C. When a reaction was set overnight, the sample was kept at 4 °C. The templates present in the mixture were digested by 1.5 µL of a methylation-sensitive nuclease *DpnI*, for at least 90 minutes at 37 °C. The presence of template was checked by examining a control, which contained the same concentration of the template in the reaction mixture without primers.

2.2.2. Agarose Gel Electrophoresis

DNA was separated in 1% (w/v) agarose gel and electrophoresed on a horizontal gel-electrophoresis system (Life technologies) with 1 x TBE at 72 mV for approximately 30 min for standard PCRs and Quickchange™ mutagenesis products. For size determination, the 1%

agarose gel was electrophoresised at 30 mV for approximately 16 h. Loading buffer containing glycerol (30 % w/v) and bromophenol blue (0.25 % w/v) was added in a 5:1 ratio to the samples prior to the separation. The DNA incorporated with ethidium bromide ($0.5 \mu\text{g}\cdot\text{mL}^{-1}$) was visualized on an ultraviolet light illuminator. A molecular marker, 1kb ladder (NEB, Bedford UK) was used as a standard to determine the sizes of DNA fragments and also to estimate the concentration of DNA.

2.2.3. Gel-purification of the PCR Products

The PCR products were purified from agarose gel using QiaQuick Gel Purification kit following the instructions provided by the manufacturer. Briefly, each piece of gel was placed in a 1.5 mL tube, and an equal volume of the dissolving solution was added. The mixture was incubated for 5 minutes at 50 °C with occasional mixing by a moderate vortex every 2 min. The solution was separated by micro column chromatography and the oligonucleotides were eluted in 30 μL sterile distilled water.

2.2.4. Restriction Enzyme Digests

The requirements for efficient enzyme activity depend on individual enzymes, and so digestions were performed according to the manufacturers' recommendations. Typically, 5 μL of plasmid DNA was digested with 2 ~10 units of restriction enzymes and their appropriate buffers in a volume of 10 μL . Samples were incubated for 3 ~ 16 h at 37 °C.

2.2.5. Ligation of cDNA

Ligation reactions contained 3:1 ratio of insert to vector, 1 - 3 units of T4 DNA ligase, ligase buffer and were made up to a final volume of 20 μL . The mixture was incubated at 16 $^{\circ}\text{C}$ for 16 h.

2.2.6. Transformation of *E.coli*

30 μL of the XL-10 Gold ultracompetent cells (Stratagene) were incubated with 1 μL of ligation mixture or QuickchangeTM mutagenesis product on ice for 30 min. Cells were heat shocked at 42 $^{\circ}\text{C}$ for 30 s, and rested on ice for 2 min. 800 μL of Luria broth (LB: containing 10 g peptone, 5g NaCl, 5g yeast extract in 1L distilled water) was added and incubated at 37 $^{\circ}\text{C}$ for 1 h. The cells were sedimented at 11,000 $\times g$ for 5 min, 800 μL of the supernatant removed, re-suspended in the remaining LB, spread onto LB agar plate containing ampicillin (100 $\mu\text{g}\cdot\text{mL}^{-1}$), and incubated at 37 $^{\circ}\text{C}$ overnight.

2.2.7. Plasmid cDNA Extraction

The plasmid cDNA were extracted from the transformed XL-10 Gold cells and purified for a small scale (1 ~ 10 μg) using the Wizard Plus SV kit (Promega) following the manufacturer's protocol. For a larger scale (0.5 ~ 3 mg), High Purity Plasmid Maxiprep System (Marligen Life Technology, Maryland USA) was used to purify the vectors following the manufacturer's instruction. The concentration of plasmid was determined by measuring the absorbance of the sample (1:2000 dilutions in distilled water). The purity of the DNA was assessed by measuring the absorbance ratio of λ 260 nm to λ 280 nm.

2.2.8. Automated Fluorescence Di-deoxy Sequencing

DNA sequences were confirmed by automated sequencing, using primers present at a pM range, by the Functional Genomics and Proteomics Laboratory in the University of Birmingham (Birmingham UK).

2.2.9. Sequence Alignments

Nucleotide sequence alignments were performed using the ClustalW (1.81) algorithm with default setting inbuilt within San Diego Super-computer (SDSC) biology workbench (California, USA) faculty. Protein sequences were obtained from Swiss-Prot/TrEMBL. Multiple sequence alignments were performed with the parameters: gap open penalty 10.0; gap extension penalty 0.2; and Gonnet series as weight matrix.

2.2.10. Cell Culture and Transfection

HEK293T cell-line with passage numbers between 15 and 32 were used for good transfection efficiency. The cells were cultured in Dulbecco's modified Eagle's medium (DMEM) supplemented with 10% (v/v) FCS, in a humidified 5 % (v/v) CO₂ in the air incubator at 37 °C. Cells were passaged twice weekly to keep approximately 50 % confluence for optimum growth.

For membrane preparations, transfection was carried out 48 h after seeding cells at a density of approximately 5×10^5 cells per 100 mm² in a culture dish. 5 µg DNA was mixed with 950 µL of 5 % (v/v) glucose solution and 120 µL of 10 mM PEI per dish, and incubated for 30 min at room temperature. 1mL of the mixture was added to each dish containing approximately 8 mL of the growth medium. Cells were harvested 48 hours after the transfection. For ELISA, cells were seeded at a density of 1.5×10^5 cells per well of a poly-*D*-

lysine coated 24-well plate. For inositol phosphate assay, the cells were seeded at a density of 2.5×10^5 cells per well of a poly-*D*-lysine coated 12-well plate. The cells on the plates were transfected after 24 h. A transfection mixture was prepared to contain (per well) 0.5 μ g DNA, 30 μ L 5 % glucose and 4 μ L PEI (10 mM) for 24-well plates, and the quantities were doubled for 12-well plates. Cells were allowed to grow for approximately 48 h after the transfection prior to each assay.

2.2.11. Membrane Preparation

Harvesting of membrane extracts for radioligand binding assays were carried out as described [421]. Cells were washed in ice-cold phosphate-buffered saline (PBS) and then scraped from plates using harvest buffer (20 mM 4-(2-hydroxyethyl)-1-piperazineethanesulfonic acid (HEPES), 1 mM glycol-bis(2-aminoethylether)-*N,N,N',N'*-tetraacetic acid (EGTA), 10 mM $\text{Mg}(\text{CH}_3\text{COO})_2$; pH 7.4) containing 250 mM sucrose and bacitracin ($0.1 \text{ mg}\cdot\text{mL}^{-1}$). Cells were sedimented by centrifugation ($4000 \times g$ at 4°C for 10 min) and re-suspended in harvest buffer containing $0.1 \text{ mg}\cdot\text{mL}^{-1}$ bacitracin. Cells were incubated on ice for 20 min before being sedimented as above. The pellets were re-suspended in harvest buffer containing 250 mM sucrose, and stored at -20°C in 500 μ L or 1 mL aliquots.

2.2.12. Protein Assay

The protein concentration of the membranes was determined using the Pierce BCA protein assay kit. A standard curve was obtained using bovine serum albumin (BSA) solution. 5 μ L of each membrane sample was diluted in distilled water for a total volume of 50 μ L. 1mL of a 50:1 mixture of Pierce assay reagents A : B was then added to each tube, and the samples were

incubated at room temperature for 2 h before reading absorbance at 562 nm. Protein concentrations were determined using linear regression against BSA standards obtained in parallel in each assay.

2.2.13. Competition Radioligand Binding Assays

All the assays were performed using [Phe³-3,4,5-³H]AVP as a tracer ligand. Membranes which had been transfected with appropriate receptor construct were diluted in 10 mL binding buffer (20 mM HEPES, 1 mM EGTA, 10 mM Mg(CH₃COO)₂, 0.1% w/v BSA; pH 7.4) per a curve. An unlabelled ligand concentration range used was 10⁻⁶ M (or 10⁻⁵M) to 10⁻¹¹ M (or 10⁻¹⁰M), depending on the affinity of ligands to the receptor constructs. Non-peptide ligands were dissolved in ≈ 100 % DMSO of molecular biology grade (Sigma-Aldrich). The final concentration of DMSO in the assay was 2 %. As for the non-peptide ligands, the total binding in the absence of competing ligand was determined in the presence of 2 % DMSO. Non-specific binding as determined by a saturating concentration (1 μM) of unlabelled ligand. The final volume of the assay was 500 μL. After mixing each tube by a gentle vortex, the samples were incubated at 30 °C for 90 min to establish a binding equilibrium. Bound and free ligands were separated by centrifugation at 13,000 x g for 10 min. From the samples prepared without competing ligand, 100 μL supernatant was collected to determine the concentration of tracer ligand. All the pellets were then washed twice gently in distilled water and dried. Each pellet was solubilised in 50 μL Soluene 350 (Packard, UK) overnight at room temperature. 1 mL of ScintiSafe™ liquid scintillation cocktail 3 (Wallac, UK) was added to each tube to facilitate radioactivity counting by a Packard 1600 TR liquid scintillation analyser counter.

2.2.14. Thermal Denaturation Assay

Membrane preparations were heat-treated in a water bath at 53 °C with a periodical time intervals in minutes determined using a sequence $n_x = 2(n_{x-1}) + 1 + \sum n_{x-2} \dots n_0$, which is similar in idea to Pell number ($P_n = 2P_{n-1} + P_{n-2}$), but it differs in that each number also add 1 and the sum of the previous numbers. After the incubation, cold binding buffer was added, and the membrane was aliquoted immediately to each microtube containing a fixed concentration (0.5 nM as the final concentration) of [³H]AVP. After brief and moderate mix by vortex, the mixtures were incubated for 90 min at 30°C, and then processed using the radioligand binding assay protocol described in section 2.2.14. The use of the denaturing temperature of 53 °C was shown to be effective by Bee *et al.* [422].

2.2.15. Determination of Cell-Surface Expression of Receptors by Enzyme-linked Immunosorbent Assay (ELISA)

Approximately 48 h after the transfection, the medium was removed by aspiration. Cells on 24-well plates were fixed using 4.8 % (v/v) formaldehyde in PBS by incubating at room temperature for 15 min. After washing cells twice in PBS, 1 % (w/v) BSA in PBS was added to provide a block to prevent nonspecific binding, and incubated with a moderate shake for 1 h. After removing the block, the primary antibody diluted (1:2000) in 1 % (w/v) BSA/PBS were added and incubated with moderate shaking for 1 h. Cells were washed three times in PBS, and re-blocked in 1 % (w/v) BSA/PBS for 15 min. Blocking buffer was removed, and the secondary antibody diluted (1:2000) in 1 % (w/v) BSA/PBS were added and incubated with moderate shake for 1 hour. The antibodies were removed, the cells were washed with PBS three times, and then horseradish peroxidase substrate (o-phenylenediamine dihydrochloride) was added.

The plates were incubated in dark for 5 - 8 min. The reaction was stopped by 1M H₂SO₄, as 100 μL of the sample and 1M H₂SO₄ were mixed in a well of 96-well plates. The peroxidase activity was measured by the quantification of the substrates in the 96-well plate using a standard plate reader with absorbance measurement at λ 492nm.

2.2.16. Determination of Agonist-induced Internalisation of Receptors

To promote the internalization, cells were exposed to AVP (1 μM) in growth media at 37 °C for the indicated time period in the relevant chapters. Prior to assaying, the cells were washed with cold PBS three times. The cells were fixed and quantification of receptors remaining at the cell surface was determined using the ELISA-based assay described in section 2.2.15. The proportion of receptor remaining on the cell-surface was determined by normalising to the expression level of the unstimulated group for each receptor construct.

2.2.17. Determination of the Effect of Non-peptide Antagonist on the Cell-Surface Expression and Internalisation by ELISA

24 h after the transfection, the two groups of cells were treated with 1 μM 5234B in DMEM containing 1% (v/v) DMSO and a control group with DMEM containing 1% (v/v) DMSO. After 24 hours incubation at 37 °C, one of the experimental groups pre-treated with 5234B was treated with AVP (1 μM) for 30 min to investigate the effect of the 5234B treatment on the agonist-induced internalisation. ELISA was performed as described in section 2.2.16.

2.2.18. Inositol Phosphate (InsP-InsP₃) Assay

AVP-induced accumulation of inositol phosphates were assayed as previously described [423]. 16 h post-transfection, the growth medium was replaced with inositol-free DMEM supplemented with 1.5 $\mu\text{Ci}\cdot\text{mL}^{-1}$ myo-[2-³H]inositol, and incubated for a further 24 hours. Cells were washed with PBS and incubated in the medium containing 10 mM LiCl for 30 min followed by 30 min incubation at 37 °C with agonist at concentration ranging from 10⁻⁶ M to 10⁻¹⁰ M. The reaction was terminated by adding 0.5 mL of 5% (v/v) percholic acid solution, which contains 1 mM EDTA and 1mg.mL⁻¹ phytic acid hydrosylate, to each well. After neutralisation with KOH, samples were kept at - 20 °C for at least 1 h to facilitate precipitation. After the centrifugation, the supernatants were loaded onto Bio-Rad AG1-X8 (formate form) filled columns. Following the elution of free inositol and glycerophosphoinositol with 60 mM NH₄COOH containing 0.1 M HCOOH, a mixed InsP fraction containing inositol mono, bis and trisphosphates was eluted with 850 mM NH₄COOH containing 0.1 M HCOOH. 10 mL of Ultima-Flo AF Scintillant (Fischer, UK) was added for liquid scintillation counting to quantify the radioactivity.

2.2.19. Data Analysis

The data for competition binding assay was analysed using Graphpad Prism version 4.0 (San Diego, USA) using its normalising function to show a percentage of maximum binding and the non-linear regression curve fitting adjusted for one-site competition (Equation 4) to determine IC₅₀. The graphs were plotted as a function of percentage binding against logarithm of the concentration of competing ligand. The IC₅₀ obtained were corrected for radioligand occupancy

to generate K_i values as described by Cheng and Prusoff [424], using equation 6. The concentration of free radioligand was calculated using equation 5.

$$Y = B + (T - B) \cdot (1 + 10^{(X - \text{LogIC}_{50})})^{-1} \quad \text{Equation 4}$$

Where B is the bottom of the curve (i.e. non-specific binding) and T is the top of the curve (i.e. the maximum binding).

$$[\text{free } [^3\text{H}]\text{ligand}] \text{ (nM)} = \text{DPM} \cdot (\text{SA} + v \cdot 2.22)^{-1} \quad \text{Equation 5}$$

Where DPM is radioactivity counts in disintegration per minute, SA is the specific activity of radioligand in $\text{Ci} \cdot \text{mmol}^{-1}$, and v is the sample volume in μL .

$$K_i \text{ (nM)} = \text{IC}_{50} \cdot (K_d \cdot (K_d \cdot [\text{free } [^3\text{H}]\text{-ligand}])^{-1}) \quad \text{Equation 6}$$

Where K_d is the equilibrium dissociation constant of $[^3\text{H}]\text{-ligand}$

For ELISA to determine the cell-surface expression, the average values plus/minus standard error of means were determined relative to values obtained for the wild-type expression, defined as $100 \cdot ((\text{OD}_{\text{mutant}} - \text{OD}_{\text{mock}}) \cdot (\text{OD}_{\text{wt}} - \text{OD}_{\text{mock}})^{-1})$.

For InsP assay, results were expressed as a percentage of maximum Wt receptor activity measured. EC_{50} values were determined by fitting the experimental data to a sigmoidal dose-response curve using Prism 4.0.

Chapter 3 Investigating the role of conserved residues among vasopressin receptors in V_{1b}R ligand binding

3.1. Introduction

Conserved residues among all the receptor subtypes are often involved in common features the receptors share, for instance in constructing binding cavities for a mutual agonist, or involved in the receptor activation. In this section, the conserved residues in the putative ligand binding cavities were subjected to study. The residues were selected based on the protein sequence alignment and the previous findings on V_{1a}R and V_{1b}R.

There have been several studies revealing the roles of conserved residues in vasopressin receptors. Some conserved polar residues in the TM domains of V_{1a}R have been shown to be involved in AVP binding by mutagenesis and computational molecular modelling studies by Mouillac *et al.* in 1995, including Gln^{2.57}, Gln^{2.61}, Lys^{3.29}, Gln^{3.32}, Gln^{4.60}, Gln^{6.55} [425]. The involvement of Gln^{2.57} in isotocin binding has also been shown in the vasotocin receptor [426]. Molecular dynamic simulation studies of AVP docking into V_{1a}R, V₂R, and OTR by Slusarz *et al.* also displayed the interactions between AVP and the residues Gln^{2.57}, Gln^{2.61}, Gln^{3.32}, Gln^{4.60}, Gln^{6.55} in all the three subtypes [427]. The ligand interactions of Gln^{2.57}, Gln^{2.61} in V_{1a}R were shown to be specific to agonist but not involved significantly in antagonist binding [425].

With a limited access for water molecules, hydrogen bonds may be sufficient as the main interaction within TM domains. However, in the N-terminal domain and juxtamembrane regions, at least a few stronger ionic interactions are required to prime a significant ligand-receptor association. In the V_{1a}R, Arg^{1.27} and Glu^{1.35} have been demonstrated by mutagenesis to

be key residues involved in AVP binding and signalling by Hawtin in 2005 [428]. Also in the OTR, Arg^{1.27} has been shown to be important in agonist binding but not in antagonist binding, by Wesley in 2002 [429].

The four residues, Gln^{2.57}, Gln^{2.61}, Arg^{1.27} and Glu^{1.35}, which have been shown by mutagenesis studies to be responsible in binding specifically to the endogenous agonist but not to antagonist, and are highly conserved among neurohypophysial hormone receptors of various species (figure 3.2). This may indicate the existence of a common binding mode in which the nonapeptide comprising a hexapeptide ring with a tripeptide tail induces the conformational change that initiates the receptor activation.

There are a few residues which have also been identified for their participations in AVP binding. In V₂R, two residues Thr^{102 (2.67)} and Arg¹⁰⁶ in ECL1 have been indicated to interact with Arg⁸ of AVP based on photoaffinity labelling studies [430]. Arg¹⁰⁶ is not conserved between the vasopressin receptor subtypes, while Thr^{102 (2.67)} is highly conserved among neurohypophysial hormone receptors. In V_{1a}R, a non-conserved Tyr^{115 (2.68)} was suggested to interact with Arg⁸ of AVP [425]. These findings suggest that although AVP may bind in a similar manner to vasopressin receptors overall, there are differences existing in the details.

Other molecular modelling-based studies have suggested that during AVP binding to V_{1a}R or V_{1b}R, Arg⁸ forms a salt bridge with Glu^{1.35} [427, 431], and Rodrigo *et al.* suggested Arg⁸ also interacted with a relatively conserved residue Asp^{2.56} in both V_{1a}R and V_{1b}R [431]. An AVP-docked molecular model of V_{1a}R produced by Simms has shown that Glu^{1.35} and Gln^{2.61} are in the proximity of the tri-peptide (Pro⁷-Arg⁸-Gly⁹-NH₂) tail of AVP (Simms J. unpublished study). Importantly, the glycinamide in particular has been related to the potency of AVP [432, 433]. Using chemically modified vasopressin and appropriate series of

mutagenesis studies, Wootten and Wheatley showed that multiple interactions occurs involving Arg⁸ with Glu^{1.35} as well as with the terminal glycineamide of AVP in V_{1a}R (manuscript in preparation). The study has also showed that although Gln^{2.61} is required for AVP binding to the V_{1a}R, Gln^{2.61} does not interact with the glycineamide, and the possibility of an interaction occurring between Glu^{1.35} and Gln^{2.61} was suggested. In contrast, in the V₂R Glu^{1.35} was shown to participate only slightly in AVP binding whereas Gln^{2.61} and Gln^{2.57} were both important for AVP binding. Although OT has Leu⁸ in place of Arg⁸ which can engage in multiple interactions, Glu^{1.35} and Gln^{2.61} were both shown to be necessary for a high affinity binding of OT, and also AVP, to the OTR (Wootten and Wheatley, manuscript in preparation). These findings have confirmed the existence of subtype differences in the molecular requirements for binding of a mutual agonist.

The conserved residues in TM7 and H8 of the V_{1b}R have recently been studied by Baker and Wheatley in 2008. There is a highly conserved region in TM7 of the neurohypophysial hormone receptors. Incorporating the NPXXY motif, the motif (N)SC(C)NPWIY is well-conserved among all the neurohypophysial hormone receptors from various species with few exceptions. Asn^{7.45} is highly conserved except in rodent V_{1b}Rs in which Ser^{7.45} is found (This residue is further mentioned in chapter 5). Cys^{7.48} is also well conserved except in V₂Rs which have Thr^{7.48}. Based on MD simulation, Ślusarz *et al.* predicted Asn^{7.45} to be a contacting point of AVP in V_{1a}R and V₂R [427]. However it was shown not to be the case in V_{1b}R. Ile^{7.52} in V_{1b}R seems important for receptor folding as [I7.52A]V_{1b}R was shown to be disrupted critically with no detectable AVP binding and with a large reduction of the cell-surface expression. Regarding the AVP binding, individual alanine substitutions of other residues within the motif were well-tolerated in the V_{1b}R (Baker, A.J. 2008, Doctoral thesis. University of Birmingham).

In this chapter, highly conserved residues within the putative binding cavities of vasopressin receptors in general were targeted for alanine mutagenesis to determine their roles in V_{1b}R function. The residues in TM domains and the extracellular juxtamembrane regions which have been demonstrated to participate in AVP binding in other subtypes were included in this study with an emphasis on TM2. This study also included a few residues conserved throughout Family A GPCRs. These included Cys^{6.47} and Trp^{6.48} of the rotamer switch, CWXP motif located in the middle of TM6 in the vicinity of the putative ligand binding cavity, Phe^{5.47} which has been proposed to interact with Trp^{6.48} during activation [427], and Tyr^{5.58} which has been shown to interact with Arg^{3.50} in the active state of opsin [295]. In addition some residues, which have been predicated to be located in the vicinity of the putative binding site of non-peptide antagonists based on molecular modelling, were also subjected to study (Dr. Grant Wishart, Schering-Plough Research Institute. private communication).

3.2. Results

3.2.1. Identification of conserved residues among vasopressin receptors by primary structure comparisons

The protein sequences of vasopressin receptors, vasotocin receptors, and OTR from various species were aligned (figure 3.1). The sequence of bovine rhodopsin was also included as a reference Family A GPCR. The regions of the N-terminus/juxtamembrane and the upper TM2 domain of the sequence alignment are shown in figure 3.2. These regions include residues Gln^{2.57}, Gln^{2.61}, Arg^{1.27} and Glu^{1.35} which have been demonstrated experimentally to be important for AVP binding to vasopressin receptors but not for antagonist binding.

Conserved residues which have been implicated in ligand binding of V_{1a}R, V₂R or OTR were selected in this study to investigate their role in ligand binding to V_{1b}R. Some aromatic or hydrogen-bonding residues were also selected additionally to investigate any functional involvement of such residues in V_{1b}R. All the residues subjected to study in this chapter are summarised in figure 3.3.

In both alignments, the entire protein sequence of each receptor was used for all the receptors except the bovine V_{1b}R, of which sequence was only available as a fragment. The regions which are remotely relevant to this section were removed from the figures to facilitate an easy viewing on a single page.

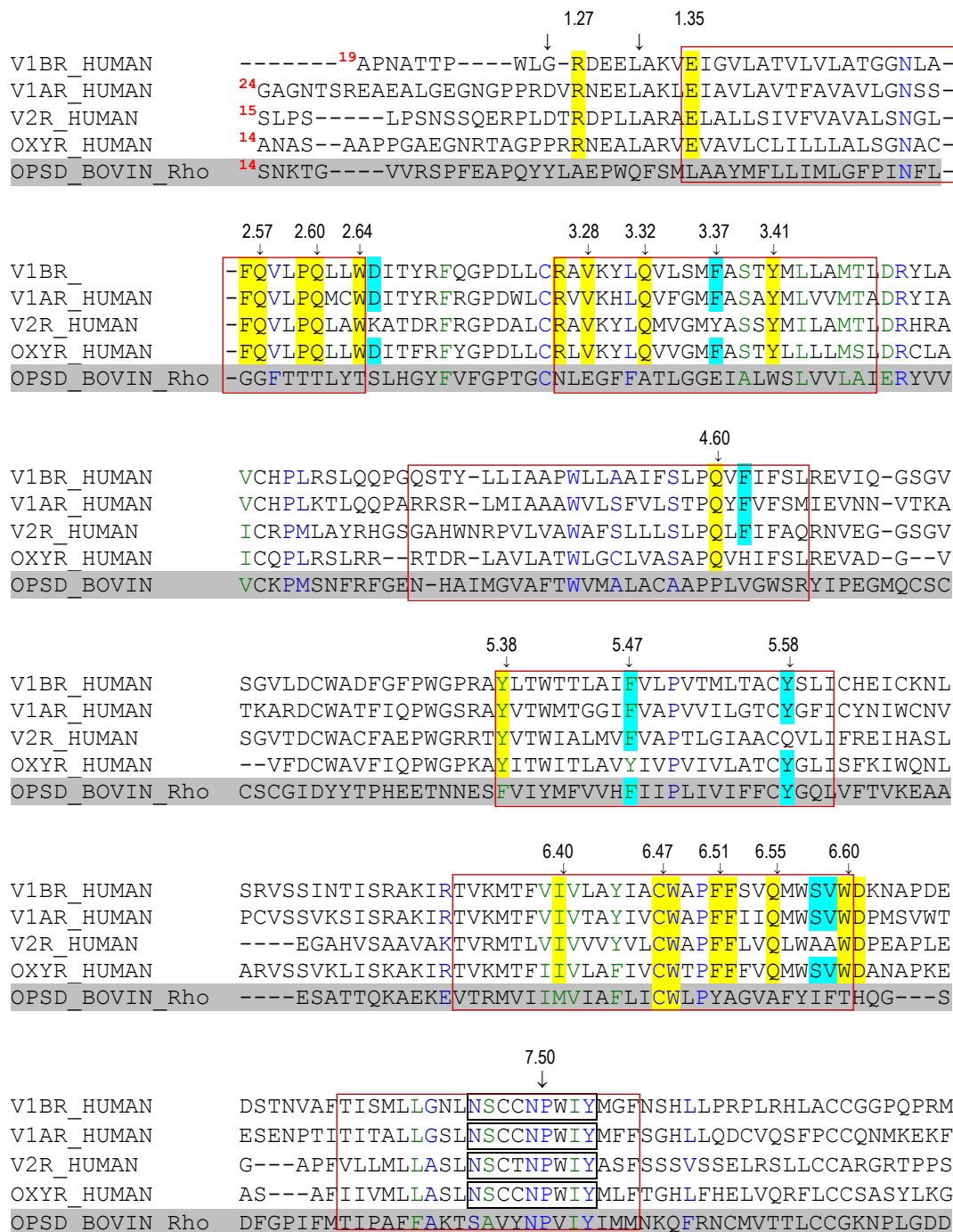


Figure 3.1 Protein sequence alignment of human neurohypophysial hormone receptors:

Multiple sequence alignment of human neurohypophysial receptors aligned with bovine rhodopsin as a reference. Selected regions of TM domains are shown, with TM domains in red boxes. The residues studied are highlighted: conserved in the four neurohypophysial hormone receptors are with yellow; conserved in three of the four receptors are indicated with turquoise. The roles of individual residues in the highly conserved region of TM7 (in black box) were previously studied in V_{1b}R by Baker (Baker A.J. Doctoral thesis 2008, University of Birmingham). The position of residues relative to the initiation Met is indicated with red numbers at the beginning.

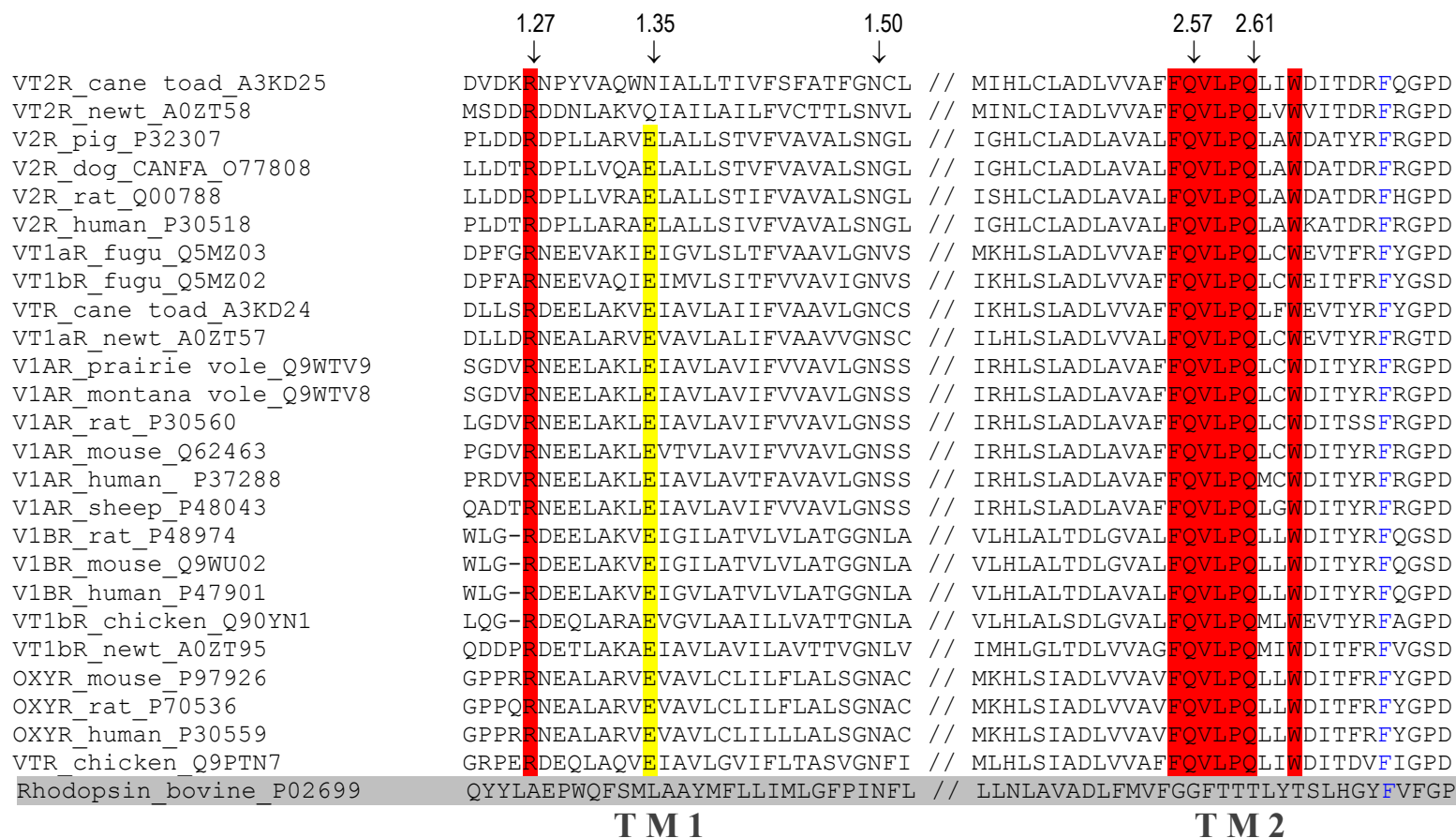


Figure 3.2 Excerpt of the multiple sequence alignment of neurohypophysial hormone receptors showing the N-terminal/juxtamembrane, the upper regions of TM1 and TM2 domains: The strictly conserved residues are shown in red, and a highly conserved residue is shown in yellow. There is a high level of conservation in the upper region of TM2 (FQVLPQ motif) including Gln^{2.57} and Gln^{2.61}, both of which have been shown previously in V_{1a}R to be involved in agonist binding and consequential activation [425].

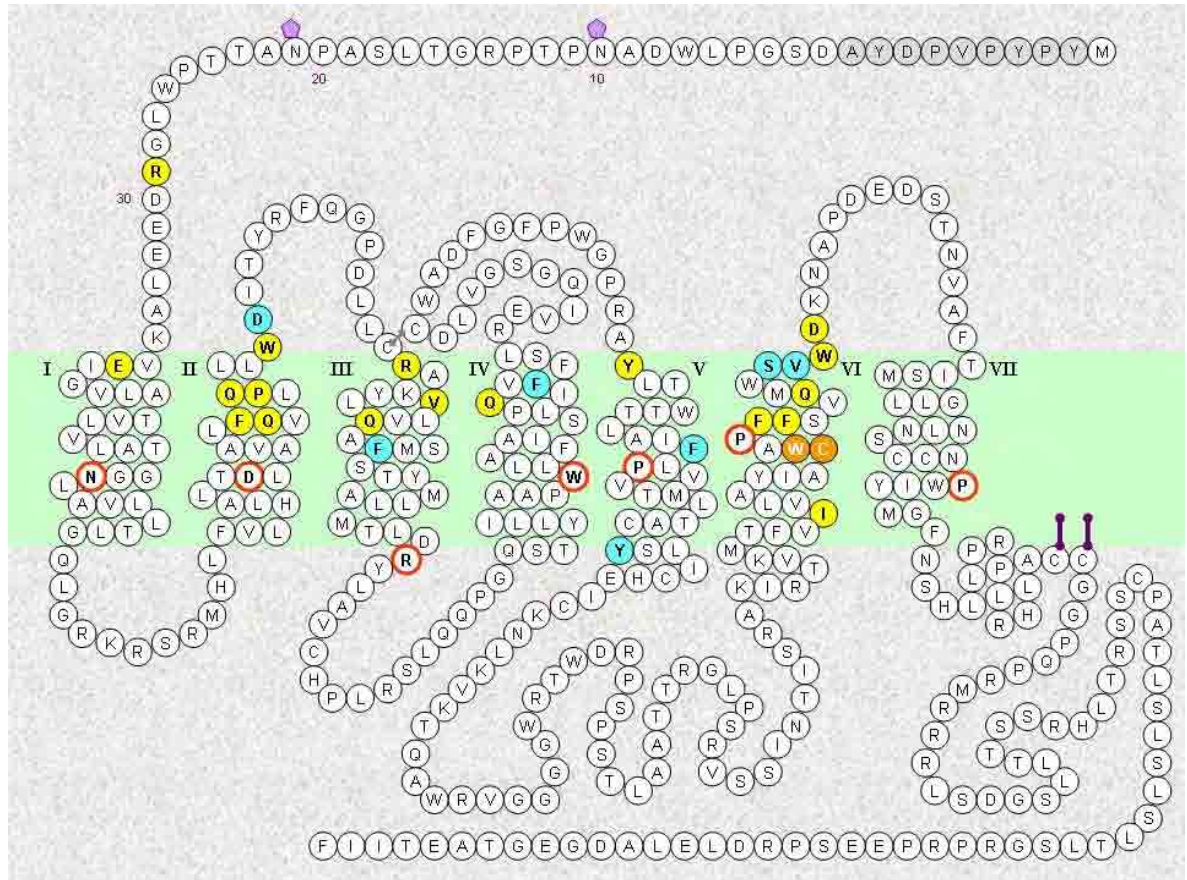


Figure 3.3 The schematic two-dimensional representation of V_{1b}R indicating residues selected for the mutagenesis study (shown as colour-filled):

The residues conserved within vasopressin receptors and OTR are shown in yellow, the residues conserved within three subtypes are shown in turquoise (as in the figure 3.1. The same colour code applied). Pale orange indicates residues within the CWXP motif of the proposed rotamer switch; the two residues were also studied.

The residues circled with orange line are indicated as reference residues used in Ballesteros-Weinstein numbering scheme. Lavender pentagons show the putative glycosylation sites. The purple lines on the right indicate putative palmitoylation sites. The residues comprising HA epitope tag are shown in pale grey.

Table 3.1 The mutagenic oligonucleotide primers for mutagenesis of V_{1b}R:

Codon altered shown underlined, and the nucleotides changed shown in **BOLD**. As for directions, (S) is sense, and (AS) is antisense.

Construct	Direction	Nucleotide Sequence
[R1.27A]V _{1b} R	(S) (AS)	5'-CCC-TGG-CTG-GGC- <u>GCG</u> -GAT-GAG-GAG-CTG-G-3' 5'-C-CAG-CTC-C'TC-ATC- <u>CGC</u> -GCC-CAG-CCA-GGG-3'
[R1.27E]V _{1b} R	(S) (AS)	5'-CCC-TGG-CTG-GGC- <u>GAG</u> -GAT-GAG-GAG-CTG-G-3' 5'-C-CAG-CTC-C'TC-ATC- <u>CTC</u> -GCC-CAG-CCA-GGG-3'
[E1.35A]V _{1b} R	(S) (AS)	5'-G-CTG-GCC-AAG-GTG- <u>GCA</u> -ATC-GGA-GTC-CTG-G-3' 5'-C-CAG-GAC-TCC-GAT- <u>TGC</u> -CAC-CTT-GGC-CAG-C-3'
[E1.35R]V _{1b} R	(S) (AS)	5'-G-CTG-GCC-AAG-GTG- <u>CGG</u> -ATC-GGA-GTC-CTG-G-3' 5'-C-CAG-GAC-TCC-GAT- <u>CCG</u> -CAC-CTT-GGC-CAG-C-3'
[E1.35D]V _{1b} R	(S) (AS)	5'-G-CTG-GCC-AAG-GTG- <u>GAC</u> -ATC-GGA-GTC-CTG-G-3' 5'-C-CAG-GAC-TCC-GAT- <u>GTC</u> -CAC-CTT-GGC-CAG-C-3'
[E1.35Q]V _{1b} R	(S) (AS)	5'-G-CTG-GCC-AAG-GTG- <u>CAG</u> -ATC-GGA-GTC-CTG-G-3' 5'-C-CAG-GAC-TCC-GAT- <u>CTG</u> -CAC-CTT-GGC-CAG-C-3'
[F2.56A]V _{1b} R	(S) (AS)	5'-GCC-GTG-GCG-CTC- <u>GCC</u> -CAG-GTG-CTG-CCA-C-3' 5'-G-TGG-CAG-CAC-CTG- <u>GGC</u> -GAG-CGC-CAC-GGC-3'
[Q2.57A]V _{1b} R	(S) (AS)	5'-C-GTG-GCG-CTC-TTC- <u>GCG</u> -GTG-CTG-CCA-CAG-3' 5'-CTG-TGG-CAG-CAC- <u>CGC</u> -GAA-GAG-CGC-CAC-G-3'
[P2.60A]V _{1b} R	(S) (AS)	5'-C-TTC-CAG-GTG-CTG- <u>GCA</u> -CAG-CTG-CTG-TGG-3' 5'-CCA-CAG-CAG-CTG- <u>TGC</u> -CAG-CAC-CTG-GAA-G-3'
[P2.60G]V _{1b} R	(S) (AS)	5'-C-TTC-CAG-GTG-CTG- <u>GGA</u> -CAG-CTG-CTG-TGG-3' 5'-CCA-CAG-CAG-CTG- <u>TCC</u> -CAG-CAC-CTG-GAA-G-3'
[Q2.61A]V _{1b} R	(S) (AS)	5'-C-CAG-GTG-CTG-CCA- <u>GCG</u> -CTG-CTG-TGG-GAC-3' 5'-GTC-CCA-CAG-CAG- <u>CGC</u> -TGG-CAG-CAC-CTG-G-3'
[W2.64A]V _{1b} R	(S) (AS)	5'-G-CCA-CAG-CTG-CTG- <u>GCC</u> -GA-CAT-CAC-CTA-CCG-3' 5'-CG-GTA-GGT-GAT-GTC- <u>CGC</u> -CAG-CAG-CTG-TGG-C-3'
[D2.65A]V _{1b} R	(S) (AS)	5'-CCA-CAG-CTG-CTG-TGG- <u>GCC</u> -ATC-ACC-TAC-CGC-3' 5'-GCG-GTA-GGT-GAT- <u>GGC</u> -CCA-CAG-CAG-CTG-TGG-3'
[D2.65Q]V _{1b} R	(S) (AS)	5'-CA-CAG-CTG-CTG-TGG- <u>CAG</u> -ATC-ACC-TAC-CGC-3' 5'-GCG-GTA-GGT-GAT- <u>CTG</u> -CCA-CAG-CAG-CTG-TG-3'
[D2.65R]V _{1b} R	(S) (AS)	5'-CA-CAG-CTG-CTG-TGG- <u>CGG</u> -ATC-ACC-TAC-CGC-3' 5'-GCG-GTA-GGT-GAT- <u>CCG</u> -CCA-CAG-CAG-CTG-TG-3'
[Q2.61D/ D2.65Q]V _{1b} R	(S) (AS)	5'-C- <u>GAC</u> -GTG-CTG-CCA- <u>CAG</u> -CTG-CTG-TGG-CAG-3' 5'-CTG-CCA-CAG-CAG- <u>CTG</u> -TGG-CAG-CAC- <u>GTC</u> -G-3'
[W2.64A/ D2.65A]V _{1b} R	(S) (AS)	5'-G-CCA-CAG-CTG-CTG- <u>GCC</u> - <u>GCC</u> -ATC-ACC-TAC-CG-3' 5'- CG-GTA-GGT-GAT- <u>GGC</u> - <u>CGC</u> -CAG-CAG-CTG-TGG-C-3'
[W2.64D/ D2.65W]V _{1b} R	(S) (AS)	5'-CCA-CAG-CTG-CTG- <u>GAC</u> - <u>TGG</u> -ATC-ACC-TAC-CGC-3' 5'- GCG-GTA-GGT-GAT- <u>CCA</u> - <u>GTC</u> -CAG-CAG-CTG-TGG-3'
[R3.26D]V _{1b} R	(S) (AS)	5'-CCC-GAC-CTC-CTG-TGC- <u>GAC</u> -GCC-GTC-AAG-TAC-CTG-3' 5'-CAG-GTA-CTT-GAC-GGC- <u>GTC</u> -GCA-CAG-GAG-GTC-GGG-3'
[V3.28A]V _{1b} R	(S) (AS)	5'-CTG-TGC-AGG-GCC- <u>GCC</u> -AAG-TAC-CTG-CAG-3' 5'-CTG-CAG-GTA-CTT- <u>GGC</u> -GGC-CCT-GCA-CAG-3'
[Q3.32A]V _{1b} R	(S) (AS)	5'-GCC-GTC-AAG-TAC-CTG- <u>GCG</u> -GTG-CTC-AGC-ATG-3' 5'- CAT-GCT-GAG-CAC- <u>CGC</u> -CAG-GTA-CTT-GAC-GGC-3'

Construct	Direction	Nucleotide Sequence
[F3.37A]V _{1b} R	(S) (AS)	5'-G-CAG-GTG-CTC-AGC-ATG- <u>GCT</u> -GCC-TCC-ACC-TAC-3' 5'-GTA-GGT-GGA-GGC- <u>AGC</u> -CAT-GCT-GAG-CAC-CTG-C-3'
[Q4.60A]V _{1b} R	(S) (AS)	5'-C-TTC-AGC-CTC-CCT- <u>GCA</u> -GTC-TTC-ATT-TTT-TCC-C-3' 5'-G-GGA-AAA-AAT-GAA-GAC- <u>TGC</u> -AGG-GAG-GCT-GAA-G-3'
[F4.62A]V _{1b} R	(S) (AS)	5'-C-CTC-CCT-CAA-GTC- <u>GCC</u> -ATT-TTT-TCC-CTG-CGG-G-3' 5'-C-CCG-CAG-GGA-AAA-AAT- <u>GGC</u> -GAC-TTG-AGG-GAG-G-3'
[Y5.38A]V _{1b} R	(S) (AS)	5'-GG-CCA-CGG-GCC- <u>GCC</u> -CTC-ACC-TGG-ACC-3' 5'-GGT-CCA-GGT-GAG- <u>GGC</u> -GGC-CCG-TGG-CC-3'
[F5.47A]V _{1b} R	(S) (AS)	5'-CC-ACC-CTG-GCT-ATC- <u>GCC</u> -GTT-CTG-CCG-GTG-3' 5'-CAC-CCG-CAG-AAC- <u>GGC</u> -GAT-AGC-CAG-GGT-GG-3'
[F5.47I]V _{1b} R	(S) (AS)	5'-CCC-TGG-CTA- <u>ATC</u> -TCG-TTC-TGC-CGG-TG-3' 5'-CA-CCG-GCA-GAA-CGA- <u>GAT</u> -TAC-CCA-GGG-3'
[F5.47V]V _{1b} R	(S) (AS)	5'-CC-CTG-GCT-ATC- <u>GTC</u> -GTT-CTG-CCG-GTG-3' 5'-CAC-CCG-CAG-AAC- <u>GAC</u> -GAT-AGC-CAG-GG-3'
[F5.47W]V _{1b} R	(S) (AS)	5'-CC-ACC-CTG-GCT-ATC- <u>TGG</u> -GTT-CTG-CCG-GTG-3' 5'-CAC-CCG-CAG-AAC- <u>CCA</u> -GAT-AGC-CAG-GGT-GG-3'
[F5.47Y]V _{1b} R	(S) (AS)	5'-CC-CTG-GCT-ATC- <u>TAC</u> -GTT-CTG-CCG-GTG-ACC-3' 5'-GGT-CAC-CCG-CAG-AAC- <u>GTA</u> -GAT-AGC-CAG-GG-3'
[Y5.58A]V _{1b} R	(S) (AS)	5'-CTC-ACG-GCC-TGC- <u>GCC</u> -AGC-CTC-ATC-TGC-C-3' 5'-G-GCA-GAT-GAG-GCT- <u>GGC</u> -GCA-GGC-CGT-GAG-3'
[I6.40A]V _{1b} R	(S) (AS)	5'-G-AAG-ATG-ACC-TTT-GTC- <u>GCC</u> -GTG-CTG-GCC-TAC-3' 5'- GTA-GGC-CAG-CAC- <u>GGC</u> -GAC-AAA-GGT-CAT-CTT-C-3'
[C6.47A]V _{1b} R	(S) (AS)	5'-GCC-TAC-ATC-GCT- <u>GCC</u> -TGG-GCT-CCC-TTC-3' 5'-GAA-GGG-AGC-CCA- <u>GGC</u> -AGC-GAT-GTA-GGC-3'
[W6.48A]V _{1b} R	(S) (AS)	5'-CC-TAC-ATC-GCT-TGC- <u>GCG</u> -GCT-CCC-TTC-TTC-AGT-G-3' 5'- C-ACT-GAA-GAA-GGG-AGC- <u>CGC</u> -GCA-AGC-GAT-GTA-GG-3'
[W6.48F]V _{1b} R	(S) (AS)	5'-CC-TAC-ATC-GCT-TGC- <u>TTC</u> -GCT-CCC-TTC-TTC-3' 5'-GAA-GAA-GGG-AGC- <u>GAA</u> -GCA-AGC-GAT-GTA-GG-3'
[F6.51A]V _{1b} R	(S) (AS)	5'-GCT-TGC-TGG-GCT-CCC- <u>GCC</u> -TTC-AGT-GTC-CAG-ATG-3' 5'-CAT-CTG-GAC-ACT-GAA- <u>GGC</u> -GGG-AGC-CCA-GCA-AGC-3'
[F6.52A]V _{1b} R	(S) (AS)	5'-GG-GCT-CCC-TTC- <u>GCC</u> -AGT-GTC-CAG-ATG-TGG-3' 5'-CCA-CAT-CTG-GAC-ACT- <u>GGC</u> -GAA-GGG-AGC-CC-3'
[Q6.55A]V _{1b} R	(S) (AS)	5'-CCC-TTC-TTC-AGT-GTC- <u>GCG</u> -ATG-TGG-TCC-GTG-TGG-3' 5'-CCA-CAC-GGA-CCA-CAT- <u>CGC</u> -GAC-ACT-GAA-GAA-GGG-3'
[S6.58A]V _{1b} R	(S) (AS)	5'-GTC-CAG-ATG-TGG- <u>GCC</u> -GTG-TG-GAC-AAG-3' 5'-CTT-GTC-CCA-CAC- <u>GGC</u> -CCA-CAT-CTG-GAC-3'
[V6.59A]V _{1b} R	(S) (AS)	5'-CAG-ATG-TGG-TCC- <u>GCG</u> -TGG-GAC-AAG-AAT-GCC-3' 5'-GGC-ATT-CTT-GTC-CCA- <u>CGC</u> -GGA-CCA-CAT-CTG-3'
[W6.60A]V _{1b} R	(S) (AS)	5'-G-ATG-TGG-TCC-GTG- <u>GCG</u> -GAC-AAG-AAT-GCC-CC-3' 5'-GG-GGC-ATT-CTT-GTC- <u>CGC</u> -CAC-GGA-CCA-CAT-C-3'
[D6.61A]V _{1b} R	(S) (AS)	5'-GG-TCC-GTG-GCG- <u>GCC</u> -AAG-AAT-GCC-CCT-G-3' 5'-C-AGG-GGC-ATT-CTT- <u>GGC</u> -CCA-CAC-GGA-CC-3'

3.2.2. The role of conserved residues in the N-terminal/juxtamembrane region of TM1 in V_{1b}R

The two residues Arg^{1.27} and Glu^{1.35} have been proven in the V_{1a}R, and OTR to be involved independently in AVP binding and the consequential signalling (Wootten and Wheatley, manuscript in preparation). Hence the two residues were studied further in the V_{1b}R to investigate whether similar mechanisms of AVP binding apply. Using QuickChange™ mutagenesis method described in section 2.2.1, both residues were initially replaced with alanine individually. The role of Glu^{1.35} was further investigated using systematic substitution. Three mutant constructs [E1.35D]V_{1b}R, [E1.35Q]V_{1b}R, and [E1.35R]V_{1b}R, specifically altered the properties of Glu^{1.35} in defined ways: Asp (one carbon atom shorter in length); Gln (replacing negative charge with a polar group); and Arg (charge reversal). The affinity and potency of AVP on these constructs were investigated by means of radioligand binding assay and InsP₃ assay. In addition, with an assumption that there may possibly be a direct interaction occurring between AVP and Glu^{1.35}, the three constructs were subjected to study using modified AVP in a complementally fashion for their proposed interactions.

Arg^{1.27} and Glu^{1.35} are eight residues apart. Since Arg^{1.27} is located at the extracellular N-terminal region possibly associated with some degrees of flexibility, it is plausible for the residue to form a mutual charge-induced interaction with Glu^{1.35} at the extracellular end of TM1 in forming a binding cavity for AVP. A reciprocal double mutant [R1.27E/E1.35R]V_{1b}R was made to investigate the effect of the positional residue changes on AVP binding and the receptor activation.

	Over 20 fold increase in affinity
	5 ~ 19 fold increase in affinity
	2 ~ 4.9 fold increase in affinity
	2 ~ 4.9 fold decrease in affinity
	5 ~ 19 fold decrease in affinity
	20 ~ 999 fold decrease in affinity
	Over 1000 fold decrease in affinity

Construct	Binding Affinity (K_i , nM \pm S.E.M.)		Cell-surface Expression (% WT)	AVP-induced Internalisation (% unstimulated)	dDAVP-induced Internalisation (% unstimulated)
	AVP	dDAVP			
WT V_{1b}R	0.90 (\pm 0.13)	10.5 (\pm 2.0)	100	47 (\pm 4)	50 (\pm 5)
[R1.27A]V _{1b} R	11.05 (\pm 4.22)	Undetectable	95 (\pm 4)	37 (\pm 7)	19 (\pm 2)
[R1.27E]V _{1b} R	Undetectable [³ H]AVP binding		36 (\pm 2)	44 (\pm 3)	-
[E1.35A]V _{1b} R	Undetectable [³ H]AVP binding		38 (\pm 2)	45 (\pm 5)	29 (\pm 2)
[E1.35R]V _{1b} R	Undetectable [³ H]AVP binding		74 (\pm 2)	46 (\pm 2)	-
[R1.27E/E1.35R]V _{1b} R	Undetectable [³ H]AVP binding		47 (\pm 2)	36 (\pm 1)	-
[E1.35Q]V _{1b} R	17.86 (\pm 1.79)	Undetectable	67 (\pm 3)	49 (\pm 3)	41 (\pm 8)
[E1.35D]V _{1b} R	Undetectable [³ H]AVP binding		25 (\pm 4)	36 (\pm 7)	38 (\pm 2)

Table 3.2 Binding affinities, the cell-surface expression levels and the responsiveness to agonist-induced receptor internalisation:

Binding affinities were determined by competition binding assay. Since tritiated AVP was the only the tracer ligand available to study V_{1b}R, mutants with largely decreased affinity to AVP could not be characterised further. The results of the cell-surface expression were analysed using ANOVA with a Dunnett's multiple comparison test with the Wt as control. The data showed significant differences from the Wt are indicated in pale red ($P < 0.01$), or pale orange ($0.01 < P < 0.05$). The binding affinity obtained as K_i in nM are shown using the colour code above (top left). Each experiment was performed in triplicate, and the average values of three experiments were shown plus/minus SEM. Dash (-) means untested.

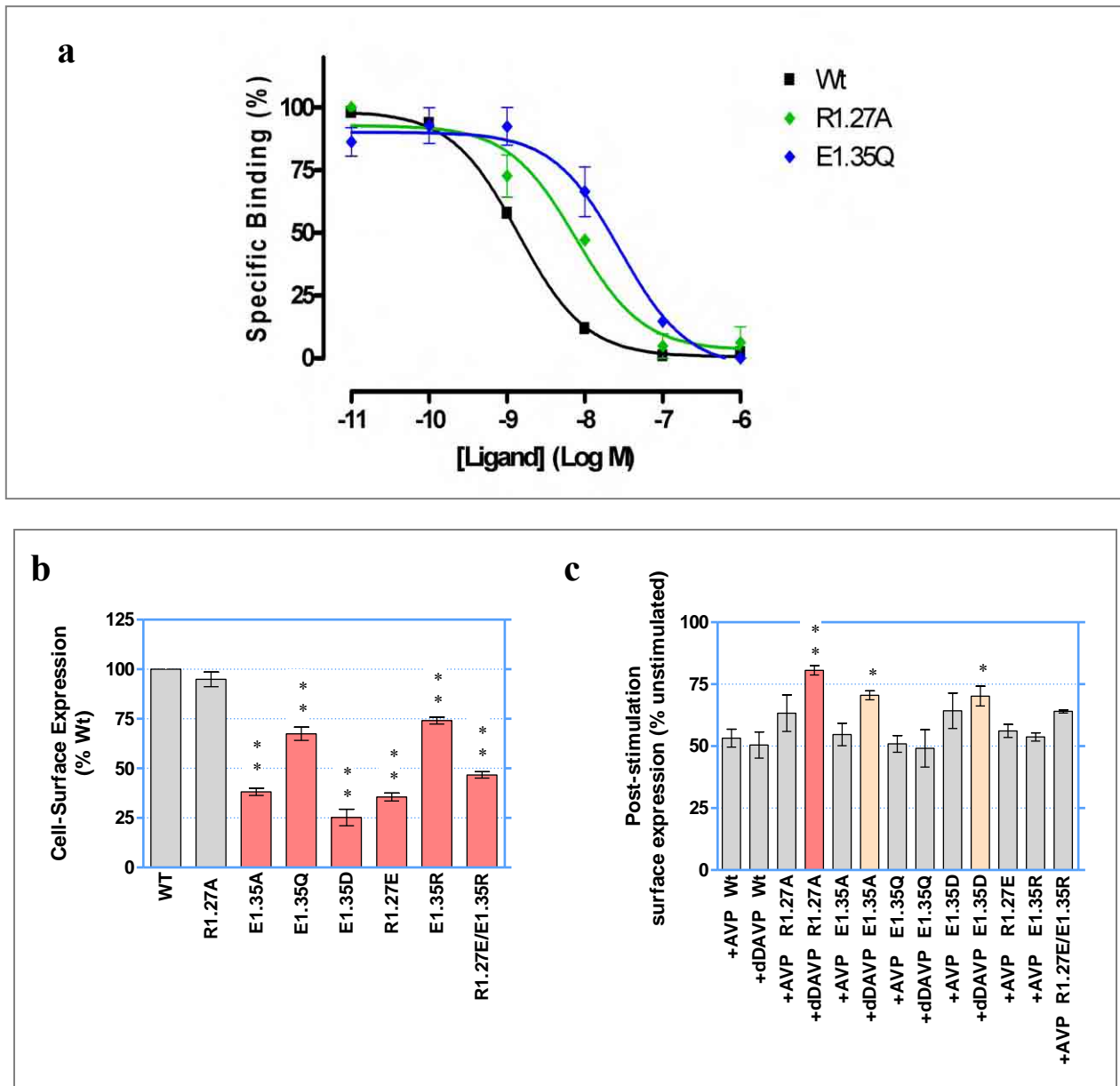


Figure 3.4 a-c AVP binding, the cell-surface expression and agonist induced internalisation of the mutant constructs:

- The competition binding of [^3H]AVP and AVP observed for the Wt $V_{1b}\text{R}$, [R1.27A] $V_{1b}\text{R}$ and [E1.35Q] $V_{1b}\text{R}$.
- The cell-surface expression levels of the mutant constructs relative to the Wt.
- The cell-surface expression after stimulation with either AVP or dDAVP as indicated (1 μM , 30 min). The data which showed significant differences after one-way ANOVA with Dunette's post test with the Wt as control, are indicated in pale red with two asterisks ($P < 0.01$) or pale orange with one asterisk ($0.01 < P < 0.05$).

The error bars represent SEM of three experiments each performed in triplicate.

AVP binding was undetectable for the constructs containing Glu^{1.35} substitution, with an exception of [E1.35Q]V_{1b}R which displayed approximately 20-fold reduction in the affinity of AVP; however the total [³H]AVP binding by the construct was low. Since [³H]AVP was the only tracer ligand available to study the V_{1b}R, the constructs were not further characterised for other ligands.

Two possible interactions occurring between Glu^{1.35} and AVP were predicted based on the AVP-docked molecular model of V_{1a}R provided by Simms. Firstly, it may be possible that there is an ionic interaction occurring between Arg⁸ of AVP and Glu^{1.35}. Secondary, the amide group of glycine of AVP could possibly form a hydrogen bond with carbonyl oxygen of Glu^{1.35}. Both interactions have been established in the V_{1a}R by Wootten and Wheatley (manuscript in preparation). In order to investigate these interactions in the V_{1b}R, three modified AVP-ligands were used. The interaction between Arg⁸ of AVP and Glu^{1.35} were tested by reversing the charged groups between AVP and V_{1b}R, using [E1.35R]V_{1b}R and [Glu⁸]vasopressin. The potential hydrogen bonding between the glycine of AVP and Glu^{1.35} were investigated in two ways: firstly using [β -Ala⁹NH₂]AVP and [E1.35D]V_{1b}R; and secondly using AVP-free acid and [E1.35Q]V_{1b}R. Figure 3.5 describes the proposed interaction between Glu^{1.35} and glycine, and also the interactions between the two alternatives. The potency of the ligands at each appropriate construct was measured by InsP-InsP₃ assay.

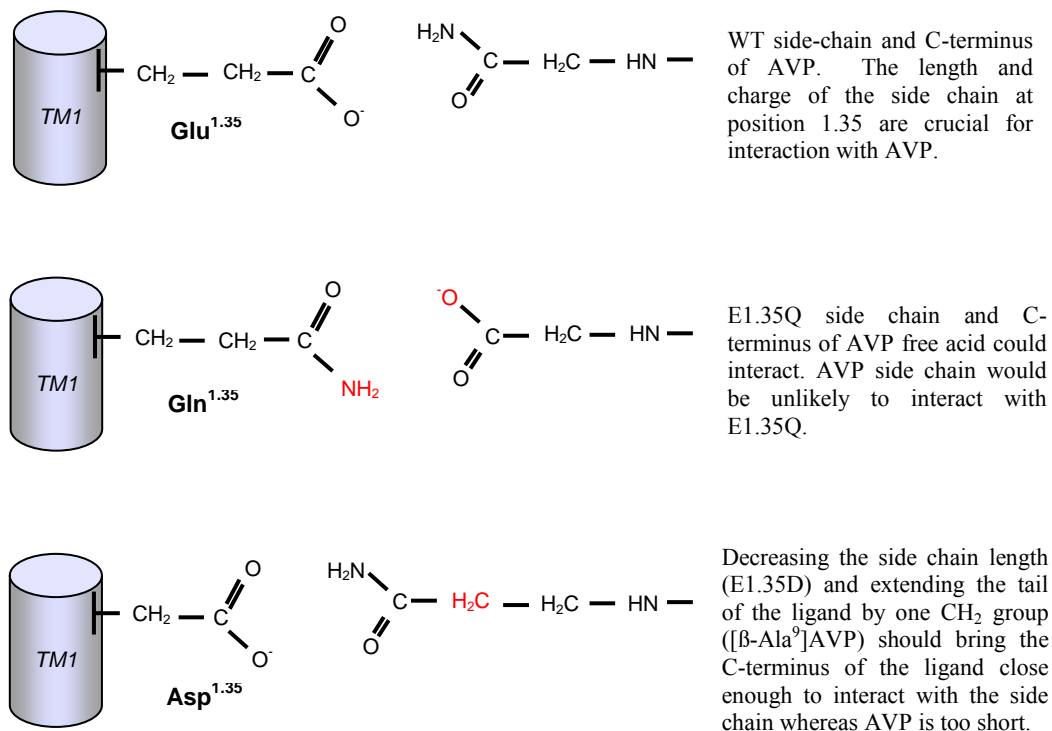


Figure 3.5 The rationale of the use of modified AVPs in specifying the interaction between Glu^{1.35} and the C-terminal glycinamide of AVP:

The plausible interactions proposed to occur between AVP and Glu^{1.35} can be determined by using modified AVP appropriately. In Wt receptor, Glu^{1.35} can be interacting with glycinamide of AVP (top). This interaction can be confirmed if AVP-free acid retains agonism upon binding to [E1.35Q]V_{1b}R. The carboxylic acid moiety and amidated C-terminal were reciprocally exchanged (middle). Alternatively, [β-Ala⁹NH₂]AVP may also induce agonism in [E1.35D]V_{1b}R in which the amino acid side chain at 1.35 was shortened one carbon length. The loss in length may be compensated by increasing the length of AVP glycinamide (bottom).

Construct	InsP-P3 accumulation (EC ₅₀ nM ±S.E.M.)			InsP-P3 accumulation E _{max} (% Wt)		
	AVP	dDAVP	dAVP	AVP	dDAVP	dAVP
WT V _{1b} R	2.8 (± 0.6)	12 (± 2)	4 (± 1)	100	100	100
[R1.27A]V _{1b} R	59 (± 4) *	12 (± 0.5)	-	76 (± 3) *	34 (± 4)	-
[E1.35A]V _{1b} R	55 (± 5) *	383 (± 93)	-	82 (± 2) *	46 (± 14)	-
[E1.35R]V _{1b} R	Undetectable	-	-	Undetectable	-	-
[R1.27E/E1.35R]V _{1b} R	Undetectable	-	-	Undetectable	-	-
[E1.35Q]V _{1b} R	19 (± 4)	90 (± 37)	105 (± 39)	50 (± 15)	31 (± 4)	70 (± 29)
[E1.35D]V _{1b} R	Undetectable	-	-	Undetectable	-	-

Construct	InsP-P3 accumulation (EC ₅₀ nM ±S.E.M.)			InsP-P3 accumulation E _{max} (% Wt, +AVP)		
	[βAla ⁹]-AVP	AVP-free acid	Glu ⁸ VP	[βAla ⁹]-AVP	AVP-free acid	Glu ⁸ VP
WT V _{1b} R	Undetectable	Undetectable	Undetectable	Undetectable	Undetectable	Undetectable
[E1.35R]V _{1b} R	-	-	13 (± 6)	-	-	22 (± 3)
[R1.27E/E1.35R]V _{1b} R	-	-	Undetectable	-	-	Undetectable
[E1.35Q]V _{1b} R	-	Undetectable	-	-	Undetectable	-
[E1.35D]V _{1b} R	Undetectable	-	-	Undetectable	-	-

Table 3.3. InsP₃ signalling properties of the V_{1b}R mutant constructs: EC₅₀ values were determined by non-linear regression and E_{max} values were obtained as a percentage of the maximum signal produced by the Wt V_{1b}R. Data shown are the mean ± SEM of three experiments each of which was performed in triplicate. Dashes (-) indicate where experiments were omitted. Data indicated with asterisk (*) was taken from doctoral thesis of Denise Wootten (Wootten D.L. 2007, University of Birmingham).

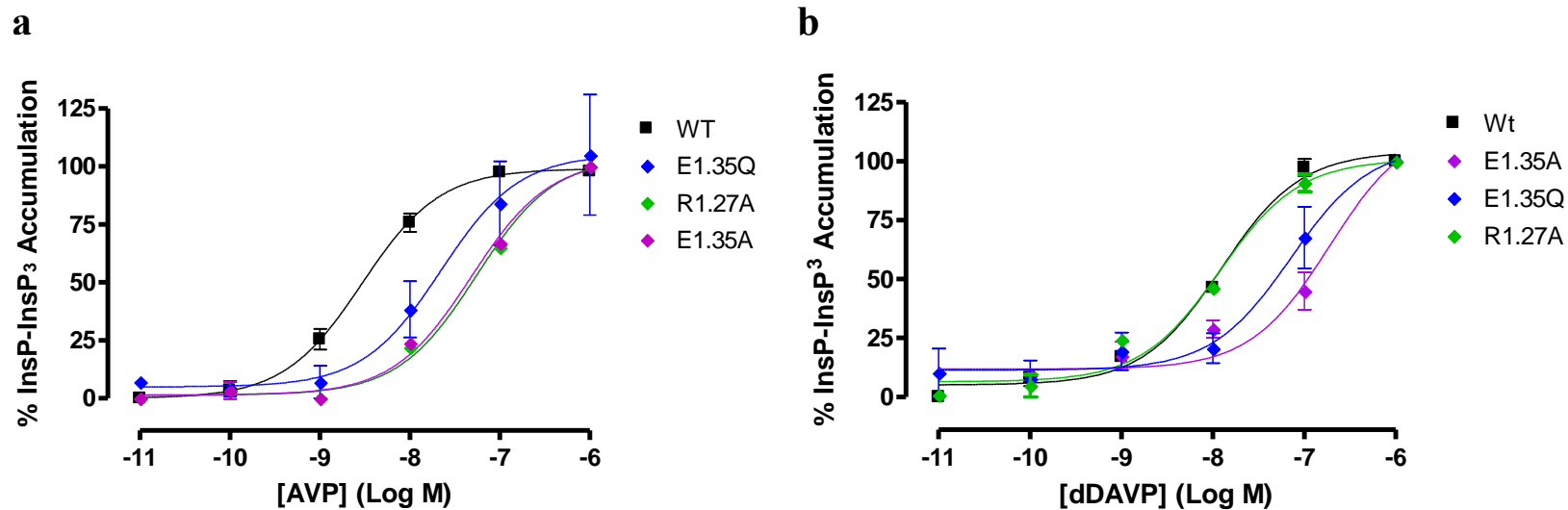


Figure 3.6 ab The InsP₃-signalling properties of V_{1b}R Wt and the mutant constructs: The percentage accumulations of InsP-Insp₃ fractions produced by the HEK293T cells transiently transfected with the mutant constructs and the Wt following agonist stimulation.

- a. InsP-Insp₃ accumulation in response to AVP.
- b. InsP-Insp₃ accumulation induced by dDAVP.

The error bars represent SEM of three experiments each performed in triplicate.

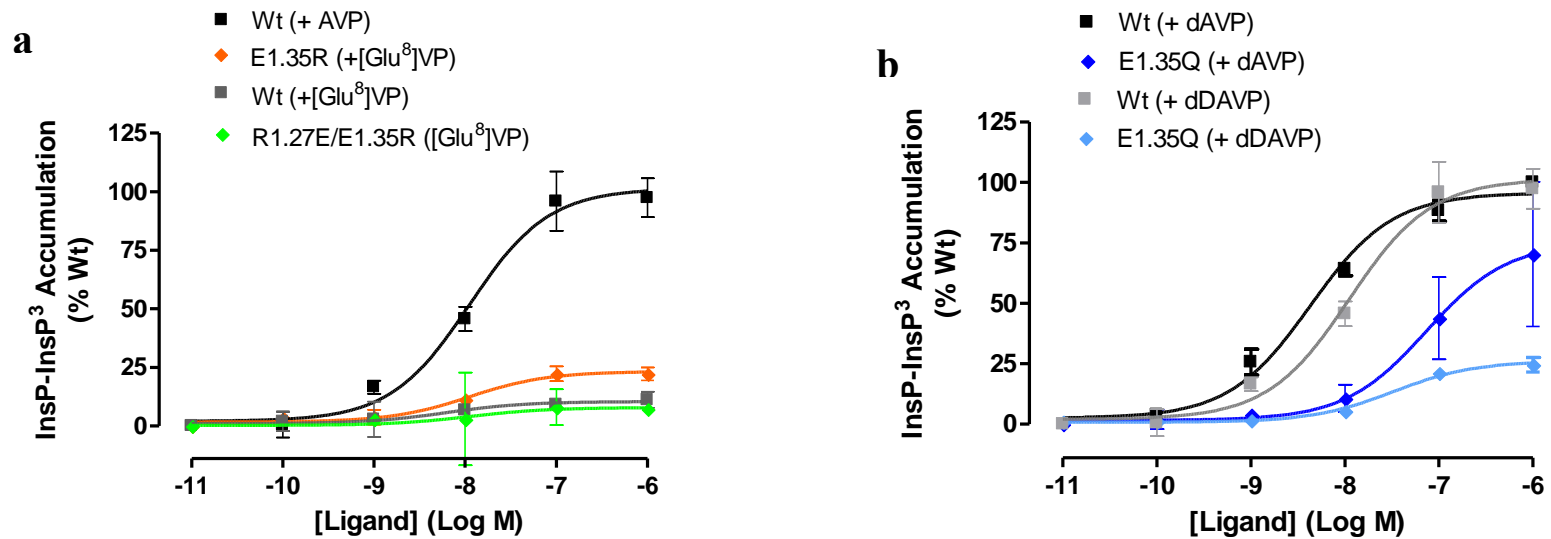


Figure 3.7 ab The InsP₃-signalling properties of V_{1b}R Wt and the mutant constructs:

The InsP-Insp₃ accumulation was normalised to the Wt data.

a. [E1.35R]V_{1b}R stimulated with [Glu⁸]vasopressin; the values were normalised to Wt stimulated with AVP to allow direct comparison.

b. Comparisons of the signalling properties of [E1.35Q]V_{1b}R initiated by dAVP or dDAVP.

The error bar represents SEM of three experiments each performed in triplicate.

Alanine substitution of Arg^{1.27} was reasonably well-tolerated in [R1.27A]V_{1b}R. The affinity of AVP for the construct was reduced about 10-fold compared to the Wt, and internalised in response to AVP stimulation at 1µM in a similar manner to the Wt. However, no detectable binding of dDAVP was observed, and only 15% of the construct was internalised following dDAVP stimulation. Although EC₅₀ value obtained was similar to the Wt, the E_{max} value was dramatically reduced to 22 % compared to the Wt.

Glu^{1.35} appeared more crucial in the V_{1b}R function. No detectable AVP binding was observed with [E1.35A]V_{1b}R, and the cell-surface expression was reduced dramatically to about 25% relative to the Wt. The construct, however, was capable of activating the PLC_β-induced signalling pathway but EC₅₀ increased approximately 20-fold for AVP, and 30-fold for dDAVP. The construct at the cell-surface was internalised following agonist stimulation with either AVP or dDAVP.

The conservative substitution of Glu by Asp at position 1.35 was poorly tolerated with complete loss of binding and signalling. The cell-surface expression of the construct was also reduced to 25% relative to the Wt. The proposed interaction between [E1.35D]V_{1b}R and [β -Ala⁹]AVP was not confirmed by the InsP₃ assay. In contrast, the substitution of Glu^{1.35} with Gln supported receptor function. The cell-surface expression level was restored to 75%, and [E1.35Q]V_{1b}R internalised in response to either AVP or dDAVP stimulation. The affinity of AVP was decreased 20-fold approximately and the potency decreased with 6-fold increase in EC₅₀ value and the lower efficacy with E_{max} value 50% relative to the Wt. The potency and the efficacy of dDAVP were lower with 10-fold increase in EC₅₀ value and E_{max} value 30% of the Wt. The signalling property of the construct induced by dAVP was apparently less affected with a high E_{max} of 70% to the Wt; however the EC₅₀ value obtained was about 100nM, in a

similar range of the value obtained for dDAVP. InsP₃ signalling in response to AVP-free acid was not detected in [E1.35Q]V_{1b}R.

InsP₃ signalling was detected in [E1.35R]V_{1b}R in response to [Glu⁸]VP with a high potency but with a low efficacy of E_{max} value 30% compared to the endogenous AVP signalling by the Wt. A reciprocal double mutant [R1.27E/E1.35R]V_{1b}R was made to investigate any interaction between these two residues, but the construct was not functional with no detectable binding nor signalling. The cell-surface expression of the construct was also compromised, ≈ 50% of the Wt. No signalling was detected by the double mutant following the [Glu⁸]VP stimulation despite the presence of Arg side chain located at position 1.35. No detectable AVP binding was obtained for each single mutant [R1.27E]V_{1b}R and [E1.35R]V_{1b}R.

3.2.3. The participation of TM2 residues in the ligand binding to the V_{1b}R

In this section, Gln^{2.61} and Asp^{2.65} which have been proven to be important for AVP binding to the V_{1a}R (Wootten D.L. Doctoral thesis, 2007, University of Birmingham) were investigated in the V_{1b}R. In addition, the conserved Phe^{2.56}, Gln^{2.57}, Pro^{2.60} and Trp^{2.64} of the FQVLPQXXW motif within the neurohypophysial hormone receptors family (figure 3.2), located at the upper region of TM2, were studied. Each residue was replaced with alanine. Pro^{2.60} may possibly provide a kink in the TM2 which is functionally relevant; therefore Pro^{2.60} was also substituted with glycine which allows the TM some degrees of flexibility. Usually, constructs contained a single alanine substitution; occasionally double mutants were produced to assess interaction between two different residues. Located at the juxtamembrane, [W2.64A/D2.65A]V_{1b}R, and also two reciprocal double mutants [Q2.61D/D2.65Q]V_{1b}R and [W2.64D/D2.65W]V_{1b}R were produced for further investigation.

The ligand binding properties of the constructs for AVP and the ligands with selectivity for V_{1b}R were investigated. A non-peptide antagonist 5234B with selectivity for V_{1b}R, synthesised by Schering-Plough Research Institute, was used to identify the contacting residues. Another V_{1b}R-selective non-peptide antagonist SSR149415, developed by Sanofi-Aventis, and also a V_{1b}R-selective peptide agonist d[Cha⁴]AVP, were also used in some constructs to further investigate the residues responsible for the ligand-selectivity of V_{1b}R. A peptide agonist dDAVP with selectivity for V_{1b}R and V₂R, and a peptide antagonist LA with selectivity for V_{1b}R and V_{1a}R, and a V_{1a}R-selective peptide antagonist CA were also used for further characterisations of some constructs.

The results of the radioligand binding assays are presented with a colour coding based on the fold-increase or -decrease observed. The cell-surface expression and the agonist-induced

internalisation of the receptor constructs are indicated with two colours depending on the significance of differences: pale red for $P < 0.01$ and pale orange for $P < 0.05$ in comparison to the WT, determined by ANOVA with a post-hoc Dunnett's test analysis. For a few constructs and the Wt, time-course study of up to one hour was performed to estimate the half-life of the cell-surface expression following exposure to the full agonist AVP.

Colour code used for the binding affinity

	Over 20 fold increase in affinity
	5 ~ 19 fold increase in affinity
	2 ~ 4.9 fold increase in affinity
	2 ~ 4.9 fold decrease in affinity
	5 ~ 19 fold decrease in affinity
	20 ~ 999 fold decrease in affinity
	Over 1000 fold decrease in affinity

Construct	Binding Affinity (K_i , nM \pm S.E.M.)			Cell-Surface Expression (% Wt)
	AVP	dDAVP	5234B	
WT V _{1b} R	0.90 (\pm 0.13)	10.5 (\pm 2.0)	7.18 (\pm 1.82)	100
[F2.56A]V _{1b} R	0.33 (\pm 0.03)	-	7.00 (\pm 2.26)	17 (\pm 1)
[Q2.57A]V _{1b} R	0.81 (\pm 0.29)	1.06 (\pm 0.22)	38.7 (\pm 4.8)	64 (\pm 2)
[P2.60A]V _{1b} R	Undetectable [³ H]AVP binding			19 (\pm 1)
[P2.60G]V _{1b} R	Undetectable [³ H]AVP binding			16 (\pm 1)
[Q2.61A]V _{1b} R	Undetectable [³ H]AVP binding			34 (\pm 9)
[W2.64A]V _{1b} R	5.06 (\pm 0.07)	10.6 (\pm 1.1)	10.1 (\pm 1.4)	119 (\pm 6)
[D2.65A]V _{1b} R	8.66 (\pm 0.13)	2.87 (\pm 0.59)	3.47 (\pm 0.40)	132 (\pm 12)
[D2.65Q]V _{1b} R	4.10 (\pm 1.51)	6.38 (\pm 1.05)	-	120 (\pm 3)
[D2.65R]V _{1b} R	3.82 (\pm 0.98)	-	-	132 (\pm 5)
[Q2.61D/D2.65Q]V _{1b} R	Undetectable [³ H]AVP binding			19 (\pm 1)
[W2.64A/D2.65A]V _{1b} R	Undetectable [³ H]AVP binding			114 (\pm 7)
[W2.64D/D2.65W]V _{1b} R	Undetectable [³ H]AVP binding			30 (\pm 1)

Table 3.4 The binding characteristics of the mutant constructs in TM2 domain of V_{1b}R:

The binding affinity (K_i) was determined by competition binding assay using [³H]AVP as a tracer ligand. Ligands are AVP, peptide agonist dDAVP, and non-peptide antagonist 5234B. Cell-surface expression of the constructs relative to the Wt was determined by ELISA. The constructs with severely compromised cell-surface expression are shown in pale red. The values shown as mean plus/minus SEM of three experiments each performed in triplicate. Dashes (-) indicates where experiments were omitted.

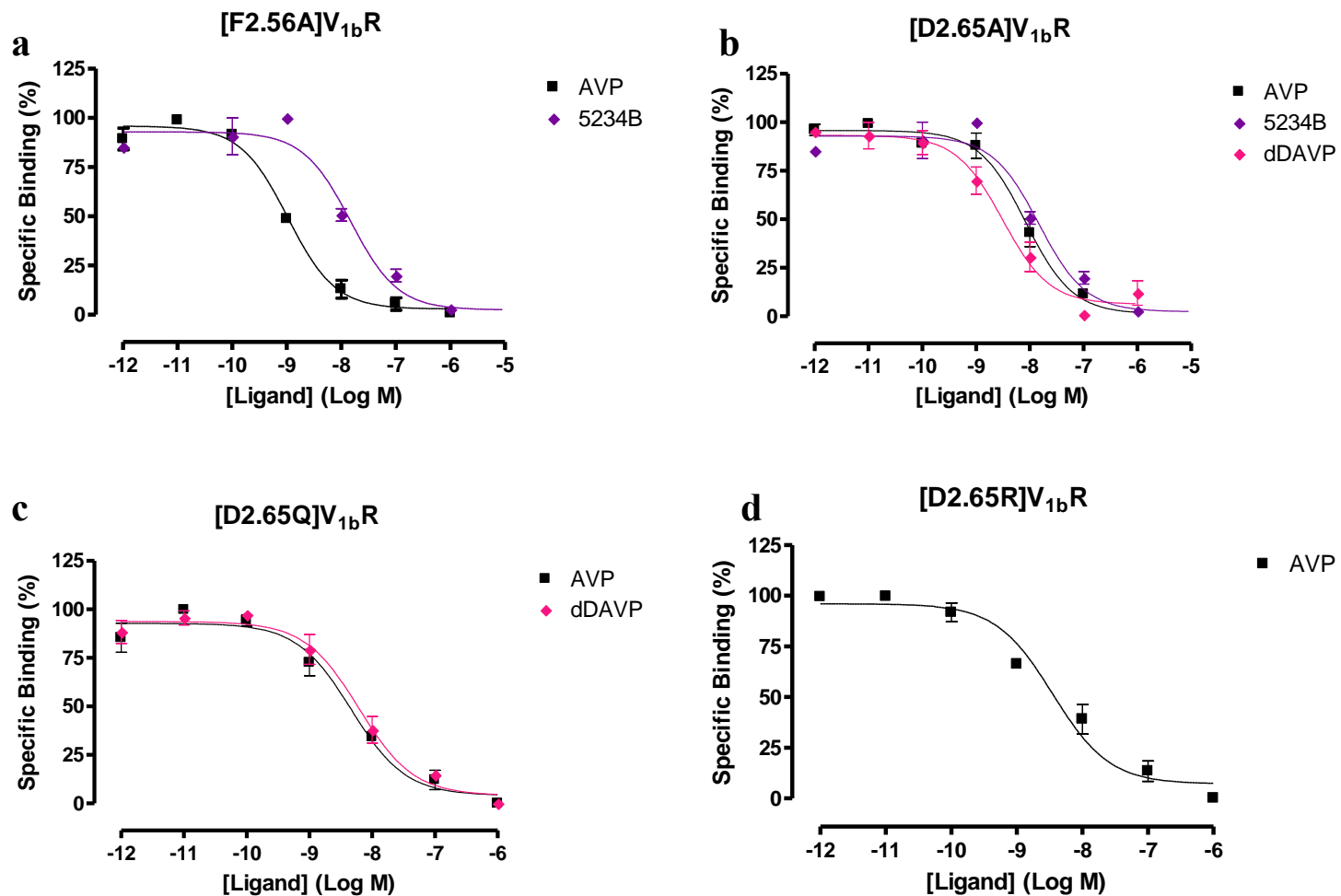
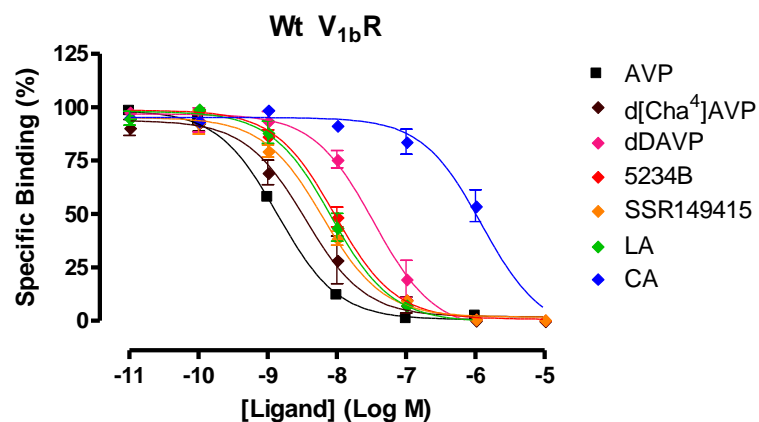


Figure 3.8 a-d Ligand binding profile of the TM2 mutant constructs:

Graphs show the competition binding of [³H]AVP and various ligands as indicated, in each construct: **a.** [F2.56A]V_{1b}R; **b.** [D2.56A]V_{1b}R; **c.** [D2.56Q]V_{1b}R; and **d.** [D2.56R]V_{1b}R. The values were normalised to show the percentage-specific bindings of [³H]AVP. The error bars represent SEM of three experiments each performed in triplicate.

Construct	Binding Affinity (K_i , nM \pm S.E.M.)							Cell-Surface Expression (% Wt)
	AVP	dDAVP	d[Cha ⁴]AVP	SSR149415	5234B	LA	CA	
WT V _{1b} R	0.90 (\pm 0.13)	10.5 (\pm 2.0)	1.35 (\pm 0.02)	3.36 (\pm 0.93)	7.18 (\pm 1.82)	6.25 (\pm 1.86)	159 (\pm 72)	100
[Q2.57A]V _{1b} R	0.81 (\pm 0.29)	1.06 (\pm 0.22)	1.07 (\pm 0.15)	2.30 (\pm 0.49)	38.7 (\pm 4.8)	0.67 (\pm 0.15)	3.58 (\pm 0.48)	64 (\pm 2)

a



b

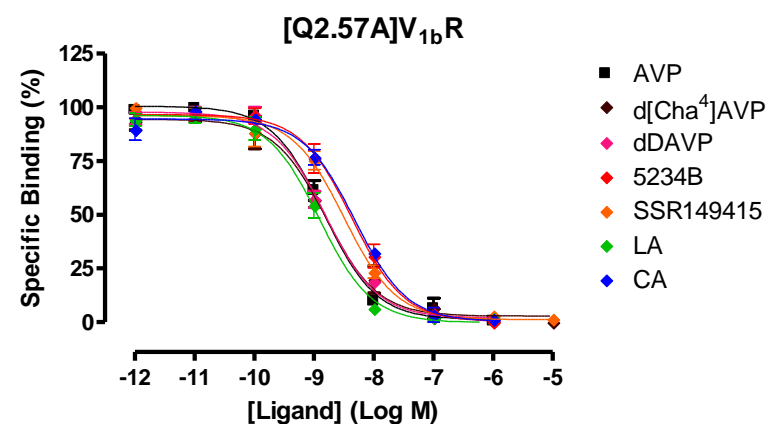


Table 3.5 The binding characteristics of the Wt V_{1b}R and [Q2.57A]V_{1b}R: The K_i values of various ligands binding to [Q2.57A]V_{1b}R are compared with the Wt. Peptide ligands: V_{1b}R-selective agonist dDAVP, d[Cha⁴]AVP, V_{1a}R/V_{1b}R-selective LA, V_{1a}R-selective CA. Non-peptide ligands: V_{1b}R-selective antagonist SSR149415, 5234B. The colour code applied as previous. The values were determined from three experiments each performed in triplicate.

Figure 3.9 ab The ligand binding properties of the Wt and [Q2.57A]V_{1b}R:

- Wt V_{1b}R The competition binding of [³H]AVP with various ligands as indicated.
- [Q2.57A]V_{1b}R The competition binding of [³H]AVP and various ligands as in the Wt. The error bars represent SEM of three experiments each performed in triplicate.

Construct	Binding Affinity (K_i , nM \pm S.E.M.)					Cell-Surface Expression (% Wt)
	AVP	dDAVP	LA	5234B	SSR149415	
WT $V_{1b}R$	0.90 (\pm 0.13)	10.5 (\pm 2.0)	6.25 (\pm 1.86)	7.18 (\pm 1.82)	3.36 (\pm 0.93)	100
[W2.64A] $V_{1b}R$	5.06 (\pm 0.07)	10.6 (\pm 1.1)	4.64 (\pm 0.54)	10.1 (\pm 1.4)	2.82 (\pm 0.41)	119 (\pm 6)

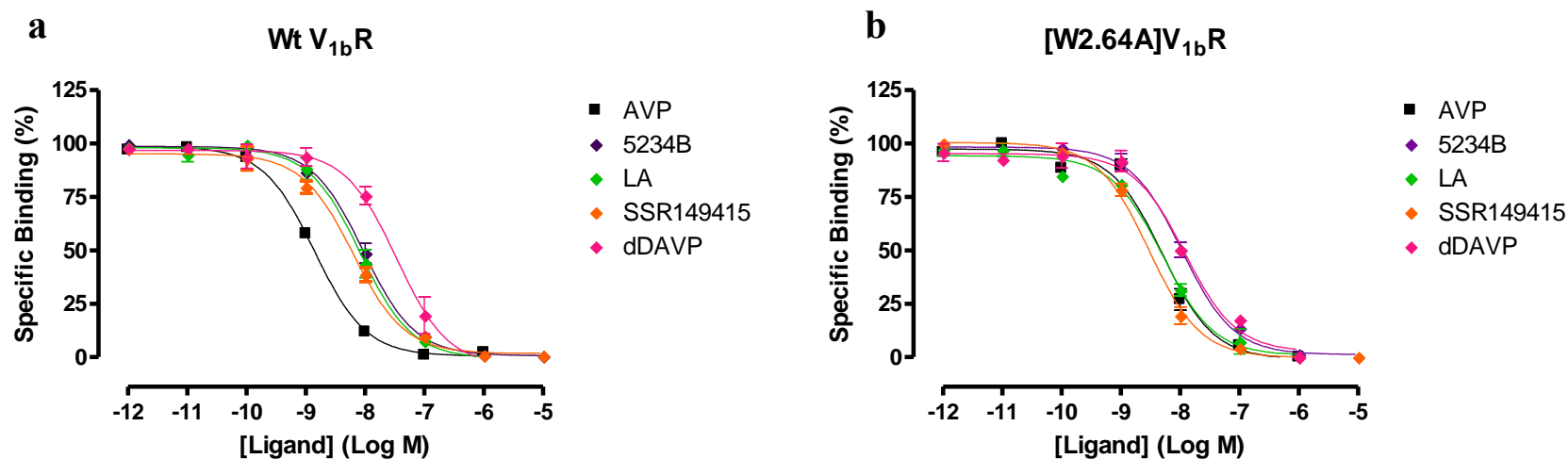
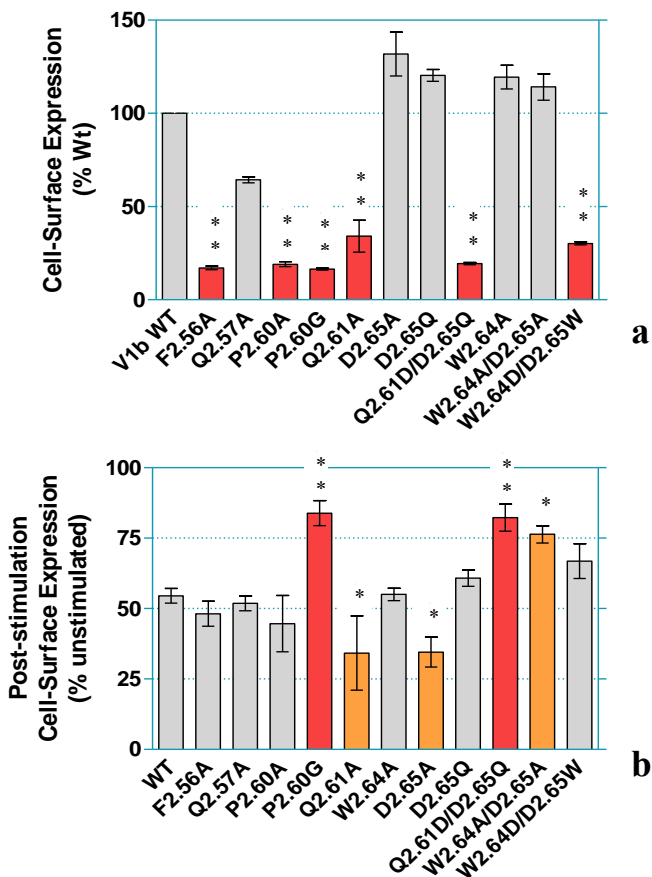


Table 3.6 The binding characteristics of the Wt $V_{1b}R$ and [W2.64A] $V_{1b}R$: The K_i values of various ligands binding to [W2.64A] $V_{1b}R$ are compared with the Wt. Peptide ligands: $V_{1b}R$ -selective agonist dDAVP and $V_{1a}R/V_{1b}R$ -selective LA. Non-peptide ligands: $V_{1b}R$ -selective antagonist SSR149415 and 5234B. The values were obtained from three experiments each performed in triplicate.

Figure 3.10 ab The ligand binding properties of the Wt and [W2.64A] $V_{1b}R$:

- Wt $V_{1b}R$ The competition binding of [3H]AVP and various ligands as indicated.
- [W2.64A] $V_{1b}R$ The competition binding of [3H]AVP and various ligands as in the Wt. The error bars represent SEM of three experiments each of which was performed in triplicate.



Construct	Cell-Surface Expression (% Wt)	AVP-induced internalisation (% unstimulated)
WT V_{1b}R	100	46 (± 3)
[F2.56A]V _{1b} R	17 (± 1)	52 (± 4)
[Q2.57A]V _{1b} R	64 (± 2)	48 (± 3)
[P2.60A]V _{1b} R	19 (± 1)	55 (± 10)
[P2.60G]V _{1b} R	16 (± 1)	16 (± 4)
[Q2.61A]V _{1b} R	34 (± 9)	66 (± 13)
[W2.64A]V _{1b} R	119 (± 6)	45 (± 2)
[D2.65A]V _{1b} R	132 (± 12)	65 (± 5)
[D2.65Q]V _{1b} R	120 (± 3)	39 (± 3)
[D2.65R]V _{1b} R	132 (± 5)	31 (± 7)
[Q2.61D/D2.65Q]V _{1b} R	19 (± 1)	18 (± 5)
[W2.64A/D2.65A]V _{1b} R	114 (± 7)	24 (± 3)
[W2.64D/D2.65W]V _{1b} R	30 (± 1)	33 (± 6)

Figure 3.11 ab The cell-surface expression of the mutant constructs and the V_{1b}R Wt:

- a.** The cell-surface expression of each mutant construct was shown relative to the Wt
- b.** The cell-surface expression after AVP-stimulation (1µM). The results were analysed statistically by one-way ANOVA with Dunett's post-test (P < 0.01 shown as pale-red, P < 0.05 shown as pale orange).
The error bars represent SEM of three experiments each performed in triplicate.

Table 3.7 The cell-surface expression and internalisation of the mutant constructs:

The cell-surface expression of the mutant constructs relative to the Wt, and the proportion of the constructs internalised are shown plus/minus SEM of three separate experiments each of which was in triplicate.

Time-course study of the agonist-induced internalisation

The cell-surface expression of [Q2.61A]V_{1b}R was significantly lower than that of the Wt, and the construct internalised proportionally more than the Wt in response to AVP stimulation. In contrast, a slightly higher cell-surface expression level was observed in [W2.64A/D2.65A]V_{1b}R compared to the Wt, and the construct internalised less proportionally to the Wt, in response to AVP stimulation. In order to investigate a possible link between the cell-surface expression level and the responsiveness of the receptors to the agonist-induced internalisation, the two constructs were subjected to a time-course study. The rate of internalisation was determined for these constructs in terms of the receptor half-life at the cell-surface, and the values were compared to that of the Wt.

Constructs (n. replicates)	$t_{1/2}$ (min)
WT (4)	7.75
Q2.61A (3)	6.17
W2.64A/D2.65A (3)	6.74

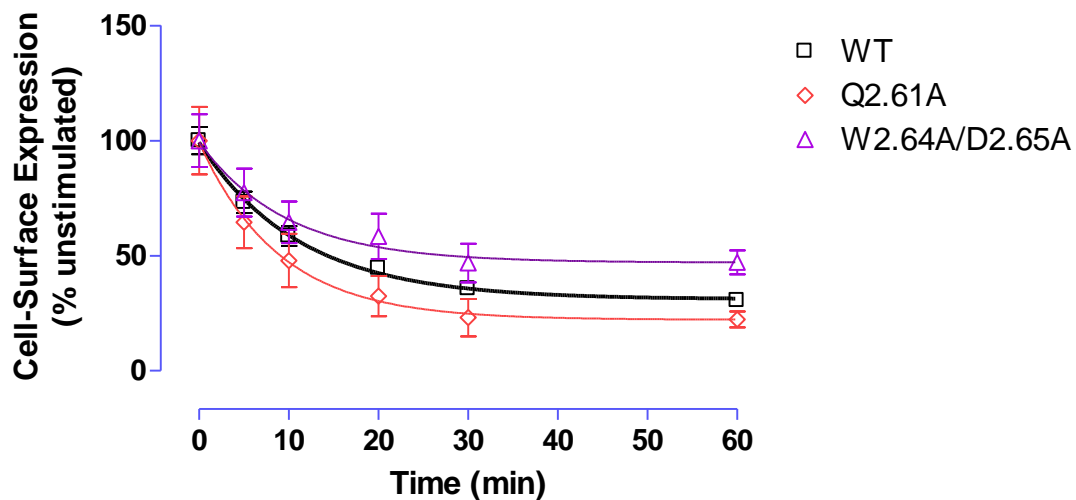


Table 3.8 The rate of internalisation of [Q2.61A] $V_{1b}R$, [W2.64A/D2.65A] $V_{1b}R$ and the Wt $V_{1b}R$: The rate of AVP-induced internalisation of the mutant constructs and the Wt were determined over one hour period. The cell-surface half-lives of the receptor constructs in HEK293T cell-line obtained are shown in minutes.

Figure 3.12 The time-course of the AVP-induced internalisation of the mutant constructs and the $V_{1b}R$ Wt: The percentage cell-surface expression after AVP-stimulation (1 μ M) relative to the unstimulated. Each set of values obtained were fitted with the one-phase exponential decay curve. Each curve represents mean plus/minus SEM of three or four separate experiments (as indicated in Table 3.8), each performed in triplicate.

3.2.3.i The summary of the results for the juxtamembrane Trp^{2.64} and Asp^{2.65}

Both Trp^{2.64} and Asp^{2.65} were shown to participate in AVP-binding as the alanine mutagenesis of either one of the residues resulted in a moderate decrease in the affinity to the V_{1b}R: \approx 5-fold decrease in [W2.64A]V_{1b}R, and \approx 10-fold decrease for [D2.65A]V_{1b}R. The substitution of Asp^{2.65} with Gln or Arg was tolerated equally well as Ala, and the affinity of AVP for [D2.65Q]V_{1b}R and [D2.65R]V_{1b}R are similar regardless of the differences in the polarities of the Gln and Arg side chains. Specific binding of [³H]AVP was undetectable in the double alanine mutant [W2.64A/D2.65A]V_{1b}R. Specific binding of [³H]AVP was not detected in the reciprocal double mutant [W2.64D/D2.65W]V_{1b}R.

The cell-surface expression was slightly but consistently elevated in the mutant constructs replacing either Trp^{2.64} or Asp^{2.65}, with an exception of [W2.64D/D2.65W]V_{1b}R. The reciprocal double mutant displayed dramatically reduced level of the cell-surface expression. Although the double alanine mutant retained the high cell-surface expression level, it showed a significantly reduced responsiveness to the agonist-induced internalisation. [D2.65A]V_{1b}R was on the other hand more responsive to the AVP-induced internalisation compared to the Wt. When the time-course study was applied to compare the rate of the internalisation between [W2.64A/D2.65A]V_{1b}R and Wt, no significant difference was recognised after t-test analysis. The cell-surface half-life of the Wt and [W2.64D/D2.65W]V_{1b}R following AVP-stimulation were both estimated to be approximately 7 minutes in HEK293T cell-line.

3.2.3.ii The summary of the results for Phe^{2.56}, Gln^{2.57}, Pro^{2.60}, and Gln^{2.61} of the conserved FQVLPQ motif

[F2.56A]V_{1b}R displayed dramatically reduced cell-surface expression. However, the mutant construct appeared to have retained binding characteristics similar to the Wt, and the receptors expressed on the cell-surface were internalised following exposure to AVP.

[Q2.57A]V_{1b}R retained Wt-like cell-surface expression and the receptor internalisation in response to AVP stimulation. The construct bound AVP, V_{1b}R-selective d[Cha⁴]AVP and V_{1b}R-selective non-peptide antagonist SSR149415 with similar affinities as the Wt. However, the affinity of the other V_{1b}R-selective antagonist 5234B to the construct was slightly compromised, with about 5-fold decrease in the K_i in comparison to the Wt. On the other hand, the relatively V_{1b}R-selective dDAVP and LA bound to [Q2.57A]V_{1b}R with increased affinities of ≈ 10-fold. Moreover, a highly V_{1a}R-selective peptide antagonist CA bound to the construct with a dramatically increased affinity of approximately 40-fold. These results suggest the involvement of Gln^{2.57} in constructing binding cavities characteristic of the V_{1b}R at least for the ligands which showed differences in this study.

The absence of Pro^{2.60} had detrimental effect on the V_{1b}R, as a dramatic decrease in the cell-surface expression was seen in [P2.60A]V_{1b}R, and the specific binding of AVP to the construct was undetectable with the concentration of [³H]AVP used. The construct was however internalised after incubating with AVP. In order to assess the role of Pro^{2.60}, [P2.60G]V_{1b}R was produced to allow the region of TM2 flexibility. Neither the cell-surface expression nor the AVP binding were recovered in [P2.60G]V_{1b}R compared to [P2.60A]V_{1b}R, and the AVP-induced internalisation was also compromised in this construct. These observations suggest that in the V_{1b}R, the cyclic structure of Pro^{2.60} with the relevant

hydrophobicity is important in this region as well as the proline-induced kink at an appropriate angle, in comparison to a mere flexibility which can also be induced by the Gly residue.

Gln^{2.61} also has a critical role in the V_{1b}R, as [Q2.61A]V_{1b}R showed a low level of the cell-surface expression and AVP binding was undetectable. However, the construct appeared to internalise more readily following AVP stimulation. Time-course study of the internalisation of [Q2.61A]V_{1b}R was carried out, and the construct appeared to internalise slightly faster with a reduced half-life of about 1.5 minutes compared to the Wt. However, t-test analysis of the results established that the difference was insignificant. The reciprocal mutant [Q2.61D/D2.65Q]V_{1b}R was produced to investigate whether the two residues were located closely and the roles could be inter-changeable. The construct did not appear to be functional with no detectable AVP binding, dramatically reduced levels of cell-surface expression and the internalisation. This suggests that both residues are likely to function independently, and the exact position of the residues is crucial in AVP binding as well as in maintaining structural integrity at the cell-surface.

3.2.3. The roles of the highly conserved residues of TM3 in the juxtamembrane region and the putative ligand binding site

Four residues of TM3 were selected for study, and these are: Arg^{3.26}, Val^{3.28}, and Gln^{3.32} which are located towards the extracellular terminal of TM3; and a core transmembrane residues Phe^{3.37}. Arg^{3.26} at the juxtamembrane is highly conserved in peptide GPCRs. Molecular modelling study on V_{1a}R by Simms predicted that Arg^{3.26} may interact with the phosphate group of phospholipids [428]. [R3.26D]V_{1b}R, in which the charge of the residue was reversed, was made to test whether the similar observation applies to the V_{1b}R.

Val^{3.28} and Gln^{3.36} are both conserved in the vasopressin receptors and OTR. Gln^{3.36} has been predicted to interact with AVP in V_{1a}R, V₂R and OTR based on the molecular modelling study by Ślusarz *et al.*. The same study has also predicted Val^{3.28} to be involved in the interaction with AVP in V_{1a}R [427]. Val^{3.28} and Gln^{3.36} were also predicted to participate in a V_{1b}R-selective antagonist Org52186 binding by molecular modelling study by Dr. Wishart in Schering-Plough (personal communication). [V3.28A]V_{1b}R and [Q3.32A]V_{1b}R were made to investigate the involvement of these residues in ligand binding by the V_{1b}R.

The aromatic residue Phe^{3.37} is conserved in vasopressin receptors and OTR with an exception of V₂R in which Tyr^{3.37} is found instead. Phe^{3.37} was suggested to be involved in AVP binding in OTR by Ślusarz *et al.*[427]. [F3.37A]V_{1b}R was made to study the involvement of this residue in the ligand binding of V_{1b}R.

Colour code applied to indicate fold-changes in binding affinity

	Over 20 fold increase in affinity
	5 ~ 19 fold increase in affinity
	2 ~ 4.9 fold increase in affinity
	2 ~ 4.9 fold decrease in affinity
	5 ~ 19 fold decrease in affinity
	20 ~ 999 fold decrease in affinity
	Over 1000 fold decrease in affinity

Construct	Binding Affinity (K_i , nM \pm S.E.M.)					Cell-Surface Expression (% Wt)
	AVP	dDAVP	SSR149415	5234B	LA	
Wt V _{1b} R	0.90 (\pm 0.13)	10.5 (\pm 2.7)	3.36 (\pm 0.93)	7.18 (\pm 1.82)	6.25 (\pm 1.86)	100
[R3.26D] V _{1b} R	Undetectable [³ H]AVP binding					49 (\pm 2)
[V3.28A]V _{1b} R	0.72 (\pm 0.22)	32.3 (\pm 6.0)	8.41 (\pm 0.40)	4.35 (\pm 0.36)	7.69 (\pm 2.08)	94 (\pm 7)
[Q3.32A]V _{1b} R	0.90 (\pm 0.23)	18.1 (\pm 2.4)	5.65 (\pm 0.91)	5.93 (\pm 0.94)	18.9 (\pm 3.0)	76 (\pm 9)
[F3.37A]V _{1b} R	0.97 (\pm 0.22)	11.2 (\pm 3.7)	1.97 (\pm 0.23)	6.23 (\pm 1.73)	0.67 (\pm 0.20)	21 (\pm 1)
[Y3.41A]V _{1b} R	0.92 (\pm 0.30)	757 (\pm 22)	55.0 (\pm 0.02)	4637 (\pm 685)	1.69 (\pm 0.23)	108 (\pm 3)

Table 3.9 The binding characteristics of the mutant constructs and the Wt V_{1b}R:

The values of K_i of various ligands, determined from three experiments each performed in triplicate, are shown plus/minus SEM. Peptide ligands: V_{1b}R-selective agonist dDAVP; peptide linear antagonists LA; V_{1a}R-selective cyclic antagonist CA. Non-peptide ligands: V_{1b}R-selective antagonist SSR149415, 5234B. The colour code applied as above. The cell-surface expression levels of the mutant and the Wt constructs were determined by ELISA. The figures in percentage relative to the Wt are shown on the far right column. The values shown are mean plus/minus SEM obtained from three experiments each performed in triplicate.

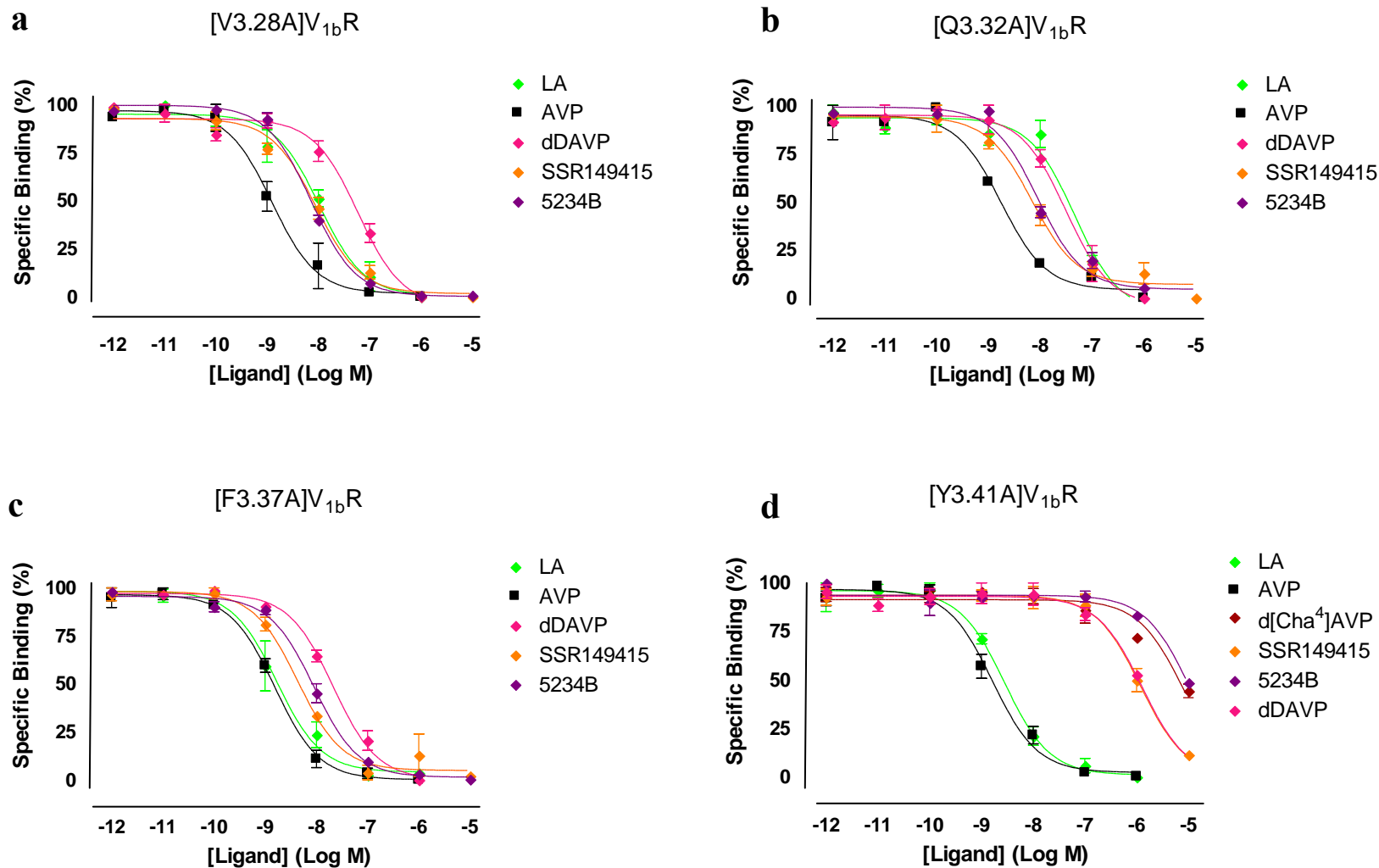
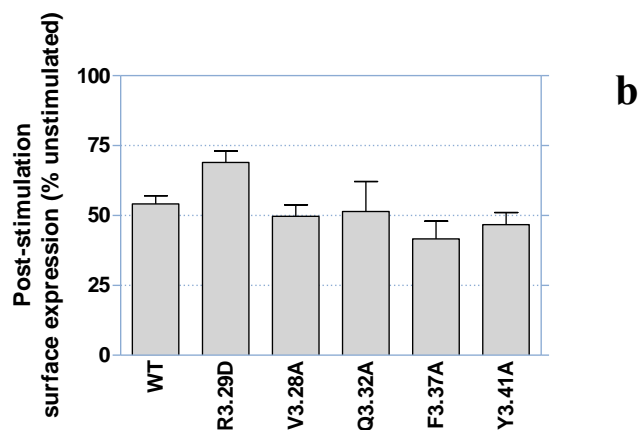
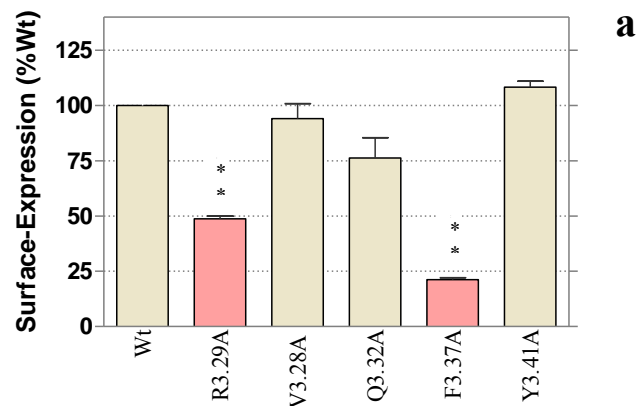


Figure 3.13.a-d Ligand binding profile of the Ala-substituted TM3 constructs:

Graphs show the competition binding of [³H]AVP and various ligands as indicated in each construct: **a** [V3.28A]V_{1b}R; **b** [Q3.32A]V_{1b}R; **c** [F3.37A]V_{1b}R; and **d** [Y3.41A]V_{1b}R. The values were normalised to show the percentage specific binding.



Construct	Cell-Surface Expression (% Wt)	AVP-induced internalisation (% unstimulated)
WT V _{1b} R	100	54 (± 3)
[R3.26A]V _{1b} R	49 (± 2)	69 (± 4)
[V3.28A]V _{1b} R	94 (± 7)	50 (± 4)
[Q3.32A]V _{1b} R	76 (± 9)	51 (± 11)
[F3.37A]V _{1b} R	21 (± 1)	42 (± 6)
[Y3.41A]V _{1b} R	108 (± 3)	53 (± 4)

Figure 3.14 ab The cell-surface expression of the mutant constructs and the V_{1b}R Wt:

- The cell-surface expression of each mutant construct was shown relative to the Wt
- The cell-surface expression after AVP-stimulation (1µM, 30 min). The results were analysed using ANOVA with Dunnett's post-test using the Wt as control (P < 0.01 indicated as pale-red with asterisks).

Table 3.10 The cell-surface expression and internalisation of the mutant constructs: The cell-surface expression of the mutant constructs relative to the Wt and the proportion of the constructs internalised in percentage are shown plus/minus SEM of three separate experiments each performed in triplicate.

3.2.4.i **The summary of the results**

Arg^{3.26} is highly conserved in peptide-GPCRs, located at the top of TM3 immediately next to Cys^{3.25} which forms the disulfide bond conserved throughout Family A GPCRs. The effect of charge reversal at this locus was investigated by studying [R3.26D]V_{1b}R. The construct did not bind to [³H]AVP. The cell-surface expression level of this construct was approximately 50% relative to the Wt.

The other three constructs, [V3.28A]V_{1b}R, [Q3.32A]V_{1b}R, and [F3.37A]V_{1b}R, all retained a high affinity binding to AVP, and that allowed further characterisations of these constructs with other ligands. [V3.28A]V_{1b}R displayed a slight decrease in affinity towards dDAVP and SSR149415, with increases in the K_i values 2 ~3 folds approximately. The affinity of LA to [Q3.32A]V_{1b}R was decreased with a 3-fold increase in the K_i , but this was the only effect observed in this construct. The cell-surface expression level of [F3.37A]V_{1b}R was reduced dramatically to 21% relative to the Wt, but the construct retained similar affinities for most ligands as Wt, with an exception of LA which increased affinity 9-fold.

The most notably, the binding characteristics of [Y3.41A]V_{1b}R were distinct from the Wt. The binding affinity of V_{1b}R-selective ligands, the agonist dDAVP and the antagonists 5234B and SSR149415, were reduced dramatically. The binding affinity of its native agonist AVP was unaffected, and the construct was internalised in a manner similar to the Wt.

3.2.5. The role of conserved aromatic, or polar residues of TM4 and TM5 in the ligand binding and receptor stability of V_{1b}R

Gln^{4.60} is a well-conserved residue in neurohypophysial hormone receptors (figure 3.1). The involvement of this residue in AVP binding to V_{1a}R, V₂R and OTR was predicted by the computational modelling study by Ślusarz *et al.* [427]. Two residues ahead of Gln^{4.60}, there is a semi-conserved Phe^{4.62}. The residue is conserved in vasopressin receptors. The OTR has a slightly smaller residue, His in place of Phe^{4.62}.

Three aromatic residues in TM5, Tyr^{5.38}, Phe^{5.47}, and Tyr^{5.58}, were subjected to Ala substitution. Phe^{5.47} is conserved in vasopressin receptors and also among many Family A GPCRs including rhodopsin (figure 3.1), while in a few GPCRs, including OTR, Tyr^{5.47} is found instead. The residue has been predicted by computational studies to be a contact site for AVP in V_{1a}R, V₂R and OTR by Ślusarz *et al.* [427], and also to be a site of interaction for SSR149415 in V_{1b}R by Derick *et al.* [434]. Tyr^{5.58} has been shown to interact with the Arg^{3.50} when the ‘ionic lock’ breaks during the rhodopsin activation [295]. To determine the ligand binding profiles of agonists and antagonists in the absence of the proposed interaction between Arg^{3.50} and Tyr^{5.58}, Tyr^{5.58} was substituted with Ala. In this section, the total of five receptor constructs [Q4.60A]V_{1b}R, [F4.62A]V_{1b}R, [Y5.38A]V_{1b}R, [F5.47A]V_{1b}R and [Y5.58A]V_{1b}R were made and characterised. The results obtained for these constructs are summarised in the first part of this section 3.2.5.I.

In transmembrane domains, aromatic or bulky hydrophobic side chains may have stabilising effects on the overall conformation of TM assembly. The constructs which did not tolerate Ala substitution were subsequently subjected to further substitution with a range of amino acids with various degrees of hydrophobicity. The results obtained for these constructs

are shown in the second part of this section 3.2.5.II. The mutant constructs were characterised for ligand binding, the cell-surface expression, and AVP-induced internalisation. The constructs containing amino acid substitution at 5.47 were also subjected to thermostability assays to assess the structural stability of these constructs.

3.2.5. I. Alanine mutagenesis

Colour code used to indicate fold-changes in binding affinity

	Over 20 fold increase in affinity
	5 ~ 19 fold increase in affinity
	2 ~ 4.9 fold increase in affinity
	2 ~ 4.9 fold decrease in affinity
	5 ~ 19 fold decrease in affinity
	20 ~ 999 fold decrease in affinity
	Over 1000 fold decrease in affinity

Construct	Binding Affinity (K_i , nM \pm S.E.M.)						Cell-Surface Expression (% Wt)
	AVP	dDAVP	d[Cha ⁴]AVP	LA	5234B	SSR149415	
WT V _{1b} R	0.90 (\pm 0.13)	10.5 (\pm 2.7)	1.35 (\pm 0.02)	6.25 (\pm 1.86)	7.18 (\pm 1.82)	3.36 (\pm 0.93)	100
[Q4.60A]V _{1b} R	2.54 (\pm 0.77)	8.88 (\pm 1.27)	1.22 (\pm 0.23)	34.5 (\pm 6.6)	105 (\pm 33)	1.85 (\pm 0.10)	126 (\pm 4)
[F4.62A]V _{1b} R	0.45 (\pm 0.18)	11.7 (\pm 2.3)	-	6.30 (\pm 0.97)	3.36 (\pm 1.00)	4.74 (\pm 0.52)	95 (\pm 11)
[Y5.38A]V _{1b} R	Undetectable [³ H]AVP binding						38 (\pm 2)
[F5.47A]V _{1b} R	Undetectable [³ H]AVP binding						9 (\pm 1)
[Y5.58A]V _{1b} R	1.85 (\pm 0.11)	9.48 (\pm 1.07)	-	6.21 (\pm 0.18)	16.1 (\pm 1.4)	5.01 (\pm 0.07)	113 (\pm 6)

Table 3.11 The binding characteristics of the mutant constructs and the Wt V_{1b}R: The values of K_i of various ligands are shown plus/minus SEM. Peptide ligands: V_{1b}R-selective agonist dDAVP and d[Cha⁴]AVP; peptide linear antagonists LA. Non-peptide ligands: V_{1b}R-selective antagonist SSR149415, 5234B. The colour code applied as above. The cell-surface expression levels of the mutant and the Wt constructs were determined by ELISA: the figures in percentage relative to the Wt are shown on the far right column. The values shown are mean plus/minus SEM of three experiments each performed in triplicate.

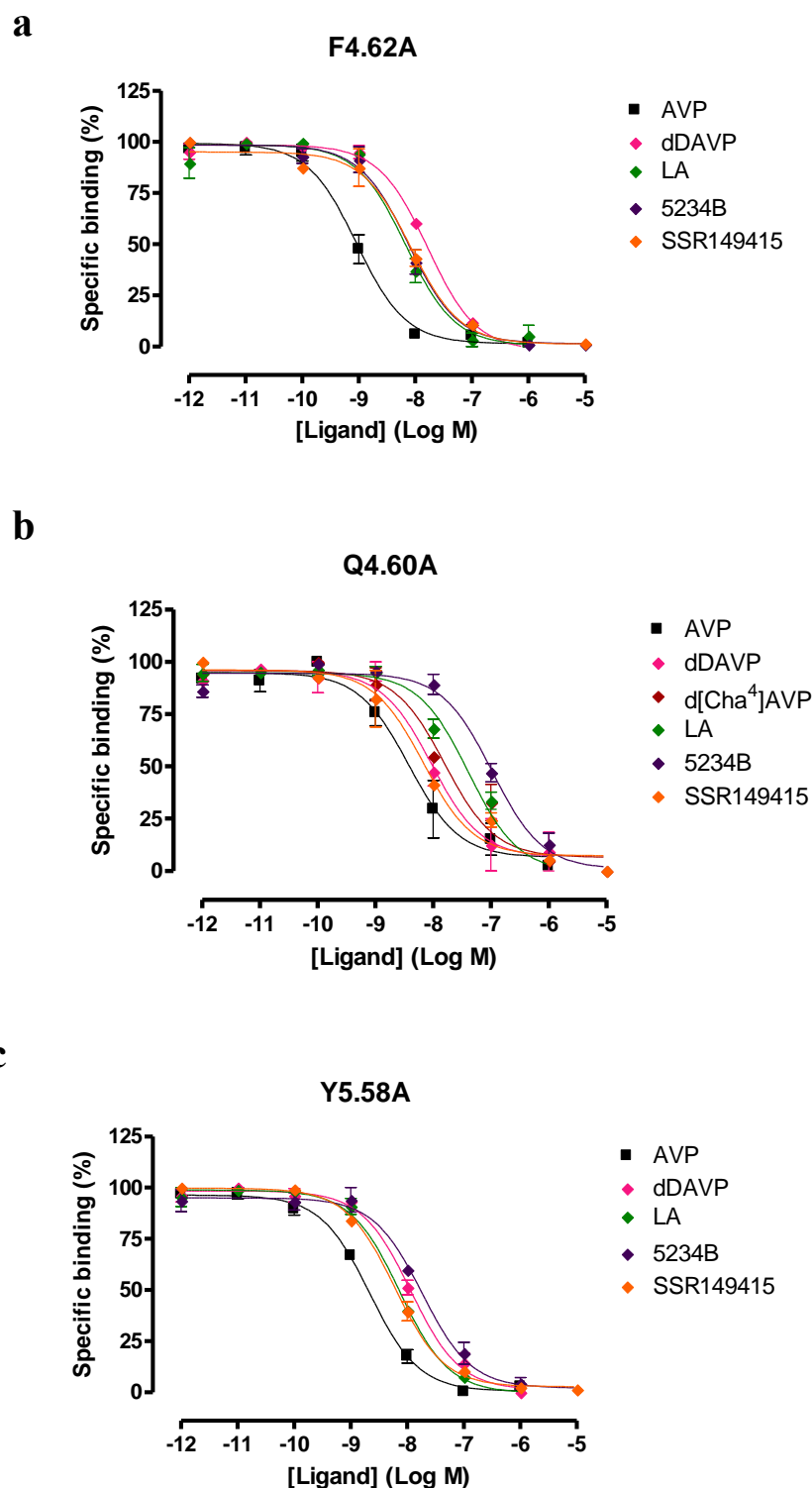
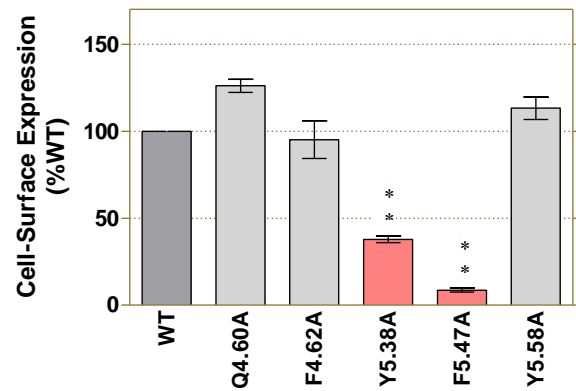
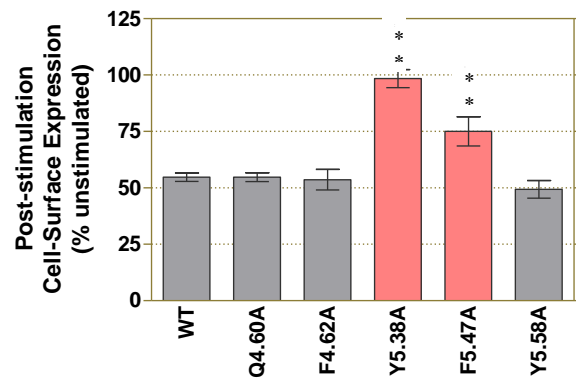


Figure 3.15.a-c Ligand binding profiles of [F4.62A]_{V_{1b}R}, [Q4.60A]_{V_{1b}R} and [Y5.58A]_{V_{1b}R}: Graphs show competition binding of [³H]AVP and various ligands as indicated, for mutant constructs each containing an alanine substitution: **a.** [F4.62A]_{V_{1b}R}; **b.** [Q4.60A]_{V_{1b}R}; **c.** [Y5.58A]_{V_{1b}R}. The values were normalised to show the percentage-specific bindings. The error bars represent SEM of three experiments performed in triplicate except dDAVP binding curves in [F4.62A]_{V_{1b}R} and [Y5.58A]_{V_{1b}R} where mean plus/minus SEM of single triplicated experiments are shown.



a



b

Construct	Cell-Surface Expression (% Wt)	AVP-induced internalisation (% unstimulated)
WT V _{1b} R	100	45 (± 2)
[Q4.60A]V _{1b} R	126 (± 4)	45 (± 2)
[F4.62A]V _{1b} R	95 (± 11)	46 (± 5)
[Y5.38A]V _{1b} R	38 (± 2)	2 (± 4)
[F5.47A]V _{1b} R	9 (± 1)	25 (± 6)
[Y5.58A]V _{1b} R	113 (± 6)	51 (± 4)

Figure 3.16 ab The cell-surface expression of the mutant constructs and the V_{1b}R Wt:

a. The cell-surface expression of each mutant construct was shown relative to the Wt

b. The cell-surface expression after AVP-stimulation (1µM, 30 min).

The results were analysed by one-way ANOVA with Dunnett's post-test with Wt as control (P < 0.01 indicated as pale-red with asterisks).

Table 3.12 The cell-surface expression and internalisation of the mutant constructs:

The cell-surface expression of the mutant constructs relative to the Wt and the proportion of the constructs internalised in percentage are shown as mean plus/minus SEM of three separate experiments each of which was performed in triplicate.

3.2.5. II. Hydrophobicity Substitutions

	Over 20 fold increase in affinity
	5 ~ 19 fold increase in affinity
	2 ~ 4.9 fold increase in affinity
	2 ~ 4.9 fold decrease in affinity
	5 ~ 19 fold decrease in affinity
	20 ~ 999 fold decrease in affinity
	Over 1000 fold decrease in affinity

Construct	Binding Affinity (K_i , nM \pm S.E.M.)			Cell-Surface Expression (% Wt)	AVP-induced internalisation (% unstimulated)
	AVP	LA	5234B		
WT V _{1b} R	0.90 (\pm 0.13)	6.25 (\pm 1.86)	7.18 (\pm 1.82)	100	50 (\pm 3)
[Y5.38F]V _{1b} R	0.50 (\pm 0.06)	5.95 (\pm 1.34)	72.7 (\pm 11.8)	82 (\pm 2)	50 (\pm 3)
[Y5.38W]V _{1b} R	1.58 (\pm 0.11)	4.93 (\pm 1.60)	9.92 (\pm 0.02)	59 (\pm 5)	65 (\pm 2)
[F5.47V]V _{1b} R	0.23 (\pm 0.05)	-	8.70 (\pm 2.24)	27 (\pm 3)	53 (\pm 13)
[F5.47I]V _{1b} R	0.93 (\pm 0.18)	-	7.05 (\pm 1.06)	27 (\pm 5)	57 (\pm 6)
[F5.47K]V _{1b} R	Undetectable [³ H]AVP binding			5 (\pm 1)	undetectable
[F5.47W]V _{1b} R	0.12 (\pm 0.04)	-	-	54 (\pm 2)	53 (\pm 4)
[F5.47Y]V _{1b} R	0.53 (\pm 0.02)	-	-	104 (\pm 11)	46 (\pm 3)

Table 3.13 The characterisation of the mutant constructs each containing a hydrophobicity substitution at residue 5.47 or 5.38: Binding affinities are shown as K_i obtained from competition binding assays using [³H]AVP as a tracer ligand. On the column on the far right, the cell-surface expression of the mutant constructs relative to the Wt and the proportion of the constructs internalised in percentage are shown plus/minus SEM of three separate experiments each of which was in triplicate.

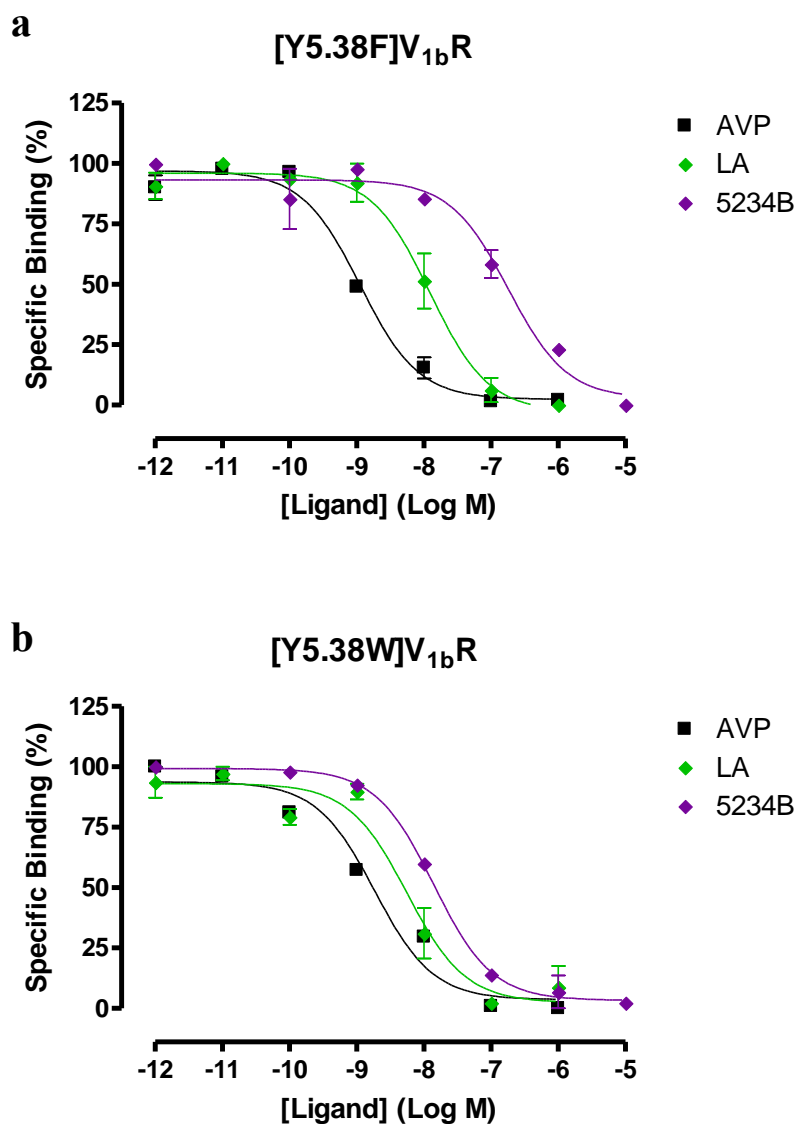


Figure 3.18 ab Ligand Binding Profile of the constructs with aromatic substitution at 5.38:

Graphs show the competition binding of [³H]AVP and various ligands as indicated, in mutant constructs each containing a substitution of amino acid at 5.38:

a. [Y5.38F]V_{1b}R, in which the terminal hydroxyl group was removed from the side chain

b. [Y5.38W]V_{1b}R.

The values were normalised to show the percentage-specific bindings. The error bars represent SEM of values obtained from three independent experiments each performed in triplicate.

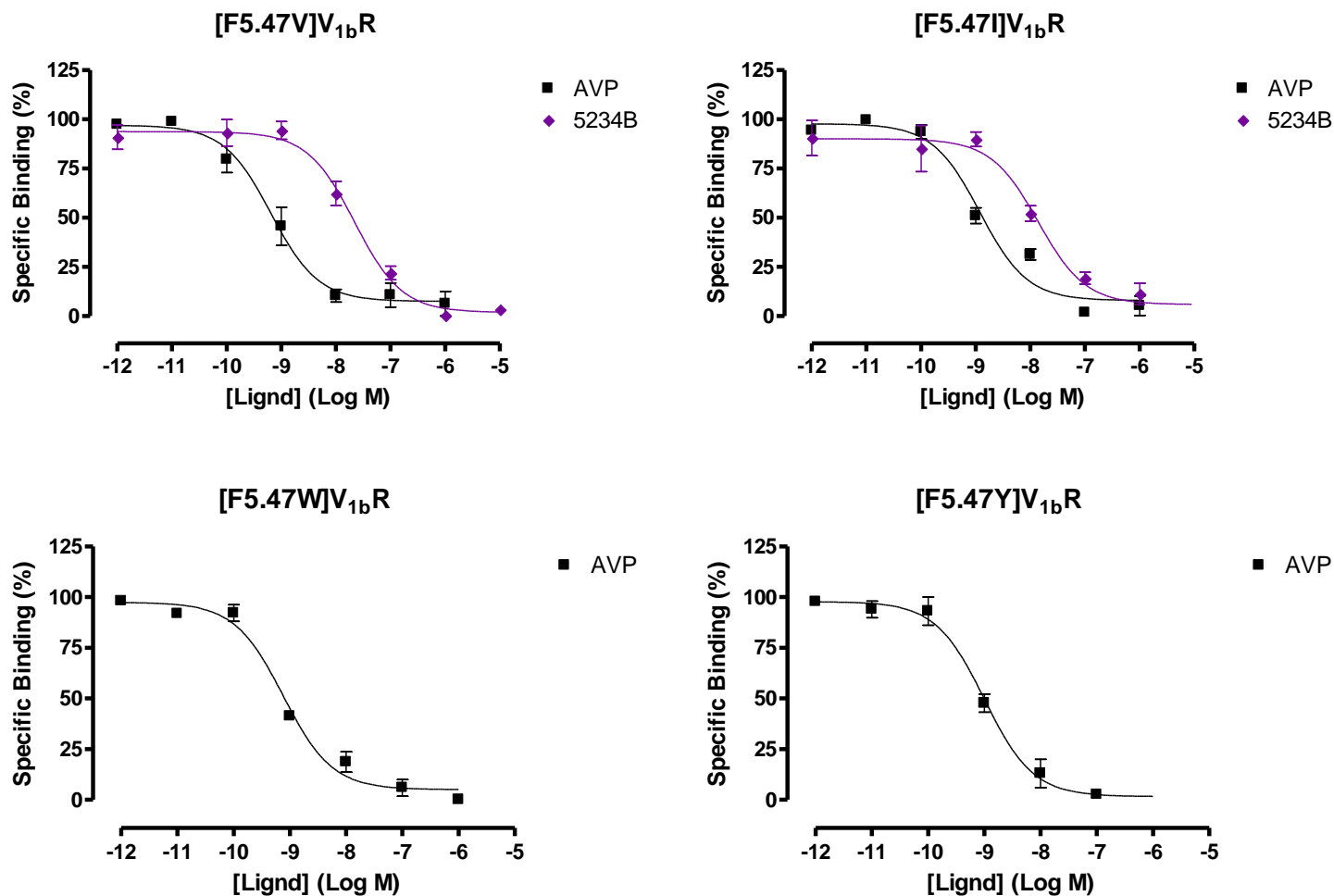
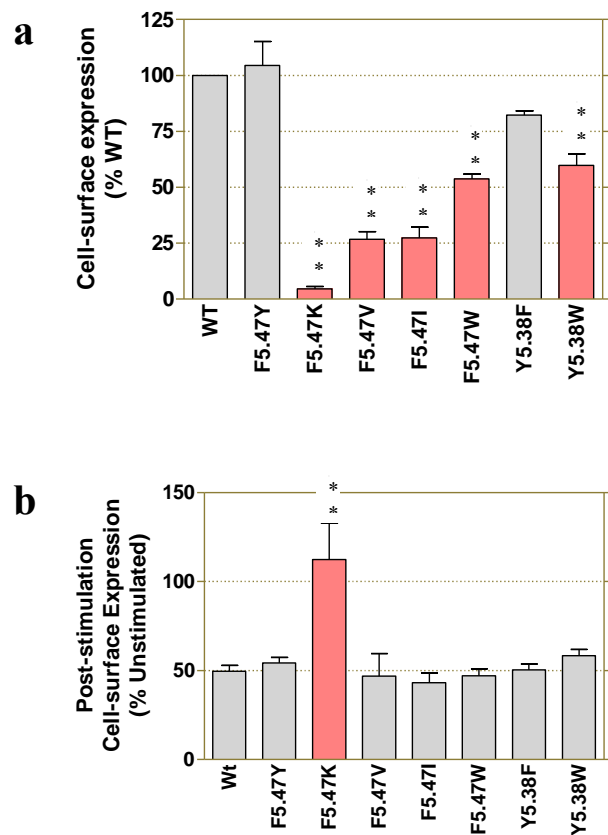


Figure 3.17.a-d Ligand Binding Profile of the constructs with modified hydrophobicity at 5.47: Graphs show the competition binding of [³H]AVP and various ligands as indicated, in mutant constructs each containing a substitution of amino acid at 5.47: **a.** [F5.47V]V_{1b}R; **b.** [F5.47I]V_{1b}R; **c.** [F5.47W]V_{1b}R; and **d.** [F5.47Y]V_{1b}R. The values were normalised to show the percentage-specific bindings. The error bars represent SEM of three experiments each performed in triplicate.



Construct	Cell-Surface Expression (% Wt)	AVP-induced internalisation (% unstimulated)
WT V _{1b} R	100	50 (± 3)
[Y5.38F]V _{1b} R	82 (± 2)	50 (± 3)
[Y5.38W]V _{1b} R	59 (± 5)	65 (± 2)
[F5.47V]V _{1b} R	27 (± 3)	53 (± 13)
[F5.47I]V _{1b} R	27 (± 5)	57 (± 6)
[F5.47K]V _{1b} R	5 (± 1)	Undetectable
[F5.47W]V _{1b} R	54 (± 2)	53 (± 4)
[F5.47Y]V _{1b} R	104 (± 11)	46 (± 3)

Figure 3.19 ab The cell-surface expression levels of the mutant constructs and the V_{1b}R Wt:

- The cell-surface expression of each mutant construct was shown relative to the Wt;
- The cell-surface expression after AVP-stimulation (1µM) for 30 min. The figures were normalised to the cell-surface expression levels of the same construct in the absence of AVP, derived from the experiments performed in parallel. The results were analysed statistically by one-way ANOVA and Dunnett's post-test with Wt as control (P < 0.01 indicated as pale-red with asterisks).

Table 3.13 The cell-surface expression of the mutant constructs relative to the Wt and the proportion of the constructs internalised in percentage are shown plus/minus SEM of three separate experiments each of which was in triplicate.

The effect of hydrophobicity substitutions at position 5.47 on the structural stability of the V_{1b}R

The substitution of Phe^{5.47} with other relatively hydrophobic residues resulted in recovery of cell-surface expression to varying degrees. From the results, it was hypothesised that the increase in the receptor expression at the cell-surface observed was due to its structural stability partially restored by increasing hydrophobicity required at the local environment. Therefore, the constructs containing hydrophobicity substitution at position 5.47 were studied further to investigate the effect of the residue substitutions on thermal stability of the V_{1b}R. The membrane preparations of [F5.47A]V_{1b}R, [F5.47V]V_{1b}R, [F5.47I]V_{1b}R, [F5.47W]V_{1b}R, [F5.47Y]V_{1b}R and the Wt V_{1b}R were pre-treated at a mildly denaturing temperature of 53 °C at various time-periods. The structural stability of the constructs was quantified as half-life of functional receptors, based on their capability in binding specifically to [³H]AVP.

Construct	Half-life (min)
Wt V _{1b} R	8.42
[F5.47V]V _{1b} R	1.61 *
[F5.47I]V _{1b} R	3.06 *
[F5.47W]V _{1b} R	1.80 *
[F5.47Y]V _{1b} R	6.40

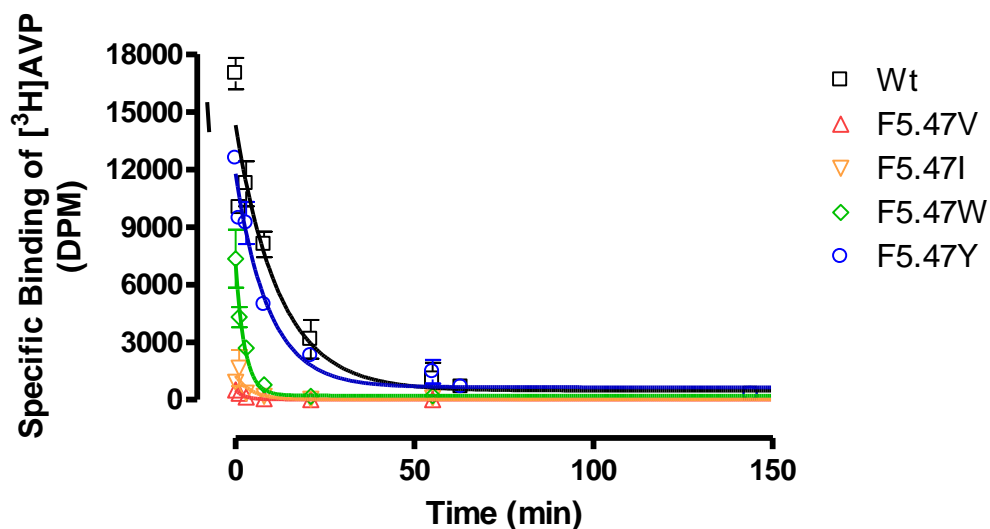


Table 3.14 The cell-surface half-life of the V_{1b}R constructs after heat-treatment:

The half-life of the functional receptors were shown in minutes, determined by capability of specific binding to [³H]AVP following heat-treatment at 53 °C. Asterisk (*) indicates results which differ significantly from the Wt (P < 0.05) indicated by two-tailed paired t-test.

Figure 3.19 Thermal stability of the mutant constructs and the V_{1b}R Wt:

The DPM values were plotted against time in minutes after subtracting non-specific binding. Non-linear regression curves were fitted optimised for one-phase exponential decay, using Prism 4.0. Each curve represents mean plus/minus SEM (error bars) of three experiments each was performed in triplicate.

The pharmacological chaperone activity of a non-peptide antagonist 5234B

Some constructs, [F5.47A]V_{1b}R, [F5.47V]V_{1b}R, [F5.47I]V_{1b}R, [F5.47K]V_{1b}R and [F5.47W]V_{1b}R, were treated with the V_{1b}R-selective non-peptide antagonist 5234B to test whether the compound can act as a chaperone assisting receptor folding. Several studies have shown that non-peptide antagonists of GPCRs can increase the cell-surface expression levels of the receptors. A notable example was seen with a 5-HT_{2A}R antagonist pipamperone, which increased the cell-surface expression of the Wt 5-HT_{2A}R, dopamine D4 receptor (D₄R), and also a D₄R mutant with compromised folding [435]. Among vasopressin receptors, a V_{1b}R-selective non-peptide antagonist SSR149415 has been demonstrated for its pharmaco-chaperone activity on a misfolding mutant [436]; and a V_{1a}R-selective antagonist SR49059 has been shown to restore the cell-surface expression of a mutant construct with compromised cell-surface expression [437]. The exact mechanisms in which certain ligands restore the cell-surface expression are yet to be established. The hydrophobic nature of non-peptide ligands may explain how these compounds act as a chaperone in assisting misfolding mutants, as these may prevent random water molecules accessing to disrupt the folding process at the core of the receptor particularly at vulnerable stages of folding intermediates. Reduced constitutive internalisation of a population of antagonist-occupied receptors is thought to be a contributing factor with a particular relevance to the increased cell-surface expression of the Wt receptors.

In each assay, a control group without treatment and two experimental groups treated with 5234B were made for each construct. One of the experimental groups was also treated additionally with AVP, to test the responsiveness of the 5234B pre-treated receptors to the AVP-induced internalisation.

Construct	Cell-Surface Expression	Cell-Surface Expression	Cell-Surface Expression
	(% Wt)	5234B pre-treated (% Wt untreated)	Post-AVP stimulation 5234B pre-treated (% Wt untreated)
WT V _{1b} R	100	163 (± 5)	103 (± 3)
[F5.47A]V _{1b} R	8 (± 2)	30 (± 2)	15 (± 1)
[F5.47V]V _{1b} R	15 (± 1)	44 (± 1)	16 (± 1)
[F5.47I]V _{1b} R	18 (± 3)	43 (± 4)	16 (± 4)
[F5.47K]V _{1b} R	5 (± 1)	15 (± 1)	6 (± 1)
[F5.47W]V _{1b} R	76 (± 6)	159 (± 6)	101 (± 9)

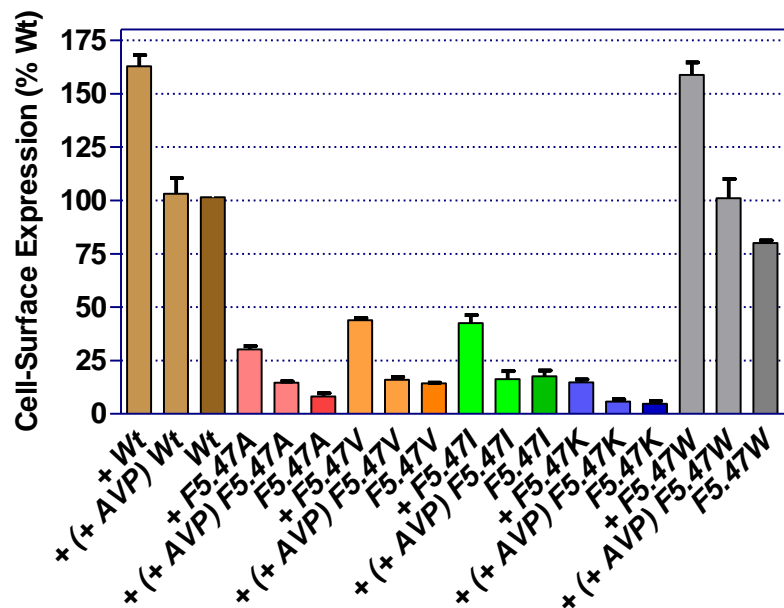


Table 3.15 The effect of a non-peptide ligand 5234B on the cell-surface expression:

The receptor constructs were treated with a V_{1b}R-selective non-peptide antagonist 5234B (1 μM) 24 h prior to the assay. The cell-surface expression level was quantified relative to the Wt untreated (the untreated group on the right, the treated group on the middle column). In each experiment one of the treatment group was stimulated with AVP for 30 min to test responsiveness of these treated constructs to the AVP-induced internalisation (right column).

3.2.5.i The summary of the results for the constructs with Ala substitution

AVP binding to [Q4.60A] $V_{1b}R$ was reduced slightly, with about 2.5-fold increase in K_i . The affinity of the construct for LA was also reduced with 5-fold increased K_i . The affinity of 5234B was most largely affected with K_i rising from 7 nM in the Wt to 105 nM, showing 15-fold increase. These changes were selective relatively as the affinities of $V_{1b}R$ -selective agonist d[Cha⁴]AVP and a non-peptide antagonist SSR149415 were unaffected. [Q4.60A] $V_{1b}R$ expressed on the cell-surface well with a slight increase of 126% relative to the Wt.

[Y5.58A] $V_{1b}R$ also displayed a slight reduction in affinities towards AVP and 5234B, with about 2-fold increase in K_i . Tyr^{5.58} is located at the lower part of the TM5 and the residue has been indicated to be involved in the activation process by interacting Arg^{3.50} in an active state of opsin. It is yet uncertain whether this residue has a similar role in the $V_{1b}R$; nevertheless the loss of Tyr^{5.58} resulted in a slight impairment (2-fold increase in K_i) of ligand binding for the agonist AVP and also the antagonist 5234B. The cell-surface expression of this construct was reduced to 38% relative to the Wt.

Ala substitution of Tyr^{5.38} or Phe^{5.47} was not tolerated in the $V_{1b}R$. The binding of [³H]AVP to [Y5.38A] $V_{1b}R$ and [F5.47A] $V_{1b}R$ were undetectable, and both constructs showed dramatic reduction in the cell-surface expression. In contrast, Phe^{4.62} appeared not to be essential in the $V_{1b}R$ structure and function, and alanine substitution of the residue was well-tolerated as [F4.62A] $V_{1b}R$ retained Wt-like characteristics in both ligand binding properties and the cell-surface expression.

3.2.5.ii The summary of the results for the constructs with altered hydrophobicity at 5.38 or 5.47

As Ala substitution of Tyr^{5.38} and Phe^{5.47} disrupted receptor function, additional substitutions were engineered to probe the role of these residues. The Phe substitution of Tyr^{5.38} recovered the receptor functionality on AVP binding and the cell-surface expression to the Wt level. However, this substitution resulted in a selective reduction of 5234B affinity to the receptor, with 10-fold increase in the K_i value. This implies a role of the terminal hydroxyl group in constructing the ligand binding cavity of 5234B. Substitution by Trp in [Y5.38W]V_{1b}R was well-tolerated with essentially the Wt binding profile for peptide agonist (AVP), peptide antagonist (LA) and non-peptide antagonist (5234B).

The substitution of Phe^{5.47} with Val or Ile resulted in a slight recovery of the receptor function. The cell-surface expression levels were still low relatively, but high affinity AVP binding to [F5.47V]V_{1b}R and [F5.47I]V_{1b}R was detected. Trp substitution resulted in an 8-fold increase in AVP affinity compared to the Wt. Cell-surface expression of [F5.47W]V_{1b}R was still compromised (54% of the Wt). The cell-surface level equivalent to the Wt was achieved by Tyr substitution. Lys substitution was not tolerated in [F5.47K]V_{1b}R, suggesting the charged nature of the residue was not suitable to be accommodated at this location of the V_{1b}R.

The mutant constructs of Phe^{5.47} were tested for their structural stability by thermal challenge as described in section 2.2.15. Half-life of [F5.47V]V_{1b}R, [F5.47I]V_{1b}R and [F5.47W]V_{1b}R were reduced to 2 - 3 min compared to the 8 min of the Wt, suggesting that the decrease in cell-surface expression was due, at least partly, to decreased receptor stability. [F5.47Y]V_{1b}R which has expressed at Wt-level at the cell-surface, unlike [F5.47V]V_{1b}R,

[F5.47I]V_{1b}R and [F5.47W]V_{1b}R, had an intermediate stability with half-life of approximately 6 min.

The pre-treatment with a V_{1b}R-selective non-peptide antagonist 5234B resulted in increased cell-surface expression levels of over 50% in all the constructs including the Wt V_{1b}R. The receptors presented on the cell-surface with aid of 5234B were internalised in response to AVP stimulation. With uncertainty in the exact mechanism of the pharmaco-chaperone activity of 5234B, it is unknown whether AVP binds to the receptor containing pharmaco-chaperone to induce internalisation, or AVP binding displaces 5234B, assuming the pharmaco-chaperone is incorporated into the receptor during the synthesis. It may also be possible that the compound may be subjected to a slow degradation by hydrolysis or other means, losing its affinity to the receptor gradually, and dissociate from it eventually over a certain period.

3.2.6. The role of conserved residues in TM6

TM6 of Family A GPCRs contain CWXP motif which has been proposed to be vital in the activation process [309]. The motif contains Cys^{6.47} and Trp^{6.48} of 'rotamer toggle switch' of the receptor activation. In addition, a hydrophobic residue is relatively conserved at position 6.40. In this study, [I6.40A]V_{1b}R was produced and the ligand binding affinities of agonist and antagonist to the construct were determined. To study the involvement of Cys^{6.47} and Trp^{6.48} of the rotamer toggle switch motif in ligand binding of the V_{1b}R, [C6.47A]V_{1b}R, [W6.48A]V_{1b}R and [W6.48F]V_{1b}R were produced.

[F6.51A]V_{1b}R, [F6.52A]V_{1b}R and [Q6.55A]V_{1b}R were also made to investigate their participation in ligand binding. The three residues were previously predicted by molecular modelling study to be involved in AVP binding to V_{1a}R, V₂R and OTR by Ślusarz et al. [427]. The three residues and also Val^{6.59} were predicted to interact with certain V_{1b}R-selective non-peptide antagonists by Dr. Wishart in Schering-Plough Research Institute (Personal communication). [V6.59A]V_{1b}R was made and characterised for ligand binding properties. In addition, Ser^{6.58} next to Val^{6.59} was also substituted with Ala to make comparison between these two residues in ligand binding, as the two residues are both semi-conserved (i.e. conserved in V_{1a}R, V_{1b}R and OTR but not in V₂R). In addition, at the extracellular end of TM6, there is a WD pair (Trp^{6.60} and Asp^{6.61}) somewhat resembling the TM2 juxtamembrane region (Trp^{2.64} and Asp^{2.65}). [W6.60A]V_{1b}R and [D6.61A]V_{1b}R were made to compare the role of the WD pair at the exofacial surface of TM2 and TM6.

	Over 20 fold increase in affinity
	5 ~ 19 fold increase in affinity
	2 ~ 4.9 fold increase in affinity
	2 ~ 4.9 fold decrease in affinity
	5 ~ 19 fold decrease in affinity
	20 ~ 999 fold decrease in affinity
	Over 1000 fold decrease in affinity

Construct	Binding Affinity (K_i , nM \pm S.E.M.)						Cell-Surface Expression (% Wt)
	AVP	dDAVP	d[Cha ⁴]AVP	LA	5234B	SSR149415	
WT V _{1b} R	0.90 (\pm 0.13)	10.5 (\pm 2.7)	1.35 (\pm 0.02)	6.25 (\pm 1.86)	7.18 (\pm 1.82)	3.36 (\pm 0.93)	100
[I6.40A]V _{1b} R	0.29 (\pm 0.05)	4.75 (\pm 0.97)	-	1.14 (\pm 0.22)	4.86 (\pm 1.06)	-	24 (\pm 3)
[C6.47A]V _{1b} R	0.50 (\pm 0.18)	-	-	1.96 (\pm 0.23)	3.59 (\pm 0.69)	2.52 (\pm 0.27)	42 (\pm 4)
[W6.48A]V _{1b} R	0.27 (\pm 0.07)	0.40 (\pm 0.06)	0.82 (\pm 0.07)	1.26 (\pm 0.21)	152 (\pm 14)	85.0 (\pm 17.1)	43 (\pm 4)
[F6.51A]V _{1b} R	2.84 (\pm 0.37)	109 (\pm 19)	1.04 (\pm 0.20)	1.10 (\pm 0.25)	336 (\pm 26)	184 (\pm 22)	64 (\pm 7)
[F6.52A]V _{1b} R	1.10 (\pm 0.13)	1.02 (\pm 0.70)	-	5.08 (\pm 0.31)	12.0 (\pm 3.8)	82.4 (\pm 12.0)	82 (\pm 13)
[Q6.55A]V _{1b} R	1.37 (\pm 0.16)	41.1 (\pm 8.3)	-	6.87 (\pm 1.67)	23.2 (\pm 4.0)	4.86 (\pm 1.26)	134 (\pm 6)
[S6.58A]V _{1b} R	1.10 (\pm 0.26)	6.01 (\pm 1.31)	-	-	3.58 (\pm 0.53)	-	66 (\pm 2)
[V6.59A]V _{1b} R	0.93 (\pm 0.29)	33.7 (\pm 11.8)	-	-	14.5 (\pm 0.9)	11.7 (\pm 2.3)	99 (\pm 14)
[W6.60A]V _{1b} R	0.59 (\pm 0.26)	15.5 (\pm 3.3)	-	8.36 (\pm 3.77)	12.2 (\pm 1.0)	-	56 (\pm 5)
[D6.61A]V _{1b} R	1.53 (\pm 0.17)	31.1 (\pm 6.8)	-	12.3 (\pm 0.8)	5.47 (\pm 0.25)	-	93 (\pm 6)

Table 3.16 The characterisation of the TM6 mutant constructs containing Ala substitution:

Binding affinities are shown as K_i obtained from competition binding assays using [³H]AVP as a tracer ligand. The colour code was applied, as indicated in the box above, to highlight changes in binding affinity relative to the Wt. The column on the far right shows cell-surface expression levels of the mutant constructs relative to the Wt, determined by ELISA. The data presented are mean values plus/minus SEM of three separate experiments, each performed in triplicate. Dash (-) means value was undetermined.

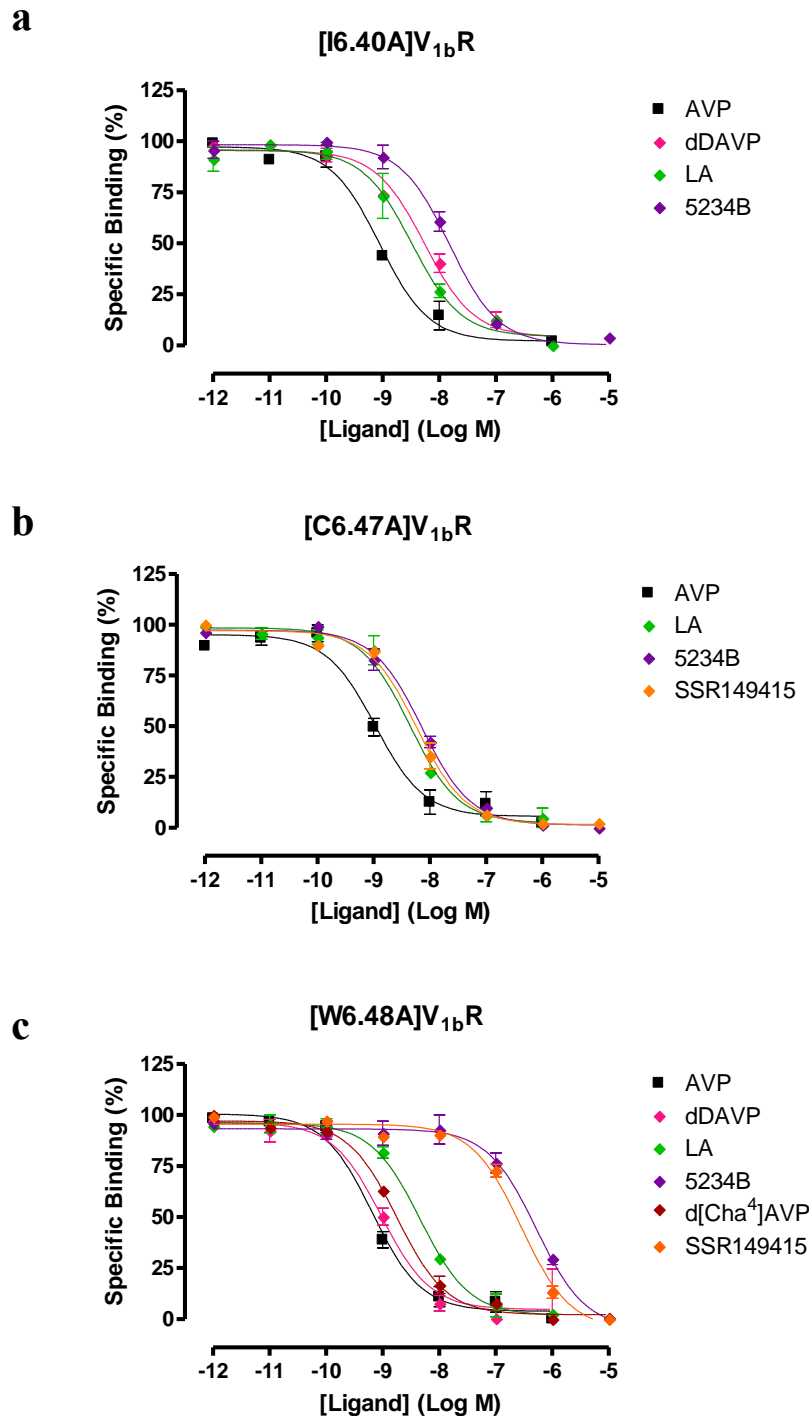


Figure 3.21 a-c Ligand Binding Profile of the TM6 constructs with Ala substitution: Graphs show the competition binding of [³H]AVP and various ligands as indicated, in the mutant constructs each containing an alanine substitution at the specified position:

a. [I6.40A]V_{1b}R with AVP, dDAVP, LA and 5234B;

b. [C6.47A]V_{1b}R with AVP, 5234B and LA;

c. [W6.48A]V_{1b}R with AVP, dDAVP, LA, 5234B, d[Cha⁴]AVP, and SSR149415.

The values plotted are normalised to show the relative specific binding of each construct.

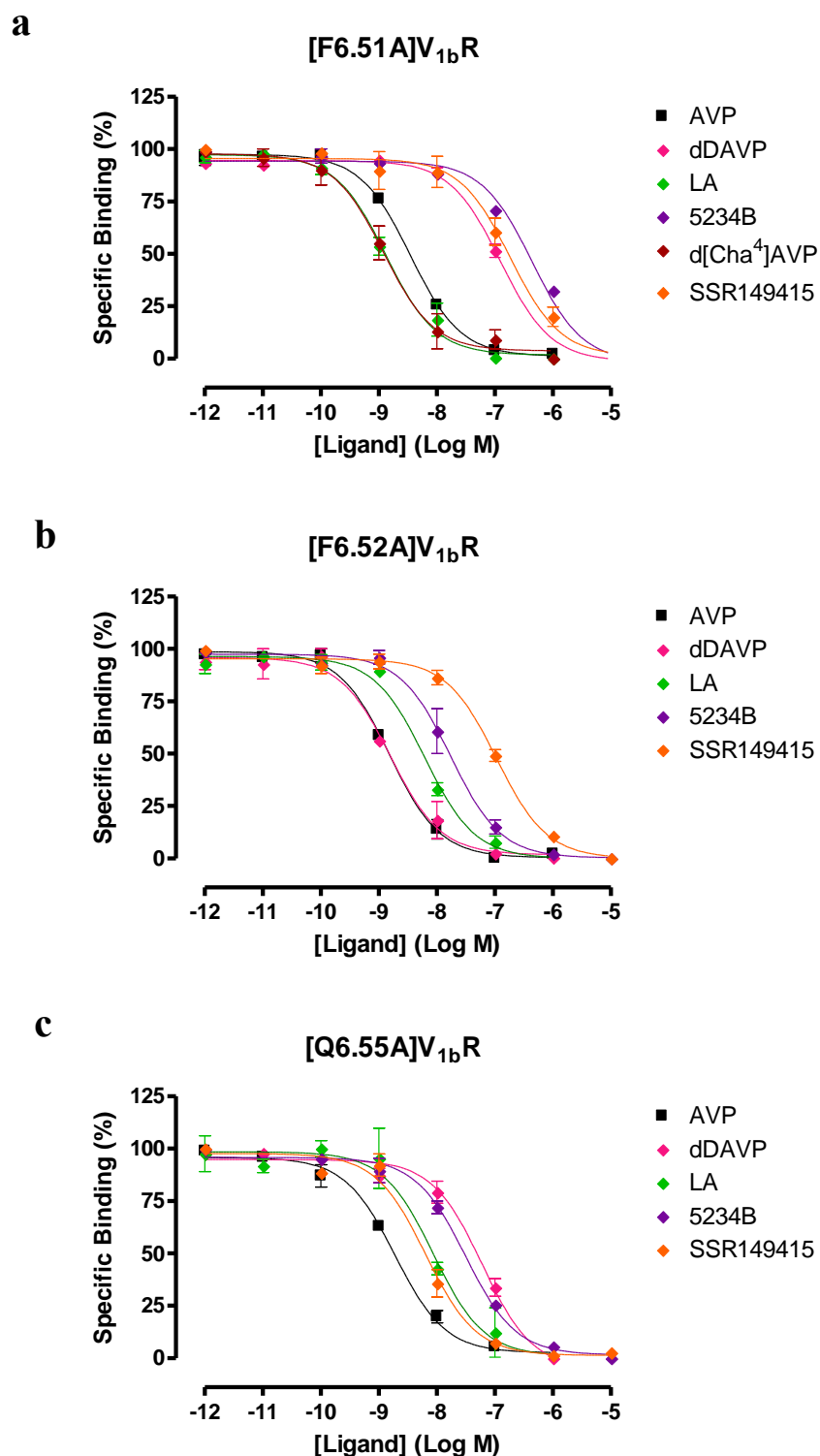


Figure 3.22 a-c Ligand Binding Profiles of the TM6 constructs with Ala-substitution:

Graphs show the competition binding of [³H]AVP and various ligands in the mutant constructs each containing an alanine substitution at the specified position. The values plotted are normalised to show the relative specific binding of each construct.

- a. [F6.51A]V_{1b}R with AVP, dDAVP, LA, d[Cha⁴]AVP, 5234B and SSR149415;
- b. [F6.52A]V_{1b}R with AVP, dDAVP, LA, 5234B and SSR149415;
- c. [Q6.55A]V_{1b}R with AVP, dDAVP, LA, 5234B, and SSR149415

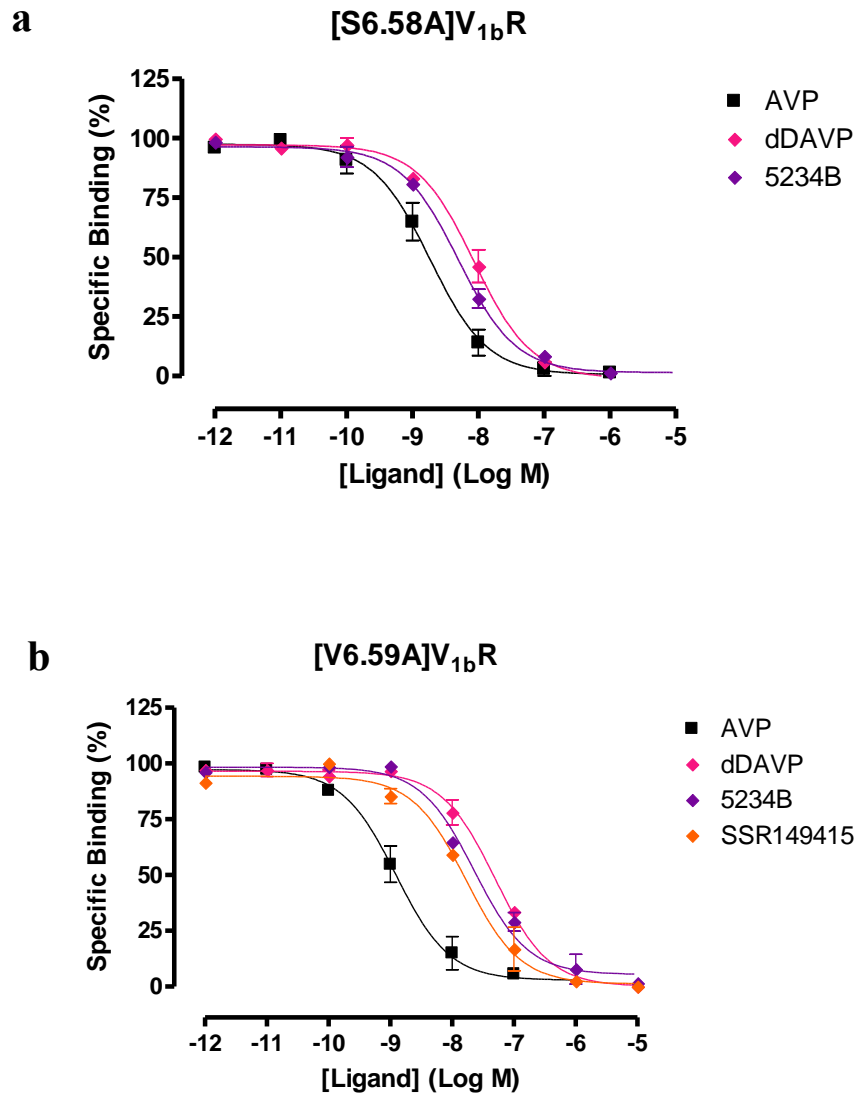


Figure 3.22 ab Ligand Binding Profiles of the TM6 constructs with Ala-substitution:

Graphs show competition binding of [³H]AVP and various ligands in the mutant constructs each containing an alanine substitution at the specified position. The values plotted are normalised to show the relative specific binding of each construct. The error bars represent SEM of three experiments each performed in triplicates.

- a. [S6.58A]V_{1b}R with AVP, dDAVP, and 5234B;
- b. [V6.59A]V_{1b}R with AVP, dDAVP, 5234B and SSR149415.

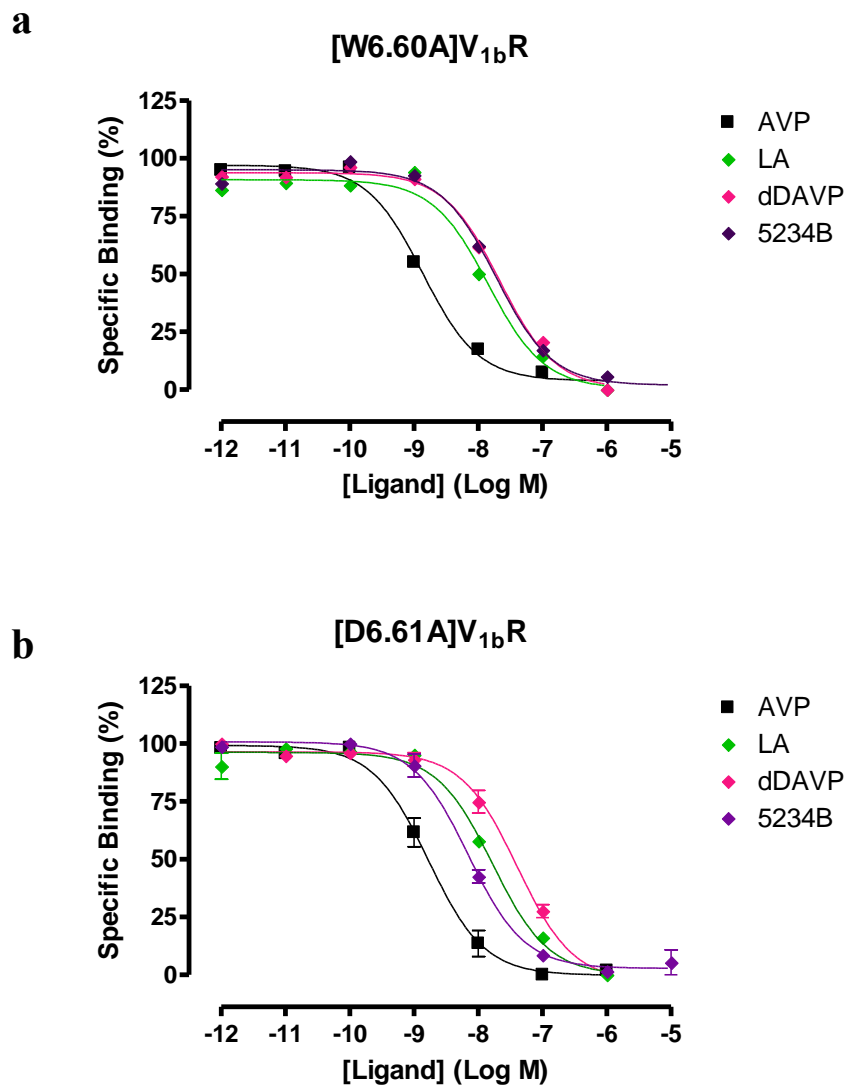
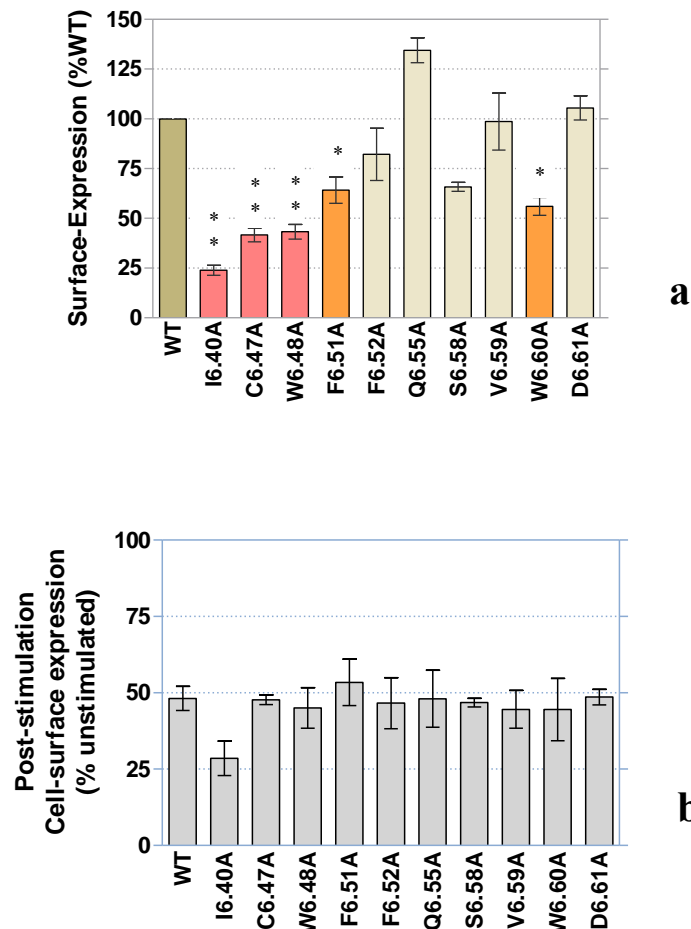


Figure 3.23 ab

Ligand Binding Profiles of the TM6 constructs with Ala-substitution:

Graphs show competition binding of [³H]AVP and various ligands in the mutant constructs each containing an alanine substitution at the specified position. The values plotted are normalised to show the relative specific binding of each construct. The error bars represent SEM of three experiments each performed in triplicates.

- a. [W6.60A]V_{1b}R with AVP, dDAVP, LA and 5234B;
- b. [D6.61A]V_{1b}R with AVP, dDAVP, LA and 5234B.



Construct	Cell-Surface Expression (% Wt)	AVP-induced Internalisation (% unstimulated)
WT V _{1b} R	100	52 (± 4)
[I6.40A]V _{1b} R	24 (± 3)	71 (± 6)
[C6.47A]V _{1b} R	42 (± 4)	52 (± 2)
[W6.48A]V _{1b} R	43 (± 4)	55 (± 7)
[F6.51A]V _{1b} R	64 (± 7)	47 (± 8)
[F6.52A]V _{1b} R	82 (± 13)	53 (± 8)
[Q6.55A]V _{1b} R	134 (± 6)	52 (± 9)
[S6.58A]V _{1b} R	66 (± 2)	53 (± 1)
[V6.59A]V _{1b} R	99 (± 14)	54 (± 6)
[W6.60A]V _{1b} R	56 (± 5)	55 (± 10)
[D6.61A]V _{1b} R	105 (± 6)	51 (± 3)

Figure 3.24 ab The cell-surface expression levels of the mutant constructs and the V_{1b}R Wt:

- The cell-surface expression of each mutant construct was shown relative to the Wt as 100%;
- The cell-surface expression determined after AVP-stimulation (1 μM, 30 min). The figures were normalised to the expression levels of the same construct in the absence of AVP, determined in parallele experiments.

The results were analysed statistically by one-way ANOVA and Dunnett's post-test with Wt as control (P < 0.05 shown in orange with asterisk, P < 0.01 in pale-red with two asterisks).

Table 3.17 The cell-surface expression of the mutant constructs relative to the Wt and the proportion of the constructs internalised in percentage are shown plus/minus SEM of three separate experiments each of which was in triplicate.

3.2.5.i The summary of the results for the constructs of TM6

Most constructs studied in this section retained a high affinity binding to AVP regardless the levels of the cell-surface expression, and this allowed the use of [³H]AVP as a tracer ligand in determining binding affinity of these constructs for other ligands. Three constructs, [I6.40A]V_{1b}R, [C6.47A]V_{1b}R and [W6.48A]V_{1b}R retained high affinity binding to AVP. The affinity of both agonists AVP and dDAVP was increased about 2 - 3-fold to [I6.40A]V_{1b}R. LA also increased affinity to [I6.40A]V_{1b}R with 5-fold decrease in K_i . In V_{1a}R, the increase in affinities observed for [I6.40A]V_{1a}R were associated specifically with agonist (Wootten, D.L. Doctoral thesis, 2007. University of Birmingham). The discrepancy in the results in the V_{1b}R may possibly be an indication of LA to be as not an effective antagonist as in V_{1a}R. Increase in agonist affinity was also seen with [W6.48A]V_{1b}R. A 3-fold increase in AVP affinity, and even a larger shift of 25-fold increased affinity of dDAVP was observed. The affinity of the peptide antagonist LA was also increased about 5-fold. In contrast, both non-peptide antagonists displayed reduced affinity to the construct with K_i value increased 20-fold for 5234B and 40-fold for SSR149415.

The affinity of many ligands was affected by the Ala substitution of Phe^{6.51} regardless of the ligands actions. The affinity of AVP was decreased 3-fold, and also that of dDAVP 10-fold. The affinity of non-peptide antagonists were affected dramatically, with a 50-fold increase in K_i for 5234B and \approx 100-fold increase in K_i for SSR149415. A selective increase in dDAVP affinity was observed with [F6.52A]V_{1b}R and a selective 25-fold decrease in the non-peptide antagonist SSR149415. In contrast, the affinity of the other non-peptide antagonist 5234B was unaffected.

Small increases of K_i between three- and four-fold were associated with dDAVP binding to [Q6.55A]V_{1b}R, [V6.59A]V_{1b}R and [D6.61A]V_{1b}R. Similar levels of decreases in affinities of 5234B and SSR149415 to [Q6.55A]V_{1b}R, and 5234B binding to [V6.59A]V_{1b}R, were also observed. The affinity of LA to [D6.61A]V_{1b}R was reduced slightly \approx 2-fold.

All constructs were internalised in response to AVP stimulation, in a similar manner to the Wt. About 50 % of the receptor expressed on the cell-surface were internalised 30 minutes following exposure to 1 μ M AVP. [I6.40A]V_{1b}R appeared to be internalised slightly more than other constructs, but statistical analysis by one-way ANOVA and paired t-test did not indicate any significance in differences.

3.3 Discussions

3.3.1. The residues required for the AVP binding to the V_{1b}R

Several residues have been identified as critical requirements in V_{1b}R for AVP binding. These are charged residues located at the N-terminus region close to TM1 and the juxtamembrane positions by TM2 and TM3. As demonstrated in V_{1a}R and OTR by Hawtin, Wesley and Wootten [428, 429, 438], Glu^{1.35} located at the juxtamembrane region of TM1, was involved critically in AVP binding of V_{1b}R. The other residue Arg^{1.27}, which was also shown to be involved critically in AVP binding of V_{1a}R and OTR, appeared also to be important in the agonist binding and activation of V_{1b}R, in particular of dDAVP. However, Arg^{1.27} is thought to be relatively less crucial in AVP binding in the V_{1b}R, since AVP binding by [R1.29A]V_{1b}R was detectable unlike in V_{1a}R and OTR.

As in V_{1a}R, Glu^{1.35} was shown to interact with Arg⁸ of AVP. Although efficacy was low, InsP₃ signalling was detected with a high potency by [E1.35R]V_{1b}R in response to [Glu⁸]vasopressin challenge. The interaction between Arg^{1.35} in the receptor and Glu⁸ of the ligand is thought possibility to have mimicked a direct interaction occurring between Arg⁸ and Glu^{1.35} in AVP binding to V_{1b}R. A high potency may also indicate that the locus at which Glu^{1.35} is present is relatively accessible by AVP. A low efficacy may possibly indicate the involvement of local residues which participate in effective activation of the V_{1b}R, and such functional interactions require the exact positioning of Arg⁸ and Glu^{1.35} in AVP and V_{1b}R. This finding is also supported by the notable reduction in AVP binding affinity observed for [E1.35Q]V_{1b}R. Glu and Gln are structurally very similar, as the only difference between the two is the atom with different electronegativity at the terminal side chain (O for Glu, N for Gln). Hence, the reduced AVP affinity observed for [E1.35Q]V_{1b}R can also be interpreted that the

high affinity binding requires a stronger ionic interaction involving the negative charge of Glu^{1.35} and a positively charged group of AVP, which is Arg⁸.

The other interaction mimicking glycinamide of AVP and Glu^{1.35} was demonstrated in V_{1a}R by Wootten using [E1.35Q]V_{1a}R and AVP-free acid, and also [E1.35D]V_{1a}R and [β -Ala⁹]AVP (Wootten and Wheatley, manuscript in preparation). However, this interaction was not observed in the V_{1b}R, indicating that AVP binds differently to V_{1b}R and V_{1a}R consistent with the slight difference noted above for Arg^{1.27}.

To investigate the possible mutual interactions between Arg^{1.27} and Glu^{1.35} in a double reciprocal mutant, the two residues were exchanged positionally. However, no recovery of AVP binding was observed in the [R1.27E/E1.35R]V_{1b}R, indicating the requirement of specific orientation for both charged groups for AVP binding at the membrane interface of the N-terminus and TM1. It is also possible that the residues participate independently in interactions in this vicinity upon activation. InsP₃ signalling was undetectable for the double mutant following the [Glu⁸]vasopressin stimulation despite the presence of Arg side chain located at position 1.35. This may suggest that the induced Glu at 1.27 was causing either a electric repulsive force or a structural obstacle to block the interaction between Arg^{1.35} and [Glu⁸]vasopressin; or alternatively the two residues Arg^{1.35} and Glu^{1.27} were forming a salt bridge which is thermodynamically more favourable than the interaction between Arg^{1.35} with Glu⁸ of the ligand.

The substitution of Asp^{2.65} with Gln or Arg was equally well-tolerated in the V_{1b}R. This observation is different from the previous studies on rat V_{1a}R, as [D2.65R]rV_{1a}R displayed a drastic fall in the receptor affinity to AVP [439], again confirming the existing differences among subtypes in the binding profiles to the mutual agonist. In the V_{1b}R, Trp^{2.64} and Asp^{2.65}

are thought to participate together in constructing the AVP-binding cavity in the V_{1b}R, since AVP binding was undetectable in the double alanine mutant [W2.64A/D2.65A]V_{1b}R and also in the reciprocal mutant [W2.64D/D2.65W]V_{1b}R. The loss of AVP binding in the latter mutant suggests that the positioning of the two residues at this vicinity is fundamental in constructing a binding cavity for AVP in the V_{1b}R. It is also plausible that the reciprocal positional change of the two residues might have caused a severe structural disruption in the V_{1b}R. The dramatically reduced cell-surface expression of [W2.64D/D2.65W]V_{1b}R observed may suggest that the large proportion of receptors might have folded incompletely and retained in the ER. In contrast, alanine substitution of either residue resulted in increased cell-surface expression of the receptor. Altogether these results suggest the importance of the two residues in the V_{1b}R architecture: at the juxtamembrane position the two residues, aromatic Trp and Asp carrying negative charge, could be responsible for keeping appropriate orientations of the upper TM2 relative to the membranes and the other TMs.

The other residues shown to be involved critically in AVP binding to V_{1b}R in this study are Pro^{2.60}, Gln^{2.61}, Arg^{3.26} and Tyr^{5.38}. The importance of Gln^{2.61} in AVP binding was also demonstrated in the other vasopressin receptors and OTR (Wootten and Wheatley, manuscript in preparation). Pro^{2.60} and Gln^{2.61} are the two residues at the end of the conserved FQVLPQ motif found in all the neurohypophysial hormone receptors identified in various species. These receptors might possibly share a similar mechanism in neurohypophysial hormone binding and the activation utilising this region, possibly involving the glycinamide terminal of the neurohypophysial hormones. The role of this motif in the agonist binding and the activation of the other neurohypophysial receptors are to be elucidated to confirm this assumption.

From the above results, the interactions between AVP and the TM1 and TM2 juxtamembrane region of V_{1b}R can be hypothesised: AVP has a tripeptide tail moiety Pro⁷-Arg⁸-Gly⁹ which ends with an amide group; Pro⁷ is probably there to induce a necessary angle in the AVP backbone, allowing the tripeptide tail to fit into the agonist binding cavity of V_{1b}R to induce activation; Arg⁸ of AVP is probably attracted to electrons on Glu^{1.35} as a driving force in this binding, while possibly the terminal amino group of AVP may become a hydrogen bond donor to carbonyl oxygen of Gln^{2.61} while a kink induced by Pro^{2.60}, as well as a Pro⁷-induced kink in AVP, make this interaction possible.

The exact angle in the Pro^{2.60}-induced kink, or Pro^{2.60} itself, is thought also to have a key role in maintaining the structural integrity of the receptor; and the point was reflected in the observation made on [P2.60G]V_{1b}R which displayed one of the most disrupted phenotype observed in the entire study. Two mutants involving substitution of Gln^{2.61} resulted in dramatically reduced cell-surface expression, implying that the residue may also have a role in stabilising the receptor structure by a dipole-dipole interaction involving a neighbouring residue along with Pro^{2.60}. This region of the exofacial end of TM2 is likely to be in a relatively unstable environment for their proximity to the N-terminal domain which is probably less restrained in their movement. This point is, however, purely speculative and it needs to be supported by MD simulation study of solvated receptor. Being involved in the agonist binding directly, this region comprising the N-terminal/TM1/TM2 is also likely to undergo structural change upon the activation.

The role of Arg^{3.26} at the juxtamembrane region of TM3 is thought to maintain the interaction between the ECL2 to the membrane plane. The residue is positioned immediately below the cysteine residue that forms a conserved disulfide bond with another cysteine residue

in ECL2. The experimental data obtained for [R3.26D]V_{1b}R matches with the findings reported for the V_{1a}R [439]. The study on rat V_{1a}R showed that the Ala substitution of Arg^{3.26} and also the charge-retained substitution with Lys did not significantly deteriorate the ligand binding properties of the receptor construct. However, the charge-reversed substitution of Arg^{3.26} with Asp resulted in the loss of the tracer ligands bindings for [³H]AVP, [³H]LA, and [³H]CA, while the cell-surface expression of the construct was detected at a compromised level of about 50% to the Wt. Molecular modelling study predicted that the substitution of Arg^{3.26} with Asp resulted in re-ordering of the phospholipids nearby due to an increase in the solvent-accessible surface at the position [439]. A similar situation is thought to apply to the V_{1b}R: in the absence of Arg^{3.26}, the AVP binding cavity involving ECL2 may not be formed appropriately as ECL2 becomes destabilised.

Tyr^{5.38}, also shown to be necessary in AVP binding in V_{1b}R, is located at the extracellular terminal of TM5 and at the top of a cluster of aromatic residues found between TM5 and TM6. Within the cluster, there is Phe^{6.51} which was also found to be involved in AVP binding to V_{1b}R. Phe^{6.51} may interact favourably with a hydrophobic region of AVP, Tyr²-Phe³, by van der Waal's interactions, and the hydroxyl terminal of Tyr^{5.38} may form a hydrogen bond with one of polar residues Gln⁴ or Asn⁵.

There is a few residues which were shown to be involved in AVP binding at magnitudes in which [³H]AVP binding was detectable. These are Arg^{1.27}, Trp^{2.64}, Asp^{2.65}, Gln^{4.60} and Phe^{6.51} mentioned above. Arg^{1.27} on the N-terminal domain is often omitted from comparative models, and so it is hard to predict *in silico* the exact role which this residue plays in AVP binding. The residue may be involved in AVP binding in an indirect manner as seen in Arg^{3.26} for instance. A

possibility is that Arg^{1.27} might be interacting with charged or polar residues nearby, for instance on an ECL domain, in forming AVP binding cavity, as an introduction of the opposite charge in [R1.27E]V_{1b}R diminished AVP binding.

In the V_{1b}R, Asp^{2.65} appears to interact with Arg⁸ of AVP along with Glu^{1.35}. The models of V_{1b}R at active and inactive states showed an alteration in the position of Asp^{2.65} which points upwards in the active state (figure 3.25). The interaction between Asp^{2.65} and Arg⁸ was also predicted by molecular modelling study by Rodrigo *et al* [431]. This is a different mechanism from the molecular model of AVP binding to the V_{1a}R, in which Asp^{2.65} has been suggested to interact with the glycinamide end of AVP, along with Glu^{1.35}. The molecular model of V_{1a}R with AVP docked predicted the three residues Glu^{1.35}, Gln^{2.61} and Asp^{2.65} to interact with the glycinamide terminal of AVP (Simms J., unpublished study: figure 3.26a). In the models of both subtypes made by Simms, Trp^{2.64} faces towards the ligand binding cavity of AVP. The residue may assist AVP binding in the V_{1b}R by interacting with the ring structure of Pro⁷. Gln^{4.60} and Tyr^{5.38} were also shown to point towards the core of the TM bundles in the both V_{1a}R and V_{1b}R (figure 3.25). The model agrees with the finding of this mutagenesis study, which showed involvement of these residues in the AVP binding.

The mutagenesis study also revealed existing differences in the binding between AVP and dDAVP to the V_{1b}R. The reduction in affinity which was seen in [W2.64A]V_{1b}R and [D2.65A]V_{1b}R was not observed with dDAVP binding. In contrast, Ala substitution of Val^{3.28} and TM6 residues had more damaging effects in dDAVP binding but not in AVP binding. The results of this study suggest that in binding to V_{1b}R, dDAVP adopts a different mechanism in which the hydrophobic residues in TM6 are more important than for AVP binding to V_{1b}R.

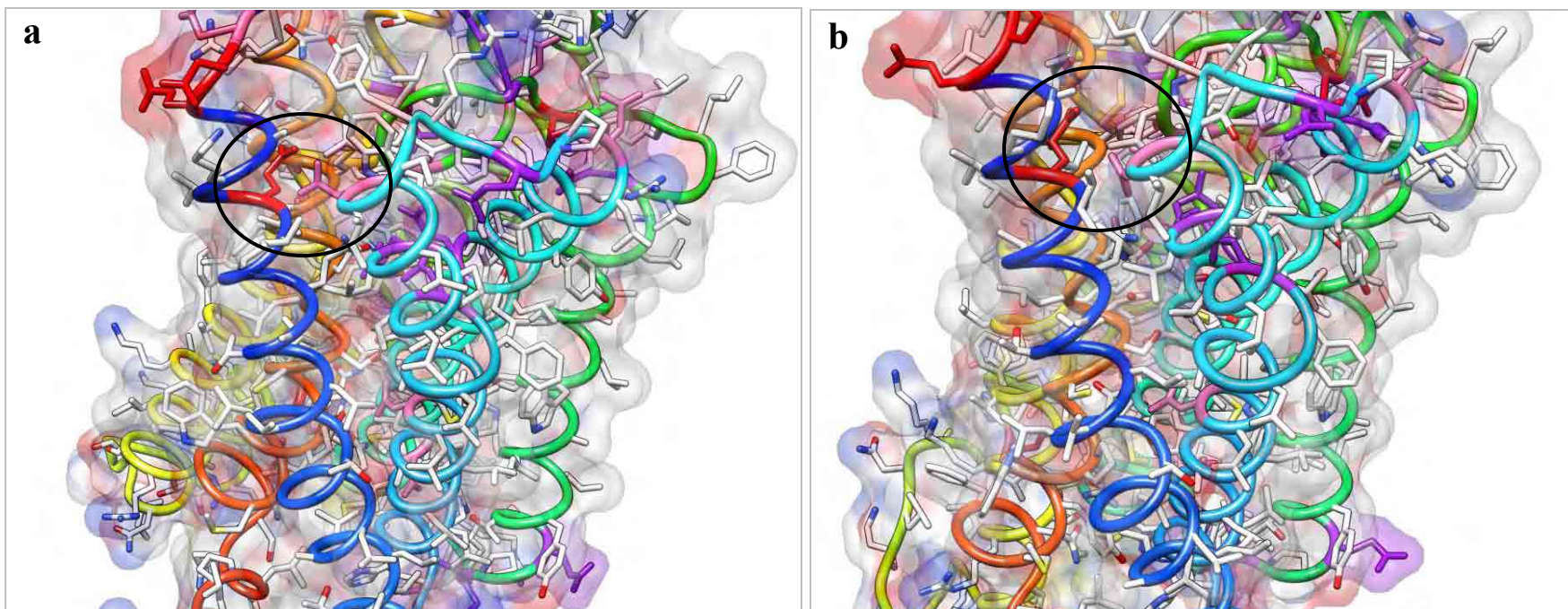


Figure 3.25 ab The molecular models of active and inactive states of V_{1b}R (side views facing TM1 and TM2):

- a.** At the active state;
- b.** At the inactive state.

Colour code on the figures: TM1 (blue), TM2 (pale blue), TM3 (turquoise), TM4 (green), TM5 (lime green), TM6 (yellow) and TM7 (orange). A few residues were also colour coded: Glu (red), Asp (pink), Gln (lavender). The black line encircles Glu^{1.35}, Asp^{2.65} and Gln^{2.61}. In the active state (a), Asp^{2.65} appears to tilt upwards.

The models were constructed by Dr. John Simms. The figures were visualised using Chimera (UCSF Computer Graphics Laboratory).

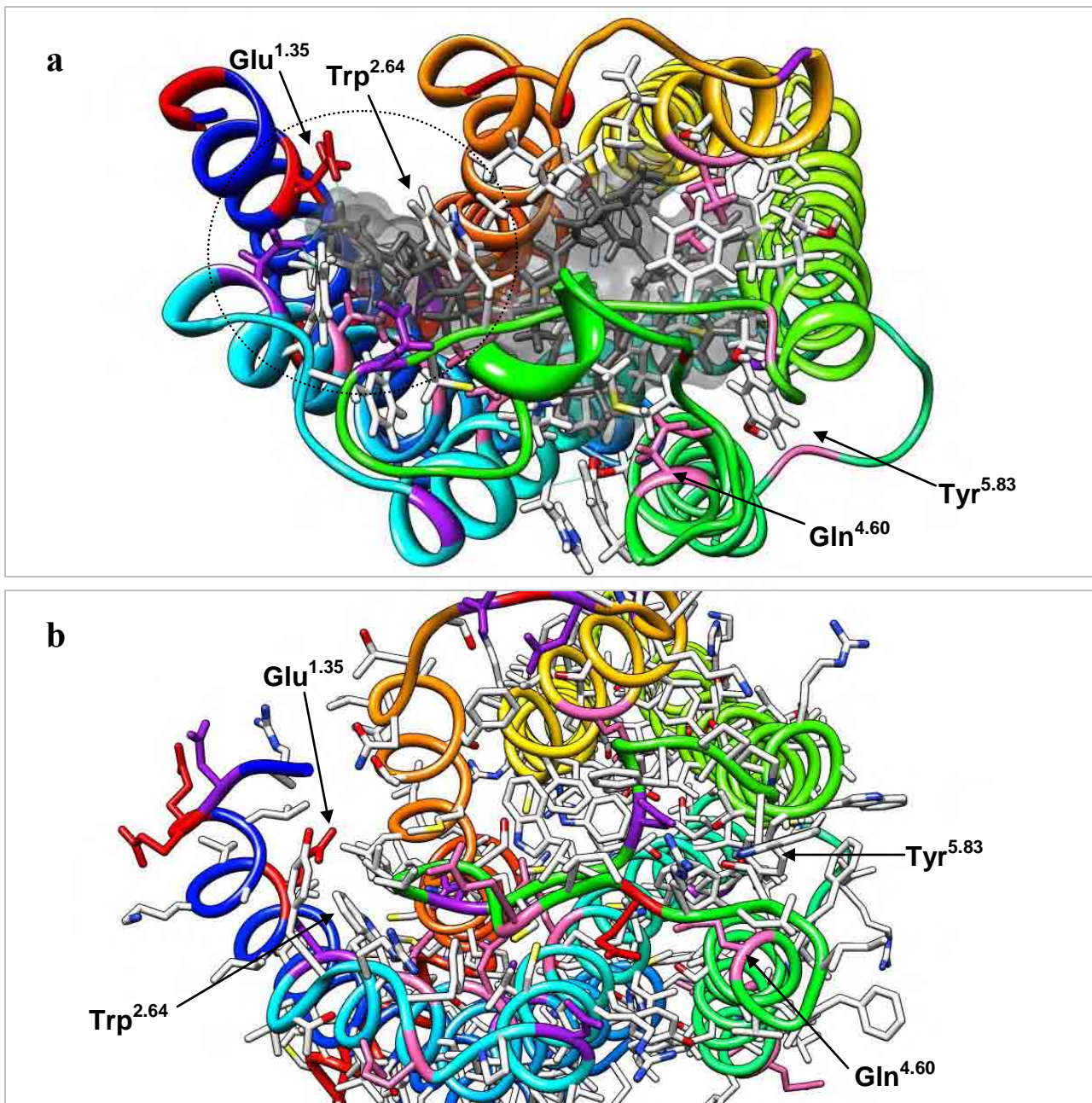


Figure 3.26 ab **The molecular model of V_{1a}R with AVP docked and V_{1b}R undocked (Viewed from the extracellular side):**

- a. V_{1a}R with bound AVP. Colour code on the figures: TM1 (blue), TM2 (pale blue), TM3 (turquoise), TM4 (green), TM5 (lime green), TM6 (yellow) and TM7 (orange). The AVP is shown in dark grey. A few residues were also colour coded: Glu (red), Asp (purple), Gln (pink). The black line encircles Glu^{1.35}, Asp^{2.65}, Trp^{2.64} and Gln^{2.61} around the glycinamide of AVP. Hydrogen bonds are shown in pale blue.
- b. V_{1b}R at inactive state. Glu^{1.35}, Gln^{4.60}, Trp^{2.64} Tyr^{5.83} are all pointing inwards towards the core of 7-TM bundles as seen in the AVP-bound V_{1a}R.

The model was constructed by Dr. John Simms. The figures were visualised using Chimera (UCSF

3.3.2. The roles of TM Gln residues in the ligand binding of V_{1b}R

Gln^{2.57} is the second residue of the conserved FQVL PQ motif of neurohypophysial hormone receptors, and this study revealed the involvement of this residue in constructing the ligand binding cavity of V_{1b}R. Although the binding properties of AVP, a V_{1b}R-selective agonist d[Cha⁴]AVP and a V_{1b}R-selective non-peptide antagonist SSR149415 were unaffected by the Ala substitution of the residue, another non-peptide antagonist 5234B exhibited decreased affinity; whereas the affinity of peptide ligands dDAVP and LA to [Q2.57A]V_{1b}R were increased significantly. Moreover, a highly V_{1a}R-selective antagonist CA was capable of binding to [Q2.57A]V_{1b}R with a high affinity unlike the V_{1b}R Wt ($K_i = 3.5$ nM and 159 nM respectively).

Gln^{2.57} is located one α -helical turn below Gln^{2.61}. The molecular models by Simms showed that the both residues are pointing inward towards the TM core, forming a cluster of a polar network along with Gln^{3.32} (figure 3.27). The upper region of TM2 is bent towards TM1, making Gln^{2.61}, Gln^{2.57}, and Gln^{3.32} almost align with Gln^{2.57} at the centre of the cluster. In the model, Gln^{2.57} in the centre appears to be holding the two other Gln residues towards TM2. The absence of Gln^{2.57} is thought to widen the ligand binding cavity as the upper region of TM2 may incline more towards TM1, and the central TM3 may tilt backwards away from the core as the interaction between TM2 and TM3 may become weaker. It should be noted that models do not include water molecules; therefore the speculation is made on incomplete assumptions. The role of Gln^{2.57} in the polar cluster may probably become clearer in the presence of water molecules. Nevertheless, the above explanation may explain why the affinity of some ligands were markedly increased for [Q2.57A]V_{1b}R.

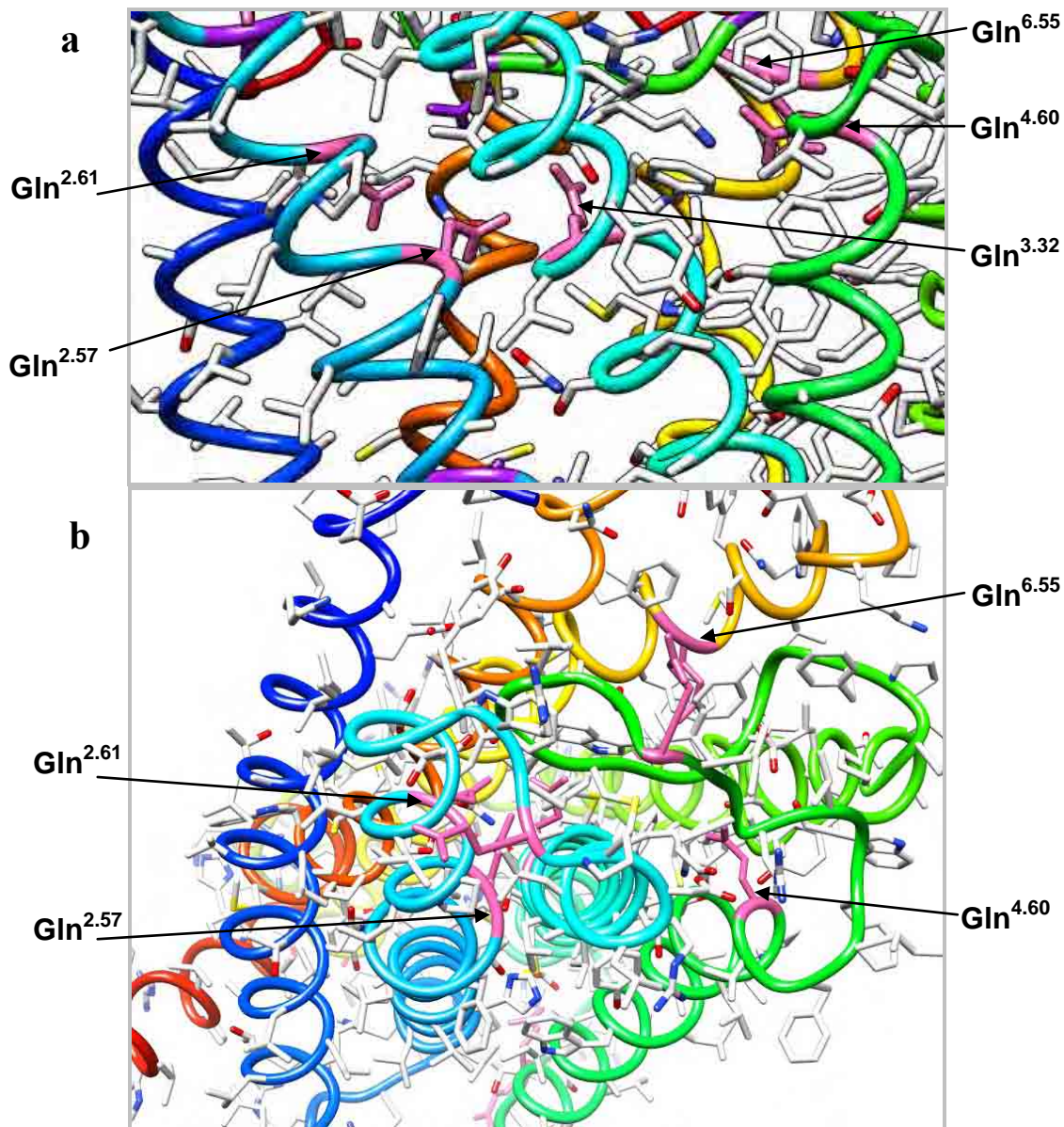


Figure 3.27 ab **The molecular model of V_{1b}R :**

- c. The side view from the side of TM2 and TM3. Colour code on the figures: TM1 (blue), TM2 (pale blue), TM3 (turquoise), TM4 (green), TM5 (lime green), TM6 (yellow) and TM7 (orange). Gln residues are shown in pink. Gln^{2.61}, Gln^{2.58}, Gln^{3.32} are all pointing inwards in the helical bundle core.
- d. Viewed from the extracellular side.

The model was constructed by Dr. John Simms. The figures were visualised using Chimera (UCSF Computer Graphics Laboratory).

Gln^{2.57} was shown also to participate in the binding of a V_{1b}R-selective non-peptide antagonist 5234B, suggesting the involvement of the TM2 portion from the polar cluster in the binding of 5234B to the V_{1b}R. Gln^{3.32} was found to be less important in binding of both non-peptide antagonists to the V_{1b}R.

The residue at position 3.32 has been reported to be involved in agonist binding of some other Family A GPCRs. Asp^{3.32} has been shown to be critically involved in the binding of acetylcholine to M₃ muscarinic receptor [440]. Asp^{3.32} in H₄ histamine receptor was shown to involve directly in histamine binding [441], and also 5-HT was shown to make direct contact with the corresponding residue in 5-HT_{2B}R [442]. In contrast, Gln^{3.32} was found not to be involved in AVP binding, suggesting differences between binding mode of a nonapeptide AVP and that of the biological amines named above.

In this study, Gln^{4.60} was shown to be involved in 5234B binding as well as in AVP binding. At the corresponding position, Phe^{4.60} in neuropeptide Y receptor was shown also to participate in binding of a non-peptide antagonist to the receptor but not of the endogenous peptide agonist [443]. In the model of V_{1b}R by Simms, the residue is pointing inwards to the helical bundle core, located on almost the same plane as the three Gln residues described above (figure 3.27a). Gln^{6.55}, which has been predicted by molecular modelling to interact with non-peptide antagonists, was shown to be required for a high affinity binding of 5234B. Gln^{6.55} points inwards towards the core of TM bundle, and is located virtually on the same plane as the Gln residues discussed above. The three Gln residues on TM2, TM4 and TM6 on this plane were all found to be involved in 5234B binding to the V_{1b}R, either directly or indirectly by constructing a suitable binding cavity.

3.3.3 The involvement of Tyr in the ligand binding of V_{1b}R

Tyr^{5.38}, located in the TM5 was shown to participate in both AVP and 5234B binding to the V_{1b}R. AVP binding appears to require bulky hydrophobic group at this position, as the loss of AVP binding resulted from Ala substitution of Tyr^{5.38} was restored by either Phe or Trp substitution. Although the high affinity binding of 5234B was restored by the Trp substitution, the Phe substitution resulted in less recovery of the affinity. This result suggests that the hydroxyl group of Tyr^{5.38} is critically important in the interaction between 5234B and the receptor. Similarly in V_{1a}R, Tyr^{5.38} was identified to be an important residue in ligand binding, and the Ala substitution reduced binding of AVP, CA and SR49059 while only LA retained a high affinity binding (Wootten D.L. Doctoral thesis, 2007. University of Birmingham).

This study identified Tyr^{3.41} as a signature residue which determines the unique binding characteristics of the V_{1b}R. The absence of this residue did not affect the binding affinity of the endogenous agonist AVP; however, the loss of the residue resulted in decreased binding affinity of all V_{1b}R-selective ligands used in this study. In the model, the aromatic ring of Tyr^{3.41} is positioned between TM4 and TM5, possibly orienting the two TMs towards TM3 by hydrophobic interactions, stabilising the local environment (Figure 3.28). Since the interhelical interactions involving Tyr^{3.41} appear to be important in constructing the ligand binding cavity unique to the V_{1b}R, further molecular docking studies using the V_{1b}R-selective ligands may clarify the exact role of Tyr^{3.41} in facilitating the formation of this unique V_{1b}R binding cavity.

The role of residue at 3.41 in stabilising the conformation of β_2 AR has been demonstrated by Roth *et al.* by hydrophobic substitutions of Glu^{3.41}. The study showed that the stability of β_2 AR can be increased by substituting the charged Glu with bulky hydrophobic Trp or Tyr

[444]. Their findings and this study altogether confirm the structural significance of hydrophobic residues at this position in Family A GPCRs. In Family A GPCRs, the D(E)RY motif found at the bottom of TM3, is known to function as an activation switch. Tyr^{3.41} is located approximately two α -helical turns above this motif, and so the stabilising effect induced by hydrophobic residues in this vicinity is thought to participate in maintaining fidelity of receptors with less agonist-independent G-protein activity. β_2 AR bearing a charged Glu^{3.41} is known to have a certain level of constitutive activity independent of agonist-stimulation. On the other hand, rhodopsin with Trp^{3.41}, and vasopressin receptors with Tyr^{3.41}, lack constitutive activity. The findings of these mutagenesis studies provide at least partially explanation for why differences in constitutive activity exist among Family A GPCRs.

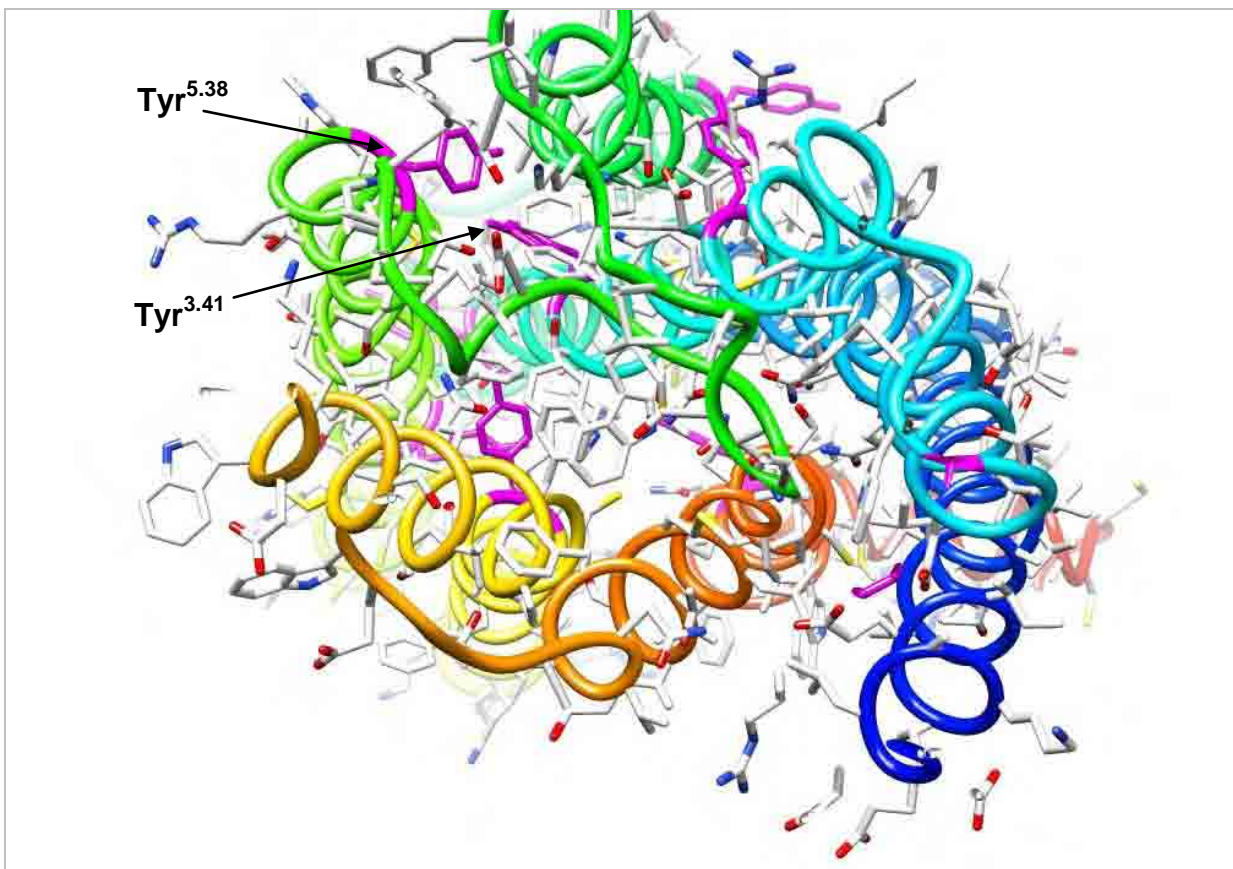


Figure 3.28 **The molecular model of V_{1b}R :**

The molecular model of V_{1b}R at an inactive state, viewed from the extracellular side. Colour code on the figures: TM1 (blue), TM2 (pale blue), TM3 (turquoise), TM4 (green), TM5 (lime green), TM6 (yellow) and TM7 (orange). Tyr residues are shown in magenta. Tyr^{5.38} is pointing inwards to the helical bundle core. Tyr^{3.41} pointing slightly upwards is also indicated in this figure.

The model was constructed by Dr. John Simms. The figures were visualised using Chimera (UCSF Computer Graphics Laboratory).

3.3.4 The participation of Ile^{6.40} and Trp^{6.48} in the V_{1b}R ligand binding

The increase in agonist affinity, both AVP and dDAVP, was seen in [I6.40A]V_{1b}R. The role of Ile^{6.40} in V_{1a}R was previously investigated by Wootten. In the study, Ile^{6.40} was shown to be important in sustaining an inactive conformation in V_{1a}R, as Ala substitution of the residue resulted in a constitutively active mutant (CAM) with an increase in AVP affinity (Wootten D.L. Doctoral thesis, 2007. University of Birmingham). Similarly in opsin, Ala substitution of Met^{6.40} resulted in CAM [445]. The increased affinity of agonists to [I6.40A]V_{1b}R was thought to suggest the involvement of this residue in sustaining inactive conformation of V_{1b}R. However, agonist-independent activity of this mutant was undetectable by InsP₃ assay (results not shown), indicating that [I6.40A]V_{1b}R is not a CAM at a significant level, and thereby Ile^{6.40} may have distinctive roles in the two subtypes.

Trp^{6.48} of the functional CWxP motif was shown in this study to be involved in bindings of both non-peptide antagonists 5234B and SSR149415. On the other hand, the affinity of agonists to [W6.48A]V_{1b}R were increased, notably for dDAVP. The loss of Trp^{6.48} might have enlarged accessibility of dDAVP to these residues dDAVP favours interacting. The facts of the affinity increase of agonists and the decrease of antagonists may altogether reflect the shift of conformational equilibrium in this construct. The construct might have favoured active states due to the loss of Trp^{6.48} which forms stabilising interaction in inactive receptors as well as initiating the activation process. However, the relatively large shift of K_i observed in the study may suggest direct interactions occurring between Trp^{6.48} and the both antagonists studied. As non-peptide antagonists usually have hydrophobic ring-based structures, the antagonists might interact with Trp^{6.48} by hydrophobic interactions. It is plausible that antagonists prevent the

rotameric change of Trp^{6.48} by direct interaction, thereby holding the receptor at an inactive state.

3.3.5 The roles of conserved Phe residues in TM domains of the V_{1b}R

Two Phe residues located at the upper TM6 above CWxP motif, Phe^{6.51} and Phe^{6.52} were proposed as interacting points for non-peptide antagonists by molecular modelling. Ala substitution of Phe^{6.51} confirmed the requirement of this residue by both 5234B and SSR149415. Ala substitution of Phe^{6.52} also affected SSR149415 binding. Similarly in V_{1a}R, the residues were shown to be required in bindings of AVP and a non-peptide antagonist SR49059 (Wootten D.L. Doctoral thesis, 2007. University of Birmingham).

In some constructs containing Ala substitution of Phe, the levels of cell-surface expression were notably decreased: in particular in receptors lacking Phe^{2.56}, Phe^{3.37}, and Phe^{5.47}. In vasopressin receptors, the upper regions of TM1 and TM2 appear to participate in agonist-induced activation, and so this region may have a certain level of conformational freedom which allows a certain structural change induced by agonist binding. Therefore Phe^{2.56} at this vicinity might have a critical role in providing temporal conformational stability of the inactive state. Although moderate decreases in cell-surface expression were seen in the absence of Phe^{6.51}, Ala-substitution of this Phe residue was relatively well-tolerated in TM6. This might be due to the nature of TM6, which undergoes relatively large conformational changes upon activation, and so the TM6 region may have a mechanism of compensating for small changes in hydrophobicity in the local vicinity.

The loss of the cell-surface expression was particularly prominent in [F5.47A]V_{1b}R. The role of Phe^{5.47} was investigated by substituting with residues of varied hydrophobicity.

Although the substitution with Val, Ile, and Trp recovered some aspect of the receptor functionality, an equivalent hydrophobicity to Phe was required for restoring the cell-surface expression level similar to the Wt, while amphipathic Lys was not tolerated at this location. The results of thermostability assay showed shorter half-lives associated with the mutant constructs, confirming the critical structural role of Phe^{5.47}. Since TM5 of Family A GPCRs appears elongated and relatively flexible, as seen in the opsin crystal structure obtained by Park *et al.* [285], the stabilising effect induced by the aromaticity of Phe^{5.47} in the middle of TM5 is thought to be critical in sustaining the receptor conformation. Biophysical studies on A₂AR have also shown that TM5 could self-associate, indicating that TM5 may possibly become part of a dimerisation interface [194]; hence could be assumed that Phe^{5.47} may have stabilising effect by facilitating homo-dimerisation. As Phe^{5.47} is highly conserved among the Family A GPCRs, the role of this residue might be universal amongst all family members, though this remains speculation until examined experimentally. Phe^{5.47} appears to face towards Phe^{6.52} in a molecular model generated by Simms (figure 3.29). The model also predicted that the two residues Phe^{5.47} and Phe^{6.52} are present at the edge of the receptor, rather than towards the helical bundle cores. These two residues may possibly be involved in hydrophobic interactions with the acyl chains of phospholipids in the membrane. The residues may also possibly involve in inter-molecular hydrophobic interactions when heterologous hydrophobic residues come close sufficiently, to facilitate dimerisation. I would also speculate that the interaction between Phe^{5.47} and Phe^{6.52} may bring the upper middle region of TM5 and TM6 into close proximity in the inactive state. The involvement of Phe^{6.52} in stabilising an inactive conformation may explain why the affinity of agonist dDAVP was increased in the absence of Phe^{6.52} as well as in the absence of Trp^{6.48}.

3.3.6. Pharmacochaperone activity of the selective antagonist 5234B

The increase in cell-surface expression observed in all the constructs, including the Wt, was thought to be due to the hydrophobic nature of the ligand with a high selectivity for the receptor. Since the mutant constructs lacking Phe^{5.47} increased the cell-surface expression following the treatment with the antagonist, the residue is said to be unlikely to have a key role in 5234B binding to the V_{1b}R.

The study on H₂R by Smit *et al.* revealed that inverse agonists can up-regulate the surface expression of the receptors while a competitive antagonist did not increase the receptor density [221]. Since vasopressin receptors lack constitutive activity, 5234B is categorically a competitive antagonist in this context. The results of this study suggest that in the receptors lacking constitutive activity, competitive antagonists can up-regulate the receptor density via yet unconfirmed mechanisms; but possibly by prolonging the cell-surface residency because of an increase in the structural stability of the receptor. It could also be assumed that a population of antagonist-bound receptors retaining the inactive state resists the process of endocytosis.

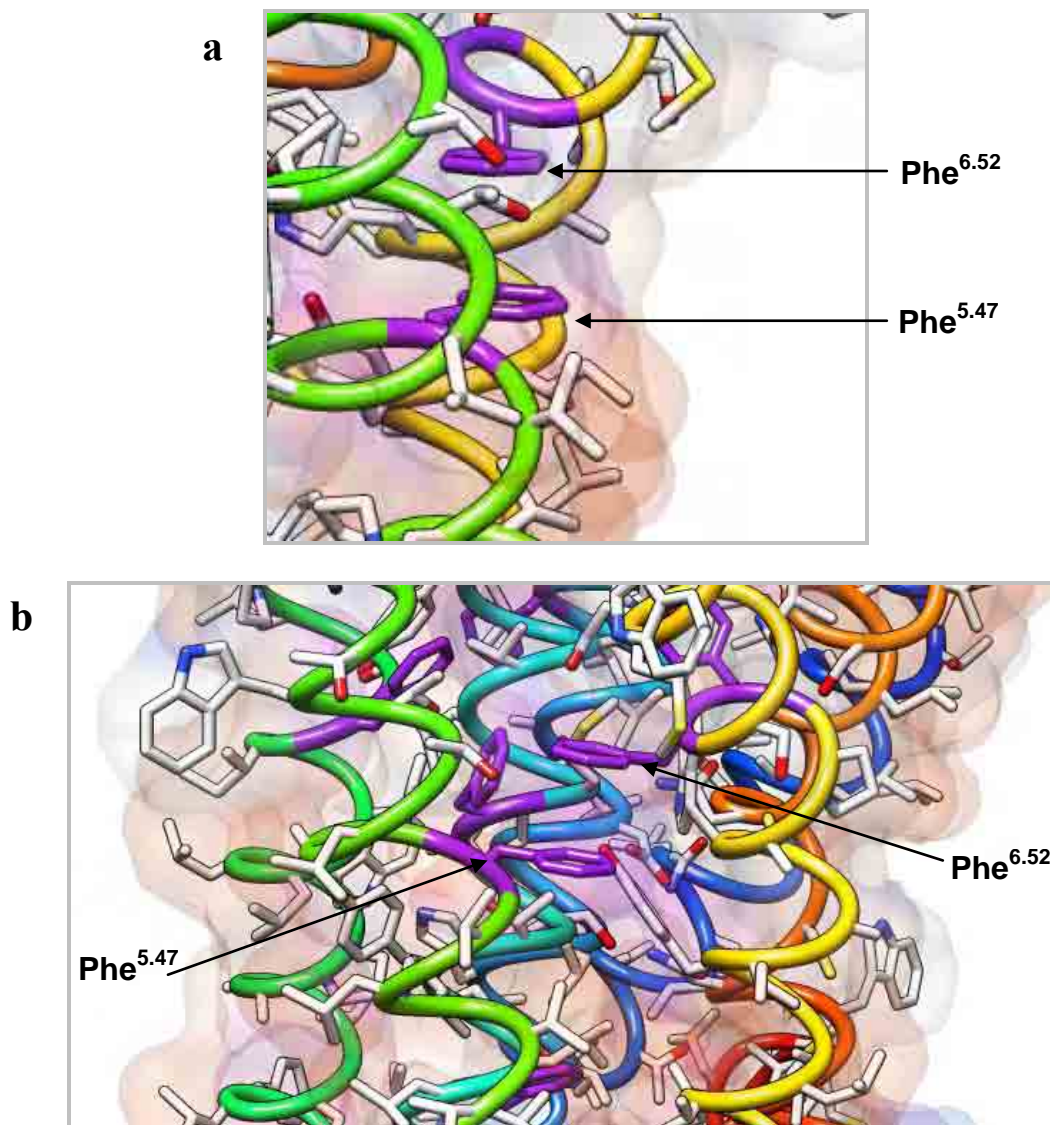


Figure 3.29 ab **The molecular model of V₁₀R, focused on Phe^{5.47} and Phe^{6.52}:**

- a.** The edge of the TM5 and TM6, showing the location of the two residues.
- b.** The side view from the side of TM4, TM5 and TM6. Colour code on the figures: TM1 (blue), TM2 (pale blue), TM3 (turquoise), TM4 (green), TM5 (lime green), TM6 (yellow) and TM7 (orange). Phe residues are shown in purple.

The model was constructed by Dr. John Simms. The figures were visualised using Chimera (UCSF Computer Graphics Laboratory).

3.4 Future Work

In addition to the above work, a further characterisation of the mutant constructs to quantify their capacities of initiating intracellular signalling cascades may give more depth to our understanding in the roles of each residue studied. The results of these experiments would likely to assist refinement of molecular models and docked ligand structures; thereby providing detailed pictures of the receptor architecture closer to reality.

By constructing a docked model of dDAVP bound to the V_{1b}R along with additional mutagenesis studies as required, differences and similarities between AVP and dDAVP in binding to the V_{1b}R could be clarified. Such investigations may possibly reveal an alternative mode of the V_{1b}R activation if differences were found to exist. Since V_{1b}R and V₂R preferentially couple to different G-protein types, establishing and comparing agonist binding and activation of V_{1b}R, V_{1a}R and V₂R in detail may allow correlating the ligand preferences of the receptor subtypes with each activation mechanism with different G-protein types.

This study has identified Try^{3.41} to be an important residue in constructing the ligand binding cavity which is a characteristic of the V_{1b}R. A series of mutagenesis study substituting this residue may reveal the role of this residue in detail, and provide a clearer picture of the subtype differences between the V_{1b}R and the V_{1a}R. Moreover, Tyr at 3.41 was identified to be structurally sustaining in the V_{1b}R, and also in β_2 AR by Roth *et al.* as Tyr-substitution of Glu^{3.41} yielded higher surface expression of the receptor [444]. As the differences in nature of the residues at 3.41 may well relate to varied degrees of constitutive activity of these receptors, protein sequence analysis of the Family A GPCRs followed by investigating constitutive activity of some of these receptors to confirm the correlation could be useful. By establishing the

correlation, in future the degrees of constitutive activity of Family A GPCRs, if unknown, could be predicted by the nature of residue at 3.41.

As Phe/Tyr^{5.47} is highly conserved among Family A GPCRs, cell-surface half-life measured for mutant constructs containing varied hydrophobicity at position 5.47 could be used as a guidance parameter in computational studies simulating denaturing or possibly folding process of Family A GPCRs. This study has demonstrated the pharmaco-chaperone activity of 5234B in assisting the cell-surface expression of the structurally unstable mutants and the Wt. As for the Wt, the observed increase could be due to the decreased constitutive internalisation of receptor recycling. The mechanisms involving internalisation and recycling of the V_{1b}R could be investigated by mutagenesis studies to find the phosphorylation sites, ubiquitination sites, and also by a co-transfection with dominant negative dynamin-1 (Dyn-K44A) or using a dynamin-inhibitor dynasore. If a comparable increase in the cell-surface expression was observed for the internalisation-defective mutants, it would confirm the increase in the cell-surface expression of the Wt observed in this study to be due to the decrease in the constitutive internalisation. Alternatively, the internalisation process and the fate of the Wt and the folding defective mutant in the absence and presence of a pharmacol-chaperone could be investigated by visualising the receptor constructs using a fluorescence microscopy.

Chapter 4 Exploring the molecular basis for ligand selectivity between $V_{1b}R$ and $V_{1a}R$

4.1. Introduction

One of the key processes in developing a novel compound for therapeutic use is to ensure the compound binds selectively to the target receptor. The aim of this study is to probe the putative binding cavity of the $V_{1b}R$ with subtype-selective compounds in order to identify residues which distinguish between the $V_{1b}R$ and a closely related subtype $V_{1a}R$ in ligand binding. This study used three non-peptide antagonists: $V_{1a}R$ -selective SR49059 and $V_{1b}R$ -selective SSR149415 both with known structures; and also $V_{1b}R$ -selective 5234B with structure undisclosed. The structures of the antagonists SR49059 and SSR149415 are presented in figure 4.23 belonging to discussion section 4.3.

The strategy adopted was to identify individual residues in the $V_{1b}R$ which had potential to interact with bound ligands, using a combination of molecular modelling and knowledge of Family A GPCRs in general. Residues suspected of contributing to the discrimination of subtype-selective ligands were investigated by studying $V_{1b}R$ and $V_{1a}R$ in parallel. In this study, each reciprocal mutation was introduced into both receptor subtypes, with each containing the corresponding residue from the other subtype. This approach provided more complete information than studying only the $V_{1b}R$. Mutation of any residue important for high affinity binding of a selective ligand would produce a reciprocal gain, and loss, of affinity respectively, in the two subtypes. A series of residues was selected for investigation. 11

residues which may confer selectivity between V_{1b}R and V_{1a}R were selected based on a computational molecular modelling study by Dr. Grant Wishart (Schering-Plough Research Institute, Newhouse). These are Tyr^{3.30}/His^{3.30}, Phe^{4.56}/Leu^{4.56}, Val^{4.61}/Tyr^{4.61}, Leu^{5.39}/Ile^{5.39}, Thr^{5.42}/Met^{5.42}, Val^{6.54}/Ile^{6.54}, Ala^{7.34}/Thr^{7.34}, Phe^{7.35}/Ile^{7.35}, Ser^{7.38}/Thr^{7.38}, Met^{7.39}/Ala^{7.39} and Asn^{7.43}/Ser^{7.43} of V_{1b}R/V_{1a}R. Three residues were also additionally studied due to their location, geometrical or functional interests. These are Thr^{2.49}/Ala^{2.49}, Phe^{4.54}/Ala^{4.54}, and Ala^{6.46}/Val^{6.46} of V_{1b}R/V_{1a}R. Thr^{2.49}/Ala^{2.49} was chosen as it is next to the highly conserved Asp^{2.50} and TM2 is heavily involved in AVP binding. Phe^{4.54}/Ala^{4.54} was chosen for its proximity to Phe^{4.56}. Ala^{6.46}/Val^{6.46} was selected due to its proximity to the CWxP motif which is functionally important. Total of 14 residues were targeted for mutagenesis in V_{1b}R and V_{1a}R to produce 28 mutant receptor constructs. The residues studied in this section are indicated in schematic diagrams of V_{1b}R and V_{1a}R in figure 4.1.

4.2 Results

The characteristics of the mutant constructs determined in this study are presented in three sections. The first section contains results obtained for V_{1b}R constructs which were engineered to incorporate the corresponding residue from the V_{1a}R, and these are [A2.49T]V_{1b}R, [Y3.30H]V_{1b}R, [A4.54F]V_{1b}R, [F4.56L]V_{1b}R, [V4.61Y]V_{1b}R, [L5.39V]V_{1b}R, [T5.42M]V_{1b}R, [A6.46V]V_{1b}R, [V6.54I]V_{1b}R, [A7.34T]V_{1b}R, [F7.35I]V_{1b}R, [S7.38T]V_{1b}R, [M7.39A]V_{1b}R and [N7.43S]V_{1b}R. The second section contains results obtained for V_{1a}R constructs which were engineered to incorporate the corresponding residue from the V_{1b}R, and these are [A2.49T]V_{1a}R, [H3.30Y]V_{1a}R, [F4.54A]V_{1a}R, [L4.56F]V_{1a}R, [V4.61Y]V_{1a}R, [V5.39L]V_{1a}R, [M5.42T]V_{1a}R, [V6.46A]V_{1a}R, [I6.54V]V_{1a}R, [T7.34A]V_{1a}R, [I7.35F]V_{1a}R, [T7.38S]V_{1a}R, [A7.39M]V_{1a}R and [S7.43N]V_{1a}R. Some of the residues targeted were predicted as potentially contacting sites of non-peptide antagonists in the V_{1b}R by Dr. Grant Wishart (Personal communication). Hence these residues were also substituted with Ala in the V_{1b}R to generate [F4.56A]V_{1b}R, [L5.39A]V_{1b}R, [T5.42A]V_{1b}R and [N7.43A]V_{1b}R. In addition [V6.54A]V_{1b}R was also made as it is located in TM6 which go under conformational changes upon receptor activation. The results obtained for these five V_{1b}R constructs are presented in the third section of results. All mutant receptor constructs were expressed in HEK293T cells and their ligand binding profiles were characterised.

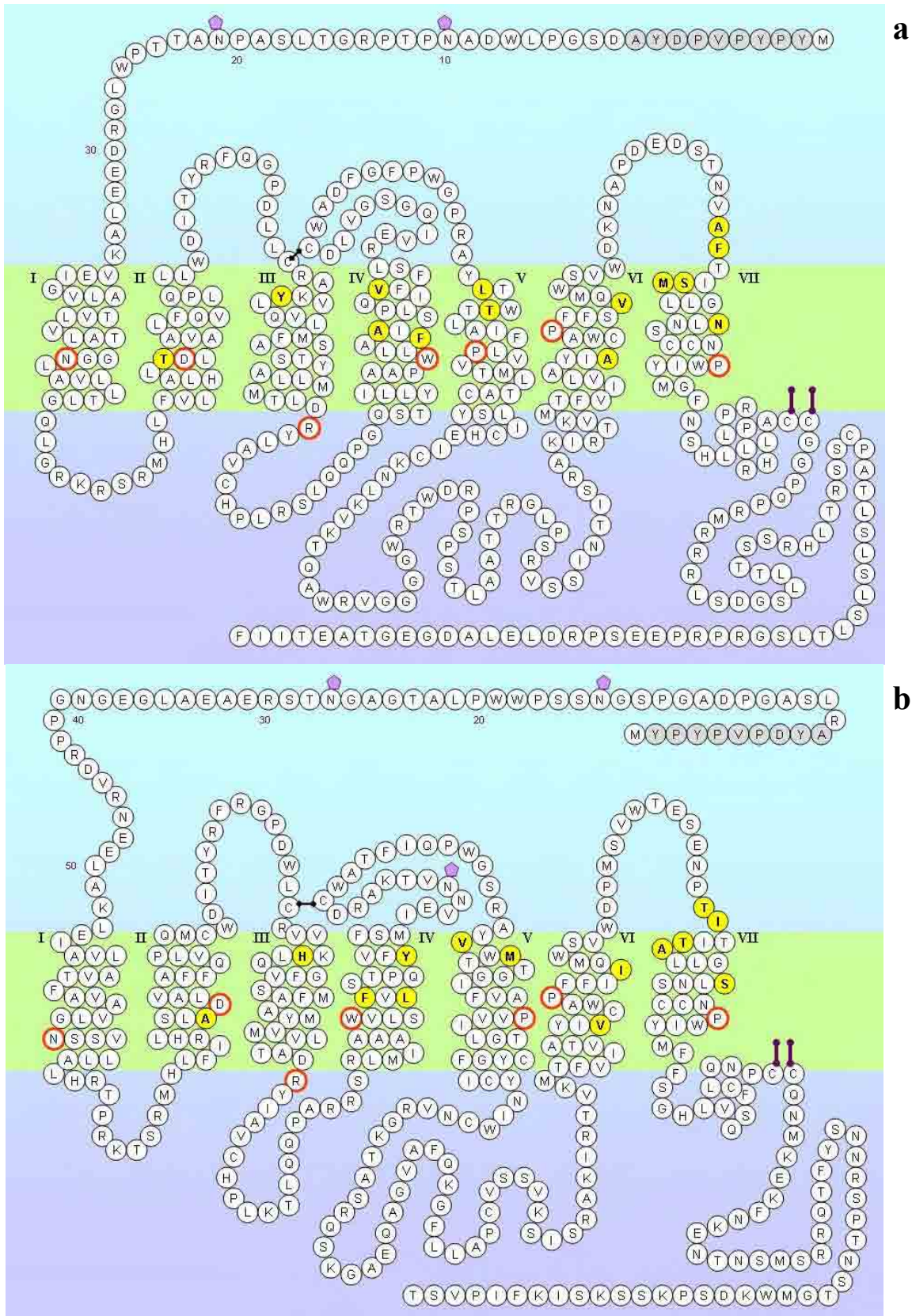


Figure 4.1 The schematic diagrams of $V_{1a}R$ and $V_{1b}R$ indicating the positions targeted for mutagenesis: **a.** $V_{1b}R$; **b.** $V_{1a}R$. The residues targeted for mutagenesis are shown in yellow. Orange lines encircle reference residues used in Ballesteros-Weinstein numbering scheme.

Table 4.1 The mutagenic oligonucleotide primers for mutagenesis:
Codon altered shown underlined, and the nucleotides changed shown in **BOLD**.

Construct	Direction	Nucleotide Sequence
[T2.49A]V _{1b} R	(S) (AS)	5'-G-CAC-TTA-GCC-CTG- <u>GCA</u> -GAC-CTG-GCC-G-3' 5'-C-GGC-CAG-GTC- <u>TGC</u> -CAG-GGC-TAA-GTG-C-3'
[Y3.30H]V _{1b} R	(S) (AS)	5'-GG-GCC-GTC-AAG- <u>CAC</u> -CTG-CAG-GTG-CTC-AGC-3' 5'-GCT-GAG-CAC-CTG-CAG- <u>GTG</u> -CTT-GAC-GGC-CC-3'
[A4.54F]V _{1b} R	(S) (AS)	5'-C-TGG-CTG-CTG-GCC- <u>TTC</u> -ATC-TTC-AGC-CTC-CC-3' 5'-GG-GAG-GCT-GAA-GAT- <u>GAA</u> -GGC-CAG-CAG-CCA-G-3'
[F4.56L]V _{1b} R	(S) (AS)	5'-G-CTG-GCC-GCC-ATC- <u>TTG</u> -AGC-CTC-CCT-CAA-G-3' 5'-C-TTG-AGG-GAG-GCT- <u>CAA</u> -GAT-GGC-GGC-CAG-C-3'
[V4.61Y]V _{1b} R	(S) (AS)	5'-C-AGC-CTC-CCT-CAA- <u>TAC</u> -TTC-ATT-TTT-TCC-CTG-CCG-G-3' 5'-C-CCG-CAG-GGA-AAA-AAT-GAA- <u>GTA</u> -TTG-AGG-GAG-GCT-G-3'
[L5.39V]V _{1b} R	(S) (AS)	5'-GGG-CCA-CGG-GCC-TAC- <u>GTC</u> -ACC-TGG-ACC-ACC-3' 5'-GGT-GGT-CCA-GGT- <u>GAC</u> -GTA-GGC-CCG-TGG-CCC-3'
[T5.42M]V _{1b} R	(S) (AS)	5'-GCC-TAC-CTC-ACC-TGG- <u>ATG</u> -ACC-CTG-GCT-ATC-TTC-G-3' 5'-C-GAA-GAT-AGC-CAG-GGT- <u>CAT</u> -CCA-GGT-GAG-GTA-GGC-3'
[A6.46V]V _{1b} R	(S) (AS)	5'-G-CTG-GCC-TAC-ATC- <u>GTT</u> -TGC-TGG-GCT-CC-3' 5'-GG-AGC-CCA-GCA- <u>AAC</u> -GAT-GTA-GGC-CAG-C-3'
[V6.54I]V _{1b} R	(S) (AS)	5'-GCT-CCC-TTC-TTC-AGT- <u>ATC</u> -CAG-ATG-TGG-TCC-G-3' 5'-C-GGA-CCA-CAT-CTG- <u>GAT</u> -ACT-GAA-GAA-GGG-AGC-3'
[A7.34T]V _{1b} R	(S) (AS)	5'-GAA-GAT-TCC-ACC-AAT-GTG- <u>ACT</u> -TTC-ACC-ATC-TCT-ATG-C-3' 5'-G-CAT-AGA-GAT-GGT-GAA- <u>AGT</u> -CAC-ATT-GGT-GGA-ATC-TTC-3'
[F7.35I]V _{1b} R	(S) (AS)	5'-CC-ACC-AAT-GTG-GCT- <u>ATC</u> -ACC-ATC-TCT-ATG-CTT-TTG-G-3' 5'-C-CAA-AAG-CAT-AGA-GAT-GGT- <u>GAT</u> -AGC-CAC-ATT-GGT-GG-3'
[S7.38T]V _{1b} R	(S) (AS)	5'-G-GCT-TTC-ACC-ATC- <u>ACT</u> -ATG-CTT-TTG-GGC-AAC-C-3' 5'-G-GTT-GCC-CAA-AAG-CAT- <u>AGT</u> -GAT-GGT-GAA-AGC-C-3'
[M7.39A]V _{1b} R	(S) (AS)	5'-G-GCT-TTC-ACC-ATC-TCT- <u>GCG</u> -CTT-TTG-GGC-AAC-CTC-3' 5'-GAG-GTT-GCC-CAA-AAG- <u>CGC</u> -AGA-GAT-GGT-GAA-AGC-C-3'
[N7.43S]V _{1b} R	(S) (AS)	5'-CT-ATG-CTT-TTG-GGC- <u>AGC</u> -CTC-AAC-AGC-TGC-TGC-3' 5'-GCA-GCA-GCT-GTT-GAG- <u>GCT</u> -GCC-CAA-AAG-CAT-AG-3'
[A2.49T]V _{1a} R	(S) (AS)	5'-CAC-CTCAGC-CTG- <u>ACC</u> -GAC-CTG-GCC-GTG-3' 5'-CAC-GGC-CAG-GTC- <u>GGT</u> -CAG-GCT-GCG-GTG-3'
[H3.30Y]V _{1a} R	(S) (AS)	5'-CGC-GTG-GTG-AAG- <u>TAC</u> -CTG-CAG-GTG-TTC-G-3' 5'-C-GAA-CAC-CTG-CAG- <u>GTA</u> -CTT-CAC-CAC-GCG-3'
[F4.54A]V _{1a} R	(S) (AS)	5'-GG-GTG-CTG-AGC- <u>GCC</u> -GTG-CTG-AGC-ACG-C-3' 5'-G-CGT-GCT-CAG-CAC- <u>GGC</u> -GCT-CAG-CAC-CC-3'
[Y4.61V]V _{1a} R	(S) (AS)	5'-G-CTG-AGC-ACG-CCG-CAG- <u>GTC</u> -TTC-GTC-TTC-TCC-3' 5'-GGA-GAA-GAC-GAA- <u>GAC</u> -CTG-CCG-CGT-GCT-CAG-C-3'
[V5.39L]V _{1a} R	(S) (AS)	5'-GT-TCT-CGT-GCC-TAC- <u>CTG</u> -ACC-TGG-ATG-ACG-G-3' 5'-C-CGT-CAT-CCA-GGT- <u>CAG</u> -GTA-GGC-ACG-AGA-AC-3'
[M5.42T]V _{1a} R	(S) (AS)	5'-CC-TAC-GTG-ACC-TGG- <u>ACG</u> -ACG-GGC-GGC-ATC-3' 5'-GAT-GCC-GCC-CGT-CGT-CCA-GGT-CAC-GTA-GG-3'
[V6.46A]V _{1a} R	(S) (AS)	5'-CG-GCT-TAC-ATC- <u>GCC</u> -TGC-TGG-GCG-CC-3' 5'-GG-CGC-CCA-GCA- <u>GGC</u> -GAT-GTA-AGC-CG-3'
[I6.54V]V _{1a} R	(S) (AS)	5'-CG-CCT-TTC-TTC-ATC- <u>GTC</u> -CAG-ATG-TGG-TCT-GTC-3' 5'-GAC-AGA-CCA-CAT-CTG- <u>GAC</u> -GAT-GAA-GAA-AGG-3'

Construct	Direction	Nucleotide Sequence
[T7.34A]V _{1a} R	(S) (AS)	5'-C-GAA-TCG-GAA-AAC-CCT- <u>GCC</u> -ATC-ACC-ATC-ACT-GC-3' 5'-GC-AGT-GAT-GGT-GAT- <u>GGC</u> -AGG-GTT-TTC-CGA-TTC-G-3'
[I7.35F]V _{1a} R	(S) (AS)	5'-G-GAA-AAC-CCT-ACC- <u>TTC</u> -ACC-ATC-ACT-GCA-TTA-CTG-3' 5'-CAG-TAA-TGC-AGT-GAT-GGT- <u>GAA</u> -GGT-AGG-GTT-TTC-C-3'
[T7.38S]V _{1a} R	(S) (AS)	5'-CCT-ACC-ATC-ACC-ATC- <u>TCT</u> -GCA-TTA-CTG-GGT-TCC-3' 5'-GGA-ACC-CAG-TAA-TGC- <u>AGA</u> -GAT-GGT-GAT-GGT-AGG-3'
[A7.39M]V _{1a} R	(S) (AS)	5'-CC-ATC-ACC-ATC-ACT- <u>ATG</u> -TTA-CTG-GGT-TCC-3' 5'-GGA-ACC-CAG-TAA- <u>CAT</u> -AGT-GAT-GGT-GAT-GG-3'
[S7.34N]V _{1a} R	(S) (AS)	5'-GCA-TTA-CTG-GGT- <u>AAC</u> -TTG-AAT-AGC-TGC-3' 5'-GCA-GCT-ATT-CAA- <u>GTT</u> -ACC-CAG-TAA-TGC-3'
[F4.56A]V _{1b} R	(S) (AS)	5'-G-CTG-GCC-GCC-ATC- <u>GCC</u> -AGC-CTC-CCT-CAA-G-3' 5'-C-TTG-AGG-GAG-GCT- <u>CGG</u> -GAT-GGC-GGC-CAG-C-3'
[L5.39A]V _{1b} R	(S) (AS)	5'-GGG-CCA-CGG-GCC-TAC- <u>GCC</u> -ACC-TGG-ACC-ACC-3' 5'-GGT-GGT-CCA-GGT- <u>GGC</u> -GTA-GGC-CCG-TGG-CCC-3'
[T5.42A]V _{1b} R	(S) (AS)	5'-GCC-TAC-CTC-ACC-TGG- <u>GCC</u> -ACC-CTG-GCT-ATC-TTC-G-3' 5'-C-GAA-GAT-AGC-CAG-GGT- <u>GGC</u> -CCA-GGT-GAG-GTA-GGC-3'
[V6.54A]V _{1b} R	(S) (AS)	5'-CCC-TTC-TTC-AGT- <u>GCC</u> -CAG-ATG-TGG-TCC-G-3' 5'-C-GGA-CCA-CAT-CTG- <u>GGC</u> -ACT-GAA-GAA-GGG-3'
[N7.43A]V _{1b} R	(S) (AS)	5'-CT-ATG-CTT-TTG-GGC- <u>GCC</u> -CTC-AAC-AGC-TGC-TGC-3' 5'-GCA-GCA-GCT-GTT-GAG- <u>GGC</u> -GCC-CAA-AAG-CAT-AG-3'

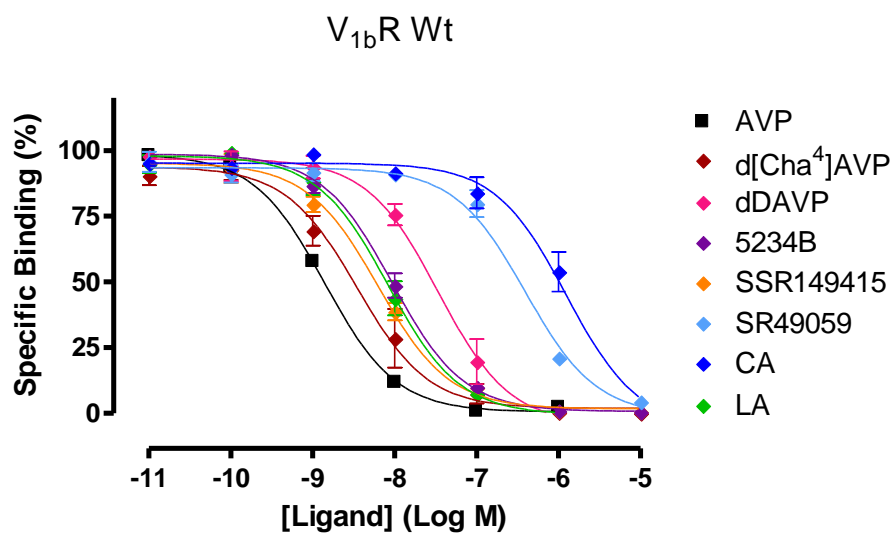
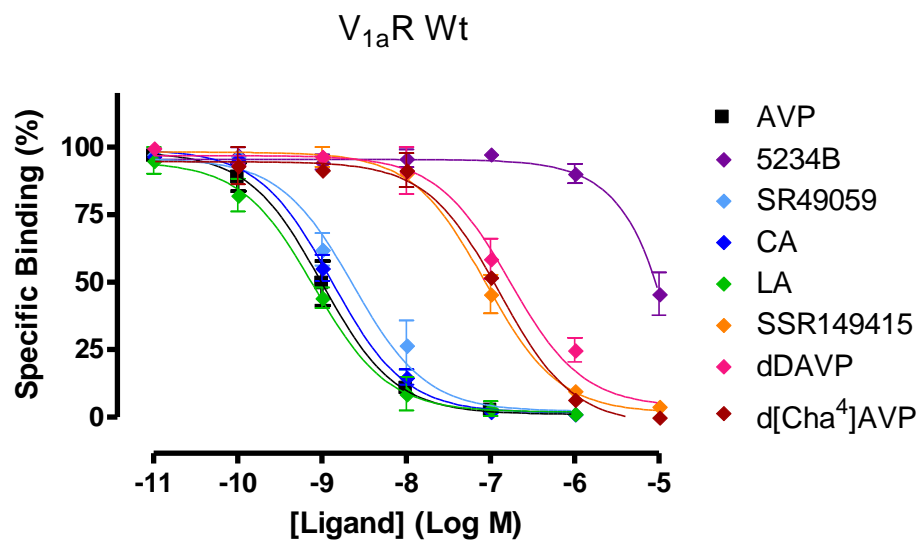
a**b**

Figure 4.2 ab The binding profiles of Wt $V_{1b}R$ and $V_{1a}R$:

a. Wt $V_{1b}R$;

b. Wt $V_{1a}R$.

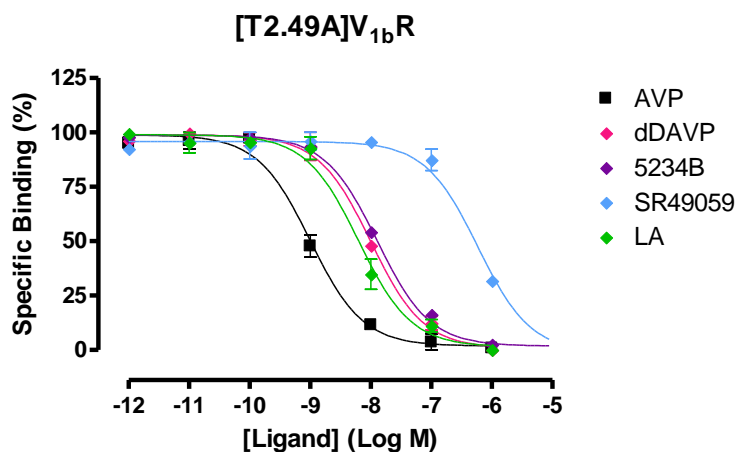
Competition binding curves of [³H]AVP and various ligands as indicated. The values plotted were normalised to show percentage specific binding. The error bars represent SEM of three separate experiments each performed in triplicate.

4.2.1. The characteristics of the V_{1b}R constructs containing the corresponding V_{1a}R residue

Construct	Binding Affinity (<i>K_i</i> , nM ±S.E.M.)						Cell-Surface Expression (% Wt)
	AVP	d[Cha ⁴]AVP	5234B	SSR149415	SR49059	LA	
WT V _{1b} R	0.90 (± 0.13)	1.35 (± 0.02)	7.18 (± 1.82)	3.36 (± 0.93)	670 (± 147)	6.25 (± 1.86)	100
WT V _{1a} R	1.02 (± 0.12)	81.9 (± 1.3)	6392 (± 655)	70.4 (± 15.3)	1.76 (± 0.54)	0.57 (± 0.05)	-
[T2.49A]V _{1b} R	0.63 (± 0.10)	-	6.75 (± 1.42)	-	343 (± 6)	4.74 (± 1.55)	95 (± 4)
[Y3.30H]V _{1b} R	0.37 (± 0.04)	-	4.21 (± 1.05)	16.6 (± 5.0)	54.0 (± 3.9)	-	25 (± 1)
[A4.54F]V _{1b} R	0.24 (± 0.08)	-	4.10 (± 1.70)	2.26 (± 0.05)	104 (± 19)	1.26 (± 0.10)	89 (± 7)
[F4.56L]V _{1b} R	0.70 (± 0.09)	1.80 (± 0.50)	7.47 (± 1.54)	10.4 (± 2.3)	155 (± 43)	4.34 (± 0.66)	71 (± 4)
[V4.61Y]V _{1b} R	0.92 (± 0.37)	-	9.01 (± 1.43)	6.95 (± 0.83)	340 (± 109)	5.13 (± 0.32)	51 (± 9)
[L5.39V]V _{1b} R	0.40 (± 0.14)	1.15 (± 0.25)	21.5 (± 1.9)	6.90 (± 1.02)	119 (± 38)	1.53 (± 0.28)	85 (± 5)
[T5.42M]V _{1b} R	0.73 (± 0.08)	2.54 (± 0.12)	69.8 (± 19.1)	35.71 (± 1.28)	1.43 (± 0.24)	7.25 (± 0.90)	101 (± 3)
[A6.46V]V _{1b} R	0.33 (± 0.12)	-	4.59 (± 1.26)	-	369 (± 27)	3.31 (± 0.35)	91 (± 5)
[V6.54I]V _{1b} R	0.46 (± 0.14)	-	5.56 (± 0.42)	-	187 (± 33)	2.42 (± 0.30)	89 (± 9)
[A7.34T]V _{1b} R	0.47 (± 0.15)	-	17.5 (± 0.4)	2.36 (± 1.11)	86.3 (± 17.3)	1.77 (± 0.50)	45(± 2)
[F7.35I]V _{1b} R	0.93 (± 0.26)	0.70 (± 0.04)	229 (± 41)	3.47 (± 0.69)	568 (± 49)	2.08 (± 0.11)	84 (± 8)
[S7.38T]V _{1b} R	1.00 (± 0.30)	-	7.19 (± 2.90)	1.90 (± 0.19)	328 (± 89)	4.25 (± 0.75)	109 (± 1)
[M7.39A]V _{1b} R	1.05 (± 0.12)	0.56 (± 0.04)	10.5 (± 1.6)	32.6 (± 0.3)	52.4 (± 9.2)	3.61 (± 1.00)	81 (± 3)
[N7.43S]V _{1b} R	0.75 (± 0.25)	-	12.84 (± 0.72)	9.07 (± 0.12)	465 (± 14)	2.04 (± 0.28)	80 (± 3)

Table 4.2 Ligand binding profiles of the constructs containing V_{1a}R residues introduced in the corresponding position of the V_{1b}R: Binding affinities of V_{1b}R-selective antagonists 5234B, SSR149415, and V_{1a}R-selective antagonist SR49059 to various V_{1b}R constructs were determined by competition binding assay using [³H]AVP as a tracer ligand. Binding affinity of peptide ligands to some constructs was also investigated. The values presented are mean plus/minus SEM of three experiments each performed in triplicate. The colour code applied as previous to show relative gain or loss of the affinity of each ligand in comparison to the Wt V_{1b}R. In essence, darker colours indicate larger shift: increase in affinity is shown in blue; loss of the affinity shown in orange/red and yellow indicates small shifts below 10-fold. Cell-surface expression levels of constructs relative to the Wt V_{1b}R were determined by ELISA.

a



b

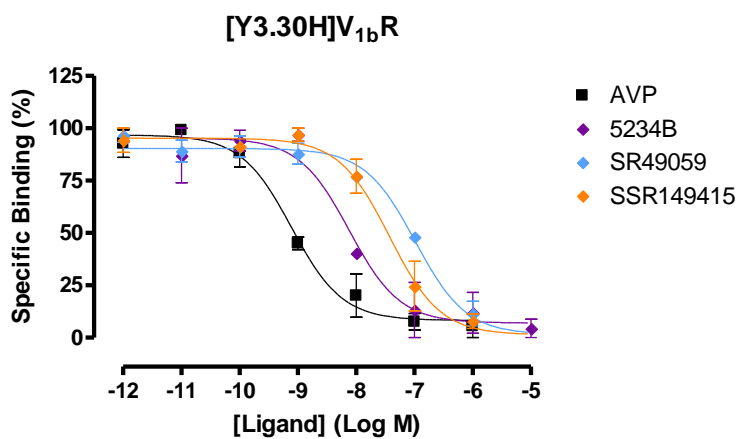


Figure 4.3 ab

The binding profiles of [T2.49A]V_{1b}R modified in TM2, and [Y3.30H]V_{1b}R modified in TM3 to contain the corresponding residues of V_{1a}R:

- a. [T2.49A]V_{1b}R;
- b. [Y3.30H]V_{1b}R.

Competition binding curves of [³H]AVP and various ligands as indicated. The values plotted were normalised to show percentage specific binding. The error bars represent SEM of three separate experiments each performed in triplicate.

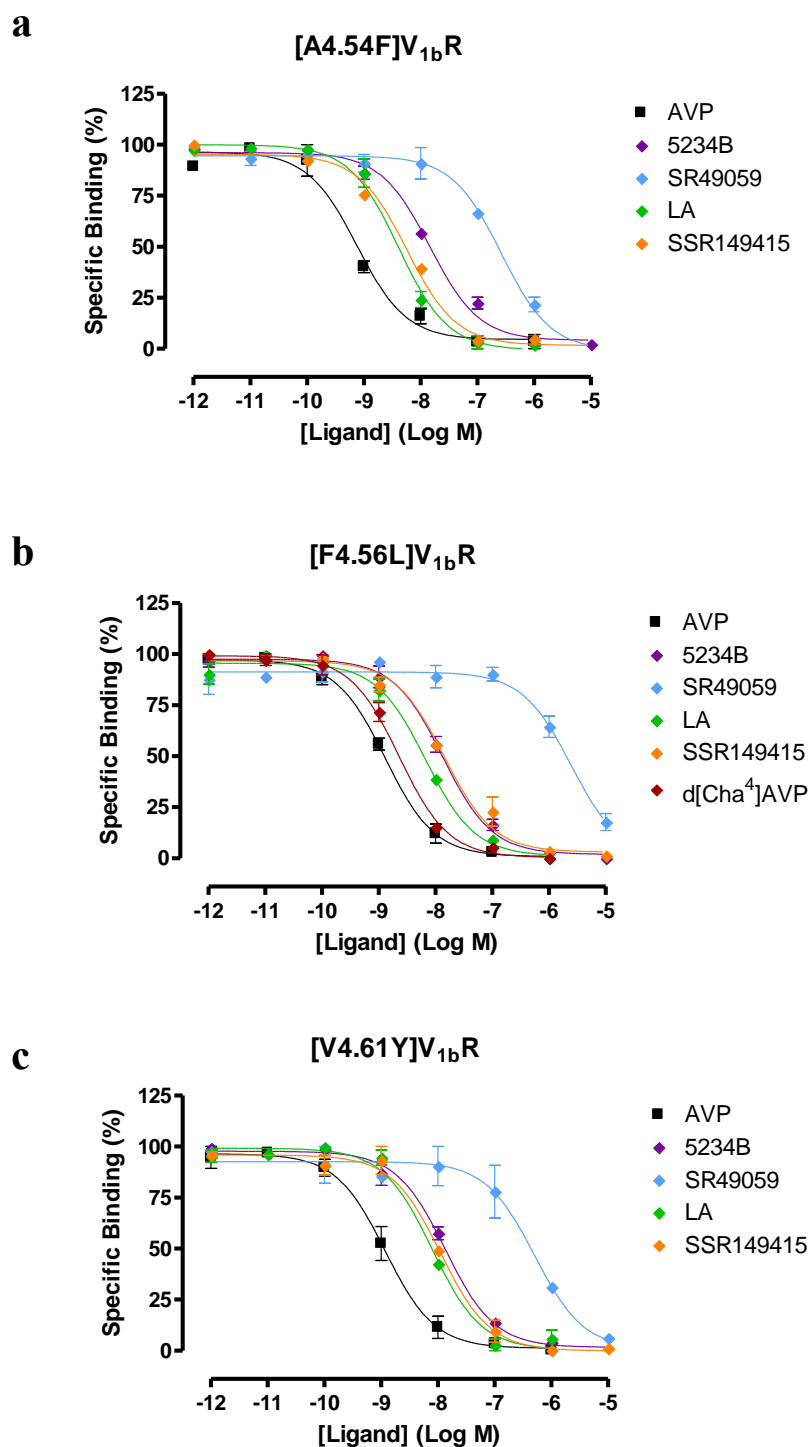


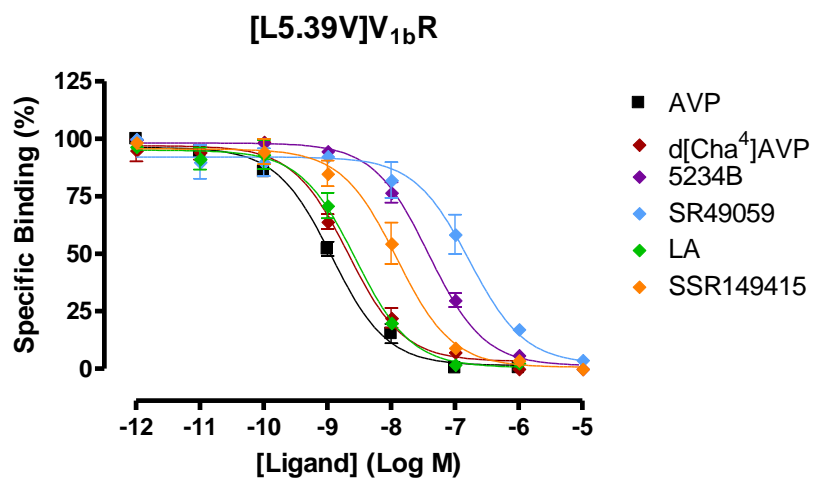
Figure 4.4 a-c

The binding profiles of V_{1b}R constructs modified in TM4 to contain the corresponding residues of V_{1a}R:

- [A4.54F]V_{1b}R;
- [F4.56L]V_{1b}R;
- [V4.61Y]V_{1b}R.

Competition binding curves of [³H]AVP and various ligands as indicated. The values plotted were normalised to show percentage specific binding. The error bars represent SEM of three separate experiments each performed in triplicate.

a



b

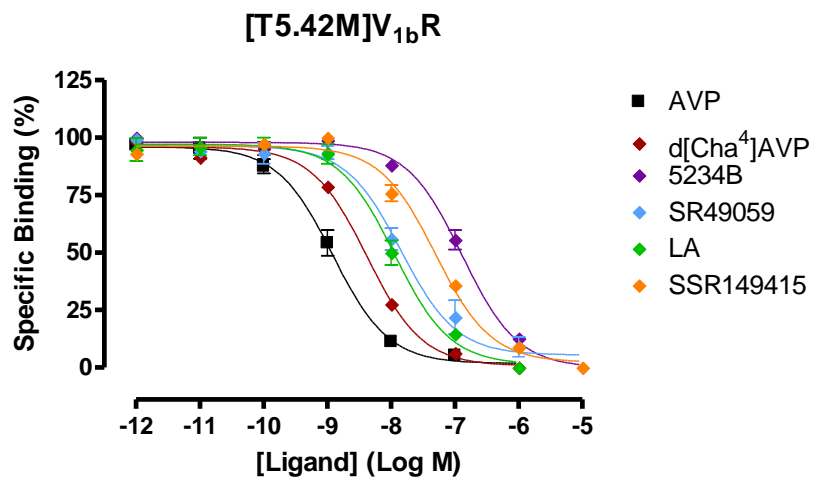


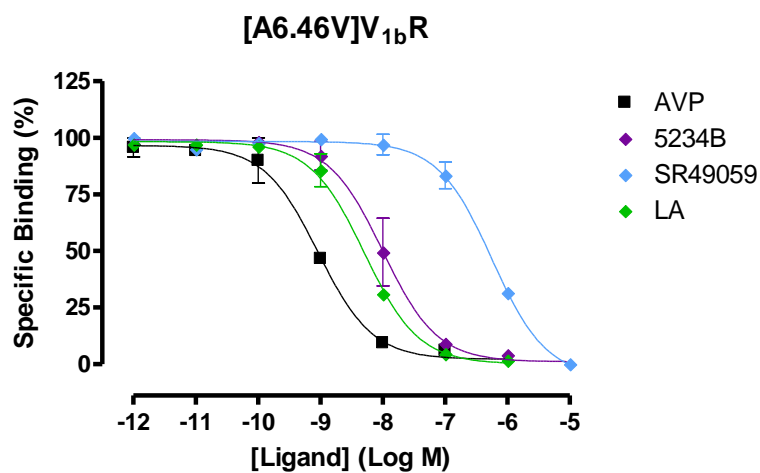
Figure 4.5 ab

The binding profiles of V_{1b}R constructs modified in TM5 to contain the corresponding residues of V_{1a}R:

- a. [L5.39V]V_{1b}R;
- b. [T5.42M]V_{1b}R.

Competition binding curves of [³H]AVP and various ligands as indicated. The values plotted were normalised to show percentage specific binding. The error bars represent SEM of three separate experiments each performed in triplicate.

a



b

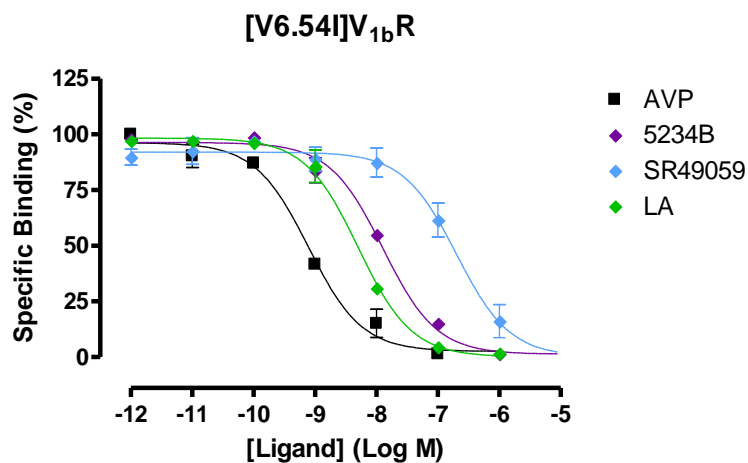


Figure 4.6 ab

The binding profiles of V_{1b}R constructs modified in TM6 to contain the corresponding residues of V_{1a}R:

- a. [A6.46V]V_{1b}R;
- b. [V6.54I]V_{1b}R.

Competition binding curves of [³H]AVP and various ligands as indicated. The values plotted were normalised to show percentage specific binding. The error bars represent SEM of three separate experiments each performed in triplicate.

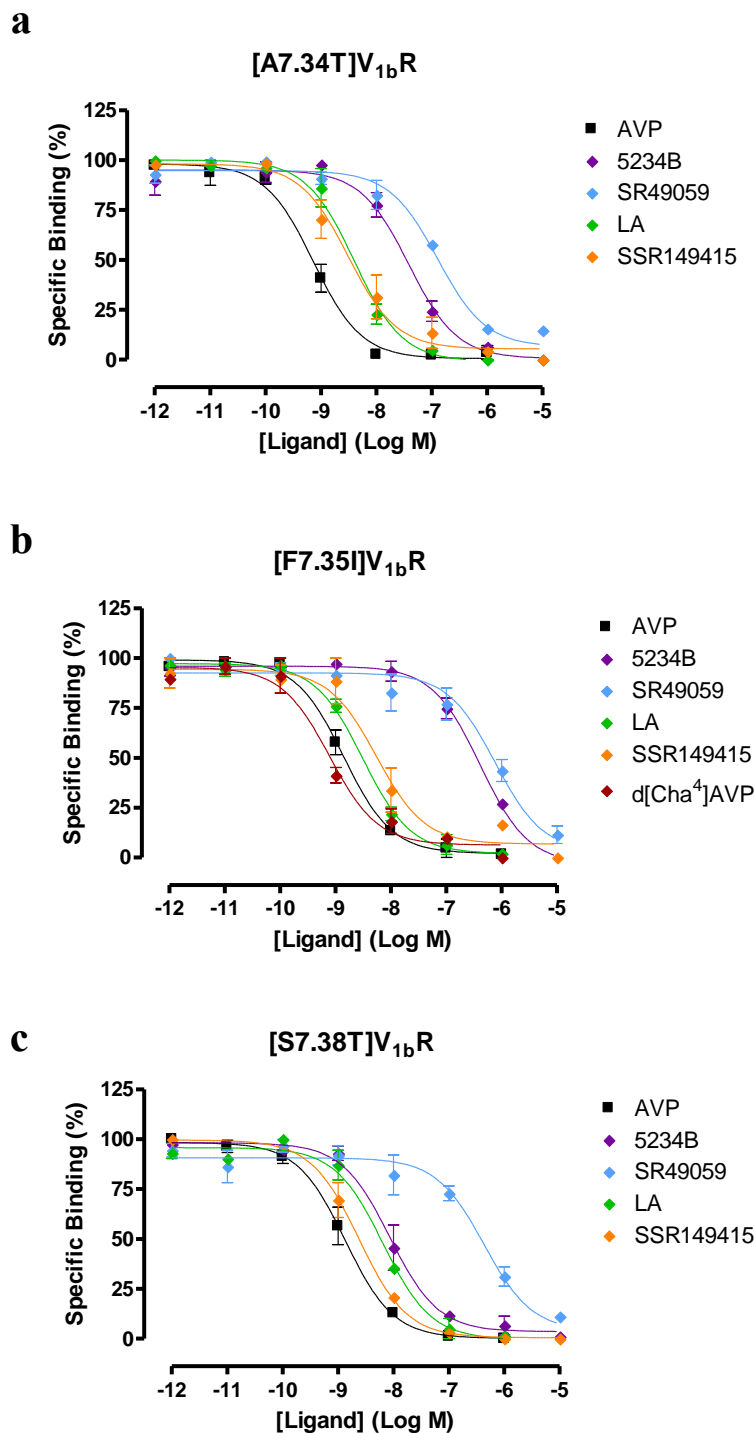


Figure 4.7 a-c

The binding profiles of V_{1b}R constructs modified in TM7 to contain the corresponding residues of V_{1a}R:

- a.** [A7.34T]V_{1b}R;
- b.** [F7.35I]V_{1b}R;
- c.** [S7.38T]V_{1b}R.

Competition binding curves of [³H]AVP and various ligands as indicated. The values plotted were normalised to show percentage specific binding. The error bars represent SEM of three separate experiments each performed in triplicate.

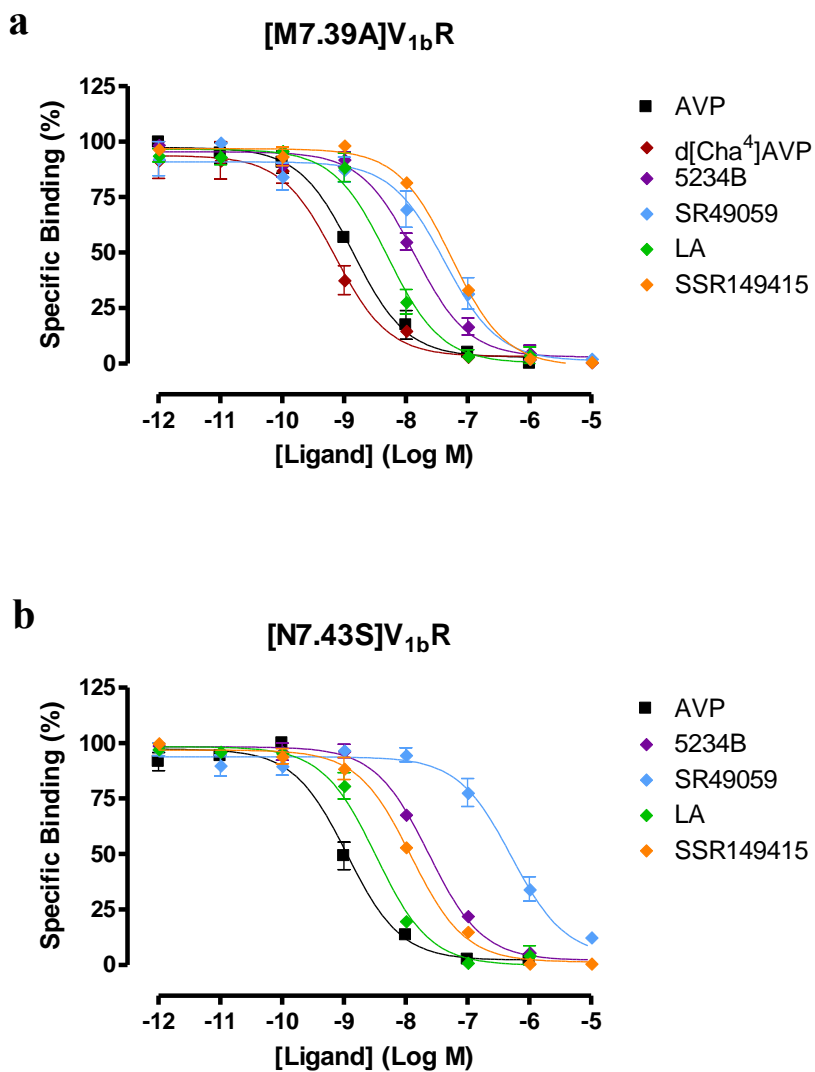
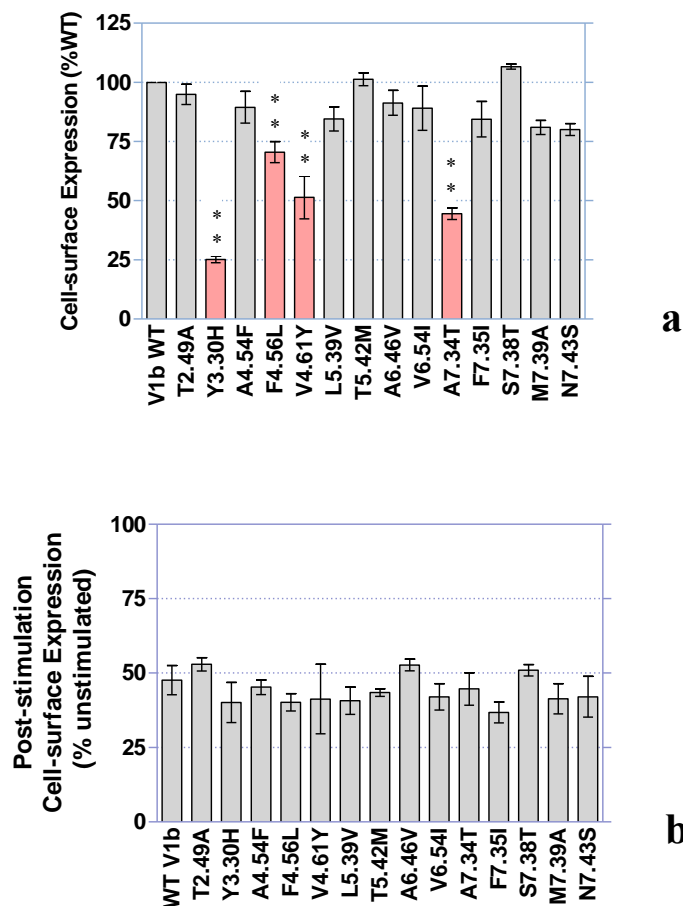


Figure 4.7 ab The binding profiles of V_{1b}R constructs modified in TM7 to contain the corresponding residues of V_{1a}R:

- a. [M7.39A]V_{1b}R;
- b. [N7.43S]V_{1b}R;

Competition binding curves of [³H]AVP and various ligands as indicated. The values plotted were normalised to show percentage specific binding. The error bars represent SEM of three separate experiments each performed in triplicate.



Construct	Cell-Surface Expression (% Wt)	AVP-induced Internalisation (% Unstimulated)
WT V _{1b} R	100	52 (± 5)
[T2.49A]V _{1b} R	95 (± 4)	43(± 2)
[Y3.30H]V _{1b} R	25 (± 1)	60 (± 7)
[A4.54F]V _{1b} R	89 (± 7)	55 (± 3)
[F4.56L]V _{1b} R	71 (± 4)	60 (± 3)
[V4.61Y]V _{1b} R	51 (± 9)	59 (± 12)
[L5.39V]V _{1b} R	85 (± 5)	59 (± 5)
[T5.42M]V _{1b} R	101 (± 3)	56 (± 1)
[A6.46V]V _{1b} R	91 (± 5)	47 (± 2)
[V6.54I]V _{1b} R	89 (± 9)	58 (± 4)
[A7.34T]V _{1b} R	45(± 2)	55 (± 5)
[F7.35I]V _{1b} R	84 (± 8)	63 (± 4)
[S7.38T]V _{1b} R	107 (± 1)	51 (± 3)
[M7.39A]V _{1b} R	81 (± 3)	59 (± 5)
[N7.43S]V _{1b} R	80 (± 3)	58 (± 7)

Figure 4.8 ab The cell-surface expression levels of the mutant constructs and the V_{1b}R Wt:

- The cell-surface expression of each mutant construct was shown relative to the Wt as 100%;
- The cell-surface expression after AVP-stimulation (1μM, 30min). The figures were normalised to the cell-surface expression levels of the same construct in the absence of AVP.

The error bars represent SEM of three experiments each was in triplicate. The significance of results was assessed by one-way ANOVA and Dunnett's post-test with Wt as a control group (P < 0.01 indicated in pale-red and asterisks).

Table 4.3 The cell-surface expression of the mutant constructs relative to the Wt and the proportion of the constructs internalised in percentage are shown plus/minus SEM of three separate experiments each of which was in triplicate.

4.2.2. The characteristics of the V_{1a}R constructs containing the corresponding V_{1b}R residue

Construct	Binding Affinity (K _i , nM ± S.E.M.)						Cell-Surface Expression (% Wt)
	AVP	d[Cha ⁴]AVP	5234B	SSR149415	SR49059	LA	
WT V _{1b} R	0.90 (± 0.13)	1.35 (± 0.02)	7.18 (± 1.82)	3.36 (± 0.93)	670 (± 147)	6.25 (± 1.86)	-
WT V _{1a} R	1.02 (± 0.12)	81.9 (± 1.3)	6392 (± 655)	70.4 (± 15.3)	1.76 (± 0.54)	0.57 (± 0.05)	100
[A2.49T]V _{1a} R	0.48 (± 0.20)	-	3469 (± 436)	104 (± 7)	2.23(± 0.61)	0.27 (± 0.07)	54 (± 2)
[H3.30Y]V _{1a} R	0.69 (± 0.25)	66.2 (± 7.2)	8150 (± 1227)	3.64 (± 0.18)	1.46 (± 0.04)	0.29 (± 0.02)	65 (± 3)
[F4.54A]V _{1a} R	0.39 (± 0.10)	-	8183(± 1233)	63.7 (± 8.4)	3.92 (± 1.11)*	0.55 (± 0.22)	105 (± 2)
[L4.56F]V _{1a} R	1.49 (± 0.31)	-	13466 (± 415)	129 (± 6.4)	2.35 (± 0.09)	-	109 (± 7)
[Y4.61V]V _{1a} R	1.07 (± 0.02)	-	10389 (± 1228)	30.1 (± 3.7)	1.21 (± 0.69)	-	71 (± 2)
[V5.39L]V _{1a} R	0.30 (± 0.06)	27.9 (± 2.0)	1244 (± 156)	26.9 (± 5.0)	0.49 (± 0.03)	0.50 (± 0.10)	67 (± 11)
[M5.42T]V _{1a} R	0.95 (± 0.13)	152 (± 23)	7568 (± 760)	6.11 (± 0.99)	9.62 (± 0.74)	0.27 (± 0.04)	57 (± 3)
[V6.46A]V _{1a} R	0.43 (± 0.06)	-	7160 (± 486)	-	0.84 (± 0.08)	0.43 (± 0.04)	43 (± 1)
[I6.54V]V _{1a} R	0.96 (± 0.36)	-	8194 (± 242)	123 (± 34)	1.65 (± 0.12)	-	108 (± 3)
[T7.34A]V _{1a} R	0.76 (± 0.10)	-	4725 (± 203)	-	0.86 (± 0.08)	0.63 (± 0.17)	92 (± 2)
[I7.35F]V _{1a} R	0.62 (± 0.08)	133 (± 21)	293 (± 69)	48.0 (± 3.5)	1.37 (± 0.05)	0.38 (± 0.04)	112 (± 2)
[T7.38S]V _{1a} R	1.00 (± 0.08)	-	12449 (± 997)	-	1.09 (± 0.21)	0.78 (± 0.12)	104 (± 5)
[A7.39M]V _{1a} R	1.06 (± 0.49)	14.0 (± 2.9)	2416 (± 269)	19.4 (± 3.7)	3.17 (± 0.15)	0.39 (± 0.01)	109 (± 7)
[S7.43N]V _{1a} R	1.16 (± 0.42)	-	6009 (± 900)	200 (± 14)	3.32 (± 0.25)	-	101 (± 4)

Table 4.4 Ligand binding characteristics of the constructs containing V_{1b}R residues within the corresponding position of V_{1a}R: Binding affinities of V_{1b}R-selective antagonists 5234B, SSR149415, and V_{1a}R-selective antagonist SR49059 to various V_{1a}R constructs were determined by competition binding assay using [³H]AVP as a tracer ligand. Binding affinity of peptide ligands to some constructs was also investigated. The colour code applied as previous to show relative gain or loss of the affinity compared to the affinity of each ligand to the Wt V_{1a}R. In essence, darker colours indicate larger shift: increase in affinity is shown in blue; loss of the affinity indicated in orange; and yellow indicates small shift below 10-fold. Cell-surface expression levels of constructs relative to the Wt V_{1a}R were determined by ELISA. The values are mean plus/minus SEM of three experiments each performed in triplicate.

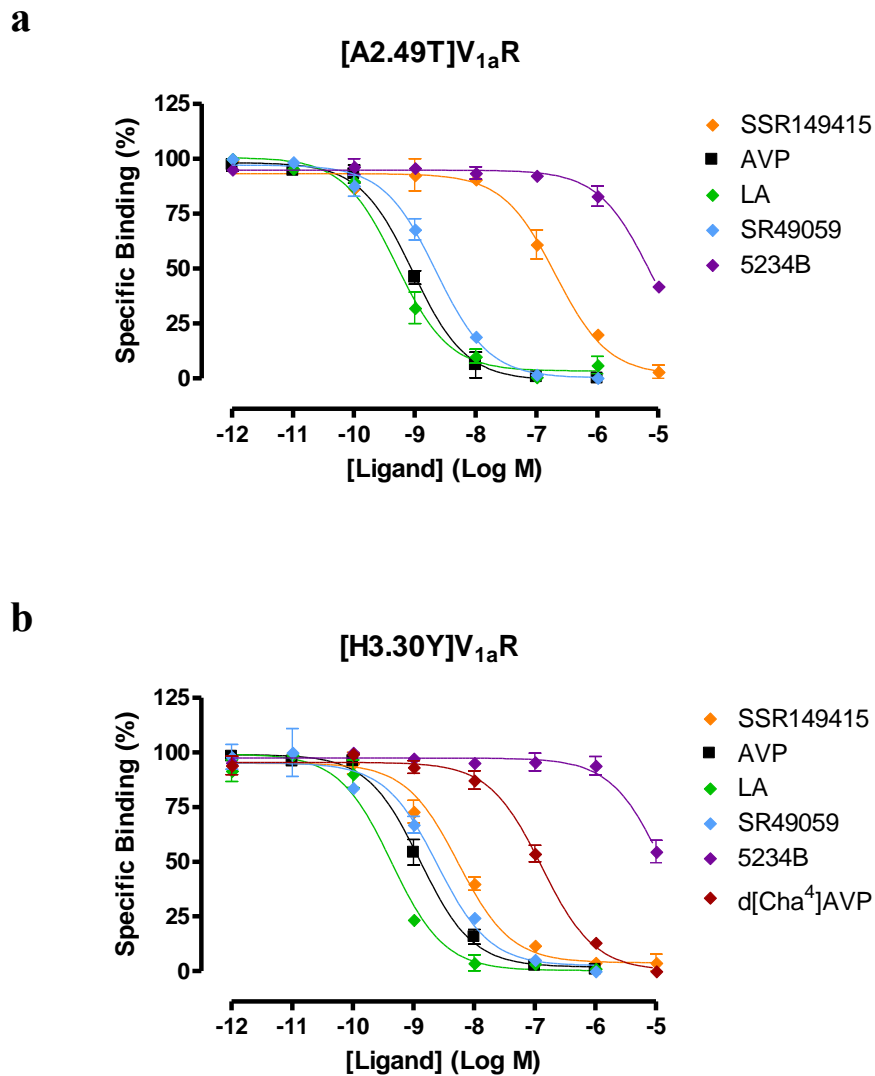


Figure 4.9 ab The binding profiles of V_{1a}R constructs modified in TM2/3 to contain the corresponding residues of V_{1b}R:

- a.** [A2.49T]V_{1a}R;
b. [H3.30Y]V_{1a}R;

Competition binding curves of [³H]AVP and various ligands as indicated. The values plotted were normalised to show percentage specific binding. The error bars represent SEM of three separate experiments each performed in triplicate.

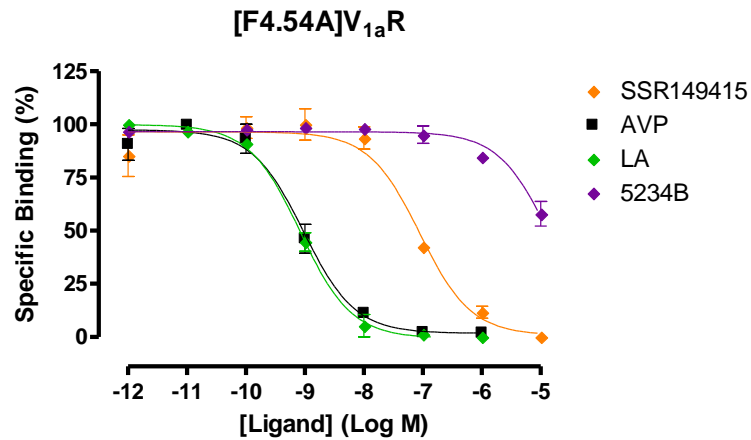
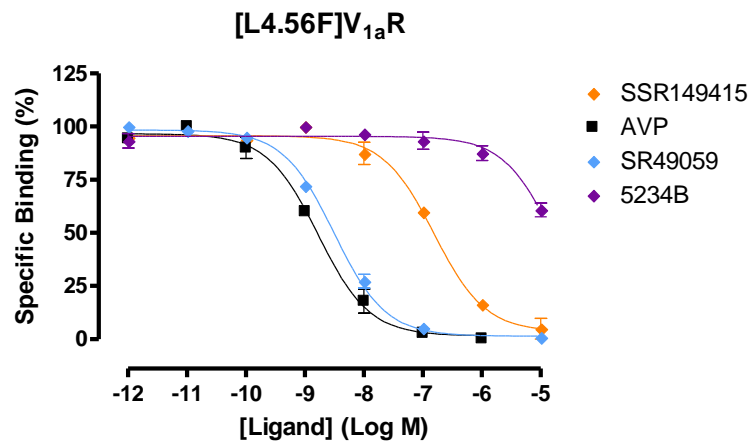
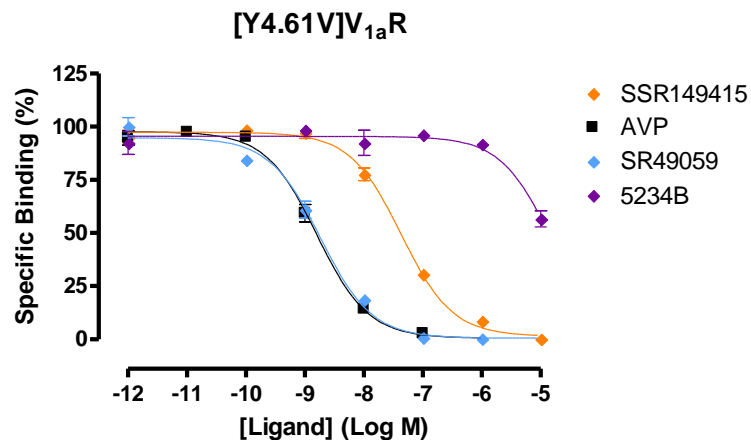
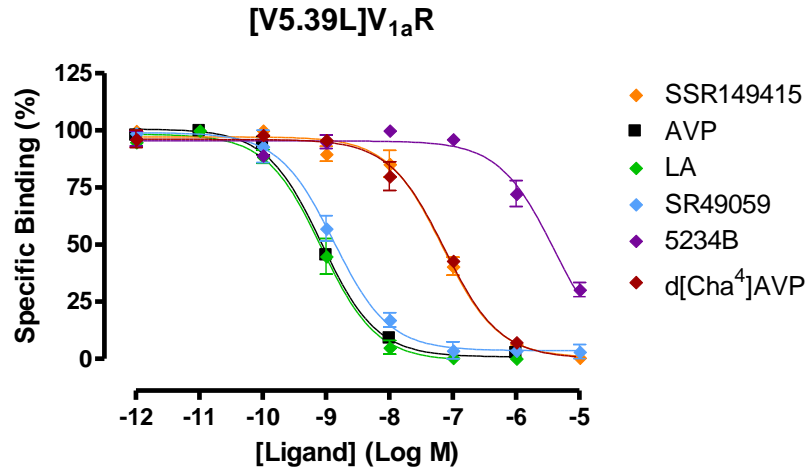
a**b****c**

Figure 4.10 ab The binding profiles of V_{1a}R constructs modified in TM4 to contain the corresponding residues of V_{1b}R:

- a. [F4.54A]V_{1a}R;
- b. [F4.56L]V_{1a}R;
- c. [Y4.61V]V_{1a}R.

Competition binding curves of [³H]AVP and various ligands as indicated. The values were normalised to show percentage specific binding. The error bars represent SEM of three separate experiments each performed in triplicate.

a



b

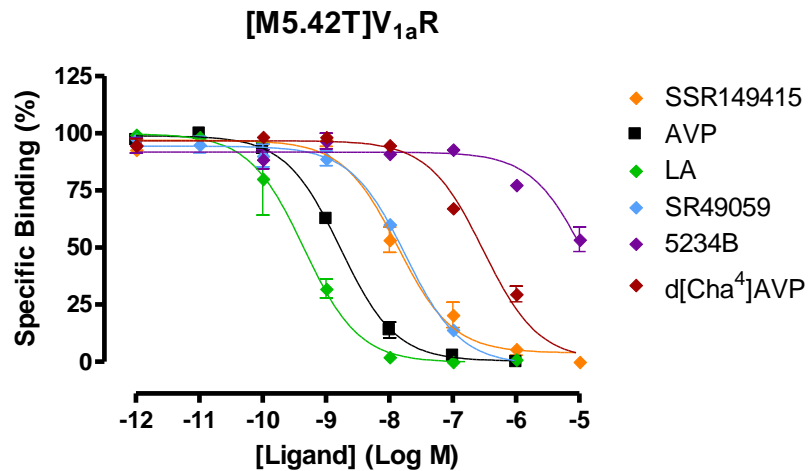


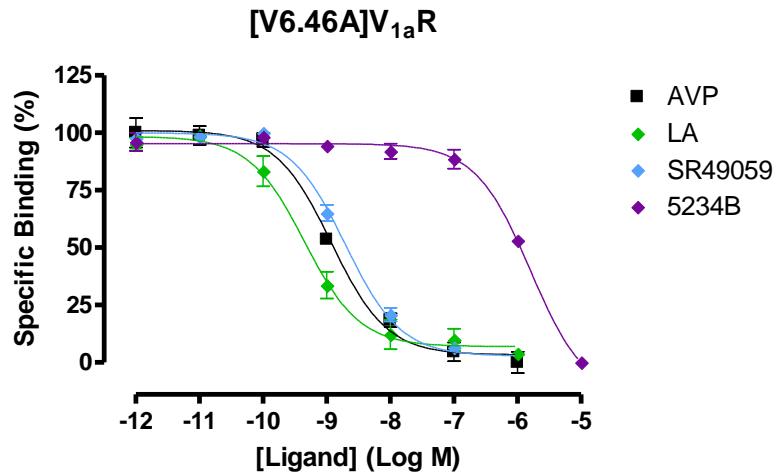
Figure 4.11 ab The binding profiles of V_{1a}R constructs modified in TM5 to contain the corresponding residues of V_{1b}R:

a. [V5.39L]V_{1a}R;

b. [M5.42T]V_{1a}R.

Competition binding curves of [³H]AVP and various ligands as indicated. The values plotted were normalised to show percentage specific binding. The error bars represent SEM of three separate experiments each performed in triplicate.

a



b

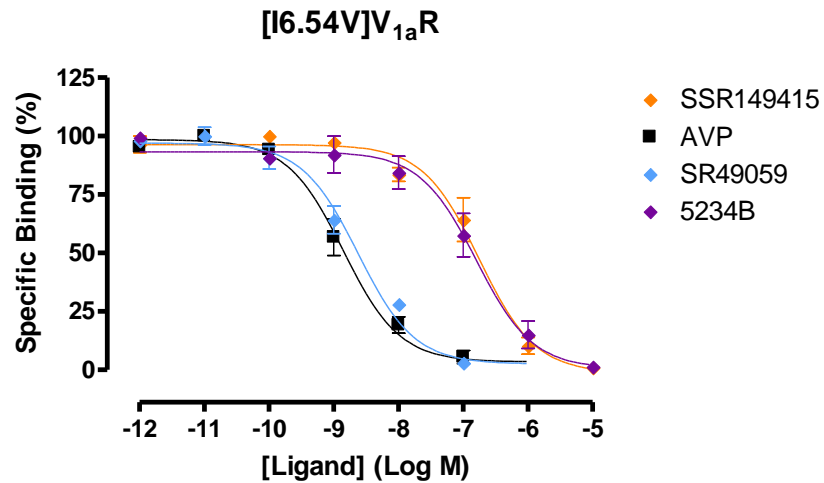


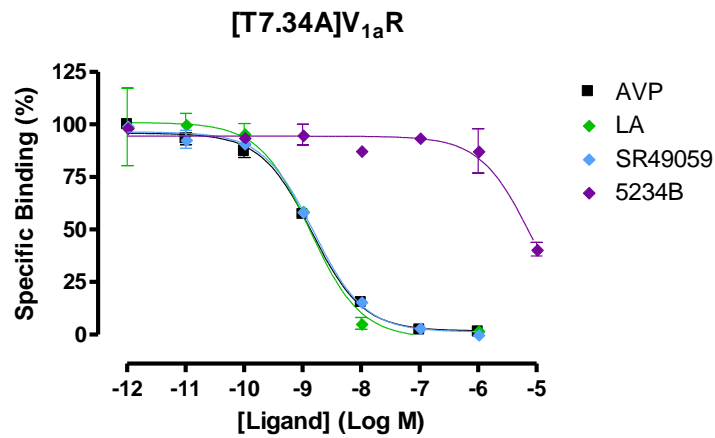
Figure 4.12 ab The binding profiles of V_{1a}R constructs modified in TM6 to contain the corresponding residues of V_{1b}R:

a. [V6.46A]V_{1a}R;

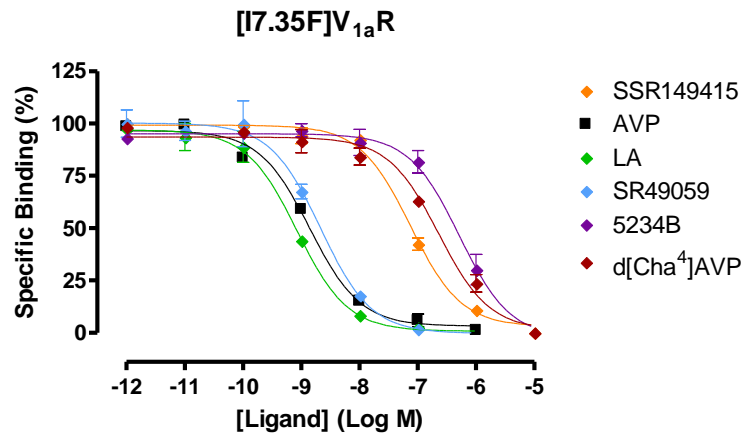
b. [I6.54V]V_{1a}R.

Competition binding curves of [³H]AVP and various ligands as indicated. The values plotted were normalised to show percentage specific binding. The error bars represent SEM of three separate experiments each performed in triplicate.

a



b



c

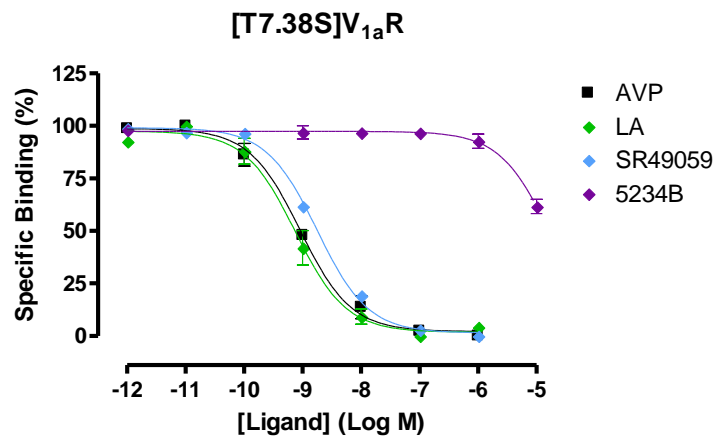


Figure 4.13 a-c The binding profiles of V_{1a}R constructs modified in TM7 to contain the corresponding residues of V_{1b}R:

a. [T7.34A]V_{1a}R;

b. [I7.35F]V_{1a}R;

c. [T7.38S]V_{1a}R.

Competition binding curves of [³H]AVP and various ligands as indicated. The values plotted were normalised to show percentage specific binding.

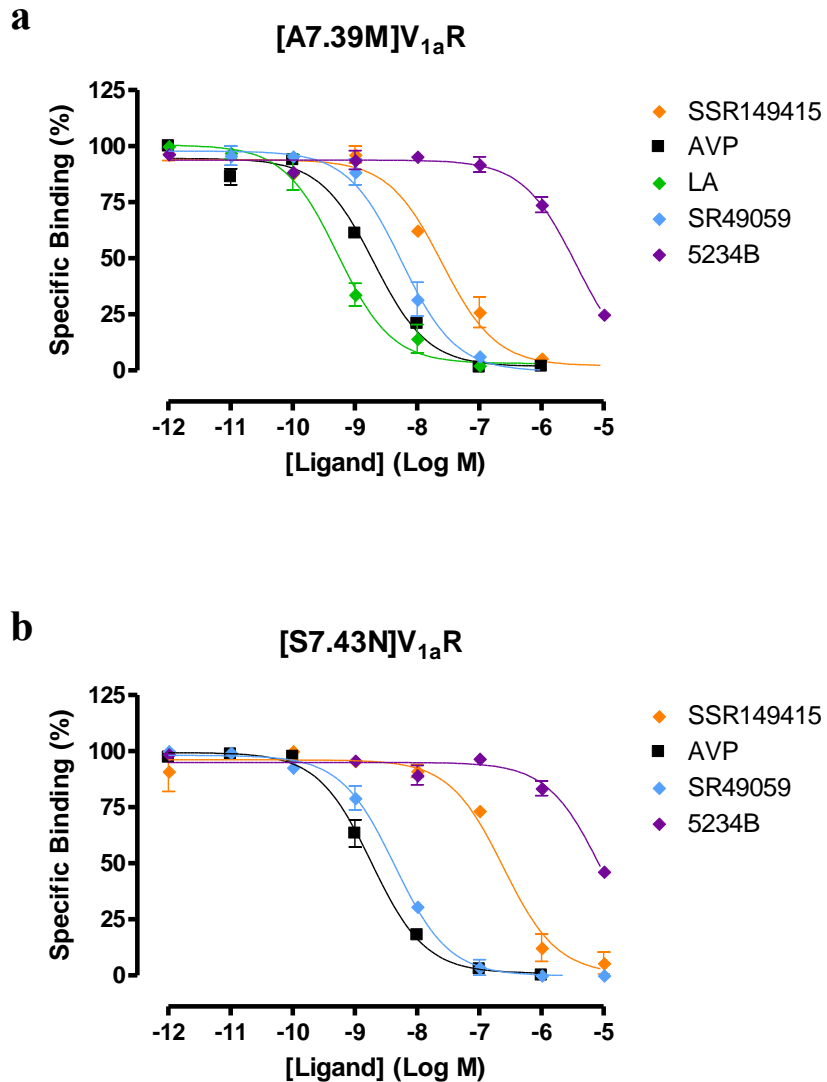
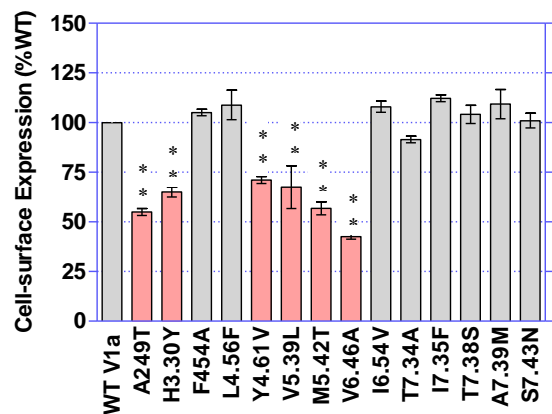


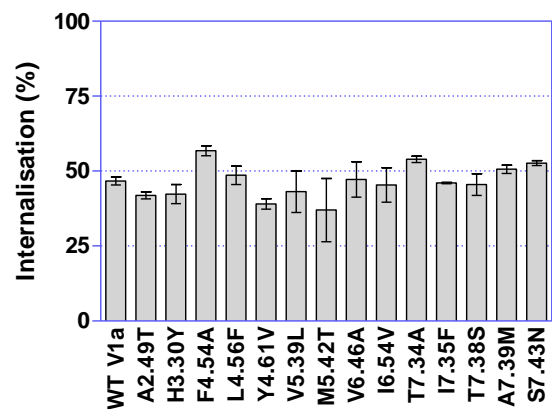
Figure 4.13 ab The binding profiles of V_{1a}R constructs modified in TM7 to contain the corresponding residues of V_{1b}R:

- a.** [A7.39M]V_{1a}R;
b. [S7.43N]V_{1a}R.

Competition binding curves of [³H]AVP and various ligands as indicated. The values plotted were normalised to show percentage specific binding. The error bars represent SEM of three separate experiments each performed in triplicate.



a



b

Construct	Cell-Surface Expression (% Wt)	AVP-induced Internalisation (% Unstimulated)
WT V _{1a} R	100	53 (± 1)
[A2.49T]V _{1a} R	54 (± 2)	58 (± 1)
[H3.30Y]V _{1a} R	65 (± 3)	58 (± 3)
[F4.54A]V _{1a} R	105 (± 2)	43 (± 2)
[L4.56F]V _{1a} R	109 (± 7)	51 (± 3)
[Y4.61V]V _{1a} R	71 (± 2)	61 (± 2)
[V5.39L]V _{1a} R	67 (± 11)	57 (± 7)
[M5.42T]V _{1a} R	57 (± 3)	63 (± 11)
[V6.46A]V _{1a} R	43 (± 1)	53 (± 6)
[I6.54V]V _{1a} R	108 (± 3)	55 (± 6)
[T7.34A]V _{1a} R	92 (± 2)	46 (± 1)
[I7.35F]V _{1a} R	112 (± 2)	54 (± 1)
[T7.38S]V _{1a} R	104 (± 5)	54 (± 4)
[A7.39M]V _{1a} R	109 (± 7)	49 (± 1)
[S7.43N]V _{1a} R	101 (± 4)	47 (± 1)

Figure 4.14 ab The cell-surface expression levels of the mutant constructs and the V_{1a}R Wt:

- The cell-surface expression of each mutant construct was shown relative to the Wt;
- The cell-surface expression after AVP-stimulation (1μM) for 30 min. The figures were normalised to the cell-surface expression levels of the same construct in the absence of AVP, determined from experiments performed in parallel. The results were analysed statistically by one-way ANOVA and Dunnett's post-test with Wt as a control group (P < 0.01 indicated as pale-red with asterisks).

Table 4.5 The cell-surface expression of the mutant constructs relative to the Wt and the proportion of the constructs internalised in percentage are shown plus/minus SEM of three separate experiments each of which was in triplicate.

4.2.3. Alanine Mutagenesis

Colour code indicates fold-changes in K_i

	Over 20 fold increase in affinity
	5 ~ 19 fold increase in affinity
	2 ~ 4.9 fold increase in affinity
	2 ~ 4.9 fold decrease in affinity
	5 ~ 19 fold decrease in affinity
	20 ~ 999 fold decrease in affinity
	Over 1000 fold decrease in affinity

Construct	Binding Affinity (K_i , nM \pm S.E.M.)					Cell-Surface Expression (% Wt)
	AVP	dDAVP	5234B	SSR149415	LA	
WT $V_{1b}R$	0.90 (\pm 0.13)	10.5 (\pm 2.7)	7.18 (\pm 1.82)	3.36 (\pm 0.93)	6.25 (\pm 1.86)	100
[F4.56A] $V_{1b}R$	0.98 (\pm 0.05)	12.6 (\pm 3.1)	6.87 (\pm 1.25)	8.89 (\pm 0.06)	6.72 $n = 1$	99 (\pm 9)
[L5.39A] $V_{1b}R$	1.36 (\pm 0.02)	58.0 (\pm 8.5)	103 (\pm 33)	20.7 (\pm 2.2)	32.8 (\pm 5.3)	85 (\pm 5)
[T5.42A] $V_{1b}R$	0.31 (\pm 0.09)	0.40 (\pm 0.04)	5.61 (\pm 0.64)	1.56 (\pm 0.13)	0.20 (\pm 0.01)	46 (\pm 2)
[V6.54A] $V_{1b}R$	0.12 (\pm 0.03)	-	7.20 (\pm 0.85)	-	1.59 (\pm 0.28)	51 (\pm 4)
[N7.43A] $V_{1b}R$	0.34 (\pm 0.02)	-	6.72 (\pm 0.92)	-	1.06 (\pm 0.11)	83 (\pm 3)

Table 4.6 Ligand binding characteristics of the $V_{1b}R$ constructs containing Ala substitution:

Binding affinity of $V_{1b}R$ -selective agonists and antagonists to $V_{1b}R$ constructs were determined by competition binding assay, using [3H]AVP as a tracer ligand. The colour code applied, as indicated above, to show relative gain or loss of the affinity compared to the affinity of each ligand to the Wt $V_{1b}R$. The column on the far right shows cell-surface expression levels of each construct relative to the Wt $V_{1b}R$, determined by ELISA utilising an engineered HA tag at the N-terminus of the receptor.

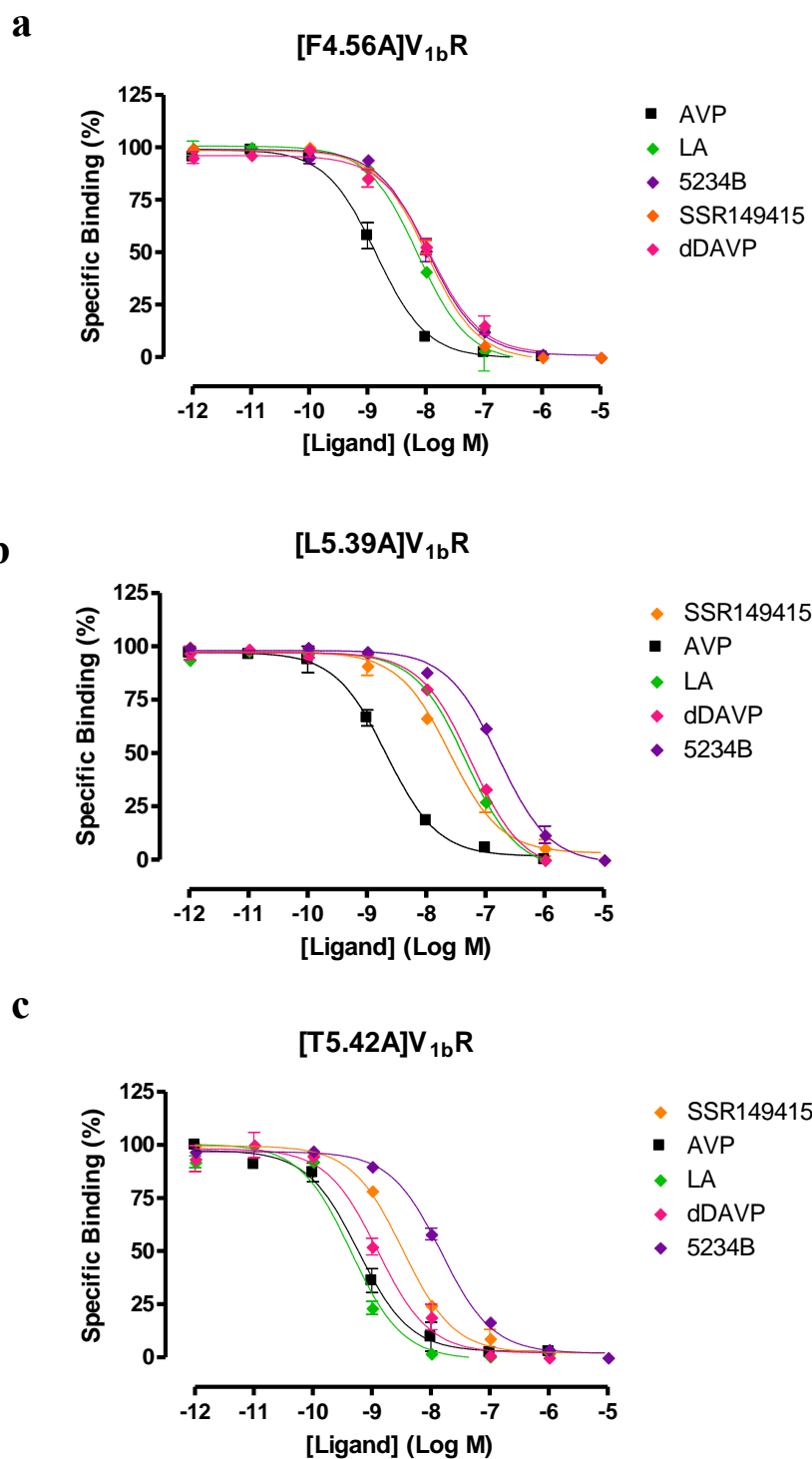


Figure 4.15 ab The binding profiles of V_{1b}R constructs with Ala substitution in TM4/TM5:

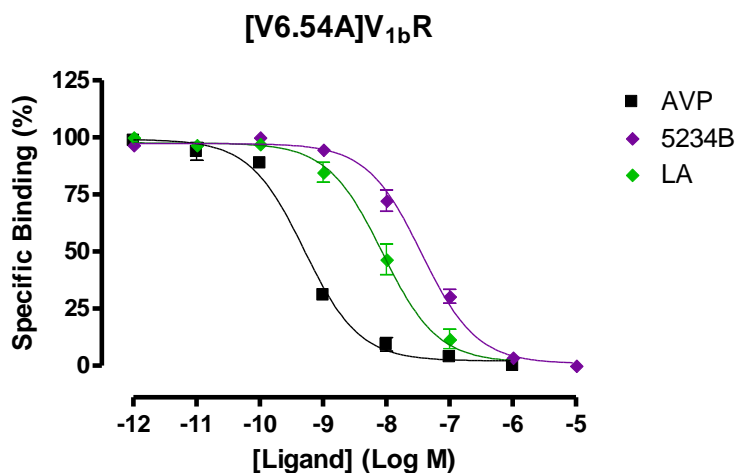
a. [F4.56A]V_{1b}R;

b. [L5.39A]V_{1b}R;

c. [T5.42A]V_{1b}R.

Competition binding curves of [³H]AVP and various ligands as indicated. The values were normalised to show percentage specific binding. The error bars represent SEM of three separate experiments each performed in triplicate.

a



b

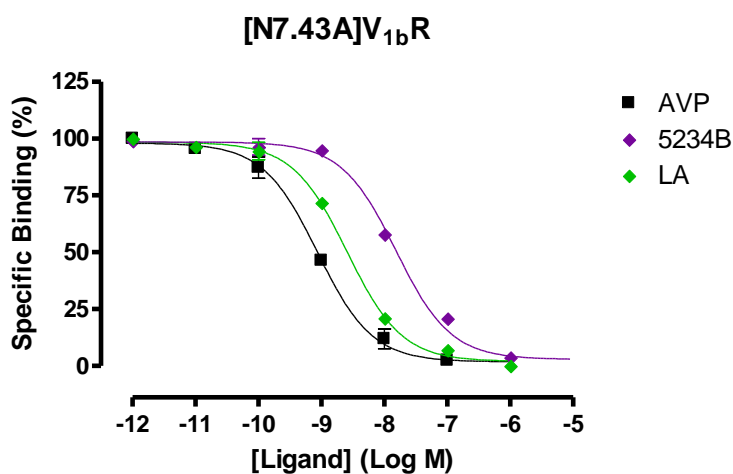


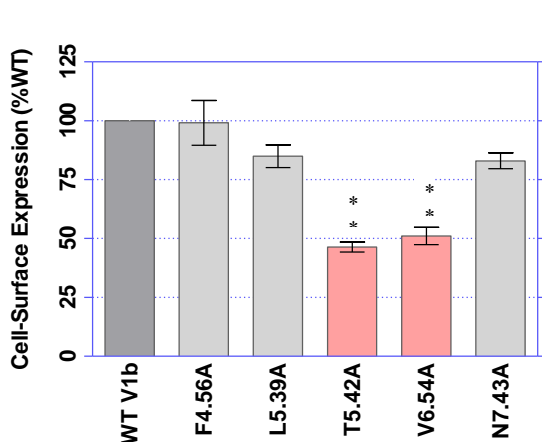
Figure 4.16 ab The binding profiles of V_{1b}R constructs with Ala substitution in TM6/TM7:

a. [V6.54A]V_{1b}R;

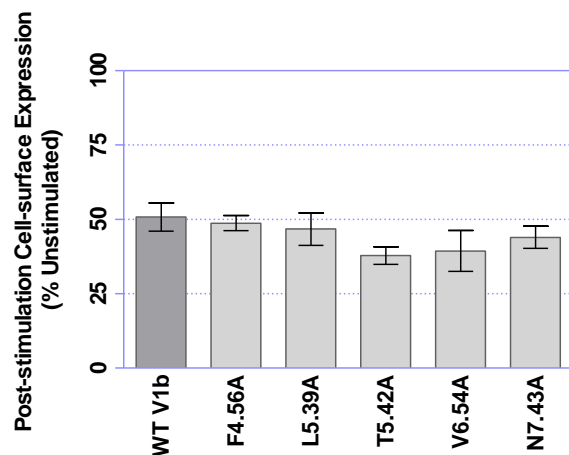
b. [N7.43A]V_{1b}R.

Competition binding curves of [³H]AVP and various ligands as indicated. The values plotted were normalised to show percentage specific binding. The error bars represent SEM of three separate experiments each performed in triplicate.

Construct	Cell-Surface Expression (% Wt)	AVP-induced Internalisation (% Unstimulated)
WT V _{1b} R	100	49 (± 5)
[F4.56A]V _{1b} R	99 (± 9)	51 (± 3)
[L5.39A]V _{1a} R	85 (± 5)	53 (± 5)
[T5.42A]V _{1a} R	46 (± 2)	62 (± 3)
[V6.54A]V _{1a} R	51 (± 4)	61 (± 7)
[N7.43A]V _{1a} R	83 (± 3)	56 (± 4)



a



b

Table 4.6 The cell-surface expression of the Ala-substituted V_{1b}R constructs: The figures on the left column are the percentage cell-surface expression of the constructs shown relative to the Wt. The proportion of the constructs internalised in percentage are shown relative to the unstimulated plus/minus SEM of three separate experiments each of which was in triplicate.

Figure 4.17 ab The cell-surface expression levels of the mutant constructs and the V_{1b}R Wt:

- The cell-surface expression of each mutant construct relative to the Wt;
- The cell-surface expression after AVP-stimulation (1 μ M) for 30 min. The figures were normalised to the cell-surface expression levels of the same construct in the absence of AVP, determined from experiments performed in parallel. The results were analysed by one-way ANOVA followed by Dunnett's post-test with Wt as a control group. The results significantly different ($P < 0.01$) are shown in pale-red and asterisks.

The reciprocal mutant constructs between V_{1b}R and V_{1ba}R were made to contain the corresponding residue of the other subtype. All the constructs bound AVP with Wt-like affinity (Table 4.2 and Table 4.4). This was important as it showed that the mutant receptors were folded appropriately, and it allowed the use of [³H]AVP as a tracer ligand in quantifying changes in the binding affinity of subtype-selective ligands. Some constructs displayed altered binding profiles to subtype-selective ligands to various degrees, whilst others retained Wt-like affinity towards the compounds used.

A few pairs of the V_{1b}R and V_{1a}R constructs showed altered affinity to a particular subtype-selective ligand correspondingly. The largest change in the affinity were seen in [F7.35I]V_{1b}R, which displayed \approx 30-fold decrease in the binding affinity for 5234B while the corresponding [I7.35F]V_{1a}R was associated with \approx 20-fold increase in its affinity for 5234B. [V4.61Y]V_{1b}R showed 10-fold reduction in affinity towards SSR149415, and 2-fold increase in the affinity of the compound to [Y4.61V]V_{1a}R was observed. The binding affinity of 5234B with [L5.39V]V_{1b}R was decreased about 3-fold, and correspondingly the affinity of the compound with [V5.39L]V_{1a}R was increased about 5-fold. Similarly, the affinity of SSR149415 to the same V_{1b}R construct was decreased about 2-fold while it was increased about 3-fold in the corresponding V_{1a}R construct. The binding affinity of SR49059 for [A4.54F]V_{1b}R was increased \approx 6-fold. This is supported by the previous finding by Wootten on [F4.54A]V_{1a}R, which was associated with 3-fold increase in K_i values to the same compound.

The affinity of [M5.42T]V_{1a}R for SSR149415 was increased about 10-fold, and also the corresponding [T5.42M]V_{1b}R showed reduced affinity towards the compound about 10-fold. Moreover, the affinity of SR49059 to [T5.42M]V_{1b}R was increased about 450-fold, resembling the affinity similar to the Wt V_{1a}R to the compound. However, the change in the affinity of the

corresponding [M5.42T]V_{1a}R was only about 5-fold. Although about 10-fold reduction in the affinity of 5234B with [T5.42M]V_{1b}R was observed, a corresponding increase in the affinity of the compound with [M5.42T]V_{1a}R was not observed. [A7.39M]V_{1a}R also displayed about 4-fold increase in the affinity for SSR149415, while the corresponding [M7.39A]V_{1b}R showed about 10-fold reduction in its binding affinity with the compound. Also the binding affinity of SR49059 with [M7.39A]V_{1b}R was increased about 10-fold, while the affinity with [A7.39M]V_{1a}R was decreased slightly about 2-fold. The increase in the binding affinity of two V_{1a}R constructs, [M5.42T]V_{1a}R and [A7.39M]V_{1a}R, for SSR149415 agrees with the mutagenesis study by Derick *et al.* [426].

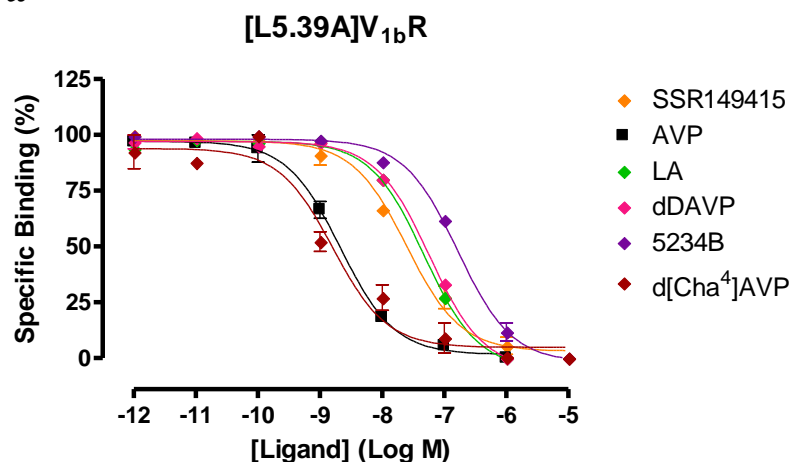
Several pairs of the reciprocal constructs showed altered binding affinity in a biased manner in which a change in affinity for a ligand was limited to only one of the subtypes. [Y3.30H]V_{1b}R showed about 10-fold reduction in the affinity with SR49059 whereas no significant difference was observed for the affinity of SR49059 at [H3.30Y]V_{1a}R. However, the latter construct showed about 20-fold increase in the binding affinity for SSR149415, whereas the corresponding decrease in the binding affinity of [Y3.30H]V_{1b}R for SSR149415 was not observed. The binding affinity of SSR149415 to [N7.43S]V_{1b}R and [S7.43N]V_{1a}R was slightly decreased \approx 3-fold for both constructs. The binding affinity of LA with [N7.43S]V_{1b}R was increased about 3-fold. The Ala-substitution of the residue in [N7.43A]V_{1b}R resulted in a larger 6-fold increase in the binding affinity for LA.

Further characterisation of [L5.39A]V_{1b}R and the constructs modified at the residue position 5.42

The reciprocal mutagenesis between V_{1a}R and V_{1b}R has shown that the residues at 5.39 (Leu in V_{1b}R, Val in V_{1a}R) and the residues at 5.42 (Thr in V_{1b}R, Met in V_{1a}R), both found in the upper region of TM5, are involved in ligand binding of the both subtypes. A further study showed that Ala-substitution of Leu^{5.39} in V_{1b}R resulted in decreased affinity of the receptor to both peptide and non-peptide ligands. In contrast, Ala-substitution of Thr^{5.42} in V_{1b}R increased the affinity of the receptor for the peptide ligands dDAVP and LA over 20-fold, while the affinity of non-peptide antagonists are relatively unaffected. Therefore, both constructs were characterised using ligands selective for the other subtype: V_{1b}R-selective peptide agonist d[Cha⁴]AVP for [L5.39A]V_{1b}R; and a V_{1a}R-selective peptide antagonist CA for [T5.42A]V_{1b}R, to test if the tendency of either decreasing or increasing affinity also apply to these ligands. Since CA is a highly selective ligand to V_{1a}R, the binding affinity of CA to [T5.42M]V_{1b}R and [M5.42T]V_{1a}R was also tested to make comparisons with [T5.42A]V_{1b}R.

Construct	Binding Affinity (K_i , nM \pm S.E.M.)						
	AVP	dDAVP	d[Cha ⁴]AVP	SSR149415	5234B	LA	CA
WT V _{1b} R	0.90 (\pm 0.13)	10.5 (\pm 2.0)	1.35 (\pm 0.02)	3.36 (\pm 0.93)	7.18 (\pm 1.82)	6.25 (\pm 1.86)	159 (\pm 72)
[L5.39A]V _{1b} R	1.36 (\pm 0.02)	58.0 (\pm 8.5)	1.24 (\pm 0.38)	20.7 (\pm 2.2)	103 (\pm 33)	32.8 (\pm 5.3)	-
[T5.42A]V _{1b} R	0.31 (\pm 0.09)	0.40 (\pm 0.04)	-	1.56 (\pm 0.13)	5.61 (\pm 0.64)	0.20 (\pm 0.01)	8.51(\pm 1.19)

a



b

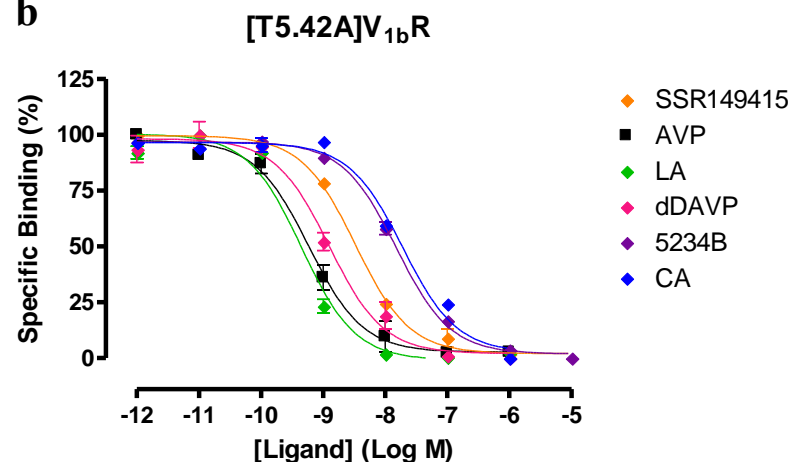


Table 4.7 The binding affinity of [L5.39A]V_{1b}R and [T5.42A]V_{1b}R: The binding affinity of various peptide and non-peptide ligands to the constructs are shown in K_i obtained from the competition binding assay.

Figure 4.18 ab The ligand binding profiles of [L5.39A]V_{1b}R and [T5.42A]V_{1b}R:

a. [L5.39A]V_{1b}R;

b. [T5.42A]V_{1b}R.

Competition binding curves of [³H]AVP and various ligands as indicated. The values were normalised to show percentage specific binding. The error bars represent SEM of three separate experiments each performed in triplicate

Construct	Binding Affinity (K_i , nM \pm S.E.M.)						
	AVP	d[Cha ⁴]AVP	SSR149415	5234B	SR49059	LA	CA
WT V _{1b} R	0.90 (\pm 0.13)	1.35 (\pm 0.02)	3.36 (\pm 0.93)	7.18 (\pm 1.82)	670 (\pm 147)	6.25 (\pm 1.86)	159 (\pm 72)
WT V _{1a} R	1.02 (\pm 0.12)	81.9 (\pm 1.3)	70.4 (\pm 15.3)	6392 (\pm 655)	1.76 (\pm 0.54)	0.57 (\pm 0.05)	1.15 (\pm 0.03)*
[M5.42T]V _{1a} R	0.95 (\pm 0.13)	152 (\pm 23)	6.11 (\pm 0.99)	7568 (\pm 760)	9.62 (\pm 0.74)	0.27 (\pm 0.04)	7.34 (\pm 0.35)
[T5.42M]V _{1b} R	0.73 (\pm 0.08)	2.54 (\pm 0.12)	35.71 (\pm 1.28)	69.8 (\pm 19.1)	1.43 (\pm 0.24)	7.25 (\pm 0.90)	1096 (\pm 20)

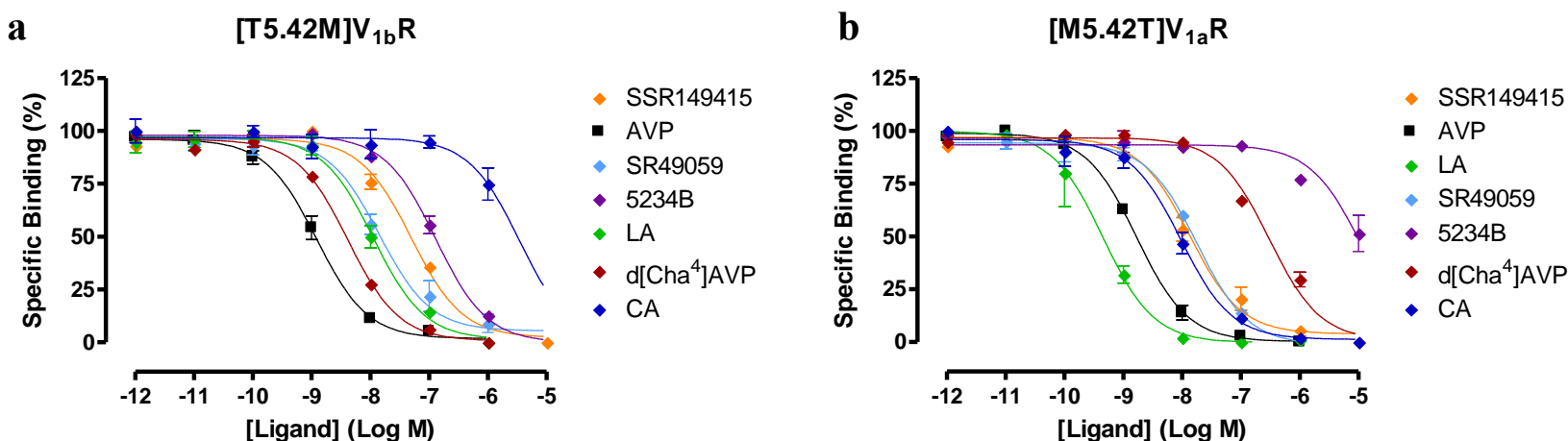


Table 4.8 The binding affinity of [T5.42M]V_{1b}R and [M5.42T]V_{1a}R: The binding affinity of various peptide and non-peptide ligands to the constructs are shown in K_i obtained from the competition binding assay.

Figure 4.19 ab The ligand binding profiles of [T5.42M]V_{1b}R and [M5.42T]V_{1a}R:

a. [T5.42M]V_{1b}R;

b. [M5.42T]V_{1a}R.

Competition binding curves of [³H]AVP and various ligands as indicated. The values plotted were normalised to show percentage specific binding. The error bars represent SEM of three separate experiments each performed in triplicate

The binding affinity of both peptide and non-peptide ligands for [L5.39A]V_{1b}R were reduced compared to the Wt V_{1b}R with the exception of the endogenous agonist AVP. Likewise, the affinity of d[Cha⁴]AVP did not change.

The affinity of a V_{1a}R-selective peptide antagonist CA to [T5.42A]V_{1b}R was markedly increased (\approx 18-fold). In contrast, a decrease (\approx 7-fold) in the affinity of CA to [T5.42M]V_{1b}R was observed. The affinity of [M5.42T]V_{1a}R to CA was decreased about 10-fold.

4.3 Discussion

4.3.1 Phe^{7.35} and Leu^{5.39} are involved in 5234B binding to V_{1b}R

Two residues were identified to be responsible for distinguishing V_{1b}R and V_{1a}R in ligand binding of a V_{1b}R-selective antagonist 5234B. The mutagenesis study showed that Phe^{7.35} residue located on the top of TM7 is likely to make direct contact with 5234B during the association between the ligand and the receptor. Regarding this compound, the largest gain and loss of the binding affinity observed in this study was consistent between the pair of reciprocal mutant constructs of V_{1b}R and V_{1a}R. This finding suggests that the ligand selectivity to V_{1b}R over V_{1a}R could be increased by targeting specifically to interact favourably with this aromatic residue. The molecular model of V_{1b}R by Simms revealed the location of Phe^{7.35} to be at a ligand accessible area, with the phenol ring facing the extracellular side. The residue types at the position 7.35 vary amongst GPCRs; however participation of the residues in ligand binding have been confirmed in some receptors: Tyr^{7.35} was identified to participate in both agonist and antagonist binding of purinergic P2Y1 receptor [446]; and Arg^{7.35} in free fatty acid receptor 1 (FFAR1) was found to involve directly in binding of synthetic agonist [447]. These findings support the models of some GPCRs in which the residues at 7.35 are present at ligand accessible surfaces.

Another residue identified to be involved in 5234B binding to V_{1b}R is Leu^{5.39}, located at the exofacial terminal of TM5. A small but consistent change in the binding affinity to 5234B was observed for the reciprocal mutants involving this residue. The results of Leu^{5.39} and Tyr^{5.38}, which was identified to be involved in 5234B binding in the previous chapter, altogether suggest that the exofacial end of TM5 is a contact site for this ligand upon binding. Upon binding to GPCRs, it makes a sense for an antagonist to have key contacting residues at TM5

and TM7, because occupying the area of TM5-TM6-TM7 interface is likely to restrict the movement of TM6, which is a critical for the receptor activation. Tyr^{5.38}, Leu^{5.39}, and Phe^{7.35} are thought to form a ligand binding cavity for 5234B along with two Gln residues Gln^{4.60} and Gln^{6.55} described in the previous chapter. Figure 4.20 shows the locations of these residues in the molecular model of V_{1b}R at an inactive state.

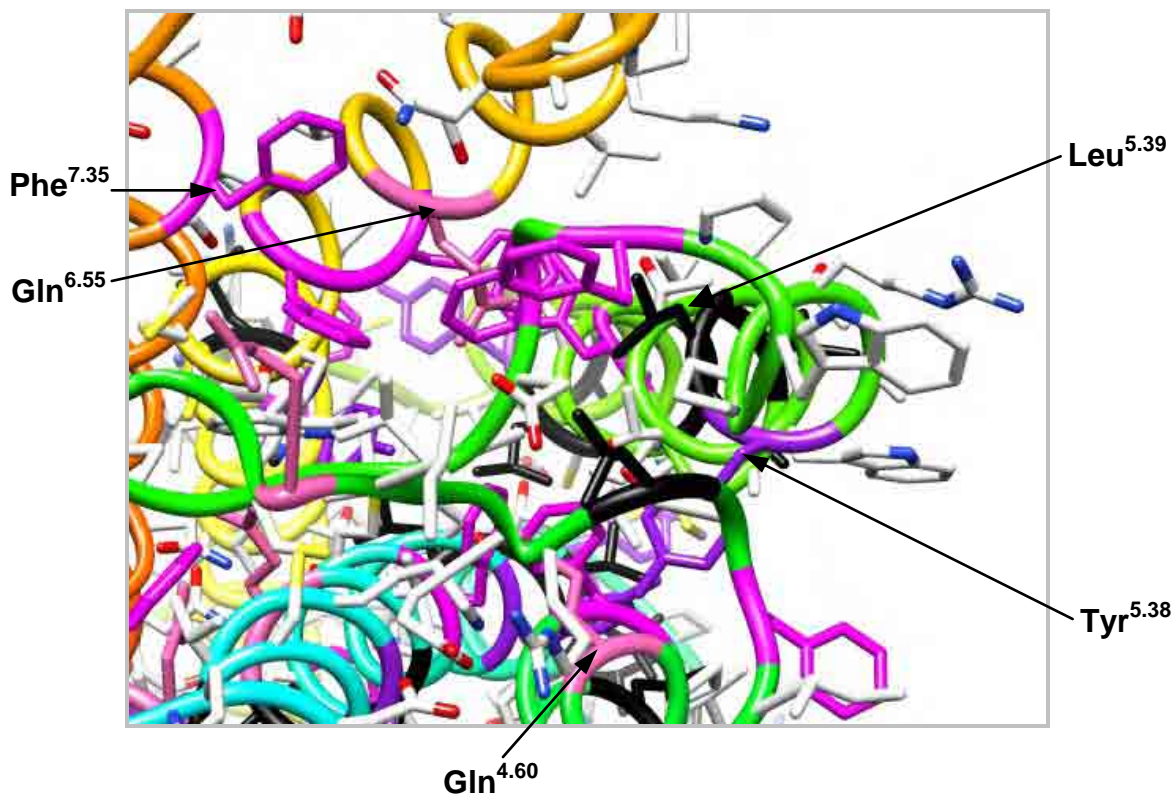


Figure 4.20 The molecular model of V_{1b}R showing the residues identified in this study to be involved in 5234B binding (view from the extracellular side):

The figure summarises the residues involved in 5234B binding to V_{1b}R, including findings from the previous chapter. A part of V_{1b}R, is shown above, including TM3 (turquoise), TM4 (green), TM5 (lime green), TM6 (yellow) and TM7 (dark orange).

A few residues were also shown colour coded: Gln (pink), Phe (magenta), Tyr (purple) and Leu (black).

The models were created by Dr. John Simms. The figures were visualised using Chimera (UCSF Computer Graphics Laboratory).

4.3.2. The residues possibly contributing indirectly in constructing the binding cavity of 5234B in V_{1b}R

Thr^{5.42} located at the upper region of TM5 is thought to engage indirectly in 5234B binding. Although the affinity of 5234B was decreased in [T5.42M]V_{1b}R, the gain of affinity was not observed in [M5.42T]V_{1b}R. In agreement with this inconsistency, [T5.42A]V_{1b}R retained a high affinity for 5234B equivalent to the Wt. This suggests that Thr^{5.42} is unlikely to make a direct contact with 5234B. The loss of the affinity observed with [T5.42M]V_{1b}R is thought to be caused by the introduction of Met, which is relatively large, in the vicinity, rather than the loss of Thr. The residue is located one α -helical turn below Leu^{5.39} and Tyr^{5.38} both of which were shown to be involved in the binding. The introduction of a large hydrophobic Met could alter the positioning of the Tyr^{5.38} and Leu^{5.39} above. Met^{5.42} may also interact favourably with the two residues in V_{1b}R via induced-dipole or van der Waal's interactions, thereby in turn making the interaction between the ligand and the two residues less favourable.

Ala^{7.34} is also thought to contribute in the 5234B binding indirectly. Although a 2-fold decrease in 5234B affinity to [A7.34T]V_{1b}R was observed, the reverse did not apply to [T7.34A]V_{1a}R. The reason for the slight decrease in 5234B affinity to [A7.34T]V_{1b}R is likely to be due to the introduction of Thr at the location. The residue is located next to Phe^{7.35} which appeared to be directly involved in the 5234B binding process. It is plausible that the presence of Thr may make the interaction slightly less favourable, hence the observed [A7.34T]V_{1b}R phenotype for the 5234B binding. Therefore these are environmental effects contributed by local residues surrounding the ligand-contacting residues. These observations made on the V_{1b}R constructs containing Met^{5.42} or Thr^{7.34} support the importance of Tyr^{5.38}, Leu^{5.39}, and Phe^{7.35} in 5234B binding.

4.3.3 The residues interacting SSR149415 and SR49059

Met^{7.39} and Thr^{5.42} were identified to be involved in SSR149415 binding. This is consistent with the findings by Derick *et al.* in 2004. Both residues were found also to be involved in SR49059 binding. A gain of affinity for SR49059 was observed with [T5.42M]V_{1b}R and [M7.39A]V_{1b}R while the reverse was seen with [A7.39M]V_{1a}R and [M5.42T]V_{1a}R. However, greater shifts in the binding affinity were observed in the V_{1b}R constructs compared to the corresponding V_{1a}R constructs. Notably, the introduction of Met in V_{1b}R to substitute Thr^{5.42} was enough to gain the Wt-like high affinity to SR49059, suggesting that the residue is a key contacting residue of SR49059. Other residues identified to be involved in SSR149415 binding to the V_{1b}R are Tyr^{3.30}, Val^{4.61} and Leu^{5.39}, with a gain of affinity observed for the V_{1a}R constructs containing each of these introduced residues.

A docking study using SR49059 and V_{1a}R was previously performed by Tahtaoui *et al.* in 2003. The model predicted that potentially interacting residues are mainly in TM3 and TM7, although some may also be in TM5, TM4 and in ECL2. About 70% of those residues are hydrophobic in nature, while some are charged, potentially forming dipole-dipole interactions [448].

The model of the V_{1b}R with docked SSR149415 has been made by Derick *et al.* The study revealed that the compound was suggested to interact between TM3, 5, 6 and 7 [434]. When the obtained structure was compared to the SR49059 bound structure of V_{1a}R, differences in orientation of those compounds were large, despite the two antagonists sharing structural similarities. The indole ring of SSR149415 was shown to be embedded in a hydrophobic crevice between TM6 and TM3 while SR49059 interacts mainly with TM5 and TM6. The dimethoxyphenyl moiety of SSR149415 seemed directed towards TM7 while the same moiety

of SR49059 appeared interacting with TM5 and TM6. Moreover, the prolinamide moieties of both antagonists were directed to opposite directions.

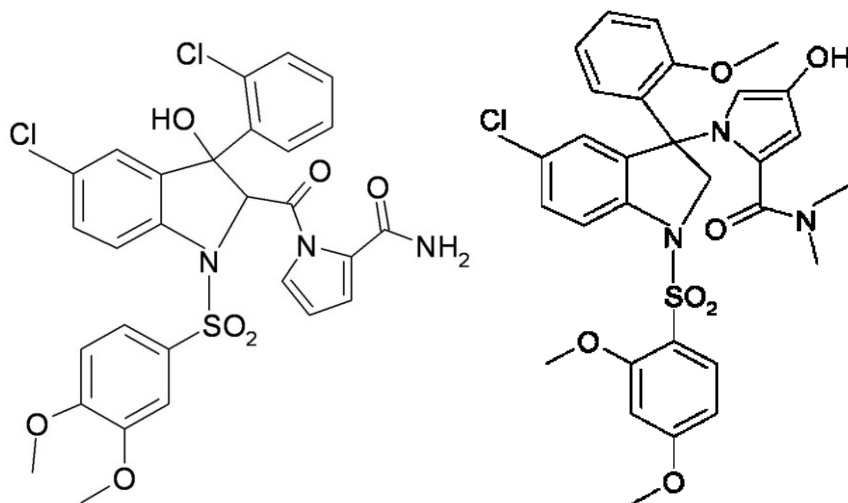


Figure 4.23 Non-peptide antagonists developed by Sanofi-Aventis:

V_{1a} selective SR49059 (left) and V_{1b} selective SSR149415 (right) are shown.

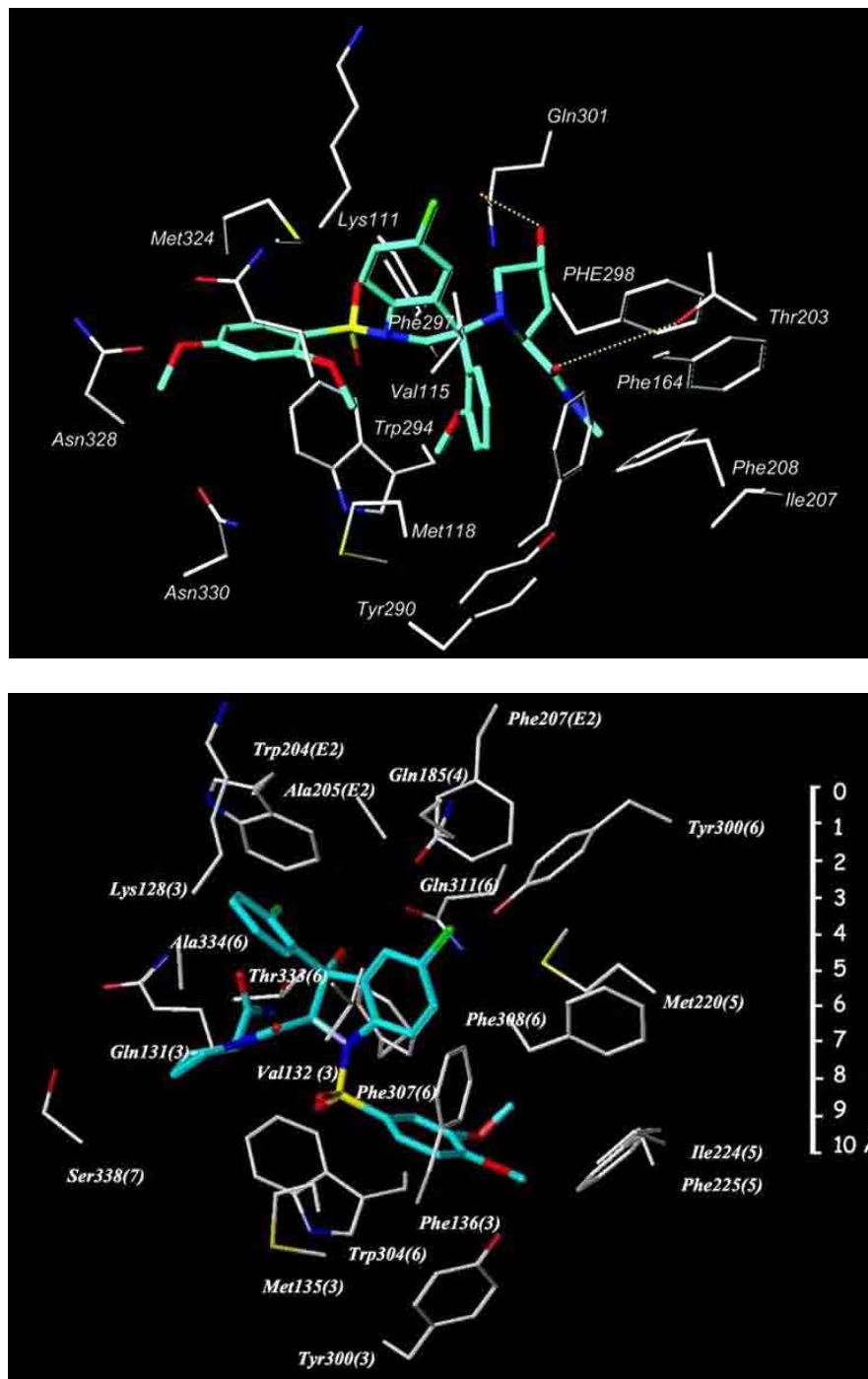


Figure 4.24 The ligand-docked model of predicted binding cavities:

Upper panel: SSR149415 in a binding cavity of $V_{1b}R$, taken from Derick *et al.*, 2004 [434]
 Lower panel: SR49059 in $V_{1a}R$, taken from Tahtaoui *et al.*, 2003 [448].
 In both models, nonpeptide antagonists are shown in turquoise.

Derrick *et al.* also investigated the subtype differences by producing a series of mutant V_{1a}Rs in which some residues were substituted to the corresponding residues of V_{1b}R. Among the mutants, M5.42T and A7.39M exhibited increased affinities to SSR149415 [434].

4.3.4. The role of Thr^{5.42} in the ligand binding of V_{1b}R

Thr^{5.42} is thought to be an important contributor in constructing the ligand binding cavity of V_{1b}R. A neutralising Ala substitution of Thr^{5.42} resulted in dramatic increases in the binding affinity for peptide ligands, including CA which is highly selective to V_{1a}R. This study showed that Thr^{5.42} distinguishes between V_{1b}R and V_{1a}R also in peptide ligand bindings with subtype-selectivity. The molecular model of V_{1b}R showed that the residue points inwards to the helical bundle core. The residue may have a crucial structural role, such as determining the location of water molecules within the TM domains, possibly in conjunction with the proceeding Thr^{5.43}, which appears to point slightly outwards. Similarly polar residues Ser^{5.42} and Ser^{5.43} are present in catecholamine receptors such as dopamine D₄R and α_2 AR; and these polar residues may possibly engage in similar intramolecular or intermolecular interactions. However, these residues were found to be involved in agonist-binding and activation [449, 450] unlike the V_{1b}R in which agonists retained a high affinity binding in the absence of Thr^{5.42}. The differences may account for overall similarities in receptor architectures among Family A GPCRs, while indicating certain differences in receptor function existing in detail.

4.3.5. The mode of LA binding to V_{1b}R and V_{1a}R

There is little correlation in this study regarding LA binding to the V_{1b}R and V_{1a}R pairs of reciprocal substitution mutants. This may suggest that LA binds to each subtype V_{1a}R and V_{1b}R

in different manners. In its linear structure, it is plausible that LA may be capable of adopting alternative conformations more easily than a partially cyclic AVP and analogues which are restrained by the intramolecular disulfide bond. Conformational flexibility and better adaptability to slight changes in the receptor binding site are likely reasons to explain why gain of affinity for LA was observed more frequently than loss of affinity.

4.4 Future studies

The sets of V_{1b}R and V_{1a}R reciprocal mutant constructs prepared in this study could be used to investigate interaction mechanisms between the receptors and other subtype-selective ligands in future development. The results obtained by this mutagenesis study could be used to refine the molecular model of the V_{1b}R and V_{1a}R containing docked ligand. Following refinement of the models, further mutagenesis studies could be carried out on the functional residues which become apparent as contacting residues. The residues which have been identified to participate in ligand binding can also be studied in more details by substituting these with other functional residues, or by utilising ligand analogues which have been modified at potentially interacting side chains or moieties. The quality of molecular model would improve with an addition of water molecules following molecular dynamic simulations and appropriate mutagenesis studies. By applying an iterative process of computational molecular docking, MD simulations, systematic mutagenesis and ligand modifications, more reliable models which approach a realistic representation of the receptor subtypes could be eventually derived. Such models would not only facilitate the further development of the subtype-selective ligands, but also would be useful in obtaining detailed kinetics of the ligand association and dissociation *in silico*.

Chapter 5 The investigation on the variants of V_{1b}R

5.1 Introduction

The majority of biochemical or pharmacological studies undertaken on the V_{1b}R were carried out using recombinant human V_{1b}Rs which are overall identical in sequence, and represent the large majority of V_{1b}R found in the human population. Overall, the studies undertaken worldwide provide descriptions highly relevant and applicable to the V_{1b}R present in the majority of human individuals.

Exceptional variants in sequence have been found in a few single nucleotide polymorphism (SNP) variants of V_{1b}R which have been identified as sequencing of human V_{1b}R was carried out on a global scale. The differences which have been identified to date are usually limited to single codon changes in those SNP cases affecting the coding regions. Also, the associations between the carriers of such variant receptors and distinctive pathophysiologies may not be obvious. Hence the effects of the codon change on the receptor pharmacology have often been assumed to be small or negligible. However, during the development of novel compounds targeting the receptor, any existing differences need to be investigated for safety reasons for the individuals who are potentially affected. Among several SNP variants of V_{1b}R sequences identified to date, three variants were selected to be studied. These are Lys⁶⁵/Asn, Gly¹⁹¹/Arg, and Arg³⁶⁴/His, where the following residue in each case represents the polymorphic variants. Among the three, two have been linked with psychological disorders. The studies on a Hungarian population identified an association of Asn⁶⁵ with childhood-onset mood disorders [451]. A correlation between His³⁶⁴ phenotype and panic disorders has also been reported by a study in Germany [452]. The prevalence of each phenotype has been reported to be: i) 4.8 %

homozygous Asn⁶⁵ and 9.5 % for heterozygous Asn/Lys⁶⁵ in Europeans; ii) 4.2 % homozygous Arg¹⁹¹, 25 % heterozygous Arg/Gly¹⁹¹ in the Sub-Saharan African population, while in Europeans no homozygous Arg¹⁹¹ were identified while 4.5 % were heterozygous Arg/Gly¹⁹¹ carrier; and iii) 5 % homozygous His³⁶⁴ and 30 % heterozygous His/Arg³⁶⁴ in the European population.

An important factor in drug development is differences in the receptor pharmacology between human and other species. In the early stages of development, novel compounds are characterised on animals before being introduced into human volunteers. Rat and other rodents have been employed traditionally as model organisms in the pharmaceutical industries. However, such studies can become pointless or hard to interpret if there are large differences in the pharmacology of the same receptor between the two species concerned. For this reason, any potential differences between the relevant species need to be examined during development prior to the compounds entering clinical trials. In this study, the residues which contribute to species differences between the rodent V_{1b}R and human V_{1b}R in the putative ligand binding sites were investigated.

5.2 Results

5.2.1 SNP variants of human V_{1b}R

The polymorphisms of human V_{1b}R gene (AVPR1B) were identified by using SNP database inbuilt within Entrez website. Three SNPs subjected to study are: i) G to C nucleotide point mutation resulting in Lys⁶⁵Asn substitution (rs35369693); ii) G to C change leading to Gly¹⁹¹Arg substitution (rs33990840); and iii) G to A producing Arg³⁶⁴His substitution (rs28632197). The three residues are indicated in the schematic diagram of the V_{1b}R (figure 5.1). Each residue was introduced into the human V_{1b}R using site-directed mutagenesis. Three mutant constructs [K65N]V_{1b}R, [G191R]V_{1b}R and [R364H]V_{1b}R were produced. The ligand binding properties, AVP-induced internalisation of the receptor and InsP-InsP₃ production in response to AVP-stimulation were measured and compared to the Wt V_{1b}R.

Table 5.1 The mutagenic oligonucleotide primers used for mutagenesis:

Codon altered shown underlined, and the nucleotides changed shown in **BOLD**. The direction (S) means sense, and (AS) means antisense.

Construct	Direction	Nucleotide Sequence
[K65N]V _{1b} R	(S)	5'-CAG-CTG-GGC-CGC- <u>AAC</u> -CGC-TCC-CGC-ATG-3'
	(AS)	5'-CAT-GCG-GGA-GCG- GTT -GCG-GCC-CAG-CTG-3'
[G191R]V _{1b} R	(S)	5'-GG-GCA-GCA-GAC-TTC- <u>CGC</u> -TTC-CCT-TGG-GGG-3'
	(AS)	5'-CCC-CCA-AGG-GAA- <u>GCG</u> -GAA-GTC-TGC-CC-3'
[R364H]V _{1b} R	(S)	5'-CAG-CCC-AGG-ATG- <u>CAC</u> -CGG-CGG-CTC-TC-3'
	(AS)	5'-GGA-GAG-CCG-CCG- GTG -CAT-CCT-GGG-CTG-3'
<i>The above three sets of primers were used to produce SNP variants of V_{1b}R constructs.</i>		
[A2.52G]V _{1b} R	(S)	5'-CTG-ACA-GAC-CTG- GGC -GTG-GCG-CTC-TTC-3'
	(AS)	5'-GAA-GAG-CGC-CAC- <u>GCC</u> -CAG-GTC-TGT-CAG-3'
[L4.44P]V _{1b} R	(S)	5'-CAG-TCC-ACC-TAC- <u>CCG</u> -CTC-ATC-GCT-GCT-C-3'
	(AS)	5'-G-AGC-AGC-GAT-GAG- CGG -GTA-GGT-GGA-CTG-3'
[F4.56A]V _{1b} R	(S)	5'-CTG-GCC-GCC-ATC- GCC -AGC-CTC-CCT-CAA-GTC-3'
	(AS)	5'-GAC-TTG-AGG-GAG-GCT- GGC -GAT-GGC-GGC-CAG-3'
[L5.39I]V _{1b} R	(S)	5'-GGG-CCA-CGG-GCC-TAC- ATC -ACC-TGG-ACC-ACC-3'
	(AS)	5'-GGT-GGT-CCA-GGT- GAT -GTA-GGC-CCG-TGG-CCC-3'
[T5.52A]V _{1b} R	(S)	5'-C-GTT-CTG-CCG-GTG- GCC -ATG-CTC-ACG-GCC-3'
	(AS)	5'-GGC-CGT-GAG-CAT- GGC -CAC-CGG-CAG-AAC-G-3'
[S5.59G]V _{1b} R	(S)	5'-C-ACG-GCC-TGC-TAC- GGC -CTC-ATC-TGC-C-3'
	(AS)	5'-G-GCA-GAT-GAG- GCC -GTA-GCA-GGC-CGT-G-3'
[N7.45S]V _{1b} R	(S)	5'-G-GGC-AAC-CTC- TCC -AGC-TGC-TGC-AAC-CCC-3'
	(AS)	5'-GGG-GTT-GCA-GCA-GCT- GGA -GAG-GTT-GCC-C-3'
<i>The above seven sets of primers were used to produce mutant constructs of human V_{1b}R containing the corresponding residues of rat V_{1b}R.</i>		

5.2.2 Characterisation of the SNP variant V_{1b}R constructs

Construct	Binding Affinity (K_i , nM \pm S.E.M.)					Cell-Surface Expression (% Wt)
	AVP	dDAVP	SSR149415	5234B	LA	
WT V _{1b} R	0.90 (\pm 0.13)	10.5 (\pm 2.0)	3.36 (\pm 0.93)	7.18 (\pm 1.82)	6.25 (\pm 1.86)	100
K ⁶⁵ N	1.46 (\pm 0.05)	4.09 (\pm 0.39)	4.48 (\pm 0.90)	10.31 (\pm 0.47)	4.27 (\pm 0.79)	89 (\pm 2)
G ¹⁹¹ R	1.05 (\pm 0.29)	8.10 (\pm 0.11)	7.51 (\pm 0.53)	6.49 (\pm 0.95)	6.94 (\pm 1.06)	157 (\pm 5)
R ³⁶⁴ H	1.31 (\pm 0.21)	6.20 (\pm 0.83)	5.83 (\pm 0.48)	7.57 (\pm 1.20)	7.29 (\pm 2.39)	100 (\pm 12)

Table 5.2 Ligand binding characteristics of the V_{1b}R constructs representing the human SNP variants:

Binding affinity of V_{1b}R-selective agonists and antagonists to V_{1b}R constructs were determined by competition binding assay, using [³H]AVP as a tracer ligand. The pale blue indicates \approx 2-fold increase in affinity, compared to the Wt V_{1b}R. Cell-surface expression levels of each construct relative to the Wt V_{1b}R, determined by ELISA utilising an engineered HA tag at the N-terminus of the receptor.

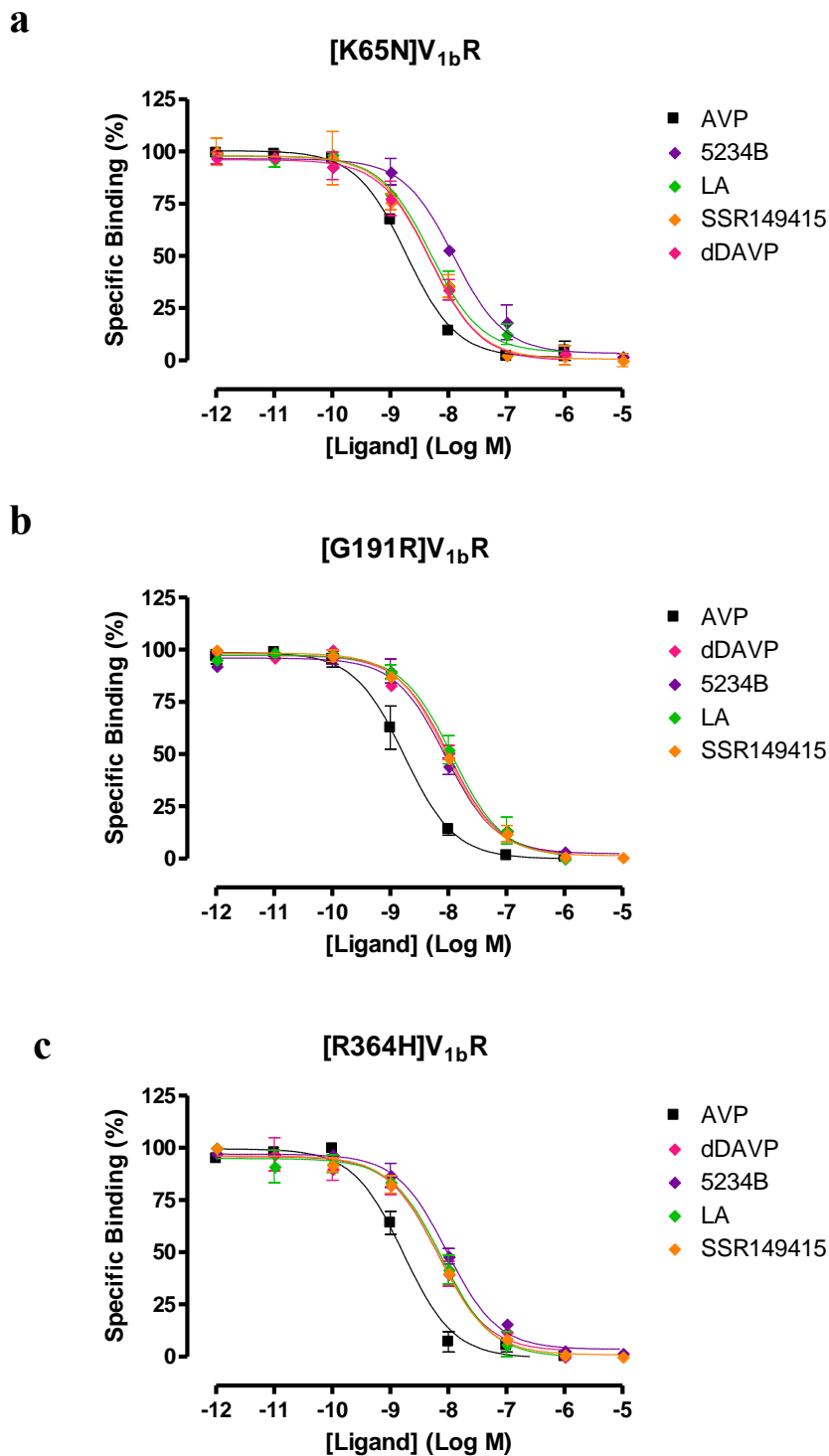


Figure 5.2 a-c The binding profiles of SNP variant constructs of V_{1b}R:

a. [K65N]V_{1b}R;

b. [G191R]V_{1b}R;

c. [R364H]V_{1b}R.

Competition binding curves of [³H]AVP and various ligands as indicated. The values were normalised to show percentage specific binding.

Construct	Cell-Surface Expression (% Wt)	AVP-induced Internalisation (% unstimulated)	dDAVP-induced Internalisation (% unstimulated)
WT V _{1b} R	100	49 (± 7)	53 (± 2)
K ⁶⁵ N	89 (± 2)	53 (± 1)	50 (± 2)
G ¹⁹¹ R	157 (± 5)	28 (± 9)	35 (± 3)
R ³⁶⁴ H	100 (± 12)	48 (± 12)	36 (± 7)

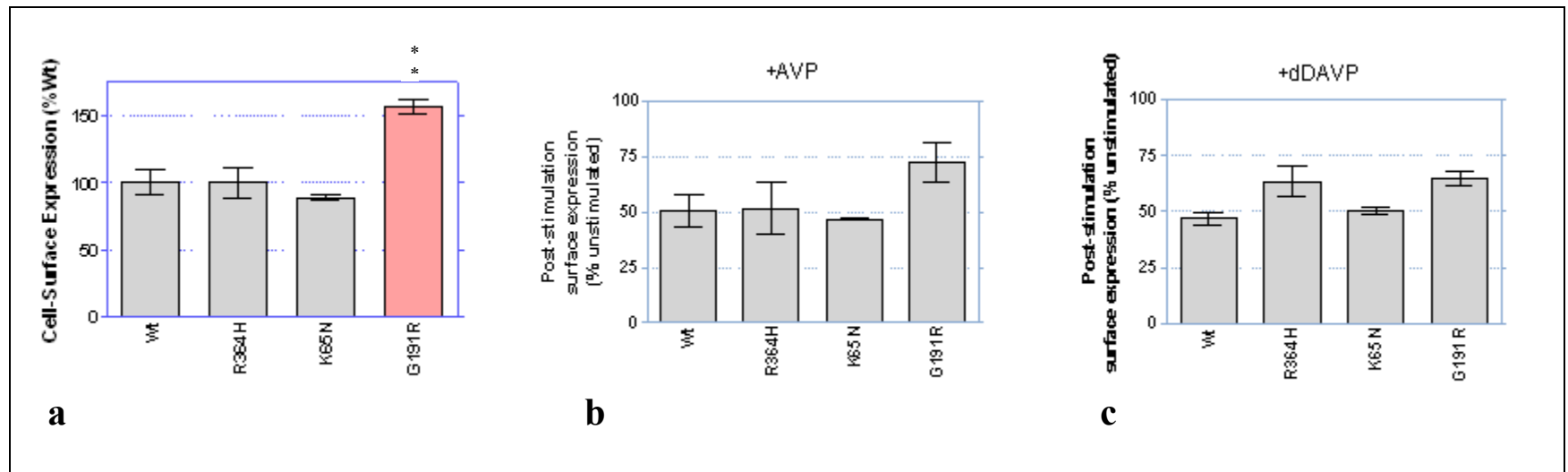


Table 5.3 The cell-surface expression and the agonist-induced internalisation of the SNP variant constructs: The percentage cell-surface expression of the constructs relative to the Wt, the proportions of constructs internalised in response to AVP-stimulation, and the internalisation induced by dDAVP. The figures are shown plus/minus SEM of three experiments each was in triplicate.

Figure 5.3 a-c The cell-surface expression of the SNP variants and the Wt V_{1b}R:

- The cell-surface expression of each mutant construct relative to the Wt;
- The expression level after AVP-stimulation (1µM) for 30 min. The figures were normalised to show the percentages relative to the unstimulated.
- The cell-surface expression after dDAVP-stimulation (1µM) for 30 min. The figures were normalised as above.

The results were analysed by one-way ANOVA followed by Dunnett's post-test with Wt as control (P < 0.01 indicated in pale red and asterisks).

Construct	AVP-induced InsP-InsP ₃ Accumulation	
	EC ₅₀ (nM, ± SEM)	E _{max} (% Wt, ± SEM)
WT V _{1b} R	1.69 (± 0.37)	100
K ⁶⁵ N	2.05 (± 0.27)	67 (± 4) *
G ¹⁹¹ R	2.59 (± 0.35)	170 (± 25) *
R ³⁶⁴ H	2.54 (± 0.23)	99 (± 20)

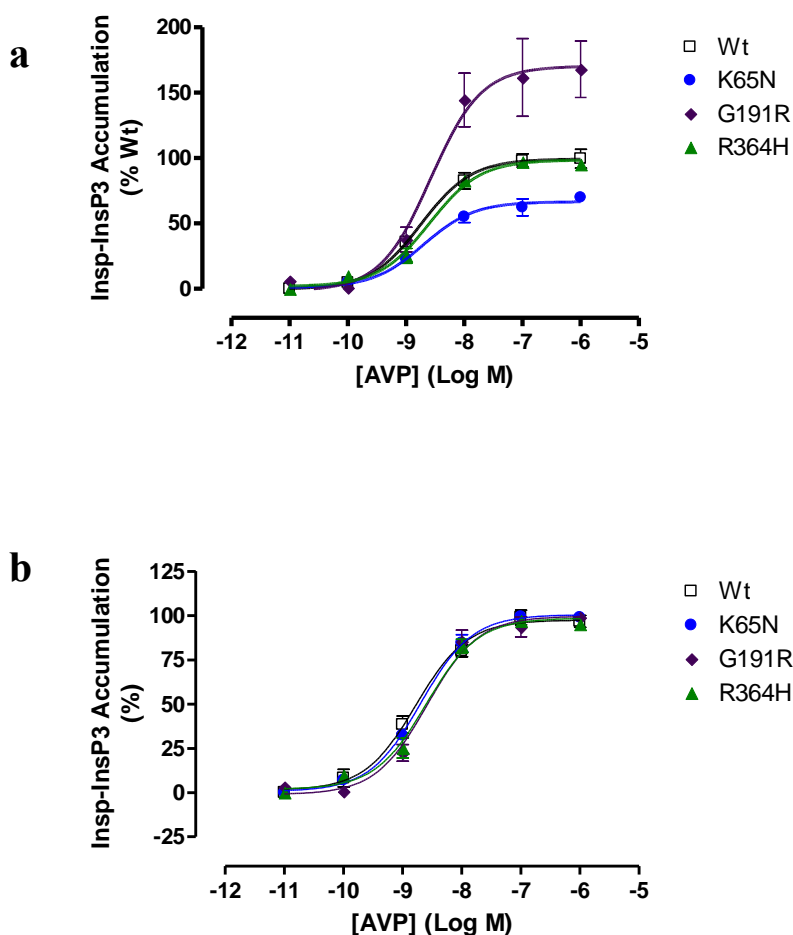


Table 5.4 InsP-InsP₃ productions by the SNP variant constructs:

The InsP-InsP₃ productions were measured 30 min after AVP-stimulation (1μM). The E_{max} was determined relative to the maximum production measured in the Wt V_{1b}R. The values were determined from three experiments each performed in triplicate. Significant differences were observed by one-tailed paired T-test (P < 0.05) as indicated in pale orange and asterisk.

Figure 5.4 ab InsP-InsP₃ productions by the SNP variants and the Wt V_{1b}R:

- The InsP-InsP₃ production relative to the Wt. The values obtained for each construct was normalised to the Wt;
- The InsP-InsP₃ production. The values were normalised to the maximum (100%) for each construct.

Construct	Agonist-induced InsP-InsP ₃ Accumulation			
	EC ₅₀ (nM, ± SEM)		E _{max} (% Wt, ± SEM)	
	AVP	dDAVP	AVP	dDAVP
WT V _{1b} R	1.78 (± 0.37)	11.9 (±1.9)	100	100
K ⁶⁵ N	2.05 (± 0.27)	8.74 (± 1.34)	67 (± 4)	60 (± 13)

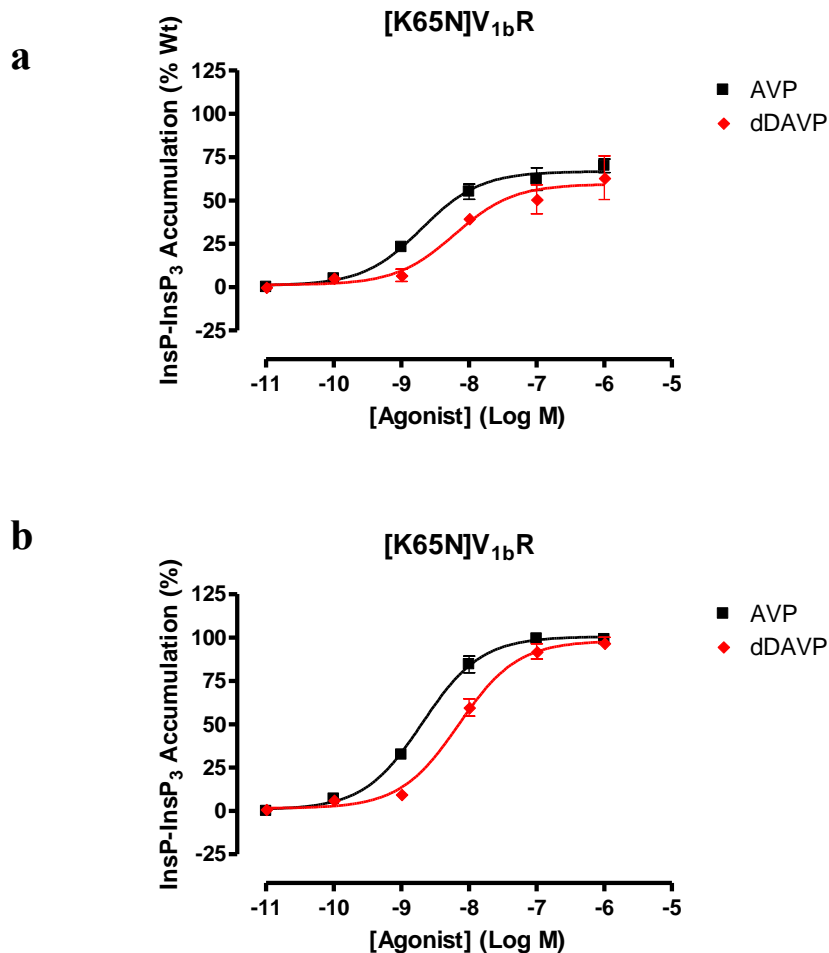


Table 5.5 InsP-InsP₃ productions by [K65N]V_{1b}R: The InsP-InsP₃ productions measured 30 mins after AVP-stimulation (1 μ M). The effectiveness in the accumulation is presented as EC₅₀ determined by non-linear regression curves. The E_{max} was determined relative to the maximum production measured in the Wt. The values were determined from three experiments each performed in triplicate.

Figure 5.5 ab InsP-InsP₃ productions by [K65N]V_{1b}R in response to AVP or dDAVP:

- The InsP-InsP₃ production relative to the Wt;
- The InsP-InsP₃ production normalised to the maximum accumulation induced by each ligand.

All three SNP variant constructs of the V_{1b}R produced in this study confirmed that any one of the codon substitutions does not abolish the V_{1b}R functionality, and each variant retained high affinity binding to AVP. In fact, the [K65N]V_{1b}R variant increased the binding affinity for dDAVP about 2-fold. When the dDAVP induced InsP-InsP₃ production by this construct was investigated, the EC₅₀ value obtained was similar to the Wt. In comparison to the Wt and the other two SNP variants, both AVP and dDAVP appeared slightly less effective in generating Ins-InsP₃ by [K65N]V_{1b}R, as seen in the relatively lower values of E_{max} obtained for this construct. Lys⁶⁵, located in the middle of the ICL1, is conserved among V_{1a}R, V_{1b}R and OTR, all of which preferentially couple to G_{q/11α}, whereas Asn⁶⁵ is found in V₂R which couples predominantly with G_{sα}. Therefore, with an assumption that the Asn substitution of Lys⁶⁵ may have increased the coupling preference of the V_{1b}R to G_{sα}, the agonist induced cAMP production by [K65N]V_{1b}R was also investigated; however no significant increase in cAMP generation by this mutant was observed (results not shown).

A significant difference in the cell-surface expression level was observed for [G191R]V_{1b}R. The cell-surface expression of the construct was markedly increased to 157 % of the Wt V_{1b}R, and a corresponding increase in E_{max} value was obtained by InsP-InsP₃ assay. The agonist induced-internalisation of the construct by both AVP and dDAVP appeared to be slightly compromised, though the differences were shown to be statistically insignificant by one-way ANOVA followed by Dunnett's post-test against the Wt control. The apparent reduction in the internalisation observed might possibly reflect a threshold of the internalisation process in the HEK293T system employed. No significant difference from the Wt was observed for [R364H]V_{1b}R in this study. The pharmacological characteristics determined for this construct in this study were similar to the Wt.

5.2.3 Characterisation of the human V_{1b}R constructs containing the equivalent residue of rat V_{1b}R

In order to identify residues which differ between human and rodent V_{1b}R in the putative ligand binding cavity for non-peptide ligands, TM domains of V_{1b}R of three species, rat, mouse and human were compared by means of protein sequence alignment (figure 5.6). The residues identified to be non-conservative substitutions were targeted for mutagenesis. The selected residues of the rat V_{1b}R were then introduced into the human recombinant V_{1b}R by site-directed mutagenesis. Initially the residues located at the upper or middle TM region were selected as these are more likely candidate for interacting ligands. However, a few residues located at the lower TM were also selected concerning indirect effects the residue could possibly have on the ligand binding cavity. In total, seven residues were selected to study. The location of these residues are indicated in a schematic diagram of human V_{1b}R (figure 5.7).

Seven human V_{1b}R constructs: [A2.52G]V_{1b}R, [L4.44P]V_{1b}R, [F4.56L]V_{1b}R, [L5.39I]V_{1b}R, [T5.52A]V_{1b}R, [S5.59G]V_{1b}R, and [N7.45S]V_{1b}R were made and characterised. The binding characteristics of three agonists AVP, dDAVP and d[Val⁴]DAVP, and also a V_{1b}R -selective non-peptide antagonists 5234B, were determined by competition binding assay. d[Val⁴]DAVP (dVDAVP) was used since the substitution of Gln⁴ of dAVP with relatively hydrophobic residues have been shown to increase selectivity to V_{1b}R [353], and d[Leu⁴, Lys⁸]VP has been shown to be a V_{1b}R -selective agonist in rat species [347]. The data from the above studies indicate that the modified peptides behave as high affinity agonists to both rat and human V_{1b}Rs but less efficacious at other subtypes. dVDAVP was originally synthesised in 1974 by Sawyer *et al.* as a V₂R-selective agonist before V_{1b}R was known to exist [453]. In this study, dVDAVP was used in search of the mutual ground between rat and human V_{1b}Rs, concerning conformations of the ligand binding cavities of V_{1b}R from the two species.

V1BR_HUMAN	MDSGPLWDANPTPRGTL SAPNATTPWL GRDEE LAKVE IGVLATVVLV LATGGNLAVLL TLG
V1BR_MOUSE	MDSEPSWTATP SPGGTL FVPMTTTPWL GRDEE LAKVE IGI LATVVLV LATGGNLAVLL ILG
V1BR_RAT	MNSEPSWTATP SPGGTL PVPNATTPWL GRDEE LAKVE IGI LATVVLV LATGGNLAVLL TLG
V1BR_HUMAN	QLGRKR SRMHL FVLHLA LTDL VVALFQVLPQL LWD ITYRFQG PDLL CRAVKY LQVLSMFA
V1BR_MOUSE	LQGHKR SRMHL FVLHLA LTDL GVALFQVLPQL LWD ITYRFQGS DLL CRAVKY LQVLSMFA
V1BR_RAT	RHGHR SRMHL FVLHLA LTDL GVALFQVLPQL LWD ITYRFQGS DLL CRAVKY LQVLSMFA
V1BR_HUMAN	STYMLL AMTLDRYLAVCHPLRSLQQPGQSTYL LIAAPWLLAAIF SLPQVFIF SLREVIQG
V1BR_MOUSE	STYMLL AMTLDRYLAVCHPLRSLQQPSQSTYP LIAAPWLLAAI LSLPQVFIF SLREVIQG
V1BR_RAT	STYMLL AMTLDRYLAVCHPLRSLRQPSQSTYP LIAAPWLLAAI LSLPQVFIF SLREVIQG
V1BR_HUMAN	SGVLDCWADFGFPWGPRAYL TWTTLAI FVLPV TMLTACYSLI CHEICKNLKVKVKTQAWRVG
V1BR_MOUSE	SGVLDCWADFYFSWGPRAYITWTTIMAI FVLPV VVLTACYGLI CHEIYKMLKVKVKTQAGREE
V1BR_RAT	SGVLDCWADFYFSWGPRAYITWTTIMAI FVLPV AVLSACYGLI CHEIYKMLKVKVKTQAGREE
V1BR_HUMAN	GGGWRTWD . RPSPSTLAATRGLPSRVSSINTISRAKIRTVKMTFVI VLAYI ACWAP FFS
V1BR_MOUSE	RRGW . . . KSSSSAAAAATRGLPSRVSSISTISRAKIRTVKMTFVI VLAYI ACWAP FFS
V1BR_RAT	RRGWRTWDKSS SAVATAATRGLPSRVSSISTISRAKIRTVKMTFVI VLAYI ACWAP FFS
V1BR_HUMAN	VQMWSV WDKNA PDEDSTNV AFTISML LGNLS CCNPWIYMGFNSHLL PRPLRHLACC GGP
V1BR_MOUSE	VQMWSV WDENA PNEDSTNV AFTISML LGNLS CCNPWIYMGFNSHLL PRSLSHRACCRGS
V1BR_RAT	VQMWSV WDENA PNEDSTNV AFTISML LGNLS CCNPWIYMGFNSRLL PRSLSHHACCTGS
V1BR_HUMAN	QPRMRRRLSDGSLSSRHTLL TRSSCPATLSL SLSLTLSGRPRPEES PRDLE LADGE GTA
V1BR_MOUSE	KPRVHRQLSNS SLASRRHTLL THTCGP STLRL SLNLS LHAKPKPAGS LKDLE QVDGE ATM
V1BR_RAT	KPQVHRQLSTS SLTSRRHTLL THACGS PTLRL SLNLS LRAKPRPAGS LKDLE QVDGE ATM
V1BR_HUMAN	ETIIF
V1BR_MOUSE	ETSI
V1BR_RAT	ETSIF

Figure 5.6 Sequence alignment of V_{1b}R from human, mouse and rat:

The protein sequence alignment of human, mouse, and rat V_{1b}R. TM domains were shown in red. TM residues that differ between the rodents and human are shown in blue. Bold letters in red indicate the most conserved residues in Family A GPCRs and are the reference residues used in Ballesteros-Weinstein's numbering scheme.

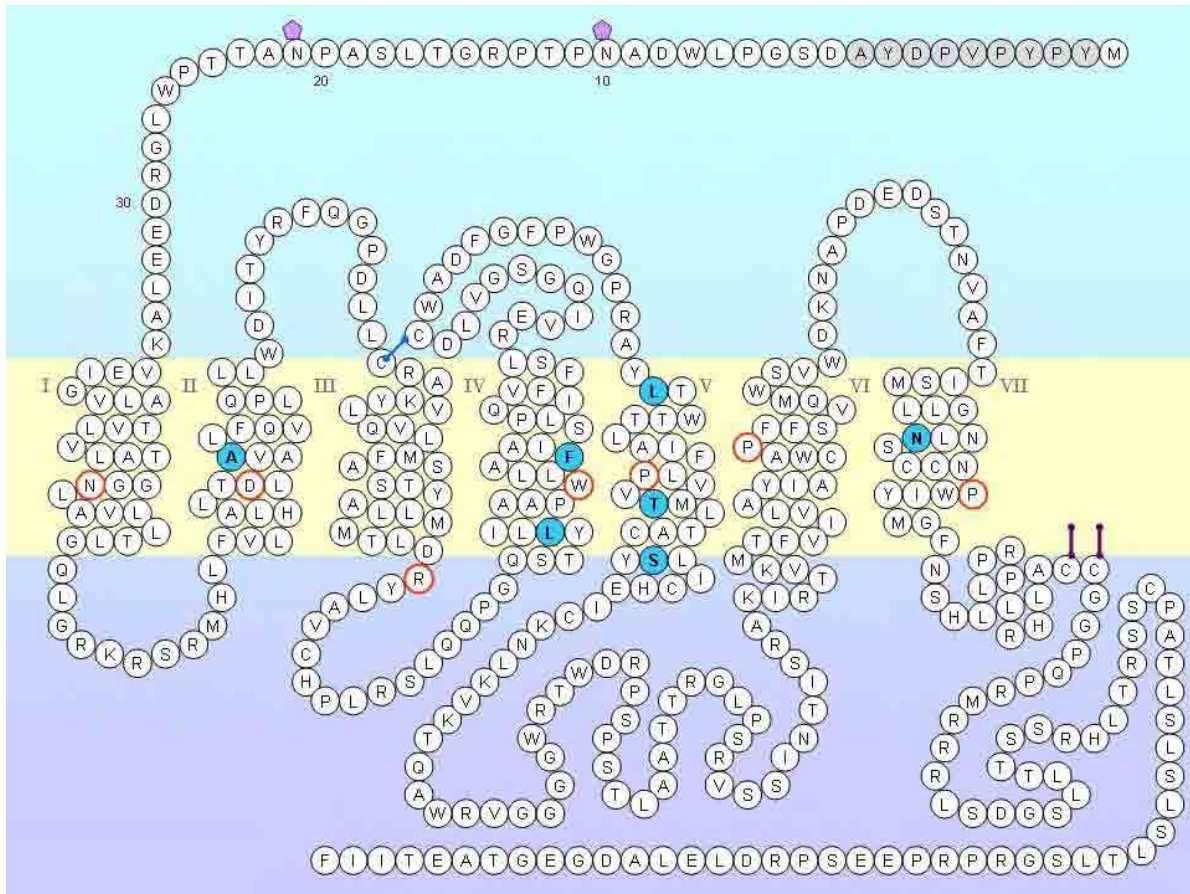


Figure 5.7 Divergent TM residues in V_{1b}Rs between human and rat:

The schematic representation of the human V_{1b}R is shown with the residues chosen for mutagenesis in turquoise. The residues circled with orange are the most conserved residues among Family A GPCRs, and are used as reference points in Ballesteros-Weinstein numbering scheme. The putative sites for post-translational modifications are indicated as follows: hexagons on Asn residues of the N-terminal domain for glycosylation; purple lines on Cys residues of the C-terminal domain for palmitoylation. The residues in grey represent HA epitope tag incorporated at the N-terminus.

Construct	Binding Affinity (K_i , nM \pm S.E.M.)				Cell-Surface Expression (% Wt)
	AVP	dDAVP	dVDAVP	5234B	
WTV_{1b}R	0.90 (\pm 0.13)	10.5 (\pm 2.7)	6.00 (\pm 0.26)	7.61 (\pm 1.18)	100
A2.52G	0.81 (\pm 0.29)	8.04 (\pm 0.85)	7.29 (\pm 1.54)	7.72 (\pm 1.27)	85 (\pm 1)
L4.44P	0.25 (\pm 0.07)	3.03 (\pm 0.15)	2.49 (\pm 0.21)	2.11 (\pm 0.61)	45 (\pm 3)
F4.56L	0.70 (\pm 0.09)	7.71 (\pm 2.79)	11.5 (\pm 0.1)	7.47 (\pm 1.54)	71 (\pm 4)
L5.39I	1.22 (\pm 0.06)	16.0 (\pm 3.6)	9.00 (\pm 0.52)	4.55 (\pm 1.42)	109 (\pm 10)
T5.52A	0.68 (\pm 0.31)	13.2 (\pm 0.7)	6.38 (\pm 0.72)	5.72 (\pm 1.89)	106 (\pm 4)
S5.59G	1.08 (\pm 0.36)	7.73 (\pm 1.04)	8.04 (\pm 1.48)	12.9 (\pm 4.3)	102 (\pm 3)
N7.45S	1.57 (\pm 0.32)	16.3 (\pm 1.6)	17.4 (\pm 4.8)	6.83 (\pm 1.23)	101 (\pm 1)

Table 5.6 Ligand binding characteristics of the human V_{1b}R constructs containing corresponding residues of rat V_{1b}R:

Binding affinity of V_{1b}R-selective agonists and antagonists to V_{1b}R constructs were determined by competition binding assay, using [³H]AVP as a tracer ligand. The pale blue indicates small gain of affinity (\approx 2~3 fold) and yellow indicates \approx 3-fold loss of affinity compared to the Wt V_{1b}R. Cell-surface expression levels of each construct relative to the Wt V_{1b}R were determined by ELISA utilising an engineered HA tag at the N-terminus of the receptor. The values presented are means plus/minus SEM of three experiments each performed in triplicate.

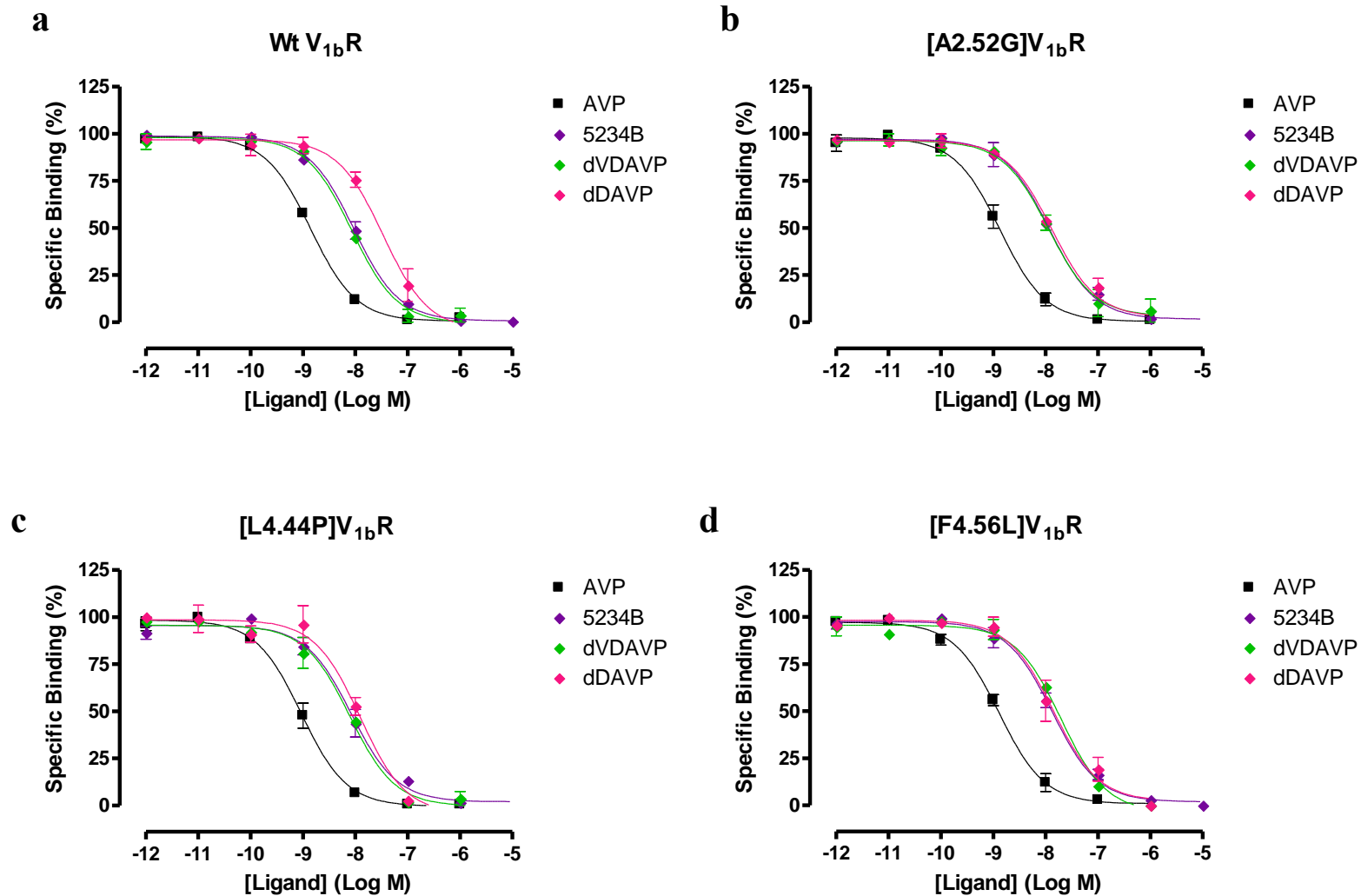


Figure 5.8 a-d The binding profiles of the Wt $V_{1b}R$ and human $V_{1b}R$ constructs each containing a rat $V_{1b}R$ residue:
 a. Wt $V_{1b}R$; b. [A2.52G] $V_{1b}R$; c. [L4.44P] $V_{1b}R$; d. [F4.56L] $V_{1b}R$.

Competition binding curves of [3H]AVP and various $V_{1b}R$ -selective ligands. The values were normalised to show percentage specific binding. The error bars represent SEM of three experiments each performed in triplicate.

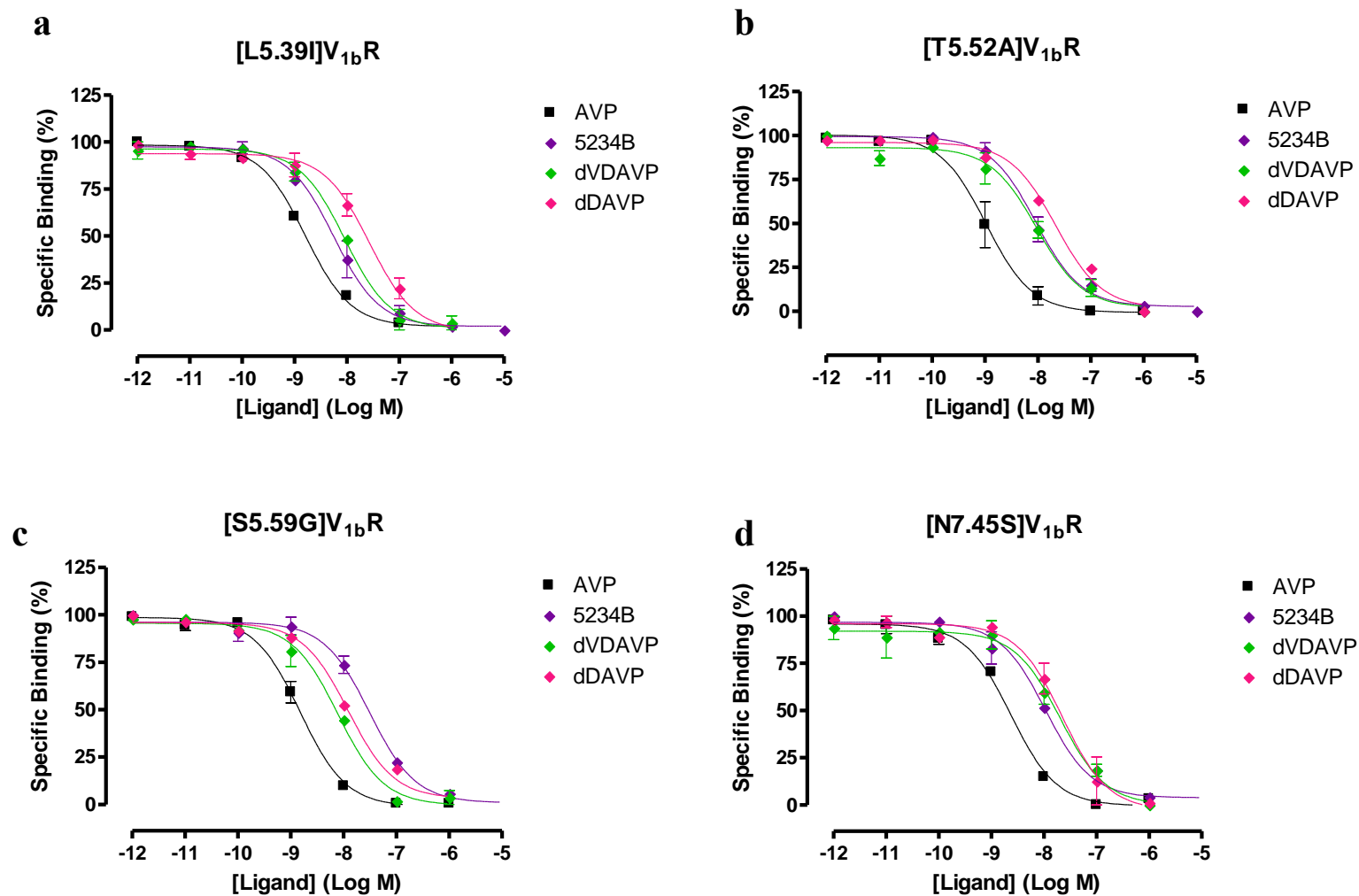


Figure 5.9 a-d The binding profiles of the human V_{1b}R constructs each containing a rat V_{1b}R residue:

a. [L5.39I]V_{1b}R; **b.** [T5.52A]V_{1b}R; **c.** [S5.59G]V_{1b}R; **d.** [N7.45S]V_{1b}R.

Competition binding curves of [³H]AVP and various V_{1b}R-selective ligands. The values were normalised to show percentage specific binding. The error bars represent SEM of three experiments each performed in triplicate.

Construct	Binding Affinity (K_i , nM \pm S.E.M.)		
	AVP	5234B	SSR149415
WT $V_{1b}R$	0.90 (\pm 0.13)	7.18 (\pm 1.82)	3.36 (\pm 0.93)
[L5.39V] $V_{1b}R$	0.40 (\pm 0.14)	21.5 (\pm 1.9)	6.90 (\pm 1.02)
[L5.39A] $V_{1b}R$	1.36 (\pm 0.02)	103 (\pm 33)	20.7 (\pm 2.2)
[L5.39I] $V_{1b}R$	1.22 (\pm 0.06)	4.55 (\pm 1.42)	5.38 (\pm 0.38)

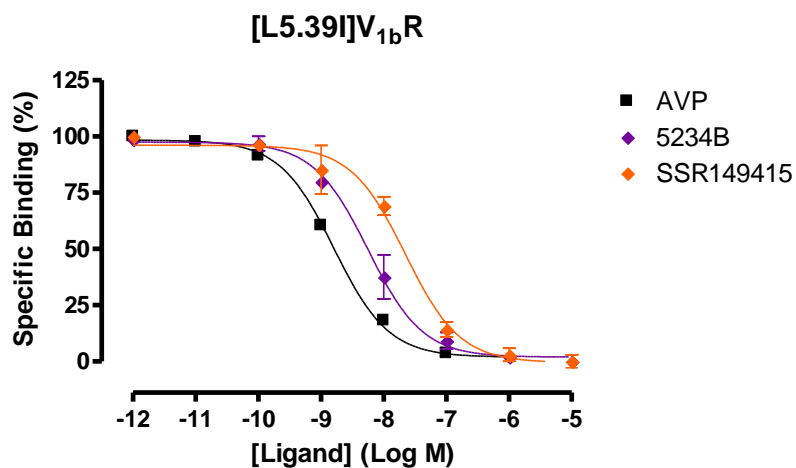


Table 5.7 The binding affinity of non-peptide antagonists to [L5.39I] $V_{1b}R$, [L5.39V] $V_{1b}R$ and [L5.39A] $V_{1a}R$:

The binding affinity of 5234B and SSR149415 to the constructs are shown in K_i obtained from three separate competition binding assays each performed in triplicate.

Figure 5.9 The binding of 5234B and SSR149415 to [L5.39I] $V_{1b}R$:

Competition binding curves of [3H]AVP and various $V_{1b}R$ -selective ligands. The values plotted were normalised to show percentage specific binding. The error bars represent SEM of three experiments each performed in triplicate.

Construct	Cell-Surface Expression (% Wt)	AVP-induced Internalisation (% unstimulated)
WT V _{1b} R	100	46 (± 6)
A2.52G	85 (± 1)	48 (± 8)
L4.44P	45 (± 3)	54 (± 3)
F4.56L	72 (± 2)	59 (± 5)
L5.39I	109 (± 10)	50 (± 4)
T5.52A	106 (± 4)	43 (± 3)
S5.59G	102 (± 3)	59 (± 7)
N7.45S	101 (± 1)	47 (± 3)

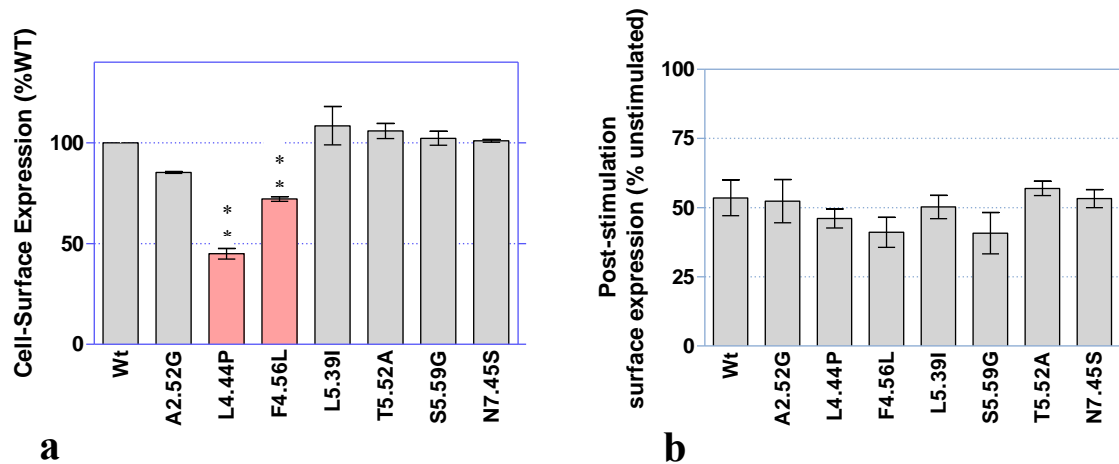


Table 5.8 The cell-surface expression and AVP-induced internalisation of the human V_{1b}R constructs containing rat V_{1b}R residues: The percentage cell-surface expression relative to the Wt, and the proportions of internalised in response to AVP-stimulation (1 μ M, 30 min). The figures are shown plus/minus SEM of three experiments each was in triplicate.

Figure 5.10 ab The cell-surface expression of the SNP variants and the Wt V_{1b}R:

- The cell-surface expression of each mutant construct relative to the Wt;
- The expression level after AVP-stimulation (1 μ M) for 30 min. The figures were normalised to show the percentages relative to the unstimulated.

The results were analysed by one-way ANOVA followed by Dunnett's post-test with Wt as control (P < 0.01 shown in pale red with asterisks).

5.2.4i Summary of results

Most mutant constructs produced in this section retained the Wt-like characteristics in ligand binding for the agonist and the antagonist used in this study. [L4.44P]V_{1b}R appeared to have shown slightly increased affinity overall, with about 2-fold decrease in K_i values obtained for all the ligands used. The cell-surface expression level of [L4.44P] V_{1b}R was 45 % relative to the Wt. Although Pro^{4.44} is mutually found in the V_{1b}R of rodents such as mouse and rat, the Pro was not well-tolerated in human V_{1b}R, which prefers to have aliphatic Leu. On the TM4, there is another hydrophobic substitution between the human and the rodents V_{1b}R at position 4.56. [F4.56L]V_{1b}R was also found to express on the cell-surface about 30% less than the Wt. The results obtained for the two constructs suggest that there are differences regarding hydrophobicity at the middle/lower region of TM4 between human and rodent V_{1b}Rs.

In the previous section of this study in Chapter 4, Leu^{5.39} was identified as involved in the ligand binding of dDAVP, LA, SSR149415 and 5234B to V_{1b}R. In rodent V_{1b}Rs, Ile^{5.39} is found. [L5.39I]V_{1b}R was produced to explore this slight difference between the species variant V_{1b}Rs. The Ile substitution of Leu^{5.39} was relatively well-tolerated in human V_{1b}R for agonists, though a slight reduction of the binding affinity remained for dDAVP. The reduction in binding affinity of antagonists were also observed in both [L5.39V]V_{1b}R and [L5.39A]V_{1b}R, but high affinity binding was restored in [L5.39I]V_{1b}R.

5.3. Discussion

5.3.1. Characteristics of SNP variants distinct from the Wt V_{1b}R

Among the three SNP variants studied, the minor SNP variant of Lys⁶⁵Asn displayed a slight but significant reduction in the cell-surface expression and reduced potency in InsP-InsP₃ generation in response to either AVP or dDAVP stimulation. Since Asn is found at the corresponding position in the V₂R which is coupled to G_{as}, a possibility of altered coupling tendency of the variant towards G_{as} was considered; however, the agonist-induced cAMP generation by this construct was not elevated (results not shown). A genetic analysis study by Dempster *et al.* has previously identified that this minor variant may have a protective effect against childhood-onset mood disorders in females [435]. The reduction in receptor functionality observed for this variant in this study support their finding, and provides an explanation at a molecular pharmacological level. The exact role of Lys⁶⁵ in the V_{1b}R conformation remains uncertain, as the reliability in predicting conformations of loop regions by molecular modelling is currently limited. The mutagenesis study of Lys residues in the intracellular domains of the V_{1a}R by Wootten showed that the Lys⁸² residue at the corresponding position in ICL1 is not subjected to ubiquitination (Wootten D.L. 2007, Doctoral thesis, University of Birmingham). This indicates that Lys⁸² is relatively unexposed and inaccessible by heterologous macromolecules in the V_{1a}R; the residue might engage in intramolecular interactions with neighbouring residues. Therefore Lys⁶⁵ at the corresponding position, as shown by multiple sequence alignment, might similarly participate in intramolecular interactions assisting conformational stability.

The other notable finding from this study on the SNP variants was the variant of Gly¹⁹¹Arg, which displayed substantially increased cell-surface expression. The result was

consistent with the large E_{\max} value representing the effective generation of InsP-InsP₃. Several hypothesis can be made to explain why the cell-surface expression level was increased in [G191R]V_{1b}R. Firstly, the introduced Arg¹⁹¹ is likely to interact with neighbouring residues by virtue of its charge, thereby making the receptor more stable. Such interactions can be achieved most likely at the intramolecular level, or even at the intermolecular level with residues of another molecule present in the close vicinity to strengthen any dimeric association. The removal of glycine itself probably contributes to stabilising the local environment of ECL2 thermodynamically as the loop would probably lose some degrees of conformational freedom in the absence of Gly. The Arg substitution of Gly¹⁹¹ is thought to have stabilised the ECL2 without distorting the ligand binding cavities, as [G191R]V_{1b}R retained high affinity binding to both agonists and antagonists used in this study.

The SNP variant carrying the Gly¹⁹¹Arg substitution is known to be relatively rare among European populations with no homozygous individual identified to date. The incidence of SNP variant is known to be more frequent in Sub-Saharan African population. It can be assumed that the SNP variant might have evolved in the Sub-Saharan African population as a coping strategy in the dry climate with high temperature, which makes individuals prone naturally to dehydration. The population might have been affected by diseases such as diarrhoea when drinking contaminated water with bacteria, which in turn cause more dehydration. Not only water but also minerals are excreted by sweating, whereas water, minerals and ACTH are also lost by excretion when affected by diarrhoea. Therefore increasing ACTH production by the stable V_{1b}R might have been a counteracting strategy in adapting to such a problematic environment. It is also possible that a rapid induction of physiological ‘fight or flight’ response enhanced by cortisol (in addition to via adrenaline) was appropriate and beneficial among

ancestral hunter-gatherers in the environment of Sub-Saharan Africa, where a range of large carnivorous animals co-habit on the same land. However, in the current modernised world, individuals possessing this SNP variant might possibly be susceptible to stress-related disorders due to the enhanced $V_{1b}R$ functionality, unless there are any counteracting function (e.g. under-active CRFR, under-production of AVP etc.) simultaneously present.

The molecular pharmacological characteristics of these minor variants determined in this study are more likely to represent the receptor functions in homologous individuals, as each construct was characterised by transfecting each construct alone. Since $V_{1b}R$ can either form homo- or heterodimers, the effects of the variants in heterologous individuals could be less, unless these variants were found to exhibit dominant effects. The heterodimerising nature of $V_{1b}R$ with CRFR1 may add another complication regarding the effect the variant has on the overall cellular events.

5.3.2 Comparisons of TM domains between human and rat $V_{1b}Rs$

The species differences between rat and human $V_{1b}Rs$ in TM domains were investigated by incorporating corresponding residues of rat $V_{1b}R$ into human $V_{1b}R$. The results of this study suggest that the TM domains of rat $V_{1b}R$ and human $V_{1b}R$ are similar regarding ligand binding properties of these receptors, and reflect the fact that both receptors are thought to share very similar ligand binding cavities. A slight difference may exist in property of TM4 and the consequential association of TM4 with neighbouring helices, as TM4 of rat $V_{1b}R$ bears Pro^{4.44} which may introduce an additional kink. The overall increase in ligand binding affinities to human $V_{1b}R$ containing Pro^{4.44} observed in this study could be the result of the altered conformation of TM4 resulting in increased accessibility of ligands to the binding cavity.

5.4 Future studies

These variant constructs produced can be used in the future to explore binding properties of different high affinity ligands of the V_{1b}R. The SNP variant constructs will remain useful tools in testing any V_{1b}R-selective agents for therapeutic purposes, prior to clinical trials in order to estimate the effect of the drugs on the affected individuals. The species variant constructs can also be used to study species differences between rodents and human V_{1b}Rs, in confirming the relevance of results obtained from rodent studies to human application.

One of SNP variants, Gly¹⁹¹Arg of the V_{1b}R was shown to be functionally enhanced compared to the Wt V_{1b}R. Since the prevalence of the SNP variant is higher in the Sub-Saharan African population compared to European populations, the prevalence of the SNP variants of CRFR1 in the same populations could also be investigated. The SNP variant of CRFR1 with enhanced function could be searched by the same approach used in this study. The additional study on CRFR1 in conjunction with investigating the cAMP signalling properties of the V_{1b}R SNP variants will provide a broader picture of the SNP variants associated with the stress response.

With considerations on both homo- and heterozygous individuals carrying the variant, the effect of homo- and hetero-dimerisation between the variant and the Wt on the functionality of the minor variant should also be investigated and quantified. Such investigations could also be extended to include heterodimerisation between the variant V_{1b}R and any other dimerisation partners such as CRFR1. The visualisation of each differentially labelled variant, the Wt, and CRFR1 upon co-expression may clarify the issue of the effect of the variant on the cell-surface expression of its dimerisation partners.

Chapter 6 Summary and concluding remarks

The results of the experiments described in this thesis have provided advanced insight into the functional and pharmacological characteristics of vasopressin receptors, with a particular focus on the V_{1b}R in molecular details. In particular, the experiments were designed to examine in considerable depth the structure of ligand binding cavities of the V_{1b}R and the similarities and differences of these sites to V_{1a}R. Additionally, because of its potential therapeutic and prognostic value, further studies on the molecular pharmacology of V_{1b}R variants were carried out.

In Chapter 3, conserved TM residues among vasopressin receptors were substituted with Ala. As shown in V_{1a}R and OTR (Wootten and Wheatley, manuscript in preparation), Arg^{1.27} and Glu^{1.35} are necessary for a high affinity AVP binding to the V_{1b}R, and the reciprocal mutagenesis between ligand and the receptor construct demonstrated the direct interaction occurring between Glu^{1.35} and Arg⁸. The individual Ala substitution of FQVLPQ (studied residues) motif conserved among the neurohypophysial hormone receptor family revealed the importance of Pro^{2.60} and Gln^{2.61} in the AVP binding to the V_{1b}R. In addition, Phe^{2.56}, Pro^{2.60} and Gln^{2.61} were found to be crucial for the V_{1b}R in achieving a high level of cell-surface expression. The role of Gln^{2.57} was identified as to restrain the peptide ligand binding cavity of the V_{1b}R. Continuing from the studies on V_{1a}R by Hawtin and Simms in 2005, Arg^{3.26} in V_{1b}R was also shown to be required to maintain the AVP binding cavity likely by the ionic interaction between Arg^{3.26} and phosphate groups of phospholipids. A crucial structural role of Phe^{5.47}, which is highly conserved among Family A GPCR, was also demonstrated in the V_{1b}R. The role of the

residue at position 5.47 in structural stabilisation was shown by thermal challenge on the mutant constructs each containing altered hydrophobicity at the position. In conjunction with the study, pharmacochaperone activity of a non-peptide antagonist 5234B was demonstrated. The participation of Tyr^{5.38} and Phe^{6.51} in ligand binding of both agonist and non-peptide antagonists was shown. The requirement of Trp^{6.48} of 'rotamer toggle switch' in non-peptide antagonists binding to the V_{1b}R was demonstrated. Chapter 3 also identified a few residues involved in dDAVP binding. Most of these residues are hydrophobic in nature, present in the upper TM region of TM3, TM5 and TM6, except a charged Asp^{6.61} present at the exofacial surface of TM6. The residues identified in this study to be involved in agonist binding of V_{1b}R are indicated in the schematic diagram (figure 6.1).

Chapter 4 discusses residues which may confer selectivity between V_{1b}R and V_{1a}R using pairs of reciprocal mutant construct each containing a corresponding residue of the other subtype. The ligands with selectivity to each subtype were used to identify potentially contacting residues. The primary aim was to identify the residues participate in the V_{1b}R-selective non-peptide antagonists. Several polar and hydrophobic residues located at the upper TM regions were found to be required for high affinity binding of 5234B, or the other V_{1b}R-selective antagonist SSR149415. The study identified Phe^{7.35} as a key residue in 5234B binding to the V_{1b}R. Including the findings from the Chapter 3, the residues participate in the V_{1b}R-selective binding of 5234B and SSR149415 are summarised in a schematic diagram of the V_{1b}R (figure 6.2).

Subsequent Ala-substitution identified that Thr^{5.42} has a role in restraining the ligand binding cavities of the V_{1b}R, since the loss of residue resulted in increased affinity of the peptide ligands otherwise less specific to the V_{1b}R. Thr^{5.42} is also thought to be important in maintaining the structural integrity of the V_{1b}R, as Ala substitution of Thr^{5.42} resulted in a significantly reduced cell-surface expression.

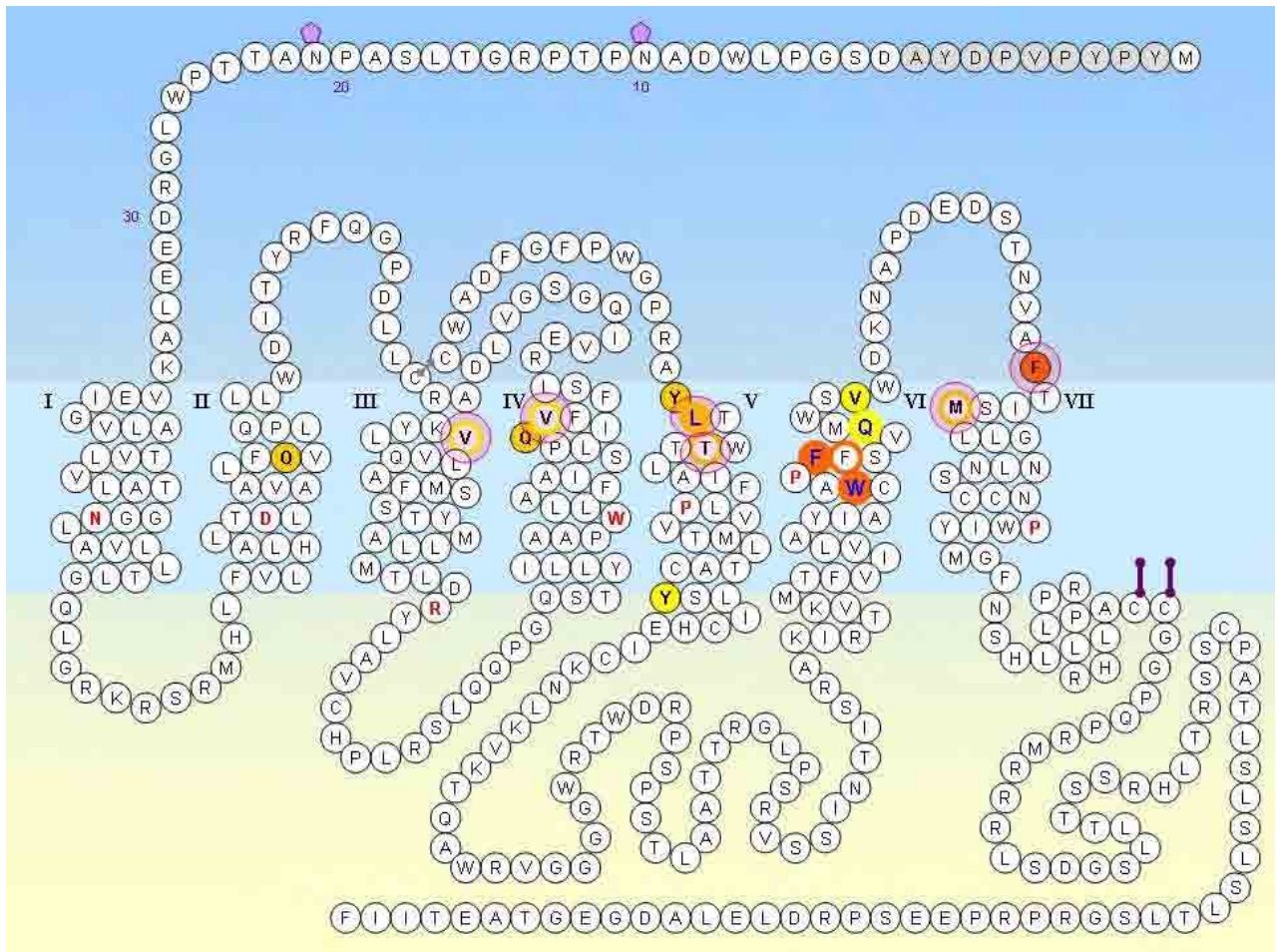


Figure 6.2. The schematic diagram of V_{1b}R highlighting the residues involved in 5234B and SSR149415 binding:

The residues involved in 5234B binding are colour-filled, and the residues involved in SSR149415 binding are circled with coloured lines. Darker the colour, larger the loss of binding affinity observed by Ala substitution or by substituting with the corresponding V_{1a}R residue: > 20-fold decrease in affinity (dark orange); 5 ~ 19 fold decrease in affinity (pale orange); and 2 ~ 4.9 fold decrease in affinity (yellow). Blue bold type indicates residues affecting both antagonists. The residues conferring selectivity between V_{1b}R and V_{1a}R are indicated with pink circle. The HA-epitope tag shown in grey, lavender hexagons indicate location of putative glycosylation sites, purple lines indicate putative palmitoylation sites, and residues in red bold type represents reference residues in Ballesteros-Weinstein numbering scheme.

Chapter 5 explored variations existing within V_{1b}Rs. Firstly, the SNP variants existing in human population were studied. Three SNP variants affecting coding regions thereby resulting in substitutions of Lys⁶⁵Asn, Gly¹⁹¹Arg, and Arg³⁶⁴His, were selected to study. The each SNP variant was reproduced by mutagenesis, and characterised. The SNP variants were shown to bind to AVP and both V_{1b}R-selective non-peptide antagonists, 5234B and SSR149415, with a high affinity. This study identified an enhancement in cell-surface expression of Gly¹⁹¹Arg. A corresponding increase in AVP-induced InsP-InsP₃ signalling by this SNP variant was observed.

In the second section of Chapter 5, inter-species differences of V_{1b}Rs were explored using human and rat V_{1b}Rs. The TM residues which differ between the two species were studied. Using human V_{1b}R as a template, reciprocal mutant constructs were made by introducing a corresponding rat V_{1b}R residue one by one. A slight structural difference was observed in TM4. TM4 of rat V_{1b}R contains Pro^{4.44} instead of Leu in human and Leu^{4.56} instead of Phe in human. The Pro-substitution of Leu^{4.44} in human V_{1b}R resulted in slight increase of binding affinity for both peptide and non-peptide ligands and decreased cell-surface expression. Another substitution of TM4 residue, Phe^{4.56} of human V_{1b}R with the corresponding Leu of rat V_{1b}R, also resulted in reduced cell-surface expression significantly.

To conclude, the results presented in this thesis have addressed some of the structural and functional characteristics of the V_{1b}R, with clinical and therapeutic implications. The results obtained from the investigation of the subtype differences between V_{1b}R and V_{1a}R will provide some useful information for current and future development of subtype-selective ligands for neurohypophysial hormone receptor subtypes. Functional and structural roles of some residues located in the TM domains and the exofacial juxtamembrane region in the V_{1b}R were

established. Certain characteristics of the $V_{1b}R$ described in this thesis may also be applicable to other GPCRs belonging to Family A. Elucidating further functional motifs and the rest of residues involved in agonist or antagonist binding of the $V_{1b}R$ will provide the complete picture of the $V_{1b}R$ functionality in detail.

Possible future studies are proposed at the end of each chapter. In general, a combination of mutagenesis, computational molecular modelling/simulations, and statistical methods, will likely remain as a useful tool in studying receptor pharmacology for a decade or so, but might be with a gradual inclination towards enhanced computing input as information technologies progress and material resources become less abundant. The studies which have been made and ongoing currently in research laboratories of molecular pharmacology and biochemistry will, hopefully one day, provide the full information required for future computational studies with refined outputs of numerical analysis.

References

1. Dale, H.H., *On some physiological actions of ergot*. J Physiol, 1906. **34**(3): p. 163-206.
2. Oliver, G. and E.A. Schafer, *On the Physiological Action of Extracts of Pituitary Body and certain other Glandular Organs: Preliminary Communication*. J Physiol, 1895. **18**(3): p. 277-9.
3. Hawthorn, J., J.M. Graham, and J.S. Jenkins, *Localization of vasopressin in synaptic vesicles of extra-hypothalamic rat brain*. Life Sci, 1984. **35**(3): p. 277-84.
4. de Wied, D., M. Diamant, and M. Fodor, *Central nervous system effects of the neurohypophyseal hormones and related peptides*. Front Neuroendocrinol, 1993. **14**(4): p. 251-302.
5. Sawchenko, P.E. and L.W. Swanson, *Immunohistochemical identification of neurons in the paraventricular nucleus of the hypothalamus that project to the medulla or to the spinal cord in the rat*. J Comp Neurol, 1982. **205**(3): p. 260-72.
6. Cechetto, D.F. and C.B. Saper, *Neurochemical organization of the hypothalamic projection to the spinal cord in the rat*. J Comp Neurol, 1988. **272**(4): p. 579-604.
7. Vandesande, F., K. Dierickx, and J. DeMey, *Identification of the vasopressin-neurophysin producing neurons of the rat suprachiasmatic nuclei*. Cell Tissue Res, 1975. **156**(3): p. 377-80.
8. Tominaga, K., S.I. Inouye, and H. Okamura, *Organotypic slice culture of the rat suprachiasmatic nucleus: sustenance of cellular architecture and circadian rhythm*. Neuroscience, 1994. **59**(4): p. 1025-42.
9. Dai, J., D.F. Swaab, and R.M. Buijs, *Distribution of vasopressin and vasoactive intestinal polypeptide (VIP) fibers in the human hypothalamus with special emphasis on suprachiasmatic nucleus efferent projections*. J Comp Neurol, 1997. **383**(4): p. 397-414.
10. Herman, J.P., D. Adams, and C. Prewitt, *Regulatory changes in neuroendocrine stress-integrative circuitry produced by a variable stress paradigm*. Neuroendocrinology, 1995. **61**(2): p. 180-90.
11. DeVries, G.J., et al., *The vasopressinergic innervation of the brain in normal and castrated rats*. J Comp Neurol, 1985. **233**(2): p. 236-54.
12. Caffé, A.R., et al., *Vasopressin and oxytocin systems in the brain and upper spinal cord of Macaca fascicularis*. J Comp Neurol, 1989. **287**(3): p. 302-25.
13. Miller, M.A., R.T. Zoeller, and D.M. Dorsa, *Detection of vasopressin messenger RNA in cells within the bed nucleus of the stria terminalis by in situ hybridization histochemistry*. Neurosci Lett, 1988. **94**(3): p. 264-8.
14. Rosen, G.J., et al., *Distribution of vasopressin in the forebrain of spotted hyenas*. J Comp Neurol, 2006. **498**(1): p. 80-92.
15. Dutertre, S., et al., *Conopressin-T from Conus tulipa reveals an antagonist switch in vasopressin-like peptides*. J Biol Chem, 2008. **283**(11): p. 7100-8.
16. Park, F., et al., *Localization of the vasopressin V1a and V2 receptors within the renal cortical and medullary circulation*. Am J Physiol, 1997. **273**(1 Pt 2): p. R243-51.
17. Ostrowski, N.L., S.J. Lolait, and W.S. Young, 3rd, *Cellular localization of vasopressin V1a receptor messenger ribonucleic acid in adult male rat brain, pineal, and brain vasculature*. Endocrinology, 1994. **135**(4): p. 1511-28.

18. Sermasi, E., et al., *Intramedullary blood vessels of the spinal cord express V1a vasopressin receptors: visualization by a biotinylated ligand*. Neuroendocrinology, 1995. **62**(6): p. 634-9.
19. Serradeil-Le Gal, C., et al., *Autoradiographic localization of vasopressin V1a receptors in the rat kidney using [3H]-SR 49059*. Kidney Int, 1996. **50**(2): p. 499-505.
20. Vittet, D., et al., *Properties of vasopressin-activated human platelet high affinity GTPase*. Biochem Biophys Res Commun, 1988. **154**(1): p. 213-8.
21. Morel, A., et al., *Molecular cloning and expression of a rat V1a arginine vasopressin receptor*. Nature, 1992. **356**(6369): p. 523-6.
22. Thibonnier, M., et al., *Molecular cloning, sequencing, and functional expression of a cDNA encoding the human V1a vasopressin receptor*. J Biol Chem, 1994. **269**(5): p. 3304-10.
23. Guillon, G., et al., *Vasopressin stimulates steroid secretion in human adrenal glands: comparison with angiotensin-II effect*. Endocrinology, 1995. **136**(3): p. 1285-95.
24. Howl, J. and M. Wheatley, *Hepatic vasopressin receptors (VPRs) exhibit species heterogeneity--absence of VPRs in sheep liver*. Comp Biochem Physiol C, 1993. **105**(2): p. 247-50.
25. Szot, P., T.L. Bale, and D.M. Dorsa, *Distribution of messenger RNA for the vasopressin V1a receptor in the CNS of male and female rats*. Brain Res Mol Brain Res, 1994. **24**(1-4): p. 1-10.
26. Phillips, P.A., et al., *Localization of vasopressin binding sites in rat brain by in vitro autoradiography using a radioiodinated V1 receptor antagonist*. Neuroscience, 1988. **27**(3): p. 749-61.
27. Tribollet, E., et al., *Binding of the non-peptide vasopressin V1a receptor antagonist SR-49059 in the rat brain: an in vitro and in vivo autoradiographic study*. Neuroendocrinology, 1999. **69**(2): p. 113-20.
28. Takemura, M., et al., *Expression and localization of human oxytocin receptor mRNA and its protein in chorion and decidua during parturition*. J Clin Invest, 1994. **93**(6): p. 2319-23.
29. Fuchs, A.R., et al., *Oxytocin and vasopressin receptors in human and uterine myomas during menstrual cycle and early pregnancy*. Hum Reprod Update, 1998. **4**(5): p. 594-604.
30. Wu, W.X., et al., *Characterization of oxytocin receptor expression and distribution in the pregnant sheep uterus*. Endocrinology, 1996. **137**(2): p. 722-8.
31. Fuchs, A.R., et al., *Oxytocin receptors in bovine cervix: distribution and gene expression during the estrous cycle*. Biol Reprod, 1996. **54**(3): p. 700-8.
32. Breton, C., D. Di Scala-Guenot, and H.H. Zingg, *Oxytocin receptor gene expression in rat mammary gland: structural characterization and regulation*. J Mol Endocrinol, 2001. **27**(2): p. 175-89.
33. Gould, B.R. and H.H. Zingg, *Mapping oxytocin receptor gene expression in the mouse brain and mammary gland using an oxytocin receptor-LacZ reporter mouse*. Neuroscience, 2003. **122**(1): p. 155-67.
34. Hansenne, I., et al., *Ontogenesis and functional aspects of oxytocin and vasopressin gene expression in the thymus network*. J Neuroimmunol, 2005. **158**(1-2): p. 67-75.
35. Thibonnier, M., et al., *Human vascular endothelial cells express oxytocin receptors*. Endocrinology, 1999. **140**(3): p. 1301-9.

36. Yoshimura, R., et al., *Localization of oxytocin receptor messenger ribonucleic acid in the rat brain*. *Endocrinology*, 1993. **133**(3): p. 1239-46.
37. Kremarik, P., M.J. Freund-Mercier, and M.E. Stoeckel, *Oxytocin and vasopressin binding sites in the hypothalamus of the rat: histoautoradiographic detection*. *Brain Res Bull*, 1995. **36**(2): p. 195-203.
38. Ostrowski, N.L., *Oxytocin receptor mRNA expression in rat brain: implications for behavioral integration and reproductive success*. *Psychoneuroendocrinology*, 1998. **23**(8): p. 989-1004.
39. Ostrowski, N.L., et al., *Expression of vasopressin V1a and V2 receptor messenger ribonucleic acid in the liver and kidney of embryonic, developing, and adult rats*. *Endocrinology*, 1993. **133**(4): p. 1849-59.
40. Fenton, R.A., et al., *Cellular and subcellular distribution of the type-2 vasopressin receptor in the kidney*. *Am J Physiol Renal Physiol*, 2007. **293**(3): p. F748-60.
41. Hirasawa, A., K. Hashimoto, and G. Tsujimoto, *Distribution and developmental change of vasopressin V1A and V2 receptor mRNA in rats*. *Eur J Pharmacol*, 1994. **267**(1): p. 71-5.
42. Sugimoto, T., et al., *Molecular cloning and functional expression of a cDNA encoding the human V1b vasopressin receptor*. *J Biol Chem*, 1994. **269**(43): p. 27088-92.
43. Grazzini, E., et al., *Molecular and functional characterization of V1b vasopressin receptor in rat adrenal medulla*. *Endocrinology*, 1996. **137**(9): p. 3906-14.
44. Guillon, G., et al., *Vasopressin : a potent autocrine/paracrine regulator of mammal adrenal functions*. *Endocr Res*, 1998. **24**(3-4): p. 703-10.
45. Ventura, M.A., et al., *Gene and cDNA cloning and characterization of the mouse V3/V1b pituitary vasopressin receptor*. *J Mol Endocrinol*, 1999. **22**(3): p. 251-60.
46. Vaccari, C., S.J. Lolait, and N.L. Ostrowski, *Comparative distribution of vasopressin V1b and oxytocin receptor messenger ribonucleic acids in brain*. *Endocrinology*, 1998. **139**(12): p. 5015-33.
47. Hernando, F., et al., *Immunohistochemical localization of the vasopressin V1b receptor in the rat brain and pituitary gland: anatomical support for its involvement in the central effects of vasopressin*. *Endocrinology*, 2001. **142**(4): p. 1659-68.
48. Young, W.S., et al., *The vasopressin 1b receptor is prominent in the hippocampal area CA2 where it is unaffected by restraint stress or adrenalectomy*. *Neuroscience*, 2006. **143**(4): p. 1031-9.
49. Kremarik, P., M.J. Freund-Mercier, and Q.J. Pittman, *Fundus striati vasopressin receptors in blood pressure control*. *Am J Physiol*, 1995. **269**(3 Pt 2): p. R497-503.
50. Cowley, A.W., Jr., *Control of the renal medullary circulation by vasopressin V1 and V2 receptors in the rat*. *Exp Physiol*, 2000. **85 Spec No**: p. 223S-231S.
51. Manning, P.T., et al., *Vasopressin-stimulated release of atriopeptin: endocrine antagonists in fluid homeostasis*. *Science*, 1985. **229**(4711): p. 395-7.
52. Levin, E.R., et al., *Arginine vasopressin stimulates atrial natriuretic peptide gene expression and secretion from rat diencephalic neurons*. *Endocrinology*, 1992. **131**(3): p. 1417-23.
53. Yip, K.P., *Epac mediated Ca²⁺ mobilization and exocytosis in inner medullary collecting duct*. *Am J Physiol Renal Physiol*, 2006.

54. Richardson, S.B., et al., *Effects of vasopressin on insulin secretion and inositol phosphate production in a hamster beta cell line (HIT)*. *Endocrinology*, 1990. **126**(2): p. 1047-52.
55. Folny, V., et al., *Pancreatic vasopressin V1b receptors: characterization in In-R1-G9 cells and localization in human pancreas*. *Am J Physiol Endocrinol Metab*, 2003. **285**(3): p. E566-76.
56. Oshikawa, S., et al., *Vasopressin stimulates insulin release from islet cells through V1b receptors: a combined pharmacological/knockout approach*. *Mol Pharmacol*, 2004. **65**(3): p. 623-9.
57. Fujiwara, Y., et al., *Mutual regulation of vasopressin- and oxytocin-induced glucagon secretion in V1b vasopressin receptor knockout mice*. *J Endocrinol*, 2007. **192**(2): p. 361-9.
58. Gillies, G.E., E.A. Linton, and P.J. Lowry, *Corticotropin releasing activity of the new CRF is potentiated several times by vasopressin*. *Nature*, 1982. **299**(5881): p. 355-7.
59. Bernardini, R., et al., *In vivo and in vitro effects of arginine-vasopressin receptor antagonists on the hypothalamic-pituitary-adrenal axis in the rat*. *Neuroendocrinology*, 1994. **60**(5): p. 503-8.
60. Aguilera, G., *Regulation of pituitary ACTH secretion during chronic stress*. *Front Neuroendocrinol*, 1994. **15**(4): p. 321-50.
61. Watters, J.J., et al., *Evidence for glucocorticoid regulation of the rat vasopressin V1a receptor gene*. *Peptides*, 1996. **17**(1): p. 67-73.
62. Hiroyama, M., et al., *Hypermetabolism of fat in V1a vasopressin receptor knockout mice*. *Mol Endocrinol*, 2007. **21**(1): p. 247-58.
63. Zerbe, R.L., F. Vinicor, and G.L. Robertson, *Plasma vasopressin in uncontrolled diabetes mellitus*. *Diabetes*, 1979. **28**(5): p. 503-8.
64. Aoyagi, T., et al., *Alteration of glucose homeostasis in V1a vasopressin receptor-deficient mice*. *Endocrinology*, 2007. **148**(5): p. 2075-84.
65. Launay, J.M., et al., *V1a-vasopressin specific receptors on human platelets: potentiation by ADP and epinephrine and evidence for homologous down-regulation*. *Thromb Res*, 1987. **45**(4): p. 323-31.
66. Inaba, K., et al., *Characterization of human platelet vasopressin receptor and the relation between vasopressin-induced platelet aggregation and vasopressin binding to platelets*. *Clin Endocrinol (Oxf)*, 1988. **29**(4): p. 377-86.
67. Ghosh, P.M., et al., *Arginine vasopressin stimulates mesangial cell proliferation by activating the epidermal growth factor receptor*. *Am J Physiol Renal Physiol*, 2001. **280**(6): p. F972-9.
68. Jeulin, A.C. and S. Nicolaidis, *Evidence for vasopressin V1 receptors of rostrodienecephalic neurons: iontophoretic studies in the in vivo rat. Responses to oxytocin and to angiotensin*. *Brain Res Bull*, 1988. **20**(6): p. 817-23.
69. Kozniowska, E. and K. Romaniuk, *Vasopressin in vascular regulation and water homeostasis in the brain*. *J Physiol Pharmacol*, 2008. **59 Suppl 8**: p. 109-16.
70. Delville, Y., et al., *Flank-marking behavior and the neural distribution of vasopressin innervation in golden hamsters with suprachiasmatic lesions*. *Behav Neurosci*, 1998. **112**(6): p. 1486-501.

71. Silver, R., et al., *Multiple regulatory elements result in regional specificity in circadian rhythms of neuropeptide expression in mouse SCN*. *Neuroreport*, 1999. **10**(15): p. 3165-74.
72. Young, L.J., et al., *Increased affiliative response to vasopressin in mice expressing the V1a receptor from a monogamous vole*. *Nature*, 1999. **400**(6746): p. 766-8.
73. Bosch, O.J. and I.D. Neumann, *Brain vasopressin is an important regulator of maternal behavior independent of dams' trait anxiety*. *Proc Natl Acad Sci U S A*, 2008. **105**(44): p. 17139-44.
74. Donaldson, Z.R. and L.J. Young, *Oxytocin, vasopressin, and the neurogenetics of sociality*. *Science*, 2008. **322**(5903): p. 900-4.
75. Bielsky, I.F., et al., *The V1a vasopressin receptor is necessary and sufficient for normal social recognition: a gene replacement study*. *Neuron*, 2005. **47**(4): p. 503-13.
76. Landgraf, R., et al., *Viral vector-mediated gene transfer of the vole V1a vasopressin receptor in the rat septum: improved social discrimination and active social behaviour*. *Eur J Neurosci*, 2003. **18**(2): p. 403-11.
77. Egashira, N., et al., *V1a receptor knockout mice exhibit impairment of spatial memory in an eight-arm radial maze*. *Neurosci Lett*, 2004. **356**(3): p. 195-8.
78. Bielsky, I.F., et al., *Profound impairment in social recognition and reduction in anxiety-like behavior in vasopressin V1a receptor knockout mice*. *Neuropsychopharmacology*, 2004. **29**(3): p. 483-93.
79. Ferris, C.F. and Y. Delville, *Vasopressin and serotonin interactions in the control of agonistic behavior*. *Psychoneuroendocrinology*, 1994. **19**(5-7): p. 593-601.
80. Ferris, C.F., et al., *Imaging the neural circuitry and chemical control of aggressive motivation*. *BMC Neurosci*, 2008. **9**: p. 111.
81. Koolhaas, J.M., et al., *Coping with stress in rats and mice: differential peptidergic modulation of the amygdala-lateral septum complex*. *Prog Brain Res*, 1998. **119**: p. 437-48.
82. Albers, H.E., et al., *Role of V1a vasopressin receptors in the control of aggression in Syrian hamsters*. *Brain Res*, 2006. **1073-1074**: p. 425-30.
83. Askew, A., et al., *Food competition and social experience effects on V1a receptor binding in the forebrain of male Long-Evans hooded rats*. *Horm Behav*, 2006. **49**(3): p. 328-36.
84. Cooper, M.A., et al., *Repeated agonistic encounters in hamsters modulate AVP V1a receptor binding*. *Horm Behav*, 2005. **48**(5): p. 545-51.
85. De Vries, G.J., R.M. Buijs, and F.W. Van Leeuwen, *Sex differences in vasopressin and other neurotransmitter systems in the brain*. *Prog Brain Res*, 1984. **61**: p. 185-203.
86. De Vries, G.J. and H.A. al-Shamma, *Sex differences in hormonal responses of vasopressin pathways in the rat brain*. *J Neurobiol*, 1990. **21**(5): p. 686-93.
87. Watters, J.J., P. Poulin, and D.M. Dorsa, *Steroid hormone regulation of vasopressinergic neurotransmission in the central nervous system*. *Prog Brain Res*, 1998. **119**: p. 247-61.
88. Miller, M.A., et al., *Sex differences in vasopressin neurons in the bed nucleus of the stria terminalis by in situ hybridization*. *Peptides*, 1989. **10**(3): p. 615-9.
89. Winslow, J.T., et al., *A role for central vasopressin in pair bonding in monogamous prairie voles*. *Nature*, 1993. **365**(6446): p. 545-8.
90. Insel, T.R., et al., *Oxytocin and the molecular basis of monogamy*. *Adv Exp Med Biol*, 1995. **395**: p. 227-34.

91. Lim, M.M. and L.J. Young, *Vasopressin-dependent neural circuits underlying pair bond formation in the monogamous prairie vole*. *Neuroscience*, 2004. **125**(1): p. 35-45.
92. Pitkow, L.J., et al., *Facilitation of affiliation and pair-bond formation by vasopressin receptor gene transfer into the ventral forebrain of a monogamous vole*. *J Neurosci*, 2001. **21**(18): p. 7392-6.
93. Winslow, J.T. and T.R. Insel, *Neuroendocrine basis of social recognition*. *Curr Opin Neurobiol*, 2004. **14**(2): p. 248-53.
94. Reymond-Marron, I., E. Tribollet, and M. Raggenbass, *The vasopressin-induced excitation of hypoglossal and facial motoneurons in young rats is mediated by V1a but not V1b receptors, and is independent of intracellular calcium signalling*. *Eur J Neurosci*, 2006. **24**(6): p. 1565-74.
95. Ogier, R., et al., *Identified motoneurons involved in sexual and eliminative functions in the rat are powerfully excited by vasopressin and tachykinins*. *J Neurosci*, 2006. **26**(42): p. 10717-26.
96. Liu, X., et al., *Presence of functional vasopressin receptors in spinal ventral horn neurons of young rats: a morphological and electrophysiological study*. *Eur J Neurosci*, 2003. **17**(9): p. 1833-46.
97. Reymond-Marron, I., M. Raggenbass, and M. Zaninetti, *Vasopressin facilitates glycinergic and GABAergic synaptic transmission in developing hypoglossal motoneurons*. *Eur J Neurosci*, 2005. **21**(6): p. 1601-9.
98. Syed, N., C.A. Martens, and W.H. Hsu, *Arginine vasopressin increases glutamate release and intracellular Ca²⁺ concentration in hippocampal and cortical astrocytes through two distinct receptors*. *J Neurochem*, 2007. **103**(1): p. 229-37.
99. Egashira, N., et al., *Disruption of the prepulse inhibition of the startle reflex in vasopressin V1b receptor knockout mice: reversal by antipsychotic drugs*. *Neuropsychopharmacology*, 2005. **30**(11): p. 1996-2005.
100. Honda, K. and Y. Takano, *New topics in vasopressin receptors and approach to novel drugs: involvement of vasopressin V1a and V1b receptors in nociceptive responses and morphine-induced effects*. *J Pharmacol Sci*, 2009. **109**(1): p. 38-43.
101. Brinton, R.E. and R. Gruener, *Vasopressin promotes neurite growth in cultured embryonic neurons*. *Synapse*, 1987. **1**(4): p. 329-34.
102. Clos, J. and J. Gabrion, *A thyroid hormone-vasopressin interaction promotes survival and maturation of hippocampal neurons dissociated postnatally*. *Neurochem Res*, 1989. **14**(10): p. 919-25.
103. Brinton, R.D., A.W. Monreal, and J.G. Fernandez, *Vasopressin-induced neurotrophism in cultured hippocampal neurons via V1 receptor activation*. *J Neurobiol*, 1994. **25**(4): p. 380-94.
104. Ikeda, K., et al., *Neurotrophic effect of angiotensin II, vasopressin and oxytocin on the ventral spinal cord of rat embryo*. *Int J Neurosci*, 1989. **48**(1-2): p. 19-23.
105. Insel, T.R. and L.E. Shapiro, *Oxytocin receptor distribution reflects social organization in monogamous and polygamous voles*. *Proc Natl Acad Sci U S A*, 1992. **89**(13): p. 5981-5.
106. Ferguson, J.N., et al., *Social amnesia in mice lacking the oxytocin gene*. *Nat Genet*, 2000. **25**(3): p. 284-8.

107. Parker, K.J., et al., *Paternal behavior is associated with central neurohormone receptor binding patterns in meadow voles (Microtus pennsylvanicus)*. Behav Neurosci, 2001. **115**(6): p. 1341-8.
108. Champagne, F. and M.J. Meaney, *Like mother, like daughter: evidence for non-genomic transmission of parental behavior and stress responsivity*. Prog Brain Res, 2001. **133**: p. 287-302.
109. Trandafir, C.C., et al., *Participation of vasopressin in the development of cerebral vasospasm in a rat model of subarachnoid haemorrhage*. Clinical and Experimental Pharmacology and Physiology, 2004. **31**(4): p. 261-266.
110. Tachikawa, K., et al., *Altered cardiovascular regulation in arginine vasopressin-overexpressing transgenic rat*. Am J Physiol Endocrinol Metab, 2003. **285**(6): p. E1161-6.
111. Hauptman, P.J., et al., *Comparison of two doses and dosing regimens of tolvaptan in congestive heart failure*. J Cardiovasc Pharmacol, 2005. **46**(5): p. 609-14.
112. Oghlakian, G. and M. Klapholz, *Vasopressin and vasopressin receptor antagonists in heart failure*. Cardiol Rev, 2009. **17**(1): p. 10-5.
113. Spanakis, E., E. Milord, and C. Gragnoli, *AVPR2 variants and mutations in nephrogenic diabetes insipidus: review and missense mutation significance*. J Cell Physiol, 2008. **217**(3): p. 605-17.
114. Quittnat, F. and P. Gross, *Vaptans and the treatment of water-retaining disorders*. Semin Nephrol, 2006. **26**(3): p. 234-43.
115. Green, L., et al., *Oxytocin and autistic disorder: alterations in peptide forms*. Biol Psychiatry, 2001. **50**(8): p. 609-13.
116. Kirsch, P., et al., *Oxytocin modulates neural circuitry for social cognition and fear in humans*. J Neurosci, 2005. **25**(49): p. 11489-93.
117. Modahl, C., et al., *Plasma oxytocin levels in autistic children*. Biol Psychiatry, 1998. **43**(4): p. 270-7.
118. Winslow, J.T. and T.R. Insel, *The social deficits of the oxytocin knockout mouse*. Neuropeptides, 2002. **36**(2-3): p. 221-9.
119. Windle, R.J., et al., *Gonadal steroid modulation of stress-induced hypothalamo-pituitary-adrenal activity and anxiety behavior: role of central oxytocin*. Endocrinology, 2006. **147**(5): p. 2423-31.
120. Scott, L.V. and T.G. Dinan, *Vasopressin and the regulation of hypothalamic-pituitary-adrenal axis function: implications for the pathophysiology of depression*. Life Sci, 1998. **62**(22): p. 1985-98.
121. de Goeij, D.C., et al., *Repeated stress-induced activation of corticotropin-releasing factor neurons enhances vasopressin stores and colocalization with corticotropin-releasing factor in the median eminence of rats*. Neuroendocrinology, 1991. **53**(2): p. 150-9.
122. Volpi, S., C. Rabadan-Diehl, and G. Aguilera, *Vasopressinergic regulation of the hypothalamic pituitary adrenal axis and stress adaptation*. Stress, 2004. **7**(2): p. 75-83.
123. Wersinger, S.R., et al., *Vasopressin V1b receptor knockout reduces aggressive behavior in male mice*. Mol Psychiatry, 2002. **7**(9): p. 975-84.
124. Wersinger, S.R., et al., *Social motivation is reduced in vasopressin 1b receptor null mice despite normal performance in an olfactory discrimination task*. Horm Behav, 2004. **46**(5): p. 638-45.

125. Blanchard, R.J., et al., *AVP V1b selective antagonist SSR149415 blocks aggressive behaviors in hamsters*. Pharmacol Biochem Behav, 2005. **80**(1): p. 189-94.
126. Alonso, R., et al., *Blockade of CRF(1) or V(1b) receptors reverses stress-induced suppression of neurogenesis in a mouse model of depression*. Mol Psychiatry, 2004. **9**(3): p. 278-86, 224.
127. Griebel, G., et al., *Anxiolytic- and antidepressant-like effects of the non-peptide vasopressin V1b receptor antagonist, SSR149415, suggest an innovative approach for the treatment of stress-related disorders*. Proc Natl Acad Sci U S A, 2002. **99**(9): p. 6370-5.
128. Griebel, G., et al., *The vasopressin V1b receptor as a therapeutic target in stress-related disorders*. Curr Drug Targets CNS Neurol Disord, 2003. **2**(3): p. 191-200.
129. Griebel, G., et al., *Non-peptide vasopressin V1b receptor antagonists as potential drugs for the treatment of stress-related disorders*. Curr Pharm Des, 2005. **11**(12): p. 1549-59.
130. Overstreet, D.H. and G. Griebel, *Antidepressant-like effects of CRF1 receptor antagonist SSR125543 in an animal model of depression*. Eur J Pharmacol, 2004. **497**(1): p. 49-53.
131. Serradeil-Le Gal, C., et al., *An overview of SSR149415, a selective nonpeptide vasopressin V(1b) receptor antagonist for the treatment of stress-related disorders*. CNS Drug Rev, 2005. **11**(1): p. 53-68.
132. Stemmelin, J., et al., *Evidence that the lateral septum is involved in the antidepressant-like effects of the vasopressin V1b receptor antagonist, SSR149415*. Neuropsychopharmacology, 2005. **30**(1): p. 35-42.
133. Arnaldi, G., et al., *Vasopressin receptors modulate the pharmacological phenotypes of Cushing's syndrome*. Endocr Res, 1998. **24**(3-4): p. 807-16.
134. Lee, S., et al., *Ectopic expression of vasopressin V1b and V2 receptors in the adrenal glands of familial ACTH-independent macronodular adrenal hyperplasia*. Clin Endocrinol (Oxf), 2005. **63**(6): p. 625-30.
135. Miyamura, N., et al., *A case of ACTH-independent macronodular adrenal hyperplasia: simultaneous expression of several aberrant hormone receptors in the adrenal gland*. Endocr J, 2003. **50**(3): p. 333-40.
136. Daidoh, H., et al., *In vivo and in vitro effects of AVP and V1a receptor antagonist on Cushing's syndrome due to ACTH-independent bilateral macronodular adrenocortical hyperplasia*. Clin Endocrinol (Oxf), 1998. **49**(3): p. 403-9.
137. Lefkowitz, R.J., *Historical review: a brief history and personal retrospective of seven-transmembrane receptors*. Trends Pharmacol Sci, 2004. **25**(8): p. 413-22.
138. George, S.R., B.F. O'Dowd, and S.P. Lee, *G-protein-coupled receptor oligomerization and its potential for drug discovery*. Nat Rev Drug Discov, 2002. **1**(10): p. 808-20.
139. Hawtin, S.R., et al., *Identification of the glycosylation sites utilized on the V1a vasopressin receptor and assessment of their role in receptor signalling and expression*. Biochem J, 2001. **357**(Pt 1): p. 73-81.
140. Kaushal, S., K.D. Ridge, and H.G. Khorana, *Structure and function in rhodopsin: the role of asparagine-linked glycosylation*. Proc Natl Acad Sci U S A, 1994. **91**(9): p. 4024-8.
141. Rands, E., et al., *Mutational analysis of beta-adrenergic receptor glycosylation*. J Biol Chem, 1990. **265**(18): p. 10759-64.

142. Hawtin, S.R., et al., *Palmitoylation of the vasopressin V1a receptor reveals different conformational requirements for signaling, agonist-induced receptor phosphorylation, and sequestration*. J Biol Chem, 2001. **276**(41): p. 38139-46.
143. Marotti, L.A., Jr., et al., *Direct identification of a G protein ubiquitination site by mass spectrometry*. Biochemistry, 2002. **41**(16): p. 5067-74.
144. Roth, A.F. and N.G. Davis, *Ubiquitination of the yeast a-factor receptor*. J Cell Biol, 1996. **134**(3): p. 661-74.
145. Shenoy, S.K., et al., *Regulation of receptor fate by ubiquitination of activated beta 2-adrenergic receptor and beta-arrestin*. Science, 2001. **294**(5545): p. 1307-13.
146. Martin, N.P., R.J. Lefkowitz, and S.K. Shenoy, *Regulation of V2 vasopressin receptor degradation by agonist-promoted ubiquitination*. J Biol Chem, 2003. **278**(46): p. 45954-9.
147. Coleman, D.E., et al., *Structures of active conformations of Gi alpha 1 and the mechanism of GTP hydrolysis*. Science, 1994. **265**(5177): p. 1405-12.
148. Lambright, D.G., et al., *Structural determinants for activation of the alpha-subunit of a heterotrimeric G protein*. Nature, 1994. **369**(6482): p. 621-8.
149. Sondek, J., et al., *GTPase mechanism of Gproteins from the 1.7-A crystal structure of transducin alpha-GDP-AIF-4*. Nature, 1994. **372**(6503): p. 276-9.
150. Wall, M.A., et al., *The structure of the G protein heterotrimer Gi alpha 1 beta 1 gamma 2*. Cell, 1995. **83**(6): p. 1047-58.
151. Camps, M., et al., *Stimulation of phospholipase C by guanine-nucleotide-binding protein beta gamma subunits*. Eur J Biochem, 1992. **206**(3): p. 821-31.
152. Tang, W.J. and A.G. Gilman, *Type-specific regulation of adenylyl cyclase by G protein beta gamma subunits*. Science, 1991. **254**(5037): p. 1500-3.
153. Lotersztajn, S., et al., *Role of G protein beta gamma subunits in the regulation of the plasma membrane Ca²⁺ pump*. J Biol Chem, 1992. **267**(4): p. 2375-9.
154. Logothetis, D.E., et al., *The beta gamma subunits of GTP-binding proteins activate the muscarinic K⁺ channel in heart*. Nature, 1987. **325**(6102): p. 321-6.
155. Higashijima, T., et al., *Effects of Mg²⁺ and the beta gamma-subunit complex on the interactions of guanine nucleotides with G proteins*. J Biol Chem, 1987. **262**(2): p. 762-6.
156. Heithier, H., et al., *Subunit interactions of GTP-binding proteins*. Eur J Biochem, 1992. **204**(3): p. 1169-81.
157. Wess, J., et al., *Structural basis of receptor/G protein coupling selectivity studied with muscarinic receptors as model systems*. Life Sci, 1997. **60**(13-14): p. 1007-14.
158. Hill-Eubanks, D., et al., *Structure of a G-protein-coupling domain of a muscarinic receptor predicted by random saturation mutagenesis*. J Biol Chem, 1996. **271**(6): p. 3058-65.
159. Abell, A.N. and D.L. Segaloff, *Evidence for the direct involvement of transmembrane region 6 of the lutropin/choriogonadotropin receptor in activating Gs*. J Biol Chem, 1997. **272**(23): p. 14586-91.
160. Liu, J. and J. Wess, *Different single receptor domains determine the distinct G protein coupling profiles of members of the vasopressin receptor family*. J Biol Chem, 1996. **271**(15): p. 8772-8.
161. Ulfers, A.L., et al., *Structure of the third intracellular loop of the human cannabinoid 1 receptor*. Biochemistry, 2002. **41**(38): p. 11344-50.

162. Urban, J.D., et al., *Functional selectivity and classical concepts of quantitative pharmacology*. J Pharmacol Exp Ther, 2007. **320**(1): p. 1-13.
163. Cordeaux, Y., et al., *Influence of receptor number on functional responses elicited by agonists acting at the human adenosine A(1) receptor: evidence for signaling pathway-dependent changes in agonist potency and relative intrinsic activity*. Mol Pharmacol, 2000. **58**(5): p. 1075-84.
164. Cabrera-Vera, T.M., et al., *Insights into G protein structure, function, and regulation*. Endocr Rev, 2003. **24**(6): p. 765-81.
165. Milligan, G. and E. Kostenis, *Heterotrimeric G-proteins: a short history*. Br J Pharmacol, 2006. **147 Suppl 1**: p. S46-55.
166. Bauer, P.H., et al., *Phosducin is a protein kinase A-regulated G-protein regulator*. Nature, 1992. **358**(6381): p. 73-6.
167. Danner, S. and M.J. Lohse, *Phosducin is a ubiquitous G-protein regulator*. Proc Natl Acad Sci U S A, 1996. **93**(19): p. 10145-50.
168. Smith, B., et al., *Dual positive and negative regulation of GPCR signaling by GTP hydrolysis*. Cell Signal, 2009. **21**(7): p. 1151-60.
169. Ladds, G., et al., *Regulators of G protein signalling proteins in the human myometrium*. Eur J Pharmacol, 2009. **610**(1-3): p. 23-8.
170. Siderovski, D.P., et al., *A new family of regulators of G-protein-coupled receptors?* Curr Biol, 1996. **6**(2): p. 211-2.
171. Carman, C.V. and J.L. Benovic, *G-protein-coupled receptors: turn-ons and turn-offs*. Curr Opin Neurobiol, 1998. **8**(3): p. 335-44.
172. Pitcher, J.A., et al., *Role of beta gamma subunits of G proteins in targeting the beta-adrenergic receptor kinase to membrane-bound receptors*. Science, 1992. **257**(5074): p. 1264-7.
173. Daaka, Y., et al., *Receptor and G betagamma isoform-specific interactions with G protein-coupled receptor kinases*. Proc Natl Acad Sci U S A, 1997. **94**(6): p. 2180-5.
174. Carman, C.V., et al., *Selective regulation of Galpha(q/11) by an RGS domain in the G protein-coupled receptor kinase, GRK2*. J Biol Chem, 1999. **274**(48): p. 34483-92.
175. Rodriguez-Munoz, M., et al., *RGS14 prevents morphine from internalizing Mu-opioid receptors in periaqueductal gray neurons*. Cell Signal, 2007. **19**(12): p. 2558-71.
176. Nobles, M., A. Benians, and A. Tinker, *Heterotrimeric G proteins precouple with G protein-coupled receptors in living cells*. Proc Natl Acad Sci U S A, 2005. **102**(51): p. 18706-11.
177. Baneres, J.L. and J. Parello, *Structure-based analysis of GPCR function: evidence for a novel pentameric assembly between the dimeric leukotriene B4 receptor BLT1 and the G-protein*. J Mol Biol, 2003. **329**(4): p. 815-29.
178. Ng, G.Y., et al., *Dopamine D2 receptor dimers and receptor-blocking peptides*. Biochem Biophys Res Commun, 1996. **227**(1): p. 200-4.
179. Cvejic, S. and L.A. Devi, *Dimerization of the delta opioid receptor: implication for a role in receptor internalization*. J Biol Chem, 1997. **272**(43): p. 26959-64.
180. Hebert, T.E., et al., *A peptide derived from a beta2-adrenergic receptor transmembrane domain inhibits both receptor dimerization and activation*. J Biol Chem, 1996. **271**(27): p. 16384-92.
181. Zeng, F.Y. and J. Wess, *Identification and molecular characterization of m3 muscarinic receptor dimers*. J Biol Chem, 1999. **274**(27): p. 19487-97.

182. Romano, C., W.L. Yang, and K.L. O'Malley, *Metabotropic glutamate receptor 5 is a disulfide-linked dimer*. J Biol Chem, 1996. **271**(45): p. 28612-6.
183. Jordan, B.A. and L.A. Devi, *G-protein-coupled receptor heterodimerization modulates receptor function*. Nature, 1999. **399**(6737): p. 697-700.
184. Gomes, I., et al., *G protein coupled receptor dimerization: implications in modulating receptor function*. J Mol Med, 2001. **79**(5-6): p. 226-42.
185. Kuner, R., et al., *Role of heteromer formation in GABAB receptor function*. Science, 1999. **283**(5398): p. 74-7.
186. Puett, D., et al., *hCG-receptor binding and transmembrane signaling*. Mol Cell Endocrinol, 1996. **125**(1-2): p. 55-64.
187. Gines, S., et al., *Dopamine D1 and adenosine A1 receptors form functionally interacting heteromeric complexes*. Proc Natl Acad Sci U S A, 2000. **97**(15): p. 8606-11.
188. AbdAlla, S., H. Lother, and U. Quitterer, *AT1-receptor heterodimers show enhanced G-protein activation and altered receptor sequestration*. Nature, 2000. **407**(6800): p. 94-8.
189. Young, S.F., C. Griffante, and G. Aguilera, *Dimerization between vasopressin V1b and corticotropin releasing hormone type 1 receptors*. Cell Mol Neurobiol, 2007. **27**(4): p. 439-61.
190. Mikhailova, M.V., et al., *Heterooligomerization between vasotocin and corticotropin-releasing hormone (CRH) receptors augments CRH-stimulated 3',5'-cyclic adenosine monophosphate production*. Mol Endocrinol, 2007. **21**(9): p. 2178-88.
191. Terrillon, S., et al., *Oxytocin and vasopressin V1a and V2 receptors form constitutive homo- and heterodimers during biosynthesis*. Mol Endocrinol, 2003. **17**(4): p. 677-91.
192. Bulenger, S., S. Marullo, and M. Bouvier, *Emerging role of homo- and heterodimerization in G-protein-coupled receptor biosynthesis and maturation*. Trends Pharmacol Sci, 2005. **26**(3): p. 131-7.
193. Kroeger, K.M., K.D. Pflieger, and K.A. Eidne, *G-protein coupled receptor oligomerization in neuroendocrine pathways*. Front Neuroendocrinol, 2003. **24**(4): p. 254-78.
194. Thevenin, D., et al., *Oligomerization of the fifth transmembrane domain from the adenosine A2A receptor*. Protein Sci, 2005. **14**(8): p. 2177-86.
195. Kunishima, N., et al., *Structural basis of glutamate recognition by a dimeric metabotropic glutamate receptor*. Nature, 2000. **407**(6807): p. 971-7.
196. Tateyama, M., et al., *Ligand-induced rearrangement of the dimeric metabotropic glutamate receptor 1alpha*. Nat Struct Mol Biol, 2004. **11**(7): p. 637-42.
197. Fan, Q.R. and W.A. Hendrickson, *Structure of human follicle-stimulating hormone in complex with its receptor*. Nature, 2005. **433**(7023): p. 269-77.
198. Salom, D., et al., *Crystal structure of a photoactivated deprotonated intermediate of rhodopsin*. Proc Natl Acad Sci U S A, 2006. **103**(44): p. 16123-8.
199. Guo, W., et al., *Crosstalk in G protein-coupled receptors: changes at the transmembrane homodimer interface determine activation*. Proc Natl Acad Sci U S A, 2005. **102**(48): p. 17495-500.
200. Torvinen, M., et al., *Adenosine A2A receptor and dopamine D3 receptor interactions: evidence of functional A2A/D3 heteromeric complexes*. Mol Pharmacol, 2005. **67**(2): p. 400-7.
201. McLatchie, L.M., et al., *RAMPs regulate the transport and ligand specificity of the calcitonin-receptor-like receptor*. Nature, 1998. **393**(6683): p. 333-9.

202. Hay, D.L., et al., *The pharmacology of CGRP-responsive receptors in cultured and transfected cells*. Peptides, 2004. **25**(11): p. 2019-26.
203. James, J.R., et al., *A rigorous experimental framework for detecting protein oligomerization using bioluminescence resonance energy transfer*. Nat Methods, 2006. **3**(12): p. 1001-6.
204. Seta, K., et al., *AT1 receptor mutant lacking heterotrimeric G protein coupling activates the Src-Ras-ERK pathway without nuclear translocation of ERKs*. J Biol Chem, 2002. **277**(11): p. 9268-77.
205. Shenoy, S.K., et al., *beta-arrestin-dependent, G protein-independent ERK1/2 activation by the beta2 adrenergic receptor*. J Biol Chem, 2006. **281**(2): p. 1261-73.
206. Charest, P.G., et al., *The V2 vasopressin receptor stimulates ERK1/2 activity independently of heterotrimeric G protein signalling*. Cell Signal, 2007. **19**(1): p. 32-41.
207. Gesty-Palmer, D., et al., *Distinct beta-arrestin- and G protein-dependent pathways for parathyroid hormone receptor-stimulated ERK1/2 activation*. J Biol Chem, 2006. **281**(16): p. 10856-64.
208. Brakeman, P.R., et al., *Homer: a protein that selectively binds metabotropic glutamate receptors*. Nature, 1997. **386**(6622): p. 284-8.
209. Oldenhof, J., et al., *SH3 binding domains in the dopamine D4 receptor*. Biochemistry, 1998. **37**(45): p. 15726-36.
210. Hall, R.A., et al., *A C-terminal motif found in the beta2-adrenergic receptor, P2Y1 receptor and cystic fibrosis transmembrane conductance regulator determines binding to the Na⁺/H⁺ exchanger regulatory factor family of PDZ proteins*. Proc Natl Acad Sci U S A, 1998. **95**(15): p. 8496-501.
211. Tang, Y., et al., *Identification of the endophilins (SH3p4/p8/p13) as novel binding partners for the beta1-adrenergic receptor*. Proc Natl Acad Sci U S A, 1999. **96**(22): p. 12559-64.
212. Cao, W., et al., *Direct binding of activated c-Src to the beta 3-adrenergic receptor is required for MAP kinase activation*. J Biol Chem, 2000. **275**(49): p. 38131-4.
213. Bouvier, M., et al., *Removal of phosphorylation sites from the beta 2-adrenergic receptor delays onset of agonist-promoted desensitization*. Nature, 1988. **333**(6171): p. 370-3.
214. Hausdorff, W.P., et al., *Phosphorylation sites on two domains of the beta 2-adrenergic receptor are involved in distinct pathways of receptor desensitization*. J Biol Chem, 1989. **264**(21): p. 12657-65.
215. Lohse, M.J., et al., *Multiple pathways of rapid beta 2-adrenergic receptor desensitization. Delineation with specific inhibitors*. J Biol Chem, 1990. **265**(6): p. 3202-11.
216. Lohse, M.J., et al., *beta-Arrestin: a protein that regulates beta-adrenergic receptor function*. Science, 1990. **248**(4962): p. 1547-50.
217. Goodman, O.B., Jr., et al., *Beta-arrestin acts as a clathrin adaptor in endocytosis of the beta2-adrenergic receptor*. Nature, 1996. **383**(6599): p. 447-50.
218. Ahn, S., et al., *Src-mediated tyrosine phosphorylation of dynamin is required for beta2-adrenergic receptor internalization and mitogen-activated protein kinase signaling*. J Biol Chem, 1999. **274**(3): p. 1185-8.

219. Doss, R.C., J.P. Perkins, and T.K. Harden, *Recovery of beta-adrenergic receptors following long term exposure of astrocytoma cells to catecholamine. Role of protein synthesis.* J Biol Chem, 1981. **256**(23): p. 12281-6.
220. Hadcock, J.R. and C.C. Malbon, *Down-regulation of beta-adrenergic receptors: agonist-induced reduction in receptor mRNA levels.* Proc Natl Acad Sci U S A, 1988. **85**(14): p. 5021-5.
221. Valiquette, M., et al., *Involvement of tyrosine residues located in the carboxyl tail of the human beta 2-adrenergic receptor in agonist-induced down-regulation of the receptor.* Proc Natl Acad Sci U S A, 1990. **87**(13): p. 5089-93.
222. Valiquette, M., et al., *Mutation of tyrosine-141 inhibits insulin-promoted tyrosine phosphorylation and increased responsiveness of the human beta 2-adrenergic receptor.* EMBO J, 1995. **14**(22): p. 5542-9.
223. Luttrell, L.M. and R.J. Lefkowitz, *The role of beta-arrestins in the termination and transduction of G-protein-coupled receptor signals.* J Cell Sci, 2002. **115**(Pt 3): p. 455-65.
224. Kohout, T.A. and R.J. Lefkowitz, *Regulation of G protein-coupled receptor kinases and arrestins during receptor desensitization.* Mol Pharmacol, 2003. **63**(1): p. 9-18.
225. Hein, L., et al., *Intracellular trafficking of angiotensin II and its AT1 and AT2 receptors: evidence for selective sorting of receptor and ligand.* Mol Endocrinol, 1997. **11**(9): p. 1266-77.
226. Tarasova, N.I., et al., *Endocytosis of gastrin in cancer cells expressing gastrin/CCK-B receptor.* Cell Tissue Res, 1997. **287**(2): p. 325-33.
227. Anborgh, P.H., et al., *Receptor/beta-arrestin complex formation and the differential trafficking and resensitization of beta2-adrenergic and angiotensin II type 1A receptors.* Mol Endocrinol, 2000. **14**(12): p. 2040-53.
228. Smit, M.J., et al., *Inverse agonism of histamine H2 antagonist accounts for upregulation of spontaneously active histamine H2 receptors.* Proc Natl Acad Sci U S A, 1996. **93**(13): p. 6802-7.
229. Wilder-Smith, C.H., et al., *Tolerance to oral H2-receptor antagonists.* Dig Dis Sci, 1990. **35**(8): p. 976-83.
230. Deakin, M. and J.G. Williams, *Histamine H2-receptor antagonists in peptic ulcer disease. Efficacy in healing peptic ulcers.* Drugs, 1992. **44**(5): p. 709-19.
231. Claing, A., et al., *Endocytosis of G protein-coupled receptors: roles of G protein-coupled receptor kinases and beta-arrestin proteins.* Prog Neurobiol, 2002. **66**(2): p. 61-79.
232. Hill, A.V., *The mode of action of nicotine and curari, determined by the form of the contraction curve and the method of temperature coefficients.* J Physiol, 1909. **39**(5): p. 361-73.
233. Langmuir, I., *The evaporation of small spheres.* Physical Review, 1918. **12**(5): p. 368-370.
234. Clark, A.J., *Discussion on the chemical and physical basis of pharmacological action, 12 November, 1936 - Opening address.* Proceedings of the Royal Society of London Series B-Biological Sciences, 1937. **121**(825): p. 580-609.
235. Stephenson, R.P., *Modification of Receptor Theory.* British Journal of Pharmacology and Chemotherapy, 1956. **11**(4): p. 379-393.

236. Del Castillo, J. and B. Katz, *Interaction at end-plate receptors between different choline derivatives*. Proc R Soc Lond B Biol Sci, 1957. **146**(924): p. 369-81.
237. Burgen, A.S., *Conformational changes and drug action*. Fed Proc, 1981. **40**(13): p. 2723-8.
238. Bond, R.A., et al., *Physiological effects of inverse agonists in transgenic mice with myocardial overexpression of the beta 2-adrenoceptor*. Nature, 1995. **374**(6519): p. 272-6.
239. Ehlert, F.J., *The relationship between muscarinic receptor occupancy and adenylate cyclase inhibition in the rabbit myocardium*. Mol Pharmacol, 1985. **28**(5): p. 410-21.
240. De Lean, A., J.M. Stadel, and R.J. Lefkowitz, *A ternary complex model explains the agonist-specific binding properties of the adenylate cyclase-coupled beta-adrenergic receptor*. J Biol Chem, 1980. **255**(15): p. 7108-17.
241. Samama, P., et al., *A mutation-induced activated state of the beta 2-adrenergic receptor. Extending the ternary complex model*. J Biol Chem, 1993. **268**(7): p. 4625-36.
242. Weiss, J.M., et al., *The cubic ternary complex receptor-occupancy model. III. resurrecting efficacy*. J Theor Biol, 1996. **181**(4): p. 381-97.
243. Leff, P., et al., *A three-state receptor model of agonist action*. Trends Pharmacol Sci, 1997. **18**(10): p. 355-62.
244. Schwartz, T.W., et al., *Molecular mechanism of 7TM receptor activation--a global toggle switch model*. Annu Rev Pharmacol Toxicol, 2006. **46**: p. 481-519.
245. Kenakin, T., *Agonist-receptor efficacy. II. Agonist trafficking of receptor signals*. Trends Pharmacol Sci, 1995. **16**(7): p. 232-8.
246. Neubig, R.R., et al., *International Union of Pharmacology Committee on Receptor Nomenclature and Drug Classification. XXXVIII. Update on terms and symbols in quantitative pharmacology*. Pharmacol Rev, 2003. **55**(4): p. 597-606.
247. Daniels, D.V., et al., *Human cloned alpha1A-adrenoceptor isoforms display alpha1L-adrenoceptor pharmacology in functional studies*. Eur J Pharmacol, 1999. **370**(3): p. 337-43.
248. Kenakin, T., *G-protein coupled receptors as allosteric machines*. Receptors Channels, 2004. **10**(2): p. 51-60.
249. Blue, D.R., et al., *Pharmacological characteristics of Ro 115-1240, a selective alpha1A/1L-adrenoceptor partial agonist: a potential therapy for stress urinary incontinence*. BJU Int, 2004. **93**(1): p. 162-70.
250. Baker, J.G., I.P. Hall, and S.J. Hill, *Agonist actions of "beta-blockers" provide evidence for two agonist activation sites or conformations of the human beta1-adrenoceptor*. Mol Pharmacol, 2003. **63**(6): p. 1312-21.
251. Pak, M.D. and P.H. Fishman, *Anomalous behavior of CGP 12177A on beta 1-adrenergic receptors*. J Recept Signal Transduct Res, 1996. **16**(1-2): p. 1-23.
252. Konkar, A.A., Y. Zhai, and J.G. Granneman, *beta1-adrenergic receptors mediate beta3-adrenergic-independent effects of CGP 12177 in brown adipose tissue*. Mol Pharmacol, 2000. **57**(2): p. 252-8.
253. Lowe, M.D., et al., *Comparison of the affinity of beta-blockers for two states of the beta 1-adrenoceptor in ferret ventricular myocardium*. Br J Pharmacol, 2002. **135**(2): p. 451-61.

254. Joseph, S.S., et al., *Binding of (-)-[3H]-CGP12177 at two sites in recombinant human beta 1-adrenoceptors and interaction with beta-blockers*. Naunyn Schmiedebergs Arch Pharmacol, 2004. **369**(5): p. 525-32.
255. Baker, J.G., *The selectivity of beta-adrenoceptor antagonists at the human beta1, beta2 and beta3 adrenoceptors*. Br J Pharmacol, 2005. **144**(3): p. 317-22.
256. Schild, H.O., *Pax and Competitive Drug Antagonism*. British Journal of Pharmacology and Chemotherapy, 1949. **4**(3): p. 277-280.
257. Nelson, C.P. and R.A. Challiss, *"Phenotypic" pharmacology: the influence of cellular environment on G protein-coupled receptor antagonist and inverse agonist pharmacology*. Biochem Pharmacol, 2007. **73**(6): p. 737-51.
258. Baker, J.G. and S.J. Hill, *Multiple GPCR conformations and signalling pathways: implications for antagonist affinity estimates*. Trends Pharmacol Sci, 2007. **28**(8): p. 374-81.
259. Niswender, C.M., et al., *RNA editing of the human serotonin 5-hydroxytryptamine 2C receptor silences constitutive activity*. J Biol Chem, 1999. **274**(14): p. 9472-8.
260. Cadet, P., *Mu opiate receptor subtypes*. Med Sci Monit, 2004. **10**(6): p. MS28-32.
261. Gentles, A.J. and S. Karlin, *Why are human G-protein-coupled receptors predominantly intronless?* Trends Genet, 1999. **15**(2): p. 47-9.
262. Baker, J.G., I.P. Hall, and S.J. Hill, *Influence of agonist efficacy and receptor phosphorylation on antagonist affinity measurements: differences between second messenger and reporter gene responses*. Mol Pharmacol, 2003. **64**(3): p. 679-88.
263. Waldhoer, M., et al., *A heterodimer-selective agonist shows in vivo relevance of G protein-coupled receptor dimers*. Proc Natl Acad Sci U S A, 2005. **102**(25): p. 9050-5.
264. Born, W., R. Muff, and J.A. Fischer, *Functional interaction of G protein-coupled receptors of the adrenomedullin peptide family with accessory receptor-activity-modifying proteins (RAMP)*. Microsc Res Tech, 2002. **57**(1): p. 14-22.
265. Armour, S.L., et al., *Pharmacological characterization of receptor-activity-modifying proteins (RAMPs) and the human calcitonin receptor*. J Pharmacol Toxicol Methods, 1999. **42**(4): p. 217-24.
266. Cussac, D., et al., *Differential activation of Gq/11 and Gi(3) proteins at 5-hydroxytryptamine(2C) receptors revealed by antibody capture assays: influence of receptor reserve and relationship to agonist-directed trafficking*. Mol Pharmacol, 2002. **62**(3): p. 578-89.
267. Cordeaux, Y., A.P. Ijzerman, and S.J. Hill, *Coupling of the human A1 adenosine receptor to different heterotrimeric G proteins: evidence for agonist-specific G protein activation*. Br J Pharmacol, 2004. **143**(6): p. 705-14.
268. Baker, J.G. and S.J. Hill, *A comparison of the antagonist affinities for the Gi- and Gs-coupled states of the human adenosine A1-receptor*. J Pharmacol Exp Ther, 2007. **320**(1): p. 218-28.
269. Chini, B. and M. Manning, *Agonist selectivity in the oxytocin/vasopressin receptor family: new insights and challenges*. Biochem Soc Trans, 2007. **35**(Pt 4): p. 737-41.
270. Azzi, M., et al., *Beta-arrestin-mediated activation of MAPK by inverse agonists reveals distinct active conformations for G protein-coupled receptors*. Proc Natl Acad Sci U S A, 2003. **100**(20): p. 11406-11.

271. Baker, J.G., I.P. Hall, and S.J. Hill, *Agonist and inverse agonist actions of beta-blockers at the human beta 2-adrenoceptor provide evidence for agonist-directed signaling*. Mol Pharmacol, 2003. **64**(6): p. 1357-69.
272. Toya, Y., et al., *Inhibition of adenylyl cyclase by caveolin peptides*. Endocrinology, 1998. **139**(4): p. 2025-31.
273. Oka, N., et al., *Caveolin interaction with protein kinase C. Isoenzyme-dependent regulation of kinase activity by the caveolin scaffolding domain peptide*. J Biol Chem, 1997. **272**(52): p. 33416-21.
274. Engelman, J.A., et al., *Caveolin-mediated regulation of signaling along the p42/44 MAP kinase cascade in vivo. A role for the caveolin-scaffolding domain*. FEBS Lett, 1998. **428**(3): p. 205-11.
275. Carman, C.V., M.P. Lisanti, and J.L. Benovic, *Regulation of G protein-coupled receptor kinases by caveolin*. J Biol Chem, 1999. **274**(13): p. 8858-64.
276. Razani, B., C.S. Rubin, and M.P. Lisanti, *Regulation of cAMP-mediated signal transduction via interaction of caveolins with the catalytic subunit of protein kinase A*. J Biol Chem, 1999. **274**(37): p. 26353-60.
277. Li, L., et al., *Caveolin-1 maintains activated Akt in prostate cancer cells through scaffolding domain binding site interactions with and inhibition of serine/threonine protein phosphatases PP1 and PP2A*. Mol Cell Biol, 2003. **23**(24): p. 9389-404.
278. Zuluaga, S., et al., *Negative regulation of Akt activity by p38alpha MAP kinase in cardiomyocytes involves membrane localization of PP2A through interaction with caveolin-1*. Cell Signal, 2007. **19**(1): p. 62-74.
279. Peters, P.J., et al., *Trafficking of prion proteins through a caveolae-mediated endosomal pathway*. J Cell Biol, 2003. **162**(4): p. 703-17.
280. Wyse, B.D., et al., *Caveolin interacts with the angiotensin II type I receptor during exocytic transport but not at the plasma membrane*. J Biol Chem, 2003. **278**(26): p. 23738-46.
281. Ostrom, R.S. and P.A. Insel, *The evolving role of lipid rafts and caveolae in G protein-coupled receptor signaling: implications for molecular pharmacology*. Br J Pharmacol, 2004. **143**(2): p. 235-45.
282. Ostrom, R.S., et al., *Localization of adenylyl cyclase isoforms and G protein-coupled receptors in vascular smooth muscle cells: expression in caveolin-rich and noncaveolin domains*. Mol Pharmacol, 2002. **62**(5): p. 983-92.
283. Gimpl, G., K. Burger, and F. Fahrenholz, *Cholesterol as modulator of receptor function*. Biochemistry, 1997. **36**(36): p. 10959-74.
284. Gimpl, G. and F. Fahrenholz, *Human oxytocin receptors in cholesterol-rich vs. cholesterol-poor microdomains of the plasma membrane*. Eur J Biochem, 2000. **267**(9): p. 2483-97.
285. Ballesteros, J.A. and H. Weinstein, *Analysis and refinement of criteria for predicting the structure and relative orientations of transmembranal helical domains*. Biophys J, 1992. **62**(1): p. 107-9.
286. Palczewski, K., et al., *Crystal structure of rhodopsin: A G protein-coupled receptor*. Science, 2000. **289**(5480): p. 739-45.
287. Okada, T., et al., *Functional role of internal water molecules in rhodopsin revealed by X-ray crystallography*. Proc Natl Acad Sci U S A, 2002. **99**(9): p. 5982-7.

288. Szundi, I., et al., *Rhodopsin photointermediates in two-dimensional crystals at physiological temperatures*. *Biochemistry*, 2006. **45**(15): p. 4974-82.
289. Rosenbaum, D.M., et al., *GPCR engineering yields high-resolution structural insights into beta2-adrenergic receptor function*. *Science*, 2007. **318**(5854): p. 1266-73.
290. Rasmussen, S.G., et al., *Crystal structure of the human beta2 adrenergic G-protein-coupled receptor*. *Nature*, 2007. **450**(7168): p. 383-7.
291. Cherezov, V., et al., *High-resolution crystal structure of an engineered human beta2-adrenergic G protein-coupled receptor*. *Science*, 2007. **318**(5854): p. 1258-65.
292. Jaakola, V.P., et al., *The 2.6 angstrom crystal structure of a human A2A adenosine receptor bound to an antagonist*. *Science*, 2008. **322**(5905): p. 1211-7.
293. Warne, T., et al., *Structure of a beta1-adrenergic G-protein-coupled receptor*. *Nature*, 2008. **454**(7203): p. 486-91.
294. Park, J.H., et al., *Crystal structure of the ligand-free G-protein-coupled receptor opsin*. *Nature*, 2008. **454**(7201): p. 183-7.
295. Scheerer, P., et al., *Crystal structure of opsin in its G-protein-interacting conformation*. *Nature*, 2008. **455**(7212): p. 497-502.
296. Teller, D.C., et al., *Advances in determination of a high-resolution three-dimensional structure of rhodopsin, a model of G-protein-coupled receptors (GPCRs)*. *Biochemistry*, 2001. **40**(26): p. 7761-72.
297. Barak, L.S., et al., *The conserved seven-transmembrane sequence NP(X)2,3Y of the G-protein-coupled receptor superfamily regulates multiple properties of the beta 2-adrenergic receptor*. *Biochemistry*, 1995. **34**(47): p. 15407-14.
298. Conner, A.C., et al., *Ligand binding and activation of the CGRP receptor*. *Biochem Soc Trans*, 2007. **35**(Pt 4): p. 729-32.
299. Eilers, M., et al., *Comparison of class A and D G protein-coupled receptors: common features in structure and activation*. *Biochemistry*, 2005. **44**(25): p. 8959-75.
300. Demene, H., et al., *Active peptidic mimics of the second intracellular loop of the V(1A) vasopressin receptor are structurally related to the second intracellular rhodopsin loop: a combined 1H NMR and biochemical study*. *Biochemistry*, 2003. **42**(27): p. 8204-13.
301. Thevenin, D., et al., *Identifying interactions between transmembrane helices from the adenosine A2A receptor*. *Biochemistry*, 2005. **44**(49): p. 16239-45.
302. Gallivan, J.P. and D.A. Dougherty, *Cation-pi interactions in structural biology*. *Proc Natl Acad Sci U S A*, 1999. **96**(17): p. 9459-64.
303. Gromiha, M.M., C. Santhosh, and S. Ahmad, *Structural analysis of cation-pi interactions in DNA binding proteins*. *Int J Biol Macromol*, 2004. **34**(3): p. 203-11.
304. Gromiha, M.M., *Influence of cation-pi interactions in different folding types of membrane proteins*. *Biophys Chem*, 2003. **103**(3): p. 251-8.
305. Gromiha, M.M., S. Thomas, and C. Santhosh, *Role of cation-pi interactions to the stability of thermophilic proteins*. *Prep Biochem Biotechnol*, 2002. **32**(4): p. 355-62.
306. Rosenbaum, D.M., S.G. Rasmussen, and B.K. Kobilka, *The structure and function of G-protein-coupled receptors*. *Nature*, 2009. **459**(7245): p. 356-63.
307. Okada, T., et al., *The retinal conformation and its environment in rhodopsin in light of a new 2.2 Å crystal structure*. *J Mol Biol*, 2004. **342**(2): p. 571-83.
308. Li, J., et al., *Structure of bovine rhodopsin in a trigonal crystal form*. *J Mol Biol*, 2004. **343**(5): p. 1409-38.

309. Ballesteros, J., et al., *Functional microdomains in G-protein-coupled receptors. The conserved arginine-cage motif in the gonadotropin-releasing hormone receptor*. J Biol Chem, 1998. **273**(17): p. 10445-53.
310. Rasmussen, S.G., et al., *Mutation of a highly conserved aspartic acid in the beta2 adrenergic receptor: constitutive activation, structural instability, and conformational rearrangement of transmembrane segment 6*. Mol Pharmacol, 1999. **56**(1): p. 175-84.
311. Vogel, R., et al., *Functional Role of the "Ionic Lock"-An Interhelical Hydrogen-Bond Network in Family A Heptahelical Receptors*. J Mol Biol, 2008.
312. Ballesteros, J.A., L. Shi, and J.A. Javitch, *Structural mimicry in G protein-coupled receptors: implications of the high-resolution structure of rhodopsin for structure-function analysis of rhodopsin-like receptors*. Mol Pharmacol, 2001. **60**(1): p. 1-19.
313. Baldwin, J.M., G.F. Schertler, and V.M. Unger, *An alpha-carbon template for the transmembrane helices in the rhodopsin family of G-protein-coupled receptors*. J Mol Biol, 1997. **272**(1): p. 144-64.
314. Farrens, D.L., et al., *Requirement of rigid-body motion of transmembrane helices for light activation of rhodopsin*. Science, 1996. **274**(5288): p. 768-70.
315. Gether, U., et al., *Agonists induce conformational changes in transmembrane domains III and VI of the beta2 adrenoceptor*. Embo J, 1997. **16**(22): p. 6737-47.
316. Jensen, A.D., et al., *Agonist-induced conformational changes at the cytoplasmic side of transmembrane segment 6 in the beta 2 adrenergic receptor mapped by site-selective fluorescent labeling*. J Biol Chem, 2001. **276**(12): p. 9279-90.
317. Shi, L., et al., *Beta2 adrenergic receptor activation. Modulation of the proline kink in transmembrane 6 by a rotamer toggle switch*. J Biol Chem, 2002. **277**(43): p. 40989-96.
318. Schwartz, T.W. and M.M. Rosenkilde, *Is there a 'lock' for all agonist 'keys' in 7TM receptors?* Trends Pharmacol Sci, 1996. **17**(6): p. 213-6.
319. Singh, R., et al., *Activation of the cannabinoid CB1 receptor may involve a W648/F336 rotamer toggle switch*. J Pept Res, 2002. **60**(6): p. 357-70.
320. Mukhopadhyay, S., et al., *Regulation of Gi by the CB1 cannabinoid receptor C-terminal juxtamembrane region: structural requirements determined by peptide analysis*. Biochemistry, 1999. **38**(11): p. 3447-55.
321. Mukhopadhyay, S., et al., *The CB(1) cannabinoid receptor juxtamembrane C-terminal peptide confers activation to specific G proteins in brain*. Mol Pharmacol, 2000. **57**(1): p. 162-70.
322. Beck, K. and B. Brodsky, *Supercoiled protein motifs: the collagen triple-helix and the alpha-helical coiled coil*. J Struct Biol, 1998. **122**(1-2): p. 17-29.
323. Pardo, L., et al., *The role of internal water molecules in the structure and function of the rhodopsin family of G protein-coupled receptors*. Chembiochem, 2007. **8**(1): p. 19-24.
324. Rubenstein, L.A., R.J. Zauhar, and R.G. Lanzara, *Molecular dynamics of a biophysical model for beta(2)-adrenergic and G protein-coupled receptor activation*. J Mol Graph Model, 2006.
325. Lin, S.W. and T.P. Sakmar, *Specific tryptophan UV-absorbance changes are probes of the transition of rhodopsin to its active state*. Biochemistry, 1996. **35**(34): p. 11149-59.
326. Crocker, E., et al., *Location of Trp265 in metarhodopsin II: implications for the activation mechanism of the visual receptor rhodopsin*. J Mol Biol, 2006. **357**(1): p. 163-72.

327. Patel, A.B., et al., *Changes in interhelical hydrogen bonding upon rhodopsin activation*. J Mol Biol, 2005. **347**(4): p. 803-12.
328. Han, S.J., et al., *Identification of an agonist-induced conformational change occurring adjacent to the ligand-binding pocket of the M(3) muscarinic acetylcholine receptor*. J Biol Chem, 2005. **280**(41): p. 34849-58.
329. Han, S.J., et al., *Pronounced conformational changes following agonist activation of the M(3) muscarinic acetylcholine receptor*. J Biol Chem, 2005. **280**(26): p. 24870-9.
330. Ahuja, S., et al., *Helix movement is coupled to displacement of the second extracellular loop in rhodopsin activation*. Nat Struct Mol Biol, 2009. **16**(2): p. 168-75.
331. Nygaard, R., et al., *Ligand binding and micro-switches in 7TM receptor structures*. Trends Pharmacol Sci, 2009. **30**(5): p. 249-59.
332. Lolait, S.J., et al., *Cloning and characterization of a vasopressin V2 receptor and possible link to nephrogenic diabetes insipidus*. Nature, 1992. **357**(6376): p. 336-9.
333. Hirasawa, A., et al., *Cloning, functional expression and tissue distribution of human cDNA for the vascular-type vasopressin receptor*. Biochem Biophys Res Commun, 1994. **203**(1): p. 72-9.
334. Thibonnier, M., et al., *The human V3 pituitary vasopressin receptor: ligand binding profile and density-dependent signaling pathways*. Endocrinology, 1997. **138**(10): p. 4109-22.
335. Abel, A., et al., *Cell cycle-dependent coupling of the vasopressin V1a receptor to different G proteins*. J Biol Chem, 2000. **275**(42): p. 32543-51.
336. Terrillon, S., C. Barberis, and M. Bouvier, *Heterodimerization of V1a and V2 vasopressin receptors determines the interaction with beta-arrestin and their trafficking patterns*. Proc Natl Acad Sci U S A, 2004. **101**(6): p. 1548-53.
337. Albizu, L., et al., *Probing the existence of G protein-coupled receptor dimers by positive and negative ligand-dependent cooperative binding*. Mol Pharmacol, 2006. **70**(5): p. 1783-91.
338. Devost, D. and H.H. Zingg, *Homo- and hetero-dimeric complex formations of the human oxytocin receptor*. J Neuroendocrinol, 2004. **16**(4): p. 372-7.
339. Manning, M., et al., *Design of potent and selective linear antagonists of vasopressor (V1-receptor) responses to vasopressin*. J Med Chem, 1990. **33**(11): p. 3079-86.
340. Jard, S., et al., *Vasopressin receptors from cultured mesangial cells resemble V1a type*. Am J Physiol, 1987. **253**(1 Pt 2): p. F41-9.
341. Sawyer, W.H., et al., *Cyclic and linear vasopressin V1 and V1/V2 antagonists containing arginine in the 4-position*. Experientia, 1991. **47**(1): p. 83-6.
342. Schmidt, A., et al., *A radioiodinated linear vasopressin antagonist: a ligand with high affinity and specificity for V1a receptors*. FEBS Lett, 1991. **282**(1): p. 77-81.
343. Ali, F.E., et al., *Potent vasopressin antagonists modified at the carboxy-terminal tripeptide tail*. J Med Chem, 1987. **30**(12): p. 2291-4.
344. Brooks, D.P., et al., *SK&F 105494 is a potent antidiuretic hormone antagonist in the rhesus monkey (Macaca mulatta)*. J Pharmacol Exp Ther, 1988. **245**(1): p. 211-5.
345. Sobocinska, M., et al., *Structure--function studies of vasopressin analogues with D-3 pyridyl-alanine in position 2*. Peptides, 1995. **16**(3): p. 389-93.
346. Guillon, G., et al., *Position 4 analogues of [deamino-Cys(1)] arginine vasopressin exhibit striking species differences for human and rat V(2)/V(1b) receptor selectivity*. J Pept Sci, 2006. **12**(3): p. 190-8.

347. Pena, A., et al., *Pharmacological and physiological characterization of d[Leu4, Lys8]vasopressin, the first V1b-selective agonist for rat vasopressin/oxytocin receptors.* Endocrinology, 2007. **148**(9): p. 4136-46.
348. Manning, M., et al., *Design of more potent antagonists of the antidiuretic responses to arginine-vasopressin.* J Med Chem, 1982. **25**(1): p. 45-50.
349. Jamil, K.M., et al., *Distinct mechanisms of action of V1 antagonists OPC-21268 and [d(CH2)5Tyr(Me)AVP] in mesangial cells.* Biochem Biophys Res Commun, 1993. **193**(2): p. 738-43.
350. Barbeis, C., et al., *Characterization of a novel, linear radioiodinated vasopressin antagonist: an excellent radioligand for vasopressin V1a receptors.* Neuroendocrinology, 1995. **62**(2): p. 135-46.
351. Bankowski, K., et al., *Design of potent antagonists of the vasopressor response to arginine-vasopressin.* J Med Chem, 1978. **21**(9): p. 850-3.
352. Saito, M., A. Tahara, and T. Sugimoto, *1-desamino-8-D-arginine vasopressin (DDAVP) as an agonist on V1b vasopressin receptor.* Biochem Pharmacol, 1997. **53**(11): p. 1711-7.
353. Derick, S., et al., *[1-deamino-4-cyclohexylalanine] arginine vasopressin: a potent and specific agonist for vasopressin V1b receptors.* Endocrinology, 2002. **143**(12): p. 4655-64.
354. Cheng, L.L., et al., *Design of potent and selective agonists for the human vasopressin V1b receptor based on modifications of [deamino-cys1]arginine vasopressin at position 4.* J Med Chem, 2004. **47**(9): p. 2375-88.
355. Pena, A., et al., *Design and synthesis of the first selective agonists for the rat vasopressin V(1b) receptor: based on modifications of deamino-[Cys1]arginine vasopressin at positions 4 and 8.* J Med Chem, 2007. **50**(4): p. 835-47.
356. Manning, M., et al., *C-terminal deletions in agonistic and antagonistic analogues of vasopressin that improve their specificities for antidiuretic (V2) and vasopressor (V1) receptors.* J Med Chem, 1987. **30**(12): p. 2245-52.
357. Manning, M., et al., *Potent and selective antagonists of the antidiuretic responses to arginine-vasopressin based on modifications of [1-(beta-mercapto-beta,beta-pentamethylenepropionic acid),2-D-isoleucine,4- valine]arginine-vasopressin at position 4.* J Med Chem, 1984. **27**(4): p. 423-9.
358. Manning, M., et al., *Synthesis and some pharmacological properties of deamino(4-threonine,8-D-arginine)vasopressin and deamino(8-D-arginine)vasopressin, highly potent and specific antidiuretic peptides, and (8-D-arginine)vasopressin and deamino-arginine-vasopressin.* J Med Chem, 1976. **19**(6): p. 842-5.
359. Manning, M., et al., *Solid phase synthesis of (1-deamino,4-valine)-8-D-arginine-vasopressin (DVDAVP), a highly potent and specific antidiuretic agent possessing protracted effects.* J Med Chem, 1973. **16**(9): p. 975-8.
360. Yamamura, Y., et al., *OPC-21268, an orally effective, nonpeptide vasopressin V1 receptor antagonist.* Science, 1991. **252**(5005): p. 572-4.
361. Serradeil-Le Gal, C., et al., *Biochemical and pharmacological properties of SR 49059, a new, potent, nonpeptide antagonist of rat and human vasopressin V1a receptors.* J Clin Invest, 1993. **92**(1): p. 224-31.
362. Freidinger, R.M. and D.J. Pettibone, *Small molecule ligands for oxytocin and vasopressin receptors.* Med Res Rev, 1997. **17**(1): p. 1-16.

363. Serradeil-Le Gal, C., et al., *Characterization of (2S,4R)-1-[5-chloro-1-[(2,4-dimethoxyphenyl)sulfonyl]-3-(2-methoxy-phenyl)-2-oxo-2,3-dihydro-1H-indol-3-yl]-4-hydroxy-N,N-dimethyl-2-pyrrolidine carboxamide (SSR149415), a selective and orally active vasopressin V1b receptor antagonist.* J Pharmacol Exp Ther, 2002. **300**(3): p. 1122-30.
364. Griffante, C., et al., *Selectivity of d[Cha4]AVP and SSR149415 at human vasopressin and oxytocin receptors: evidence that SSR149415 is a mixed vasopressin V1b/oxytocin receptor antagonist.* Br J Pharmacol, 2005. **146**(5): p. 744-51.
365. Andersen, P.H. and J.A. Jansen, *Dopamine Receptor Agonists - Selectivity and Dopamine-D1 Receptor Efficacy.* European Journal of Pharmacology-Molecular Pharmacology Section, 1990. **188**(6): p. 335-347.
366. Neumeyer, J.L., et al., *(+/-)-3-Allyl-6-bromo-7,8-dihydroxy-1-phenyl-2,3,4,5-tetrahydro-1H-3-benzazepin, a new high-affinity D1 dopamine receptor ligand: synthesis and structure-activity relationship.* J Med Chem, 1991. **34**(12): p. 3366-71.
367. Weinstock, J., et al., *Synthesis and dopaminergic activity of some halogenated mono- and dihydroxylated 2-aminotetralins.* J Med Chem, 1986. **29**(9): p. 1615-27.
368. Andersen, P.H., et al., *Nnc-112, Nnc-687 and Nnc-756, New Selective and Highly Potent Dopamine D1 Receptor Antagonists.* European Journal of Pharmacology, 1992. **219**(1): p. 45-52.
369. Chumpradit, S., et al., *Synthesis and Resolution of (+/-)-7-Chloro-8-Hydroxy-1-(3'-Iodophenyl)-3-Methyl-2,3,4,5-Tetrahydro-1h-3-Benzazepine (Tisch) - a High-Affinity and Selective Iodinated Ligand for Cns D1 Dopamine Receptor.* Journal of Medicinal Chemistry, 1991. **34**(3): p. 877-883.
370. Baidur, N., et al., *(+/-)-3-Allyl-7-Halo-8-Hydroxy-1-Phenyl-2,3,4,5-Tetrahydro-1h-3-Benzazepines as Selective High-Affinity D1 Dopamine Receptor Antagonists - Synthesis and Structure Activity Relationship.* Journal of Medicinal Chemistry, 1992. **35**(1): p. 67-72.
371. Andres, J.I., et al., *2-(dimethylaminomethyl)-tetrahydroisoxazopyridobenzazepine derivatives. Synthesis of a new 5-HT2C antagonist with potential anxiolytic properties.* Bioorganic & Medicinal Chemistry Letters, 2002. **12**(24): p. 3573-3577.
372. Thomsen, W.J., et al., *Lorcaserin, a novel selective human 5-hydroxytryptamine2C agonist: in vitro and in vivo pharmacological characterization.* J Pharmacol Exp Ther, 2008. **325**(2): p. 577-87.
373. Aramaki, Y., et al., *Synthesis of 1-benzothiepine and 1-benzazepine derivatives as orally active CCR5 antagonists.* Chemical & Pharmaceutical Bulletin, 2004. **52**(2): p. 254-258.
374. Seto, M., et al., *Orally active CCR5 antagonists as anti-HIV-1 agents 2: Synthesis and biological activities of anilide derivatives containing a pyridine N-oxide moiety.* Chemical & Pharmaceutical Bulletin, 2004. **52**(7): p. 818-829.
375. Seto, M., et al., *Highly potent and orally active CCR5 antagonists as anti-HIV-1 agents: Synthesis and biological activities of 1-benzazocine derivatives containing a sulfoxide moiety.* Journal of Medicinal Chemistry, 2006. **49**(6): p. 2037-2048.
376. Van den Eynde, I., et al., *A new structural motif for mu-opioid antagonists.* Journal of Medicinal Chemistry, 2005. **48**(10): p. 3644-3648.
377. Evans, P., A.T.L. Lee, and E.J. Thomas, *Synthesis of a 6-aryloxymethyl-5-hydroxy-2,3,4,5-tetrahydro-[1H]-2-benzazepin-4-one: a muscarinic (M-3) antagonist.* Organic & Biomolecular Chemistry, 2008. **6**(12): p. 2158-2167.

378. Emura, T., et al., *Efficient asymmetric synthesis of novel gastrin receptor antagonist AG-041R via highly stereoselective alkylation of oxindole enolates*. Journal of Organic Chemistry, 2006. **71**(22): p. 8559-8564.
379. Stevens, F.C., et al., *Potent oxindole based human beta(3) adrenergic receptor agonists*. Bioorganic & Medicinal Chemistry Letters, 2007. **17**(22): p. 6270-6273.
380. Nagamine, J., et al., *Pharmacological profile of a new orally active growth hormone secretagogue, SM-130686*. J Endocrinol, 2001. **171**(3): p. 481-9.
381. Nagamine, J., et al., *Synthesis and pharmacological profile of an orally-active growth hormone secretagogue, SM-130686*. Combinatorial Chemistry & High Throughput Screening, 2006. **9**(3): p. 187-196.
382. Tokunaga, T., et al., *Structure-activity relationships of the oxindole growth hormone secretagogues*. Bioorg Med Chem Lett, 2005. **15**(7): p. 1789-92.
383. Burrell, L.M., et al., *Effects of an orally active vasopressin V1 receptor antagonist*. Clin Exp Pharmacol Physiol, 1993. **20**(5): p. 388-91.
384. Serradeil-Le Gal, C., et al., *Effect of a new, potent, non-peptide V1a vasopressin antagonist, SR 49059, on the binding and the mitogenic activity of vasopressin on Swiss 3T3 cells*. Biochem Pharmacol, 1994. **47**(4): p. 633-41.
385. Ferris, C.F., et al., *Orally active vasopressin V1a receptor antagonist, SRX251, selectively blocks aggressive behavior*. Pharmacol Biochem Behav, 2006. **83**(2): p. 169-74.
386. Guillon, C.D., et al., *Azetidinones as vasopressin V1a antagonists*. Bioorg Med Chem, 2007. **15**(5): p. 2054-80.
387. Shimada, Y., et al., *Synthesis and biological activity of novel 4,4-difluorobenzazepine derivatives as non-peptide antagonists of the arginine vasopressin V1A receptor*. Bioorg Med Chem, 2006. **14**(6): p. 1827-37.
388. Morita, M., et al., *Molecular analysis of antilipemic effects of FR218944, a novel vasopressin V1a receptor antagonist, in genetically diabetic db/db mice in comparison with pioglitazone and fenofibrate*. Drug Development Research, 2003. **60**(4): p. 241-251.
389. Kakefuda, A., et al., *Synthesis and pharmacological evaluation of 5-(4-biphenyl)-3-methyl-4-phenyl-1,2,4-triazole derivatives as a novel class of selective antagonists for the human vasopressin V(1A) receptor*. J Med Chem, 2002. **45**(12): p. 2589-98.
390. Bleickardt, C.J., et al., *Characterization of the V1a antagonist, JNJ-17308616, in rodent models of anxiety-like behavior*. Psychopharmacology (Berl), 2009. **202**(4): p. 711-8.
391. Serradeil-Le Gal, C., et al., *Biological characterization of rodent and human vasopressin V1b receptors using SSR-149415, a nonpeptide V1b receptor ligand*. Am J Physiol Regul Integr Comp Physiol, 2007. **293**(2): p. R938-49.
392. Craighead, M., et al., *Characterization of a novel and selective V1B receptor antagonist*. Prog Brain Res, 2008. **170**: p. 527-35.
393. MacSweeney, C.P., *Neurobiological basis and preclinical evidence for the anxiolytic/antidepressant potential of org 52186, a novel and selective V1B receptor antagonist*. Biological Psychiatry, 2008. **63**(7): p. 161s-161s.
394. Yamamura, Y., et al., *Characterization of a Novel Aquaretic Agent, Opc-31260, as an Orally Effective, Nonpeptide Vasopressin V2-Receptor Antagonist*. British Journal of Pharmacology, 1992. **105**(4): p. 787-791.

395. Kondo, K., et al., *7-Chloro-5-hydroxy-1-[2-methyl-4-(2-methylbenzoyl-amino)benzoyl]-2,3,4,5-tetrahydro-1H-1-benzazepine (OPC-41061): a potent, orally active nonpeptide arginine vasopressin V2 receptor antagonist*. *Bioorg Med Chem*, 1999. **7**(8): p. 1743-54.
396. Miyazaki, T., et al., *Tolvaptan, an orally active vasopressin V(2)-receptor antagonist - pharmacology and clinical trials*. *Cardiovasc Drug Rev*, 2007. **25**(1): p. 1-13.
397. Venkatesan, H., et al., *Total synthesis of SR 121463 A, a highly potent and selective vasopressin v(2) receptor antagonist*. *J Org Chem*, 2001. **66**(11): p. 3653-61.
398. Serradeil-Le Gal, C., *Nonpeptide antagonists for vasopressin receptors. Pharmacology of SR 121463A, a new potent and highly selective V2 receptor antagonist*. *Adv Exp Med Biol*, 1998. **449**: p. 427-38.
399. Soupart, A., et al., *Successful long-term treatment of hyponatremia in syndrome of inappropriate antidiuretic hormone secretion with satavaptan (SR121463B), an orally active nonpeptide vasopressin V2-receptor antagonist*. *Clin J Am Soc Nephrol*, 2006. **1**(6): p. 1154-60.
400. Gines, P., et al., *Effects of satavaptan, a selective vasopressin V-2 receptor antagonist, on ascites and serum sodium in cirrhosis with hyponatremia: A randomized trial*. *Hepatology*, 2008. **48**(1): p. 204-213.
401. Chan, P.S., et al., *VPA-985, a nonpeptide orally active and selective vasopressin V2 receptor antagonist*. *Adv Exp Med Biol*, 1998. **449**: p. 439-43.
402. Muralidharan, G., et al., *Pharmacokinetics and pharmacodynamics of a novel vasopressin receptor antagonist, VPA-985, in healthy subjects*. *Clinical Pharmacology & Therapeutics*, 1999. **65**(2): p. 189-189.
403. Guyader, D., et al., *Pharmacodynamic effects of a nonpeptide antidiuretic hormone V2 antagonist in cirrhotic patients with ascites*. *Hepatology*, 2002. **36**(5): p. 1197-1205.
404. Abraham, W.T., et al., *Aquaretic effect of Lixivaptan, an oral, non-peptide, selective V2 receptor vasopressin antagonist, in New York Heart Association functional class II and III chronic heart failure patients*. *Journal of the American College of Cardiology*, 2006. **47**(8): p. 1615-1621.
405. Ashwell, M.A., et al., *The design, synthesis and physical chemical properties of novel human vasopressin V2-receptor antagonists optimized for parenteral delivery*. *Bioorg Med Chem Lett*, 2000. **10**(8): p. 783-6.
406. Ohtake, Y., et al., *Novel vasopressin V2 receptor-selective antagonists, pyrrolo[2,1-a]quinoxaline and pyrrolo[2,1-c][1,4]benzodiazepine derivatives*. *Bioorganic & Medicinal Chemistry*, 1999. **7**(6): p. 1247-1254.
407. Matthews, J.M., et al., *Synthesis and biological evaluation of novel indoloazepine derivatives as non-peptide vasopressin V2 receptor antagonists*. *Bioorg Med Chem Lett*, 2003. **13**(4): p. 753-6.
408. Tahara, A., et al., *Effect of YM087, a potent nonpeptide vasopressin antagonist, on vasopressin-induced protein synthesis in neonatal rat cardiomyocyte*. *Cardiovasc Res*, 1998. **38**(1): p. 198-205.
409. Matsuhisa, A., et al., *Nonpeptide arginine vasopressin antagonists for both V1A and V2 receptors: synthesis and pharmacological properties of 4-(1,4,5,6-tetrahydroimidazo[4,5-d][1]benzoazepine-6-carbonyl)benzanilide derivatives and 4'-(5,6-dihydro-4H-thiazolo[5,4-d][1]benzoazepine-6-carbonyl)benzanilide derivatives*. *Chem Pharm Bull (Tokyo)*, 2000. **48**(1): p. 21-31.

410. Tsukuda, J., et al., *Pharmacological characterization of YM471, a novel potent vasopressin V-1A and V-2 receptor antagonist*. European Journal of Pharmacology, 2002. **446**(1-3): p. 129-138.
411. Cho, H., et al., *Synthesis and structure-activity relationships of 5,6,7,8-tetrahydro-4H-thieno[3,2-b]azepine derivatives: novel arginine vasopressin antagonists*. J Med Chem, 2004. **47**(1): p. 101-9.
412. Hartupee, D.A., et al., *Effects of CL-385004, a nonpeptidic vasopressin V-1a/V-2 receptor antagonist, in a rat model of heart failure*. Circulation, 1997. **96**(8): p. 3416-3416.
413. Aranapakam, V., et al., *5-fluoro-2-methyl-N-[5-(5H-pyrrolo[2,1-c][1,4] benzodiazepine-10(11H)-YL carbonyl)-2-pyridinyl] benzamide (CL-385004) and analogs as orally active arginine vasopressin receptor antagonists*. Bioorganic & Medicinal Chemistry Letters, 1999. **9**(13): p. 1737-1740.
414. Sum, F.W., et al., *Structure-activity study of novel tricyclic benzazepine arginine vasopressin antagonists*. Bioorganic & Medicinal Chemistry Letters, 2003. **13**(13): p. 2195-2198.
415. Xiang, M.A., et al., *Synthesis and evaluation of spirobenzazepines as potent vasopressin receptor antagonists*. Bioorg Med Chem Lett, 2004. **14**(11): p. 2987-9.
416. Coltamai, L., et al., *Vascular effects of RWJ-676070, a selective combined V1a/V2 vasopressin receptor antagonist*. Clin Pharmacol Ther, 2009. **85**(2): p. 145-8.
417. Ajay and M.A. Murcko, *Computational methods to predict binding free energy in ligand-receptor complexes*. J Med Chem, 1995. **38**(26): p. 4953-67.
418. Bohm, H.J., *The development of a simple empirical scoring function to estimate the binding constant for a protein-ligand complex of known three-dimensional structure*. J Comput Aided Mol Des, 1994. **8**(3): p. 243-56.
419. Sobolev, V., et al., *Molecular docking using surface complementarity*. Proteins, 1996. **25**(1): p. 120-9.
420. Thibonnier, M., et al., *Molecular pharmacology and modeling of vasopressin receptors*. Prog Brain Res, 2002. **139**: p. 179-96.
421. Wheatley, M., et al., *Preparation of a membrane fraction for receptor studies and solubilization of receptor proteins with retention of biological activity*. Methods Mol Biol, 1997. **73**: p. 305-22.
422. Bee, M.S. and E.C. Hulme, *Functional analysis of transmembrane domain 2 of the M1 muscarinic acetylcholine receptor*. J Biol Chem, 2007. **282**(44): p. 32471-9.
423. Howl, J., et al., *Rat testicular myoid cells express vasopressin receptors: receptor structure, signal transduction, and developmental regulation*. Endocrinology, 1995. **136**(5): p. 2206-13.
424. Cheng, Y. and W.H. Prusoff, *Relationship between the inhibition constant (K₁) and the concentration of inhibitor which causes 50 per cent inhibition (I₅₀) of an enzymatic reaction*. Biochem Pharmacol, 1973. **22**(23): p. 3099-108.
425. Mouillac, B., et al., *Identification of agonist binding sites of vasopressin and oxytocin receptors*. Adv Exp Med Biol, 1995. **395**: p. 301-10.
426. Hausmann, H., et al., *Mutational analysis and molecular modeling of the nonapeptide hormone binding domains of the [Arg⁸]vasotocin receptor*. Proc Natl Acad Sci U S A, 1996. **93**(14): p. 6907-12.

427. Slusarz, M.J., et al., *Analysis of interactions responsible for vasopressin binding to human neurohypophyseal hormone receptors-molecular dynamics study of the activated receptor-vasopressin-G(alpha) systems*. J Pept Sci, 2006. **12**(3): p. 180-9.
428. Hawtin, S.R., et al., *The N-terminal juxtamembrane segment of the V1a vasopressin receptor provides two independent epitopes required for high-affinity agonist binding and signaling*. Mol Endocrinol, 2005. **19**(11): p. 2871-81.
429. Wesley, V.J., et al., *Agonist-specific, high-affinity binding epitopes are contributed by an arginine in the N-terminus of the human oxytocin receptor*. Biochemistry, 2002. **41**(16): p. 5086-92.
430. Kojro, E., et al., *Direct identification of an extracellular agonist binding site in the renal V2 vasopressin receptor*. Biochemistry, 1993. **32**(49): p. 13537-44.
431. Rodrigo, J., et al., *Mapping the binding site of arginine vasopressin to V1a and V1b vasopressin receptors*. Mol Endocrinol, 2007. **21**(2): p. 512-23.
432. Du Vigneaud, V., *Hormones of the posterior pituitary gland: oxytocin and vasopressin*. Harvey Lect, 1954. **50**: p. 1-26.
433. Manning, M., et al., *Carboxy terminus of vasopressin required for activity but not binding*. Nature, 1984. **308**(5960): p. 652-3.
434. Derick, S., et al., *Key amino acids located within the transmembrane domains 5 and 7 account for the pharmacological specificity of the human V1b vasopressin receptor*. Mol Endocrinol, 2004. **18**(11): p. 2777-89.
435. Van Craenenbroeck, K., et al., *Influence of the antipsychotic drug pipamperone on the expression of the dopamine D4 receptor*. Life Sci, 2006. **80**(1): p. 74-81.
436. Robert, J., et al., *Mechanisms of cell-surface rerouting of an endoplasmic reticulum-retained mutant of the vasopressin V1b/V3 receptor by a pharmacological chaperone*. J Biol Chem, 2005. **280**(51): p. 42198-206.
437. Hawtin, S.R., *Pharmacological chaperone activity of SR49059 to functionally recover misfolded mutations of the vasopressin V1a receptor*. J Biol Chem, 2006. **281**(21): p. 14604-14.
438. Wheatley, M., et al., *Extracellular loops and ligand binding to a subfamily of Family A G-protein-coupled receptors*. Biochem Soc Trans, 2007. **35**(Pt 4): p. 717-20.
439. Hawtin, S.R., et al., *Charged extracellular residues, conserved throughout a G-protein-coupled receptor family, are required for ligand binding, receptor activation, and cell-surface expression*. J Biol Chem, 2006. **281**(50): p. 38478-88.
440. Wess, J., et al., *Selectivity profile of the novel muscarinic antagonist UH-AH 37 determined by the use of cloned receptors and isolated tissue preparations*. Br J Pharmacol, 1991. **102**(1): p. 246-50.
441. Shin, N., et al., *Molecular modeling and site-specific mutagenesis of the histamine-binding site of the histamine H4 receptor*. Mol Pharmacol, 2002. **62**(1): p. 38-47.
442. Manivet, P., et al., *The serotonin binding site of human and murine 5-HT2B receptors: molecular modeling and site-directed mutagenesis*. J Biol Chem, 2002. **277**(19): p. 17170-8.
443. Sjodin, P., et al., *Re-evaluation of receptor-ligand interactions of the human neuropeptide Y receptor Y1: a site-directed mutagenesis study*. Biochem J, 2006. **393**(Pt 1): p. 161-9.

444. Roth, C.B., M.A. Hanson, and R.C. Stevens, *Stabilization of the human beta2-adrenergic receptor TM4-TM3-TM5 helix interface by mutagenesis of Glu122(3.41), a critical residue in GPCR structure*. J Mol Biol, 2008. **376**(5): p. 1305-19.
445. Han, M., S.O. Smith, and T.P. Sakmar, *Constitutive activation of opsin by mutation of methionine 257 on transmembrane helix 6*. Biochemistry, 1998. **37**(22): p. 8253-61.
446. Costanzi, S., et al., *Architecture of P2Y nucleotide receptors: structural comparison based on sequence analysis, mutagenesis, and homology modeling*. J Med Chem, 2004. **47**(22): p. 5393-404.
447. Tikhonova, I.G., et al., *Bidirectional, iterative approach to the structural delineation of the functional "chemoprint" in GPR40 for agonist recognition*. J Med Chem, 2007. **50**(13): p. 2981-9.
448. Tahtaoui, C., et al., *Identification of the binding sites of the SR49059 nonpeptide antagonist into the V1a vasopressin receptor using sulfhydryl-reactive ligands and cysteine mutants as chemical sensors*. J Biol Chem, 2003. **278**(41): p. 40010-9.
449. Peltonen, J.M., et al., *Molecular mechanisms of ligand-receptor interactions in transmembrane domain V of the alpha2A-adrenoceptor*. Br J Pharmacol, 2003. **140**(2): p. 347-58.
450. Floresca, C.Z. and J.A. Schetz, *Dopamine receptor microdomains involved in molecular recognition and the regulation of drug affinity and function*. J Recept Signal Transduct Res, 2004. **24**(3): p. 207-39.
451. Dempster, E.L., et al., *Evidence of an association between the vasopressin V1b receptor gene (AVPR1B) and childhood-onset mood disorders*. Arch Gen Psychiatry, 2007. **64**(10): p. 1189-95.
452. Keck, M.E., et al., *Combined effects of exonic polymorphisms in CRHR1 and AVPR1B genes in a case/control study for panic disorder*. Am J Med Genet B Neuropsychiatr Genet, 2008.
453. Sawyer, W.H., et al., *Structural changes in the arginine vasopressin molecule that enhance antidiuretic activity and specificity*. Endocrinology, 1974. **94**(4): p. 1106-15.

Appendix

Table I: pEC₅₀ values determined for the V_{1b}R constructs by InsP-InsP₃ assay

	AVP	dDAVP	dAVP	[Glu ⁸]VP
Wt V _{1b} R	8.740 ± 0.021	7.942 ± 0.093	7.592 ± 0.128	Undetectable
[R1.27A]V _{1b} R	7.260 ± 0.042	7.924 ± 0.096	—	—
[E1.35A]V _{1b} R	7.318 ± 0.045	6.417 ± 0.177	—	—
[E1.35Q]V _{1b} R	Undetectable	7.484 ± 0.111	7.133 ± 0.042	Undetectable
[E1.35R]V _{1b} R	Undetectable	—	—	7.818 ± 0.115
[K65N]V _{1b} R	8.689 ± 0.037	8.213 ± 0.175	—	—
[G191R]V _{1b} R	8.588 ± 0.124	—	—	—
[R364H]V _{1b} R	8.595 ± 0.106	—	—	—